THÈSE

En vue de l'obtention du

DOCTORAT DE L'UNIVERSITÉ DE TOULOUSE

Délivré par : *l'Université Toulouse 3 Paul Sabatier (UT3 Paul Sabatier)*

Présentée et soutenue le *16/12/2014* **par :**

Ronan MONJARRET

The multi-layer shallow water model with free surface: Treatment of the open boundaries

---

JURY

Rémy BARAILLE	Ingénieur	SHOM
Christophe BESSE	Professeur des Universités	Université Toulouse 3
Philippe BONNETON	Directeur de Recherche	Université de Bordeaux
Florent CHAZEL	Maître de Conférences	INSA Toulouse
Sergey GAVRILYUK	Professeur des Universités	Université d'Aix-Marseille
David LANNES	Directeur de Recherche	Université de Bordeaux
Carole NAHUM	Docteur	DGA
Jean-Paul VILA	Professeur des Universités	INSA Toulouse

École doctorale et spécialité :
MITT : Domaine Mathématiques : Mathématiques appliquées
Unité de Recherche :
Institut de Mathématiques de Toulouse - UMR 5219
Directeur(s) de Thèse :
Rémy BARAILLE, *Florent CHAZEL* et *Jean-Paul VILA*
Rapporteurs :
Sergey GAVRILYUK et *David LANNES*

Acknowledgements

Merci à tous.

Contents

1

Introduction générale

Contents

La coopération et les échanges d'idées entre des entités scientifiques, dont les compétences techniques sont complémentaires, est cruciale pour l'avancement de la recherche. Dans le cas présent, les domaines concernés sont : l'océanographie et les mathématiques appliquées à la physique. Le but de cette thèse est la réduction des barrières entre ces deux mondes. Cette alliance permet un débat constructif entre les participants, pour que les mathématiciens soient à même de proposer des solutions originales aux problèmes techniques des océanographes. Cette thèse est née de la cooperation entre le SHOM, Service Hydrographique et Océanographique de la Marine, et l'IMT, Institut de Mathématiques de Toulouse.

Le SHOM est un établissement public français à caractère administratif, placé sous la tutelle du ministère de la Défense. Sa mission se divise en trois principaux volets :

- le service hydrographique national : le SHOM répond aux besoins de tous les usagers de la mer en ce qui concerne l'hydrographie générale. Il se conforme à la convention internationale SOLAS [95], adoptée en 1974, pour la sauvegarde de la vie humaine en mer, ainsi que la convention de l'ONU sur le droit de la mer [135], adoptée en 1982,

- le soutien à la défense : le SHOM assure l'efficacité des besoins d'expertise et d'appui opérationnel de la défense en connaissance de l'environnement hydrographique, océanographique et météorologique. Il se fait de la côte au large et de la surface au plancher océanique,
- le soutien aux politiques publiques maritimes et du littoral : le SHOM recueille et met à disposition des données numériques nécessaires aux actions de l'État en mer. Par exemple, les travaux relatifs à la délimitation des frontières maritimes, les projets pour le développement durable, la lutte contre les pollutions maritimes ou la mise en place de réseaux d'alertes pour la prévention des risques et des catastrophes.

Intégré au sein de l'université *Paul Sabatier* - Toulouse III, l'IMT est une unité mixte de recherche. Il est constitué de trois équipes de recherche couvrant la quasi-totalité du spectre des mathématiques pures et appliquées. Les principales missions du laboratoire sont :

- L'enseignement des mathématiques à l'université, avec notamment un large spectre de formations de niveau Master, incluant la formation des futurs enseignants, l'initiation à la recherche des scientifiques en devenir et la professionnalisation des ingénieurs de demain,
- la promotion et la diffusion des connaissances mathématiques à destination des scolaires et du grand public. Par exemple, le projet Hippocampe qui vise à décloisonner le laboratoire pour l'ouvrir à des lycéens lord d'un mini-stage d'initiation à la recherche,
- le développement de toutes les mathématiques, notamment pour les applications les plus diverses et les interactions avec les autres sciences, comme par exemple la médecine [32].

L'étude menée dans le cadre de ce doctorat s'articule autour de cette philosophie : promouvoir les intérêts communs et trouver des solutions innovantes qui permettent une meilleur prédiction de la météorologie marine grâce à la contribution des outils mathématiques. L'objectif de cette thèse est d'étudier les conditions limites d'un modèle océanique pour que le SHOM puisse, in fine, les intégrer dans son code opérationnel : HYCOM.

Dans cette introduction, le contexte scientifique, dans lequel se situe ce doctorat, est présenté : l'étude des océans. Puis, les techniques, utilisées jusqu'à présent pour répondre à la problématique posée, seront décrites dans l'état de l'art. Enfin les principaux objectifs de cette thèse seront énoncés, ainsi que le plan de ce manuscrit.

1.1 L'étude des océans

Bien que les grands navigateurs et les explorateurs d'hier ont eu l'audace de mettre au grand jour l'étendue des océans, ce ne fût que la partie immergée de l'iceberg et la conquête marine est loin d'être aboutie. En effet, l'extension géographique des mers a répondu à quelques grandes interrogations, mais a surtout été le point de départ d'études importantes sur la compréhension de notre planète. Dans un premier temps, la cartographie marine se développe lors des grandes expéditions, telle que celle menée par *Magellan* en 1521, où il tente en vain de mesurer la profondeur de l'océan Pacifique. Cette tâche s'avère complexe car ses lignes plombées ne dépassent pas 800m. Ce n'est qu'en 1840 que *J.C. Ross* procède aux premiers sondages modernes des mers profondes [112].

Dans un second temps, les mécanismes de fonctionnement de nos océans, telle que les vagues, les marées, les courants marins ou la distribution de température, sont étudiés méthodiquement. Effectivement, dès le début du 19eme siècle, *J. Rennell* et *J. Purdy* publient leurs premiers écrits scientifiques, [109], sur l'observation des courants marins dans les océans Atlantique et Indien. Les principaux courants connus aujourd'hui sont représentés en figure 1.1.

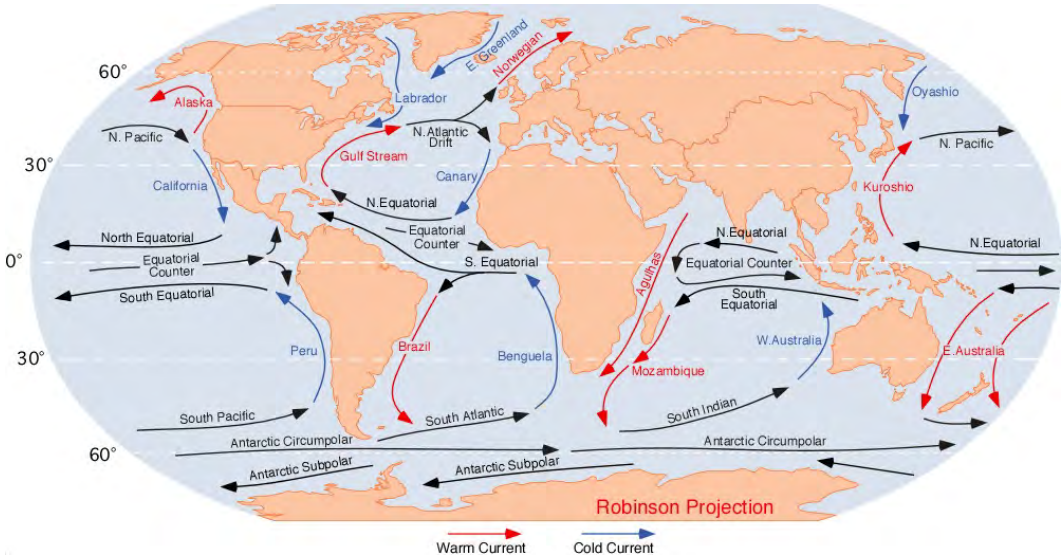

Figure 1.1: Principaux courants mondiaux - Extrait de [105].

L'étude de la biologie marine n'est pas en reste quand *C. Darwin* révèle son célèbre *Journal et remarques* [38], en 1839, dans lequel il suggère notamment la théorie de formation des atolls. Le 20eme siècle et le développement de technologies avancées voient l'essor de l'étude microscopique des eaux marines. Cette analyse cherche à comprendre l'évolution des éléments chimiques des océans qui

jouent un rôle essentiel dans la régulation du climat mondial. Enfin, la deuxième moitié du 20eme siècle et la conquête spatiale ont permis le déploiement et la mise au point des mesures océaniques à l'aide de l'imagerie satellitale.

Cet historique chargé a amené 40 États, en 1960, à créer la *Commission océanographique intergouvernementale*, sous l'égide de l'UNESCO. Sa mission est de promouvoir la coopération internationale dans le but d'améliorer la connaissance des océans et d'appliquer ce savoir afin d'améliorer durablement les actions gouvernementales en matière de développement et de protection du milieu marin. Les États ont compris que l'enjeu est primordial : cette commission compte 147 États membres, en 2014. Par ailleurs, l'Europe s'est dotée d'une *Directive cadre "stratégie pour le milieu marin"*, en 2008, et a établi un plan d'action communautaire visant à prendre les mesures nécessaires pour réaliser ou maintenir un bon état écologique du milieu marin d'ici l'horizon 2020.

Les connaissance océaniques actuelles permettent de prédire précisément la météo marine :

- pour la pêche et la navigation de plaisance, à une échelle locale (voir figure 1.2),
- pour les politiques publiques de développement durable, à une échelle globale.

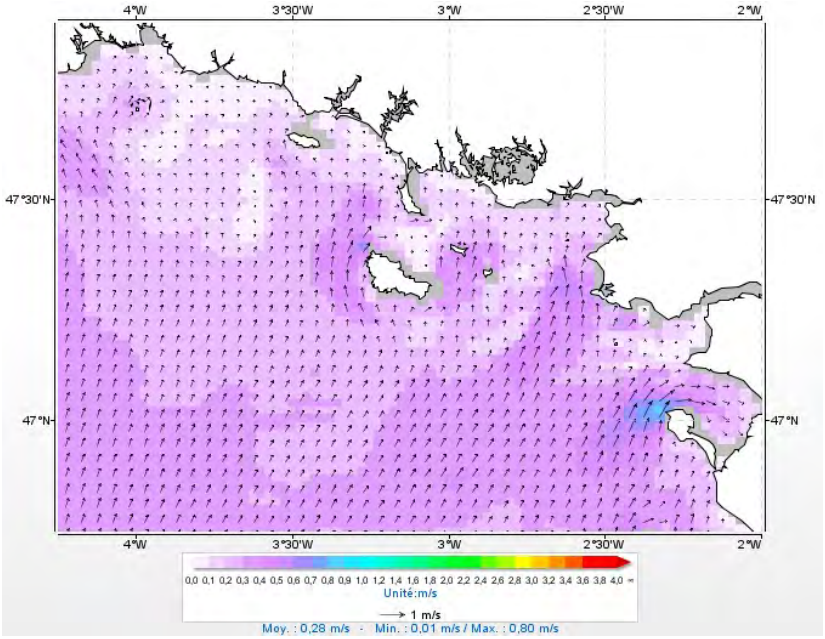

Figure 1.2: Direction et intensité des courants de surface au large du Golfe du Morbihan - Tempête du 6 Janvier 2014.

L'étude des océans est donc une problématique charnière majeure pour :

- ◇ la prédiction locale et précise des tempêtes permet de protéger les populations, à court terme,
- ◇ l'observation et la surveillance des espèces invasives sont nécessaires pour conserver durablement les écosystèmes marins, à moyen terme,
- ◇ la prévision pertinente de l'évolution climatique globale est un argument fort pour changer les comportements des sociétés, à long terme.

La dernière décennie nous a donné des exemple concrets de la nécessité de cette étude. Ces études permettent la prévision du comportement des océans, ce qui est une avancée majeure, mais aussi la description de la qualité quotidienne de nos mers.

Par exemple, lors du séisme de magnitude 9,0, au large des côtes nord-est de l'île de Honshu au Japon, le 11 Mars 2011, les scientifiques ont pu, au moment de la catastrophe, prédire rapidement les conséquences directes sur les côtes de l'océan Pacifique. Un effet inattendu a été l'exposition des quatre centrales nucléaires de Fukushima Daiichi, suite à la violence du tsunami. Les scientifiques de l'entreprise *ASR ltd*, aux U.S.A., ont pu décrire l'impact de la contamination de l'océan Pacifique par la radioactivité des réacteurs (comme l'illustre la figure 1.3). Cette étude de l'état radioactif de l'océan pacifique a été menée à partir de données générées par HYCOM.

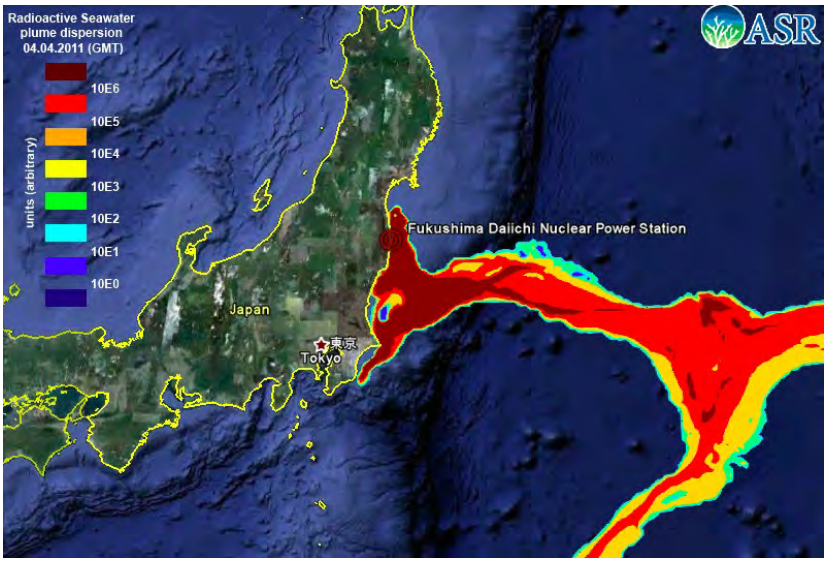

Figure 1.3: Dispersion du panache radioactif en surface au large du Japon (usi) - Le 4 Avril 2011.

Cette dernière figure est particulièrement intéressante. En effet, elle a été confondue, dans une large majorité de la presse internationale, avec une autre image présentant l'élévation maximale du niveau de l'océan Pacifique, engendrée par le tsunami du 11 Mars 2011. La figure 1.4 a été divulguée par la *National Oceanic and Atmospheric Administration* (NOAA). Cette image a été interprétée, dans de nombreux médias, comme la carte de contamination radioactive des eaux salées, suite au drame nucléaire de Fukushima Daiichi. Malgré cette information erronée, il est à noter qu'une image telle que la figure 1.4 peut être rapidement générée, aujourd'hui, avec la donnée du lieu géographique et de l'intensité du tremblement de Terre.

En résumé, les effets directs sur l'océan d'une catastrophe naturelle ont pu être prédits précisément. Mais les modèle d'océan permettent aussi de connaître l'évolution de quantités invisibles, qui peuvent contaminer le milieu marin.

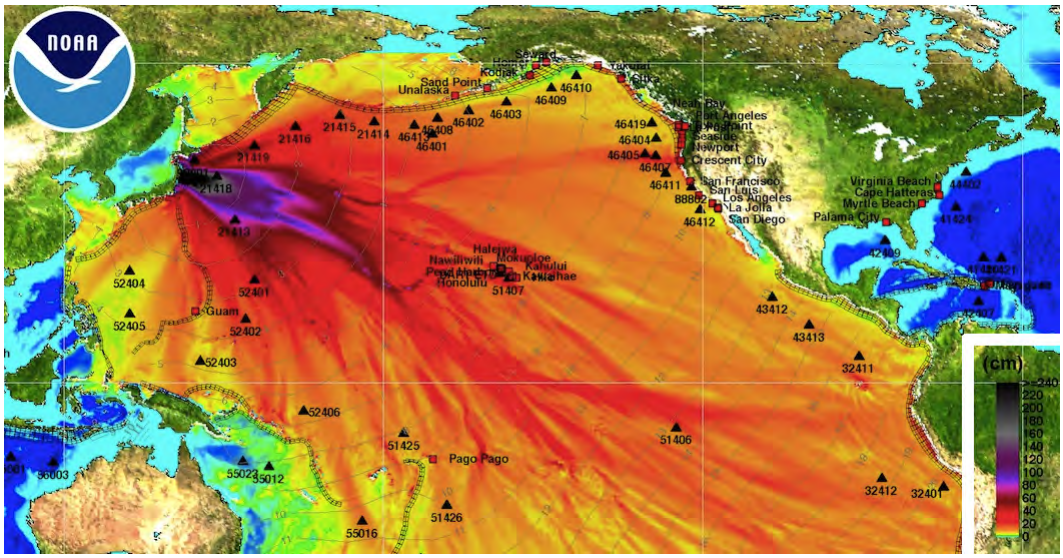

Figure 1.4: Élévation maximale de la surface de l'océan Pacifique (cm) - Le 11 Mars 2011.

Un autre exemple marquant est le passage de la tempête *Xynthia*, sur la façade Atlantique de l'Europe. Les prévisions de cet épisode météorologique, survenu entre le 26 Février et le 1er Mars 2010, n'avaient pas alerté les autorités compétentes. Cette tempête a pourtant eu pour conséquence la mort de 59 personnes. Malgré le caractère non-exceptionnel de cette tempête, elle s'est conjuguée avec une pression basse et une marée haute de vives-eaux. Cette concomitance de phénomènes s'est traduite par une surcôte de 1,5 mètres et a été à l'origine de *Xynthia*. Cette catastrophe est la preuve directe qu'il est nécessaire de prédire rigoureusement le comportement des eaux marines. De plus,

elle souligne l'un des nouveaux enjeux actuels : la nécessité de faire communiquer les connaissances de l'océanographie avec celles de la météorologie atmosphérique. Les prévisions de ces deux milieux sont fortement liées. Par conséquent, elles nécessitent une interaction forte, suivie d'un programme d'alerte adapté visant à informer la population locale.

En résumé, l'étude des océans est un enjeu majeur dans le développement durable de nos sociétés. De plus, l'appauvrissement des ressources poissonnières, l'exploitation des énergies marines ainsi que le dérèglement climatique terrestre placeront l'océanographie, avec la météorologie terrestre, au centre des activités scientifiques de demain.

1.2 L'état de l'art

Avant la 2^{eme} moitié du 20^{eme} siècle, la prévision complète de la météo marine n'était pas envisageable. Le développement des capacités de calculs informatiques et l'apparition des supercalculateurs l'ont rendue envisageable.

En 1965, le co-fondateur de la multi-nationale *Intel*, *G.E. Moore*, annonce le doublement annuel de la capacité des circuits imprimés (voir [89]). Cependant, sa conjecture est modifiée en 1975 : il prévoit la multiplication par 2 des transistors présents dans les microprocesseurs tous les deux ans (voir la figure 1.5). Il se trouve que cette dernière prédiction a été relativement bien vérifiée, jusqu'à aujourd'hui.
Le développement exponentiel de la puissance informatique est crucial pour la prévision océanique. En effet, la mer s'avère souvent difficile d'accès et ne peut être explorée, découverte et surveillée de manière exhaustive. C'est pour cela que les calculs informatiques sont nécessaires pour comprendre le comportement global de nos océans. Cependant, la puissance ne fait pas tout, il faut aussi comprendre les propriétés des fluides qui forment notre sujet d'étude. Cette connaissance nous permettra d'effectuer des simplifications, sans dégrader grossièrement nos résultats.

La modélisation est l'autre outil majeur de l'océanographe dans sa conquête des prévisions marines. Cette technique joue le rôle d'un traducteur : elle exprime, avec des équations mathématiques, une certaine réalité correspondant à des hypothèses. Le modèle, formé de ces équations, coïncide alors avec un système vérifiant ces hypothèses. Il est donc nécessaire de trouver les simplifications qui s'accordent le mieux à notre réalité, les océans.

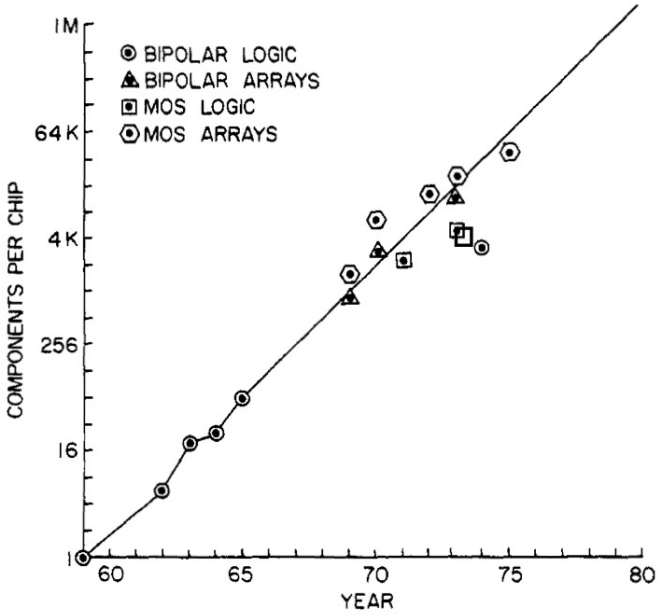

Figure 1.5: Capacité des microprocesseurs en fonction de l'année d'introduction - Extrait de [90].

Le lecteur avisé remarquera que les techniques développées dans ce manuscrit sont directement liées au modèle considéré. Si un modèle plus avantageux apparaît dans le futur, les résultats que nous présentons dans cet écrit ne s'appliquerons peut-être pas directement. Cependant, la méthode développée restera intéressante et pourra être adaptée.

1.2.1 Le modèle de *Saint-Venant* multi-couches

Les équations de *Navier-Stokes*, détaillées dans [15], décrivent avec précision un fluide newtonien tel que l'océan. Cependant, aujourd'hui encore, ce système d'équations s'avère à la fois trop coûteux en temps de calcul et trop général pour notre application : la mer se caractérise par une physique particulière et un fort hydrodynamisme. Pour ces raisons, les scientifiques utilisent des modèles simplifiés, dérivés des équations de *Navier-Stokes*.

Une première hypothèse est de supposer notre fluide comme un fluide non-visqueux. D'après les propriétés de l'eau marine, cette simplification paraît pertinente. On peut donc débuter notre modélisation avec les équations d'*Euler*, détaillées dans [10] et [131]. De plus, les eaux salées permettent d'ajouter des hypothèses supplémentaires. Une première approximation est de considérer la densité de tout l'océan comme constante. Ceci paraît peu pertinent puisque nous savons que

la température et la salinité, et donc la densité, varient de manière non-négligeable des pôles à l'équateur. Cependant, il est raisonnable de se restreindre à une partie de l'océan. Il n'est pas raisonnable de vouloir modéliser toute sa diversité des courants marins mondiaux dès le premier jet. En considérant donc une latitude donnée et les eaux s'étendant jusqu'à quelques centaines de kilomètres autour, il n'est pas invraisemblable de supposer la densité constante. Effectivement, comme nous pouvons le constater sur les valeurs de densité présentes en figure 1.6 (à retrouver dans [116]), il est envisageable de supposer, dans un premier temps, que la densité est constante. Il est à noter que cette figure 1.6 ne présente les caractéristiques de l'eau marine que jusqu'à 1000 mètres. L'évolution de ces quantités au-delà de cette profondeur est similaire à son évolution entre 500 mètres et 1000 mètres.

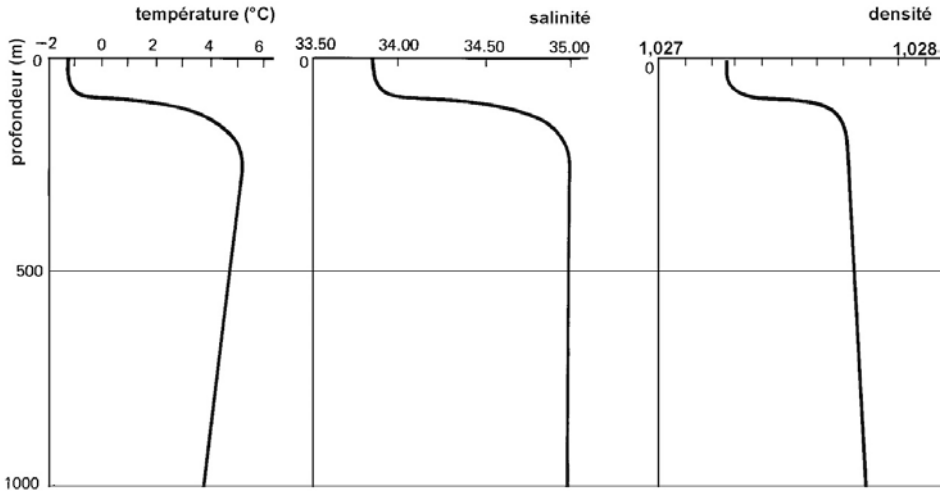

Figure 1.6: Évolution de la température, de la salinité et de la densité en fonction de la profondeur.

Enfin, deux dernières hypothèses complètent les précédentes. Tout d'abord, la pression est supposée hydrostatique : elle ne dépend que de la hauteur d'eau au-dessus du point considéré. Cette supposition permet d'éliminer certaines équations telles que la conservation de quantité de mouvement selon la coordonnée verticale. Enfin, la dernière simplification est la clé du modèle que l'on va obtenir. Elle suppose l'existence de deux longueurs caractéristiques, pour notre fluide, telles que :

- une longueur caractéristique horizontale notée L,
- une longueur caractéristique verticale notée H,

telles que la longueur L est très supérieure à la longueur H :

$$\frac{H}{L} \ll 1. \tag{1.1}$$

Cette hypothèse (1.1) est communément appelée l'hypothèse *shallow water*, *i.e.* eau peu profonde.
Les simplifications présentées ci-dessus permettent de dériver un nouveau modèle, à partir des équations d'*Euler*. Ce modèle a été introduit par *A.B. de Saint-Venant* [113], qui a donné le système d'équations de *Saint-Venant* :

$$\begin{cases} \frac{\partial h}{\partial t} + \frac{\partial (hu)}{\partial x} + \frac{\partial (hv)}{\partial y} = 0, \\ \frac{\partial (hu)}{\partial t} + \frac{\partial}{\partial x}\left(hu^2 + \frac{1}{2}gh^2\right) + \frac{\partial (huv)}{\partial y} + gh\frac{\partial b}{\partial x} - fv = 0, \\ \frac{\partial (hv)}{\partial t} + \frac{\partial (huv)}{\partial x} + \frac{\partial}{\partial y}\left(hv^2 + \frac{1}{2}gh^2\right) + gh\frac{\partial b}{\partial y} + fu = 0, \end{cases} \tag{1.2}$$

où (x,y) et t correspondent respectivement aux coordonnées cartésiennes horizontales et au temps; h est la hauteur d'eau en (t,x,y) et ${}^{\top}(u,v)$ est le vecteur des vitesses horizontales moyennes sur la couche d'eau; g est l'accélération gravitationnelle, f est le paramètre de *Coriolis* et b est la topographie du fond océanique. Le modèle (1.2) est aussi nommé le modèle *shallow water*.
Les équations (1.2) ont été étudiées de manière exhaustive (voir par exemple [54] ou [100]). Il a été prouvé rigoureusement, dans [3] pour le cas irrotationnel et [26] pour le cas rotationnel, que (1.2) est un modèle asymptotique issu des équations d'*Euler*. Bien que les équations de *Saint-Venant* décrivent relativement bien le comportement moyen de notre système, il est impossible de l'utiliser pour détailler le comportement du fluide, dans la zone supérieure, entre 0m et 300m : la zone de mélange. Cette région de l'océan est cruciale dans la dynamique des mers. Il est donc nécessaire de revoir nos hypothèses afin d'améliorer le modèle (1.2) pour obtenir une description des océans plus précise.

Comme il est possible de le constater sur la figure 1.6, la zone de mélange est caractérisée par une variation de température, de salinité et de densité élevée. Afin de capturer le comportement de cette région, la densité n'est plus considérée constante mais constante par morceaux. Ainsi, notre système n'est plus un fluide homogène mais plusieurs couches homogènes, non-miscibles et superposées. Avec une hypothèse similaire à (1.1) pour chaque couche, un nouveau modèle peut être dérivé à partir des équations d'*Euler* : le modèle *Saint-Venant* multi-couches, aussi appelé *shallow water* multi-couches.

Si on considère une stratification en densité à $n > 1$ couches, les équations du nouveau modèle s'écrivent sous la forme suivante :

$$\forall i \in [\![1,n]\!], \begin{cases} \frac{\partial h_i}{\partial t} + \nabla\cdot(h_i \boldsymbol{u_i}) = 0, \\ \frac{\partial \boldsymbol{u_i}}{\partial t} + (\boldsymbol{u_i}\cdot\nabla)\boldsymbol{u_i} + \nabla P_i - f\boldsymbol{u_i}^{\perp} = 0, \end{cases} \tag{1.3}$$

où ρ_i est la densité de la couche i, h_i et $\boldsymbol{u_i} := {}^{\top}(u_i, v_i)$ sont respectivement la hauteur en (t,x,y) et le vecteur des vitesses horizontales moyennes, de cette couche. $\boldsymbol{u_i^{\perp}} := {}^{\top}(-v_i, u_i)$ est le vecteur orthogonal au vecteur vitesse, P_i est la pression à l'interface i, entre la couche i et la couche $i+1$, et a pour expression:

$$P_i := g\big(b + \sum_{k=1}^{n} \alpha_{i,k} h_k\big), \tag{1.4}$$

et les coefficients $\alpha_{i,k}$ sont les ratios de densité définis par :

$$\alpha_{i,k} = \begin{cases} \frac{\rho_k}{\rho_i}, & k < i \\ 1, & k \geq i. \end{cases} \tag{1.5}$$

Ce modèle généralise le modèle *shallow water* (1.2) et permet, *a priori*, de décrire le comportement de la zone de mélange. La dérivation de ce modèle est détaillée dans [125] et les propriétés d'ondes planes qui lui sont associées dans [126].

Les ondes associées à l'ensemble de l'épaisseur d'eau, *i.e.* à la surface libre, sont appelées barotropes. Celles associées aux interfaces internes sont nommées baroclines.

Bien que cela paraisse surprenant de premier abord, ce modèle est physique. En effet, les océans présentent réellement des couches de densité constante. Par exemple, l'eau de la mer Méditerranée est chaude, saline et plus dense que celle de l'océan Atlantique. Lorsque l'eau de la mer Méditerranée pénètre dans l'océan Atlantique, au niveau du détroit de Gibraltar, elle avance de plusieurs centaines de kilomètres dans l'Atlantique à une profondeur d'environ 1000 mètres, tout en conservant la température, la salinité et la densité qui la caractérisent (détaillé dans [40] et [68]). C'est à cette profondeur que l'eau de la Méditerranée se stabilise.
Le code HYCOM est un acronyme signifiant HYbrid Coordinate Ocean Model. Effectivement, le modèle implémenté dans HYCOM possède une définition de la coordonnée verticale qui est hybride:

- géopotentielle dans les couches de surface, *i.e.* elle suit les variations de hauteur,
- sigma par petits fonds, *i.e.* elle suit les variations de bathymétrie,
- isopycnale dans l'océan intérieure, *i.e.* elle suit les variations de densité.

L'intérêt d'un tel choix de coordonnée verticale est multiple. Tout d'abord, la coordonnée géopotentielle permet de discrétiser précisément la couche de mélange. Celle en sigma permet d'augmenter la résolution près du fond. La coordonnée isopycnale est à la fois une coordonnée naturelle pour la dynamique tourbillonnaire et permet de préserver les caractéristiques des masses d'eau intermédiaires et profondes. Elle permet de ne pas avoir de mélange induit par des imprécisions

numériques. De plus, la grille de calcul peut être adaptée à chaque instant à la configuration de la zone et aux phénomènes physiques. La coordonnée verticale hybride permet aussi de gérer une bathymétrie à fort gradient sans générer d'instabilités, comme par exemple sur le talus océanique au large du Golfe de Gascogne. Ce choix implique aussi des limitations. En effet, la coordonnée hybride nécessite de définir des densités cibles dont le paramétrage peut être délicat pour certains processus. Elle exige aussi des schémas numériques sophistiqués et coûteux en temps de calcul. Pour plus de détails sur le code HYCOM, se reporter à [31].

Dans ce manuscrit, nous nous focalisons sur le modèle de *Saint-Venant* multi-couches à surface libre. Ce système d'équations aux dérivées partielles (1.3), quasi-linéaire et du 1er ordre, correspond exactement au modèle associé à la coordonnée isopycnale du code HYCOM. Il a été étudié, dans un premier temps, dans des cas simplifiés. Le cas le plus simple, sans revenir au modèle à une couche (1.2), est le modèle bi-couche à toit rigide, *i.e.* la hauteur totale du système de fluides est supposée constante. Ce cas simple est étudié dans [80]. Le cas bi-couches à surface libre, quant à lui, est analysé dans [114], [97] et [79]. Dans le cas irrotationnel, il a été prouvé rigoureusement dans [41] que (1.3) avec $n = 2$ est un modèle asymptotique issu des équations d'*Euler*.

Une propriété fondamentale pour les modèles tel que (1.3) est l'hyperbolicité. Un tel système est hyperbolique lorsque l'opérateur différentiel en espace, associé à ce modèle, n'a que des valeurs propres réelles. L'hyperbolicité de (1.3) a été étudié dans des cas particuliers. Le cas du bi-couches est identifié depuis les études récentes de [27]. Pour 3 couches, dans [127], l'hyperbolicité est étudié numériquement, alors que dans [50], elle est analysée formellement. Dans [5], un cas légèrement différent est abordé : des termes d'échanges entre les couches sont ajoutés.

1.2.2 Analyse du modèle de *Saint-Venant*

Pour le traitement des conditions limites, il est nécessaire d'analyser méticuleusement le modèle. Dans cette section, nous considérons, tout d'abord, le modèle (1.2) linéarisé autour de l'état constant $\mathbf{u_0} := {}^{\top}(h_0, {}^{\top}\boldsymbol{u_0}) \in \mathbb{R}_+^* \times \mathbb{R}^2$. Puis nous considérons le modèle (1.2), dans le cas non-linéaire .

Le modèle linéaire

Les nouvelles variables sont : l'élévation de surface $\eta := h - h_0$ et les variations de vitesse dans chaque direction $\tilde{u} := u - u_0$ et $\tilde{v} := v - v_0$ (avec $\boldsymbol{u_0} := {}^{\top}(u_0, v_0)$). Ces quantités vérifient le système

suivant :

$$\frac{\partial \tilde{\mathbf{u}}}{\partial t} + \mathsf{A}_x^{sw}(\mathbf{u_0})\frac{\partial \tilde{\mathbf{u}}}{\partial x} + \mathsf{A}_y^{sw}(\mathbf{u_0})\frac{\partial \tilde{\mathbf{u}}}{\partial y} + \mathsf{C}^{sw}\tilde{\mathbf{u}} = 0 \tag{1.6}$$

où le vecteur des inconnues, $\tilde{\mathbf{u}}$, est défini par :

$$\tilde{\mathbf{u}} := {}^{\top}(\eta, \tilde{u}, \tilde{v}), \tag{1.7}$$

et $\mathsf{A}_x^{sw}(\mathbf{u_0})$, $\mathsf{A}_y^{sw}(\mathbf{u_0})$ et C^{sw} sont des matrices 3×3 définies par :

$$\mathsf{A}_x^{sw}(\mathbf{u_0}) := \begin{bmatrix} u_0 & h_0 & 0 \\ g & u_0 & 0 \\ 0 & 0 & u_0 \end{bmatrix},\ \mathsf{A}_x^{sw}(\mathbf{u_0}) := \begin{bmatrix} v_0 & 0 & h_0 \\ 0 & v_0 & 0 \\ g & 0 & v_0 \end{bmatrix},\ \mathsf{C}^{sw} := \begin{bmatrix} 0 & 0 & 0 \\ 0 & 0 & -f \\ 0 & f & 0 \end{bmatrix}. \tag{1.8}$$

Nous rappelons quelques éléments de théorie des ondes nécessaires pour la suite (voir [69] pour plus de détails). Considérons une frontière dont la normale sortante est $\mathbf{n} := {}^{\top}(\cos(\theta), \sin(\theta))$, avec $\theta \in [0, 2\pi]$. Pour le traitement des conditions limites ouvertes, il est crucial d'étudier la diagonalisatbilité, dans $\mathcal{M}_3(\mathbb{R})$, de la matrice :

$$\mathsf{A}^{sw}(\mathbf{u_0}, \theta) := \mathsf{A}_x^{sw}(\mathbf{u_0})\cos(\theta) + \mathsf{A}_x^{sw}(\mathbf{u_0})\sin(\theta). \tag{1.9}$$

Après analyse, cette matrice est toujours diagonalisable dans $\mathcal{M}_3(\mathbb{R})$. En notant $(\,\cdot\,)$ le produit scalaire canonique de $\mathbb{R}^2$, les valeurs propres sont :

$$\begin{cases} \lambda_1^-(\mathbf{u_0}, \theta) & := (\boldsymbol{u_0}\cdot\mathbf{n}) - \sqrt{gh_0}, \\ \lambda_2(\mathbf{u_0}, \theta) & := (\boldsymbol{u_0}\cdot\mathbf{n}), \\ \lambda_1^+(\mathbf{u_0}, \theta) & := (\boldsymbol{u_0}\cdot\mathbf{n}) + \sqrt{gh_0}, \end{cases} \tag{1.10}$$

et les vecteurs propres, à gauche, sont :

$$\begin{cases} \boldsymbol{l}^{\lambda_1^-}(\mathbf{u_0}, \theta) & := (-\sqrt{\frac{g}{h_0}}, \cos(\theta), \sin(\theta)), \\ \boldsymbol{l}^{\lambda_2}(\mathbf{u_0}, \theta) & := (0, \sin(\theta), -\cos(\theta)), \\ \boldsymbol{l}^{\lambda_1^+}(\mathbf{u_0}, \theta) & := (\sqrt{\frac{g}{h_0}}, \cos(\theta), \sin(\theta)), \end{cases} \tag{1.11}$$

Pour chaque valeur propre λ, les invariants de *Riemann* r_λ, s'ils existent, sont définis par :

$$\exists \alpha > 0,\ ({}^{\top}\boldsymbol{l}^{\lambda}\cdot\frac{\partial \tilde{\mathbf{u}}}{\partial t}) = \alpha\frac{\partial r_\lambda}{\partial t}. \tag{1.12}$$

Ces quantités sont aussi appelées les variables caractéristiques et vérifient l'équation suivante :

$$\frac{\partial r_\lambda}{\partial t} + \lambda(\mathbf{u_0}, \theta)\frac{\partial r_\lambda}{\partial \mathbf{n}} + ({}^{\top}\boldsymbol{l}^{\lambda}(\mathbf{u_0}, \theta)\cdot\mathsf{C}^{sw}\tilde{u}) = 0. \tag{1.13}$$

De plus, dans le cas homogène, *i.e.* sans terme source, l'invariant de *Riemann* r_λ est constant le long d'une courbe particulière, appelée courbe caractéristique, définie par :

$$\frac{ds}{dt} = \lambda(\mathbf{u_0}, \theta). \tag{1.14}$$

Dans le cas présent d'un système linéaire, les caractéristiques sont des droites affines. Pour le modèle de *Saint-Venant* linéarisé, ces quantités existent toujours et sont alors égales à :

$$\begin{cases} r_{\lambda_1^-}(\mathbf{u_0}, \tilde{\mathbf{u}}, \theta) & := (\tilde{\boldsymbol{u}} \cdot \mathbf{n}) - \sqrt{\frac{g}{h_0}}\eta, \\ r_{\lambda_2}(\mathbf{u_0}, \tilde{\mathbf{u}}, \theta) & := (\tilde{\boldsymbol{u}} \cdot \mathbf{n}), \\ r_{\lambda_1^+}(\mathbf{u_0}, \tilde{\mathbf{u}}, \theta) & := (\tilde{\boldsymbol{u}} \cdot \mathbf{n}) + \sqrt{\frac{g}{h_0}}\eta, \end{cases} \tag{1.15}$$

avec $\tilde{\boldsymbol{u}} := {}^\top(\tilde{u}, \tilde{v})$.

De plus, comme nous le verrons ultérieurement, il est important, pour les conditions limites, de connaître le signe des valeurs propres. Le régime est alors caractérisé de la manière suivante :

- sous-critique si $\lambda_1^-(\mathbf{u}, \theta) < 0$ et super-critique sinon,
- entrant si $\lambda_2(\mathbf{u}, \theta) < 0$ et sortant sinon.

Sachant que les inégalités suivantes sont toujours vérifiées :

$$\lambda_1^-(\mathbf{u_0}, \theta) < \lambda_2(\mathbf{u_0}, \theta) < \lambda_1^+(\mathbf{u_0}, \theta), \tag{1.16}$$

le régime considéré permet de connaître exactement le signe des valeurs propres.

Le modèle non-linéaire

Dans le cas non-linéaire, il est naturel de se demander si le système (1.2) possède des courbes caractéristiques et des invariants de *Riemann*. Tout d'abord, nous décrivons le modèle de *Saint)Venant* de la manière suivante, dans le cas d'une topographie constante :

$$\frac{\partial \mathbf{u}}{\partial t} + \mathsf{A}_x^{sw}(\mathbf{u})\frac{\partial \mathbf{u}}{\partial x} + \mathsf{A}_y^{sw}(\mathbf{u})\frac{\partial \mathbf{u}}{\partial y} + \mathsf{C}^{sw}\tilde{\mathbf{u}} = 0 \tag{1.17}$$

où le vecteur des inconnues, $\mathbf{u}$, est défini par :

$$\mathbf{u} := {}^\top(h, u, v), \tag{1.18}$$

Les valeurs propres de la matrice $\mathsf{A}^{sw}(\mathbf{u}, \theta)$ sont alors toujours réelles et définies par :

$$\begin{cases} \lambda_1^-(\mathbf{u}, \theta) & := (\boldsymbol{u} \cdot \mathbf{n}) - \sqrt{gh}, \\ \lambda_2(\mathbf{u}, \theta) & := (\boldsymbol{u} \cdot \mathbf{n}), \\ \lambda_1^+(\mathbf{u}, \theta) & := (\boldsymbol{u} \cdot \mathbf{n}) + \sqrt{gh}, \end{cases} \tag{1.19}$$

Les vecteurs propres à gauche associés sont alors :

$$\begin{cases} \boldsymbol{l}^{\lambda_1^-}(\mathbf{u},\theta) & := (-\sqrt{\frac{g}{h}},\cos(\theta),\sin(\theta)), \\ \boldsymbol{l}^{\lambda_2}(\mathbf{u},\theta) & := (0,\sin(\theta),-\cos(\theta)), \\ \boldsymbol{l}^{\lambda_1^+}(\mathbf{u},\theta) & := (\sqrt{\frac{g}{h}},\cos(\theta),\sin(\theta)), \end{cases} \tag{1.20}$$

Enfin, les invariants de *Riemann* existent toujours, dans le cas non-linéaire, et sont définis par

$$\begin{cases} r_{\lambda_1^-}(\mathbf{u},\theta) & := (\boldsymbol{u}\cdot\mathbf{n}) - 2\sqrt{gh}, \\ r_{\lambda_2}(\mathbf{u},\theta) & := (\boldsymbol{u}\cdot\mathbf{n}), \\ r_{\lambda_1^+}(\mathbf{u},\theta) & := (\boldsymbol{u}\cdot\mathbf{n}) + 2\sqrt{gh}, \end{cases} \tag{1.21}$$

avec $\boldsymbol{u} := {}^{\top}(u,v)$. Enfin, chaque courbe caractéristique est toujours une droite affine, mais dont le coefficient directeur varie en fonction de la valeur propre correspondante au temps initial.

1.2.3 Le traitement des conditions limites

Les zones océaniques les plus intéressantes sont proches des côtes. La précision de la prévision marine doit y être d'autant plus grande. De plus, la puissance de calcul actuelle est élevée mais reste finie. Il faut donc faire des choix et il n'est pas possible de prédire le comportement de l'ensemble des océans mondiaux avec une précision infinie. Ce sont ces principales raisons qui imposent d'implémenter un maillage raffiné proche des continents et de ne calculer l'évolution de l'océan que sur une partie finie et restreinte de celui-ci. Ce domaine est noté par la suite $\mathcal{D}$. Il y a par conséquent deux types de conditions limites, au bord du domaine considéré :

- des conditions de non-perméabilité au niveau côtier,
- des conditions ouvertes au niveau hauturier.

Les conditions ouvertes sont au cœur de notre analyse. La difficulté est de prescrire des conditions, au bord du domaine, afin de minimiser l'erreur induite. Il est vrai que le calcul des points intérieurs du domaine $\mathcal{D}$ nécessitent les valeurs des points directement autour. Il ressort alors un problème : au bord du domaine, il manque certains points voisins. Il est donc nécessaire de prescrire ces valeurs pour obtenir une prédiction cohérente.

Il existe plusieurs techniques pour le traitement des conditions limites ouvertes, pour les écoulements marins. Les difficultés du problème aux limites sont de trouver et de démontrer la pertinence des conditions limites. De plus, il est nécessaire qu'elles puissent être implémentées simplement dans un code de calcul, qu'elles ne nécessitent pas un grand nombre d'opérations et qu'elles aient une

signification intrinsèque au modèle considéré. Dans la littérature, il est possible de référencer ces méthodes ainsi :

- ◇ radiative,
- ◇ absorbante,
- ◇ de relaxation,
- ◇ des caractéristiques.

Nous décrivons ces différentes méthodes ci-dessous, en s'inspirant de [14]. Dans la suite, nous considérons le modèle de *Saint-Venant* linéarisé (1.17) et une frontière particulière : une frontière Est, dont la normale sortante est égale à $\mathbf{n} := {}^{\top}(1,0)$, *i.e.* $\theta = 0$.

La méthode radiative

Après avoir étudié la théorie de la diffraction optique, en 1896 dans [119], et la propagation des ondes radio, en 1909 dans [120], *A. Sommerfeld* exprime une méthode pour traiter les conditions limites ouvertes, d'abord dans [121] puis plus tard dans [122]. Elle est basée sur l'équation suivante :

$$\frac{\partial \phi}{\partial t} + c\frac{\partial \phi}{\partial \boldsymbol{n}} = 0, \tag{1.22}$$

qui correspond au transport de la quantité ϕ, à la vitesse c et à travers la frontière $\partial\mathcal{D}$ ($\boldsymbol{n}$ est le vecteur normal à $\partial\mathcal{D}$, dirigé vers l'extérieur). Pour plus de détails sur cette méthode, nous nous reportons à [115], ainsi qu'aux références qui y sont présentes. Pour les problèmes non-linéaires, l'implémentation numérique de la condition (1.22) nécessite une évaluation adaptative de c : la vitesse de propagation. Dans [96], une première technique est proposée. Puis d'autres dérivations suivent, prenant en compte la dérivée tangentielle et avec le rajout d'un terme de relaxation (se référer à [24], [87], [107], [7] et [81]).

Bien que ces méthodes radiatives sont répandues dans la communauté océanographique, l'efficacité pour des fluides complexes n'est pas évidente. Plusieurs études montrent qu'elle induit une erreur non-négligeable et que le calcul de c est problématique (voir [111], [98], [94], [134] et [46]). La raison première de ce manque d'efficacité est dû au fait que la condition de *Sommerfeld* (1.22) n'est valable que pour une équation d'onde à vitesse de propagation constante. Pourtant, les méthodes de radiation sont communément utilisées dans les simulations numériques océaniques. Elles possèdent une apparente efficacité grâce aux données extérieures $\phi = \phi_{ext}$ (voir [134], [25] et [103]).

La méthode absorbante

Cette méthode est introduite dans [47] et qui est exactement satisfaite par les quantités sortantes du domaine. Cependant, c'est une méthode globale en temps et en espace. Elle est donc difficile de l'implémenter et elle doit être approchée pour devenir une condition locale.

Avec le rappel fait précédemment sur les invariants de *Riemann*, on peut alors expliciter l'approximation des conditions absorbantes. Une estimation au 1$^{\text{er}}$ ordre de ces conditions est :

$$\begin{cases} r_{\lambda_1^-} = 0, & \text{si } u_0 > 0, \\ r_{\lambda_1^-} = r_{\lambda_2} = 0, & \text{si } u_0 < 0. \end{cases} \tag{1.23}$$

Alors qu'une estimation au 2$^{\text{nd}}$ ordre est :

$$\begin{cases} \frac{\partial r_{\lambda_1^-}}{\partial t} + u_0 \frac{\partial \tilde{v}}{\partial y} - \frac{u_0}{\sqrt{gh_0}} f \tilde{v} = 0, & \text{si } u_0 > 0, \\ \begin{cases} \frac{\partial r_{\lambda_1^-}}{\partial t} - \frac{u_0+\sqrt{gh_0}}{2} \frac{\partial \tilde{v}}{\partial y} = 0, \\ \frac{\partial \tilde{v}}{\partial t} - v_0 \frac{u_0-\sqrt{2}(u_0+\sqrt{gh_0})}{\sqrt{2gh_0}} \frac{\partial \tilde{v}}{\partial y} + \frac{u_0+\sqrt{gh_0}}{2} \frac{\partial r_{\lambda_1^+}}{\partial y} + f \frac{u_0+\sqrt{gh_0}}{2\sqrt{gh_0}} r_{\lambda_1^+} = 0, \end{cases} & \text{si } u_0 < 0. \end{cases} \tag{1.24}$$

Il est alors possible de résumer ces conditions (1.23) ou (1.24) dans un opérateur différentiel B défini par :

$$\mathsf{B}\tilde{\mathbf{u}} = 0. \tag{1.25}$$

Alors, les données extérieures, juste au-delà de la frontière, permettent d'améliorer les résultats obtenus avec les conditions absorbantes (voir [94]). Les nouvelles conditions limites deviennent alors :

$$\mathsf{B}\tilde{\mathbf{u}} = \mathsf{B}\tilde{\mathbf{u}}_{ext}. \tag{1.26}$$

La méthode de relaxation

Cette méthode a pour objectif de relaxer la solution $\mathbf{u}$, vers une donnée extérieure $\mathbf{u}_{ext}$. Une manière brutale de le faire est d'imposer une condition de *Dirichlet* à la frontière $\partial\mathcal{D}$:

$$\mathbf{u} = \mathbf{u}_{ext}. \tag{1.27}$$

Cependant, avec une telle condition limite, la valeur de $\mathbf{u}$ à la frontière ne dépend que de la donnée extérieure $\mathbf{u}_{ext}$. La solution à l'intérieur du domaine ne l"influence pas du tout. Par conséquent, une onde sortante du domaine va être partiellement réfléchie, dès que la donnée extérieure n'est pas parfaitement consistante avec la dynamique intérieure.

La méthode de relaxation permet de résoudre ce problème et est initialement proposé dans [39]. Le principe est de rajouter une *couche éponge* $\mathcal{D}_{ce}$, tout autour du domaine $\mathcal{D}$. Le modèle est alors résolu

sur l'ensemble des domaines $\mathcal{D} \cup \mathcal{D}_{ce}$. Et à chaque pas de temps, la solution dans $\mathcal{D}_{ce}$ est remplacée par la quantité :

$$(1-r)\mathbf{u} + r\mathbf{u}_{ext}, \tag{1.28}$$

où r est une fonction de relaxation : elle augmente de 0 à 1, de la frontière $\partial\mathcal{D}$ à la frontière extérieure de $\mathcal{D} \cup \mathcal{D}_{ce}$. Si la *couche éponge* $\mathcal{D}_{ce}$ est assez grande, la transition de $\mathbf{u}$ à $\mathbf{u}_{ext}$ est douce et les résultats obtenus sont satisfaisants (*cf* [111], [98] et [94]).

Dans [82], il est prouvé que la solution approchée par cette méthode revient à rajouter un terme source aux équations de départ, de la forme :

$$K(\mathbf{u} - \mathbf{u}_{ext}) \tag{1.29}$$

où K est une fonction positive qui dépend de la fonction r et du schéma numérique utilisé.
Cependant, les principaux inconvénients de cette méthode sont :

- la nécessité de calculer la solution approchée sur un domaine $\mathcal{D}_{ce}$ qui sera inexploitable,
- la signification de la solution continue dans la couche éponge n'est pas évidente.

Enfin, [13] propose une amélioration de la méthode de relaxation, appliquée aux modèles d'électromagnétisme. Ce perfectionnement est appelé méthode PML, pour *perfectly matched layer*, et est basée sur une combinaison bien choisie d'un *splitting* des équations et d'ajouts de termes de relaxation. La technique PML a été appliquée aux équations d'*Euler*, dans [61] et [62], et aux équations *Saint-Venant*, dans [37] et [92].

La méthode des caractéristiques

Dans [58], une condition limite parfaitement non-réfléchissante pour un problème hyperbolique homogène non-linéaire. Cette condition impose une dérivée temporelle nulle à tous les invariants de *Riemann* rentrants :

$$\frac{\partial r_\lambda}{\partial t} = 0, \text{ si } \lambda < 0. \tag{1.30}$$

Dans le cas non-linéaire, une équation similaire à (1.13) est vérifiée pour chaque invariant de *Riemann*. La condition (1.30) implique donc :

$$\lambda \frac{\partial r_\lambda}{\partial \mathbf{n}} = 0, \text{ si } \lambda < 0. \tag{1.31}$$

Cette dernière condition possède une interprétation simple. Il a été expliqué ci-dessus que les invariants de *Riemann* sont des quantités conservées le long de courbes particulières : les courbes caractéristiques. Pour calculer l'approximation de $\mathbf{u}$ à un temps t_{n+1} et en un point (x,y), intérieur du domaine $\mathcal{D}$, l'approximation de $\mathbf{u}$, au temps précédent t_n et en un point voisin à (x,y), sera nécessaire.

Ce point voisin sera bien dans le domaine $\mathcal{D}$ et dépendra de la courbe caractéristique. Supposons maintenant le point (x,y) au bord du domaine $\mathcal{D}$. Si l'invariant de *Riemann* est sortant, il n'y aura pas de problème pour calculer l'approximation au temps t_{n+1}. Par contre, s'il est entrant, il serait nécessaire de connaître la valeur approchée de $\mathbf{u}$ juste au-delà de la frontière $\partial\mathcal{D}$. Le modèle seul ne peut pas évaluer une telle valeur. D'où la nécessité d'imposer une conditions limite telle que (1.31).
Cette approche a été utilisé dans [55] et comparé aux méthodes précédemment présentées dans [111], [64] et [98]. Elle a aussi été appliquée dans le cadre des équations d'*Euler* et de *Navier-Stokes*, avec des résultats probants (voir [106], [22] et [23]). Enfin, un moyen d'améliorer cette méthode est encore d'utiliser les données extérieures en imposant :

$$\lambda\frac{\partial r_\lambda}{\partial \mathbf{n}} = \lambda\frac{\partial r_\lambda^{ext}}{\partial \mathbf{n}},\ \text{si}\ \lambda < 0. \tag{1.32}$$

Pour le modèle *shallow water*, les conditions limites les plus populaires ont été introduites par *R.A. Flather*, dans [49], et se présente sous la forme suivant :

$$(\tilde{\boldsymbol{u}}\cdot\mathbf{n}) - \sqrt{\frac{g}{h_0}}\eta = (\tilde{\boldsymbol{u}}_{ext}\cdot\mathbf{n}) - \sqrt{\frac{g}{h_0}}\eta_{ext}. \tag{1.33}$$

Cette condition (1.33), dite de *Flather*, peut être obtenue à partir de l'équation de *Sommerfeld* (1.22). Elle a été étudiée dans [98], [81] et [94] et est l'une des plus efficaces conditions limites. Cependant, il est plus naturelle de voir la formulation (1.33) non pas comme un condition radiative mais comme issue de la méthode des caractéristiques. En effet, dans le cas du modèle *shallow water* linéarisé, la condition (1.33) est exactement la condition (1.32), dans le cas d'un régime sous-critique rentrant (détails dans [21] et [20]).
Cette méthode apparaît donc efficace. Par conséquent, il serait intéressant de la développer pour le modèle *shallow water* multi-couches (1.3).

Les codes de calcul combinent ces différentes méthodes pour prescrire les conditions limites au niveau des frontières artificielles. Dans HYCOM, les conditions limites ont les caractéristiques suivantes :

- les modes barotropes et baroclines sont traités séparément,
- une condition type *Flather* est appliquée aux modes barotropes,
- une condition de relaxation est appliquée aux modes baroclines,
- pas de distinction entre régime entrant et sortant.

Comme nous l'avons présenté ci-dessus, il serait intéressant de caractériser des conditions limites liées intrinsèquement au modèle et prenant en compte les différents régimes.

1.3 Objectifs et plan de la thèse

Les prédictions océaniques sont un des enjeux scientifiques majeurs de ce début de siècle. Les récents tsunamis et tempêtes en sont la preuve. Il est donc nécessaire de continuer d'améliorer les résolutions approchées des océans, effectuées par les codes de calculs.

Dans la partie précédente, la présentation des différentes méthodes de traitement des conditions limites ouvertes a permis de mettre en exergue la pertinence de la méthode des caractéristiques. D'une part, cette méthode possède une justification intrinsèque au modèle. D'autre part, il est possible de l'implémenter facilement dans un code numérique. Enfin, à la différence de la méthode de relaxation, elle évite de calculer de manière superficielle une solution approchée sur un domaine qui restera inexploitable.

Pour améliorer les prédictions marines, le SHOM a besoin d'avoir un code de calcul performant. Le traitement des conditions limites est donc un point clé qu'il est nécessaire de perfectionner. Les objectifs principaux de cette thèse sont :

- ◇ caractériser l'hyperbolicité du modèle *Saint-Venant* multi-couches,
- ◇ déterminer les conditions limites à prescrire aux frontières ouvertes, pour ce modèle,
- ◇ valider ces conditions limites numériquement.

De plus, les problèmes rencontrés par le SHOM sont à deux dimensions, il n'est donc pas envisageable de se placer dans un cas à une dimension. De même, nous ne pouvons pas considérer un problème irrotationnel. Il faut ainsi développer des conditions limites valables pour tous types de

frontières et tous types de régimes.

Cependant, comme nous l'avons présenté précédemment, HYCOM est basé sur une coordonnée verticale hybride. Nous restreignons donc notre étude au cas de la coordonnée isopycnale. Ce manuscrit se divise en 3 parties :

- Partie I : Étude de l'hyperbolicité du modèle bi-couches, ainsi que le caractère localement bien-posé de ce modèle; introduction d'un nouveau modèle conservatif; comparaison des deux modèles,
- Partie II : Analyse de l'hyperbolicité du modèle général à n couches, ainsi que le caractère localement bien-posé de ce modèle; généralisation du nouveau modèle conservatif, introduit dans la partie I, à n couches; comparaison des deux modèles multi-couches,
- Partie III : Validation numérique des conditions limites dérivées des résultats obtenus en partie II. Les calculs seront effectués pour 2 cas tests : une onde de gravité et un vortex barotrope; et 3 modèles sont considérés : 1, 2 et 4 couches (comme synthétisé dans le tableau 1.1).

	1 couche	**2 couches**	**4 couches**
Cas test 1	✓ linéaire ✓ non-linéaire	✓ linéaire ✓ non-linéaire	✓ linéaire ✓ non-linéaire
Cas test 2	✓ linéaire ✓ non-linéaire	✓ linéaire ✓ non-linéaire	✓ linéaire ✓ non-linéaire

Table 1.1: Plan de validation numérique des conditions limites.

Les modèles linéaires ne seront pas exactement les modèles linéarisés des modèles de *Saint-Venant* multi-couches car le terme source associé à la force de *Coriolis* sera légèrement modifiée. Cependant, ils permettront une validation de la méthode utilisé, augmentée de la vorticité, car ces modèles linéaires possèdent certaines solutions analytiques non-triviales, associées à la condition initiale 2. De plus, le cas test 1 permettra de valider les conditions limites dans un cas tests simple et rapide d'exécution.

La première partie de ce manuscrit a été publiée dans le journal international à comité de lecture : *SIAM Journal on Appliad Mathematics* en 2015 (lien). La seconde partie a aussi été soumise à publication dans un journal international à comité de lecture. Par conséquent, les articles n'ont pas été retouchés. De plus, le lecteur pourra consulter chacune des 3 parties principales de la thèse de façon indépendante : les prérequis nécessaires sont rappelés au début de chacune d'entre elles.

J'ouvre les yeux, et je vois la mer. Ce n'est pas la mer d'émeraude que je voyais autrefois, dans les lagons, ni l'eau noire devant l'estuaire de la rivière du Tamarin. C'est la mer comme je ne l'avais jamais vue encore, libre, sauvage, d'un bleu qui donne le vertige, la mer qui soulève la coque du navire, lentement, vague après vague, tachée d'écume, parcourue d'étincelles.

Le chercheur d'or, J.M.G. Le Clézio, 1985.

Figure 1.7: ”Danger : eau peu profonde” - Mars 2014 sur l’île de Kauai, Hawaii, U.S.A.

Part I

The two-layer model with free surface

Introduction

Dans cette partie, toute notre attention est portée sur le modèle bi-couches à surface libre. Quelques résultats connus sont à nouveau démontrés et de nombreux développements originaux sont prouvés. Le plan est le suivant :

- Premièrement, le modèle ainsi que les hypothèses supposées sont rappelées dans l'introduction. Une propriété, qui est à la base des développements de tous les résultats de ce chapitre, est justifiée : l'invariance par rotation. Cette caractéristique du modèle de *Saint-Venant* bi-couches à surface libre, et de nombreux autres modèles physiques, permet de réduire le problème à deux dimensions, à un problème à une dimension,
- Deuxièmement, les définitions d'hyperbolicité et de symétrisabilité sont rappelées, ainsi que leurs liens. Un critère de symétrisabilité du modèle bi-couches est alors déduit : il permet alors de vérifier l'existence de conditions initiales assurant l'hyperbolicité du modèle. Il est alors intéressant de savoir si ce critère est optimal ou s'il est possible d'en déduire un nouveau plus général,
- Troisièmement, l'ensemble des conditions initiales, permettant d'assurer l'hyperbolicité du modèle, est déterminé exactement. Une différence majeure apparaît, entre le cas à une dimension d'espace et à deux dimensions : il n'y a que dans le cas à une dimension que la différence de vitesse, entre les deux couches, ne doit pas être nécessairement bornée pour assurer l'hyperbolicité du modèle. De plus, la caractérisation du domaine d'hyperbolicité est implicite. Il est donc pertinent d'effectuer un développement asymptotique pour caractériser explicitement cet ensemble,
- Quatrièmement, le développement asymptotique du domaine d'hyperbolicité est effectué sous l'approximation de *Boussinesq* : le saut de densité, entre les deux couches, est supposé très faible. Sous cette hypothèse, il est aussi possible d'obtenir les développements asymptotiques des éléments propres de l'opérateur différentiel associé au modèle bi-couches. Il sera alors possible de démontrer le caractère localement bien-posé du problème bi-couches, sous condition initiale hyperbolique,

- Cinquièmement, un nouveau modèle bi-couches est introduit : le modèle augmenté de la vorticité. Ce modèle conserve les propriétés du modèle de*Saint-Venant* bi-couches initial, et possède un atout en plus : il est conservatif. Les développement asymptotiques, sous hypothèse de *Boussinesq*, prouvés pour le modèle non-augmenté, sont adaptés au modèle augmenté. Il est alors démontré le caractère localement bien-posé de ce nouveau modèle, ainsi que les liens entre les solutions de ces deux modèles,
- Enfin, la conclusion permet de souligner les résultats prouvés ainsi que les difficultés rencontrées lors de ce chapitre. Les différences entre le modèle de *Saint-Venant* bi-couches et multi-couches sont abordés.

Ce chapitre a été publié dans le journal international à comité de lecture : *SIAM Journal on Applied Mathematics* en 2015 (lien). Par conséquent, il n'a pas été retouché et est à lecture indépendante.

2

Local well-posedness of the two-layer shallow water model with free surface

Contents

2.1 Introduction

We consider two immiscible, homogeneous, inviscid and incompressible superposed fluids, with no surface tension; the pressure is assumed to be hydrostatic, constant at the free surface and continuous at the internal surface. Moreover, the shallow water assumption is considered: there exist vertical and horizontal characteristic lengths and the vertical one is assumed much smaller than the horizontal one.

For more details on the derivation of these equations, see [113], [100] and [54] for the one-layer model; [80] for the two-layer model with rigid lid; [114], [97] and [79] for the two-layer model with free surface. In the *curl*-free case, these models have been rigorously obtained as an asymptotic model of the three-dimensional *Euler* equations, under the shallow water assumption, in [3] for the one-layer model with free surface and in [41] for the two-layer one. With no assumption on the vorticity, it has been obtained, only in the one layer case, in [26].

The aim of this paper is to obtain criteria of symmetrizability and hyperbolicity of the two-layer shallow water model, in order to insure the local well-posedness of the associated initial-value problem. Moreover, the hyperbolicity and local well-posedness are also proved for a new *conservative* two-layer shallow water model.

Outline: In this section, the model is introduced. In the 2nd one, useful definitions are reminded and a sufficient condition of hyperbolicity and local well-posedness in $\mathcal{H}^s(\mathbb{R}^2)$, is given. In the 3rd section, the hyperbolicity of the model is exactly characterized in one and two dimensions. In the 4th one, asymptotic analysis is performed, in order to deduce a new criterion of local well-posedness in $\mathcal{H}^s(\mathbb{R}^2)$. Finally, in the last section, after reminding the horizontal vorticity, a new model is introduced: benefits of this model are explained, local well-posedness, in $\mathcal{H}^s(\mathbb{R}^2)$, is proved and links, with the two-layer shallow water model, are justified.

2.1.1 Governing equations

The i^{th} layer of fluid, $i \in \{1,2\}$, has a constant density ρ_i, a depth-averaged horizontal velocity $\boldsymbol{u_i}(t,X) := {}^{\top}(u_i(t,X), v_i(t,X))$ and a thickness designated by $h_i(t,X)$, where t denotes the time and $X := (x,y)$ the horizontal cartesian coordinates, as drawn in figure 2.1.

The governing equations of the two-layer shallow water model with free surface are given by one mass conservation for each layer:

$$\frac{\partial h_i}{\partial t} + \nabla\cdot(h_i \boldsymbol{u_i}) = 0,\ i \in \{1,2\}, \tag{2.1}$$

and an equation on the depth-averaged horizontal velocity in each layer:

$$\frac{\partial \boldsymbol{u_i}}{\partial t} + (\boldsymbol{u_i}\cdot\nabla)\boldsymbol{u_i} + \nabla P_i - f\boldsymbol{u_i}^{\perp} = 0,\ i \in \{1,2\}, \tag{2.2}$$

where $\boldsymbol{u_i^{\perp}} := {}^{\top}(v_i, -u_i)$, $P_i := g\left(b + \sum_{k=1}^{2} \alpha_{i,k} h_k\right)$ is the fluid pressure, with g the gravitational acceleration, b the bottom topography, f the *Coriolis* parameter and $(\alpha_{i,k})_{(i,k)\in[\![1,n]\!]}$ given by

$$\alpha_{i,k} = \begin{cases} \frac{\rho_1}{\rho_2}, & \text{if } k = i-1 = 1, \\ 1, & \text{otherwise.} \end{cases}$$

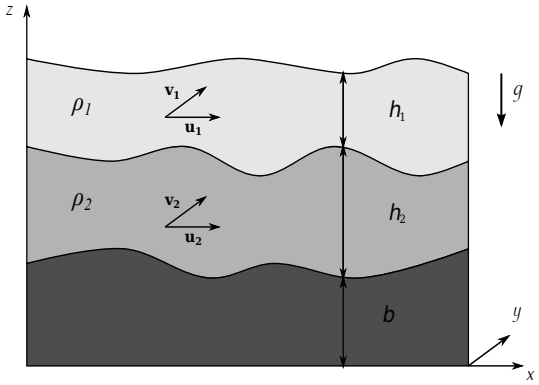

Figure 2.1: Configuration of the two-layer shallow water model with free surface

The multi-layer shallow water model with free surface describes fluids such as the ocean: the evolution of the density can be assumed piecewise-constant, the horizontal characteristic length is much greater than the vertical one and the pressure can be expected only dependent of the height of fluid. The two-layer model is a simplified case, where we consider the density has only two values. This model describes well the straits of *Gibraltar*, where the Mediterranean sea meets the Atlantic ocean. By introducing the vector

$$\mathbf{u} := {}^{\top}(h_1, h_2, u_1, u_2, v_1, v_2), \tag{2.3}$$

and $\gamma := \frac{\rho_1}{\rho_2}$, the system (2.1-2.2) can be written as

$$\frac{\partial \mathbf{u}}{\partial t} + \mathsf{A}_x(\mathbf{u})\frac{\partial \mathbf{u}}{\partial x} + \mathsf{A}_y(\mathbf{u})\frac{\partial \mathbf{u}}{\partial y} + \mathbf{b}(\mathbf{u}) = 0, \tag{2.4}$$

where $\mathsf{A}_x(\mathbf{u})$, $\mathsf{A}_y(\mathbf{u})$ and $\mathbf{b}(\mathbf{u})$ are defined by

$$\mathsf{A}_x(\mathbf{u}) := \begin{bmatrix} u_1 & 0 & h_1 & 0 & 0 & 0 \\ 0 & u_2 & 0 & h_2 & 0 & 0 \\ g & g & u_1 & 0 & 0 & 0 \\ \gamma g & g & 0 & u_2 & 0 & 0 \\ 0 & 0 & 0 & 0 & u_1 & 0 \\ 0 & 0 & 0 & 0 & 0 & u_2 \end{bmatrix}, \; \mathsf{A}_y(\mathbf{u}) := \begin{bmatrix} v_1 & 0 & 0 & 0 & h_1 & 0 \\ 0 & v_2 & 0 & 0 & 0 & h_2 \\ 0 & 0 & v_1 & 0 & 0 & 0 \\ 0 & 0 & 0 & v_2 & 0 & 0 \\ g & g & 0 & 0 & v_1 & 0 \\ \gamma g & g & 0 & 0 & 0 & v_2 \end{bmatrix}, \tag{2.5}$$

$$\mathbf{b}(\mathbf{u}) := {}^{\top}\left(0, 0, -fv_1 + g\frac{\partial b}{\partial x}, -fv_2 + g\frac{\partial b}{\partial x}, fu_1 + g\frac{\partial b}{\partial y}, fu_2 + g\frac{\partial b}{\partial y}\right). \tag{2.6}$$

Remark: The two-layer shallow water model is expanded from the full *Euler* system. However, this last system is ill-posed in *Sobolev* spaces in the absence of surface tension, because of the so-called *Kelvin-Helmholtz* instabilities: this is proved in [71] for the two-layer model with rigid lid. As it will be proved in this article, the two-layer shallow water model with free surface is locally well-posed, even if there is no such stabilizing phenomena.

2.1.2 Rotational invariance

As the two-layer shallow water model with free surface is based on physical partial differential equations, it is predictable that it verifies the so-called rotational invariance:

$$\mathsf{A}(\mathbf{u},\theta) := \cos(\theta)\mathsf{A}_x(\mathbf{u}) + \sin(\theta)\mathsf{A}_y(\mathbf{u}) \tag{2.7}$$

depends only on the matrix A_x and the parameter θ. Indeed, there is the following relation:

$$\forall(\mathbf{u},\theta) \in \mathbb{R}^6 \times [0,2\pi],\ \mathsf{A}(\mathbf{u},\theta) = \mathsf{P}(\theta)^{-1}\mathsf{A}_x(\mathsf{P}(\theta)\mathbf{u})\,\mathsf{P}(\theta), \tag{2.8}$$

with

$$\mathsf{P}(\theta) := \begin{bmatrix} 1 & 0 & 0 & 0 & 0 & 0 \\ 0 & 1 & 0 & 0 & 0 & 0 \\ 0 & 0 & \cos(\theta) & 0 & \sin(\theta) & 0 \\ 0 & 0 & 0 & \cos(\theta) & 0 & \sin(\theta) \\ 0 & 0 & -\sin(\theta) & 0 & \cos(\theta) & 0 \\ 0 & 0 & 0 & -\sin(\theta) & 0 & \cos(\theta) \end{bmatrix}, \tag{2.9}$$

and an important point is $\mathsf{P}(\theta)^{-1} = {}^{\top}\mathsf{P}(\theta)$. The equality (2.8) will permit to simplify the analysis of $\mathsf{A}(\mathbf{u},\theta)$ to the analysis of $\mathsf{A}_x(\mathsf{P}(\theta)\mathbf{u})$ (see [132] for more details). This property has been also used in [93].

2.2 Well-posedness of the model: a first criterion

In this section, we remind useful criteria of hyperbolicity and local well-posedness in $\mathcal{H}^s(\mathbb{R}^2)$. Connections between each one will be given and a 1$^{\text{st}}$ criterion of local well-posedness of the model (2.4) will be deduced.

2.2.1 Hyperbolicity

First, we give the definition, a useful criterion of hyperbolicity and an important property of hyperbolic model. We will consider the euclidean space $\mathcal{L}^2(\mathbb{R}^2), \|\cdot\|_{\mathcal{L}^2})$.

Definition (Hyperbolicity) Let $\mathbf{u} : \mathbb{R}^2 \to \mathbb{R}^6$. The system *(2.4)* is hyperbolic if and only

$$\exists\, c > 0,\ \forall \theta \in [0, 2\pi],\ \sup_{\tau \in \mathbb{R}} \| \exp\left(-i\tau \mathsf{A}(\mathbf{u}, \theta)\right) \|_{\mathcal{L}^2} \leq c. \tag{2.10}$$

A useful criterion of hyperbolicity is in the next proposition.

Proposition 2.2.1 *Let* $\mathbf{u} : \mathbb{R}^2 \mapsto \mathbb{R}^6$. *The model* (2.4) *is hyperbolic if*

$$\forall \theta \in [0, 2\pi],\ \sigma(\mathsf{A}(\mathbf{u}, \theta)) \subset \mathbb{R}. \tag{2.11}$$

Proof See in [117].

Proposition 2.2.2 *Let* $\mathbf{u} : \mathbb{R}^2 \mapsto \mathbb{R}^6$ *a constant function. If the model* (2.4) *is hyperbolic, then the* Cauchy *problem, associated with the linear system*

$$\frac{\partial \mathbf{v}}{\partial t} + \mathsf{A}_x(\mathbf{u}) \frac{\partial \mathbf{v}}{\partial x} + \mathsf{A}_y(\mathbf{u}) \frac{\partial \mathbf{v}}{\partial y} = 0, \tag{2.12}$$

and the initial data $\mathbf{v^0} \in \mathcal{L}^2(\mathbb{R}^2)^6$, *is locally well-posed in* $\mathcal{L}^2(\mathbb{R}^2)$ *and the unique solution* $\mathbf{v}$ *is such that*

$$\begin{cases} \forall\, T > 0,\ \exists\, c_T > 0,\ \sup_{t \in [0,T]} \|\mathbf{v}(t)\|_{\mathcal{L}^2} \leq c_T \|\mathbf{v^0}\|_{\mathcal{L}^2}, \\ \mathbf{v} \in \mathcal{C}(\mathbb{R}_+; \mathcal{L}^2(\mathbb{R}^2))^6 \end{cases} \tag{2.13}$$

Remark: More details about the hyperbolicity in [117].

2.2.2 Symmetrizability

In order to prove the local well-posedness of the model (2.4), in $\mathcal{H}^s(\mathbb{R}^2)$, we give below a useful criteria.

Definition (Symmetrizability) Let $\mathbf{u} \in \mathcal{H}^s(\mathbb{R}^2)^6$. If there exists a $\mathcal{C}^\infty$ mapping $\mathsf{S} : \mathcal{H}^s(\mathbb{R}^2)^6 \times [0, 2\pi] \to \mathcal{M}_6(\mathbb{R})$ such that for all $\theta \in [0, 2\pi]$,

1. $\mathsf{S}(\mathbf{u}, \theta)$ is symmetric,
2. $\mathsf{S}(\mathbf{u}, \theta)$ is positive-definite,
3. $\mathsf{S}(\mathbf{u}, \theta)\mathsf{A}(\mathbf{u}, \theta)$ is symmetric,

then, the model *(2.4)* is said symmetrizable and the mapping S is called a symbolic-symmetrizer.

Proposition 2.2.3 *Let* $\mathbf{u^0} \in \mathcal{H}^s(\mathbb{R}^2)^6$. *If the model* (2.4) *is symmetrizable, then the* Cauchy *problem, associated with* (2.4) *and initial data* $\mathbf{u^0}$, *is locally well-posed in* $\mathcal{H}^s(\mathbb{R}^2)$, *with* $s > 2$. *Furthermore, there exists* $T > 0$ *such that the unique solution* $\mathbf{u}$ *verifies*

$$\begin{cases} \mathbf{u} \in \mathcal{C}^1([0,T] \times \mathbb{R}^2)^6, \\ \mathbf{u} \in \mathcal{C}([0,T]; \mathcal{H}^s(\mathbb{R}^2))^6 \cap \mathcal{C}^1([0,T]; \mathcal{H}^{s-1}(\mathbb{R}^2))^6. \end{cases} \tag{2.14}$$

Remark: The proof of the last proposition is in [12], for instance.

One the difficulties of the model (2.1–2.2) lies in the non-conservative terms of the depth-averaged horizontal vorticity equations: this is why we do not name it momentum conservations. Such a non-conservative model needs a new theory to define weak solutions and to resolve it numerically, as it explained in [36], [91] and [99]. However, some negative results have been shown, in [60] and more recently in [2], concerning the failure of the convergence of non-conservative schemes to weak solutions of conservative problems. Consequently, we are interested in founding a formulation of the equations with zero non-conservative terms. Using a change of variables, one can look for conservative forms. Surprisingly, in one spatial dimension, with the unknowns h_i and $q_i := h_i u_i$, the equations of the two-layer shallow water model with free surface are not conservative, while there are so with the unknowns h_i and u_i. In two spatial dimensions, as far as we know, there is no conservative unknowns. Consequently, we have kept the best unknows: h_i and u_i. *Remark*: We will give a way to avoid the necessity of conservative path, in the last part of this article.

As it was noticed in [117], if the model is conservative, there exists a natural symmetrizer: the hessian of the energy of the model. This energy is defined, modulo a constant, by:

$$e_1 := \frac{1}{2}\gamma h_1 \left(u_1^2 + g(h_1 + 2h_2)\right) + \frac{1}{2} h_2 \left(u_2^2 + g h_2\right). \tag{2.15}$$

As the model (2.1–2.2), in one dimension and variables (h_i, u_i), is conservative, it is straightforward the hessian of e_1 is a symmetrizer of the one-dimensional model. However, it is not anymore a symmetrizer with the non-conservative variables $(h_i, h_i u_i)$. This is why the analysis, in this paper, is performed with variables (h_i, u_i).

Remarks: 1) In all this paper, the parameter $s \in \mathbb{R}$ is assumed such that

$$s > 1 + \frac{d}{2}, \tag{2.16}$$

where $d := 2$ is the dimension. 2) The criterion (2.11) is a necessary and sufficient condition of hyperbolicity, whereas the symmetrizability is only a sufficient condition of local well-posedness in $\mathcal{H}^s(\mathbb{R}^2)$.

2.2.3 Connections between hyperbolicity and symmetrizability

In this subsection, we do not formulate all the connections between the hyperbolicity and the local well-posedness in $\mathcal{H}^s(\mathbb{R}^2)$ but only the useful ones for this paper.

Proposition 2.2.4 *If the model* (2.4) *is symmetrizable, then it is hyperbolic.*

Remark: See [12] or [117] for more details.

Proposition 2.2.5 *Let* $\mathbf{u^0} \in \mathcal{H}^s(\mathbb{R}^2)^6$ *such that the model is hyperbolic and*

$$\forall (X,\theta) \in \mathbb{R}^2 \times [0,2\pi], \text{ the matrix } \mathsf{A}(\mathbf{u^0}(X),\theta) \text{ is diagonalizable.} \tag{2.17}$$

Then, the model (2.4) *is symmetrizable and the unique solution verifies the conditions* (2.14).

Proof Let $\mu \in \sigma(\mathsf{A}(\mathbf{u^0},\theta))$, we denote $\mathsf{P}^\mu(\mathbf{u^0},\theta)$ the projection onto the μ-eigenspace of $\mathsf{A}(\mathbf{u^0},\theta)$. One can construct a symbolic symmetrizer:

$$\mathsf{S}_1(\mathbf{u^0},\theta) := \sum_{\mu \in \sigma(\mathsf{A}(\mathbf{u^0},\theta))} {}^{\top}\mathsf{P}^\mu(\mathbf{u^0},\theta)\mathsf{P}^\mu(\mathbf{u^0},\theta). \tag{2.18}$$

Then, $\mathsf{S}_1(\mathbf{u^0},\theta)$ verifies conditions of the proposition 2.2.3 because $\mathsf{A}(\mathbf{u^0},\theta)$ is diagonalizable and $\sigma(\mathsf{A}(\mathbf{u^0},\theta)) \subset \mathbb{R}$. Then, proposition 2.2.3 implies the local well-posedness of the model (2.4), in $\mathcal{H}^s(\mathbb{R}^2)$, and there exists $T > 0$ such that conditions (2.14) are verified.

To conclude, the analysis of the eigenstructure of $\mathsf{A}(\mathbf{u},\theta)$ is a crucial point, in order to provide its diagonalizability. Moreover, it provides also the characterization of the *Riemann* invariants (see [118]), which is an important benefit for numerical resolution.
Remark: This proposition was proved in [130], in the particular case of a strictly hyperbolic model (*i.e.* all the eigenvalues are real and distinct).

2.2.4 A criterion of symmetrizability of the two-layer shallow water model

According to the proposition 2.2.4, the symmetrizability implies the hyperbolicity. Then, we give a rough criterion of symmetrizability to insure the local well-posedness in $\mathcal{H}^s(\mathbb{R}^2)$ and $\mathcal{L}^2(\mathbb{R}^2)$.

Theorem 2.2.6 *Let* $\gamma \in]0,1[$ *and* $\mathbf{u^0} \in \mathcal{H}^s(\mathbb{R}^2)^6$ *such that*

$$\begin{cases} \inf_{X\in\mathbb{R}^2} h_1^0(X) > 0,\ \inf_{X\in\mathbb{R}^2} h_2^0(X) > 0, \\ \inf_{X\in\mathbb{R}^2} (1-\gamma) g h_2^0(X) - (u_2^0(X) - u_1^0(X))^2 - (v_2^0(X) - v_1^0(X))^2 > 0. \end{cases} \tag{2.19}$$

Then, the Cauchy *problem, associated with* (2.4) *and the initial data* $\mathbf{u^0}$*, is hyperbolic, locally well-posed in* $\mathcal{H}^s(\mathbb{R}^2)$ *and the unique solution verifies conditions* (2.14).

Proof First, we prove the next lemma

Lemma 2.2.7 *Let $\mathcal{S}$ be an open subset of $\mathcal{H}^s(\mathbb{R}^2)^6$ and $\mathsf{S}_\mathsf{x}(\mathbf{u})$ be a symmetric matrix such that $\mathsf{S}_\mathsf{x}(\mathbf{u})\mathsf{A}_x(\mathbf{u})$ is symmetric. If there exists $\mathbf{u^0} \in \mathcal{S}$ such that*

$$\forall \theta \in [0,2\pi],\ \mathsf{S}_\mathsf{x}(\mathsf{P}(\theta)\mathbf{u^0}) > 0, \tag{2.20}$$

then the system (2.4), with initial data $\mathbf{u^0}$, is locally well-posed in $\mathcal{H}^s(\mathbb{R}^2)$, hyperbolic and the unique solution verifies (2.14).

Proof Considering $\mathbf{u^0} \in \mathcal{S}$ such that for all $\theta \in [0,2\pi]$, $\mathsf{S}_\mathsf{x}(\mathsf{P}(\theta)\mathbf{u})$ is positive-definite, it is clear that $\mathsf{S} : (\mathbf{u},\theta) \mapsto \mathsf{P}(\theta)^{-1}\mathsf{S}_\mathsf{x}(\mathsf{P}(\theta)\mathbf{u})\mathsf{P}(\theta)$ verifies assumptions of proposition 2.2.3, with $\mathbf{u^0} \in \mathcal{H}^s(\mathbb{R}^2)^6$. Consequently, propositions 2.2.3 and 2.2.4 are verified.

Then, to verify the lemma 2.2.7, we use a perturbation of the hessian of e_1 (which is a symmetrizer of the one-dimensional model, as we noticed it before):

$$\mathsf{S}_\mathsf{x}(\mathbf{u},u_0) := \begin{bmatrix} g\gamma & g\gamma & \gamma(u_1-u_0) & 0 & 0 & 0 \\ g\gamma & g & 0 & u_2-u_0 & 0 & 0 \\ \gamma(u_1-u_0) & 0 & \gamma h_1 & 0 & 0 & 0 \\ 0 & u_2-u_0 & 0 & h_2 & 0 & 0 \\ 0 & 0 & 0 & 0 & \gamma h_1 & 0 \\ 0 & 0 & 0 & 0 & 0 & h_2 \end{bmatrix}, \tag{2.21}$$

where $u_0 \in \mathbb{R}$ is a parameter, which will be chosen in order to simplify the calculus. Then, it is clear that $\mathsf{S}_\mathsf{x}(\mathbf{u},u_0)$ and $\mathsf{S}_\mathsf{x}(\mathbf{u},u_0)\mathsf{A}_x(\mathbf{u})$ are symmetric for all $(\mathbf{u},u_0) \in \mathbb{R}^6 \times \mathbb{R}$. From now on u_0 is set as $u_0 := u_1$. Then, using the leading principal minors characterization of a positive-definite matrix (also known as *Sylvester*'s criterion), for $(X,\theta) \in \mathbb{R}^2 \times [0,2\pi]$, $\mathsf{S}_\mathsf{x}(\mathsf{P}(\theta)\mathbf{u^0}(X)) > 0$ if and only if

$$\begin{cases} \gamma \in]0,1[, \\ h_1^0(X) > 0,\ h_2^0(X) > 0, \\ (1-\gamma)gh_2^0(X) > \left(\cos(\theta)(u_2^0(X)-u_1^0(X)) + \sin(\theta)(v_2^0(X)-v_1^0(X))\right)^2. \end{cases} \tag{2.22}$$

Finally, as conditions (2.22) must be verified for all $(X,\theta) \in \mathbb{R}^2 \times [0,2\pi]$ and remarking that for all $(\alpha,\beta) \in \mathbb{R}^2$,

$$\max_{\theta \in [0,2\pi]} (\cos(\theta)\alpha + \sin(\theta)\beta)^2 = \alpha^2 + \beta^2, \tag{2.23}$$

then, according to the lemma 2.2.7, the system is locally well-posed in $\mathcal{H}^s(\mathbb{R}^2)$ and hyperbolic, under conditions (2.19), with $\gamma \in]0,1[$.

Remark: The conditions (2.22) have already been found in [41], in the *curl*-free case. However, in [41], the symmetrizer is a *Friedrichs*-symmetrizer as it does not depend of the parameter θ. Moreover,

it is the hessian of the energy of the model and in our case, the symmetrizer is not the hessian of any energy.

To conclude, let $\gamma \in]0,1[$, we define $\mathcal{S}^s_\gamma \subset \mathcal{H}^s(\mathbb{R}^2)^6$, an open subset of initial conditions such that the model (2.4) is symmetrizable:

$$\mathcal{S}^s_\gamma := \left\{ \mathbf{u^0} \in \mathcal{H}^s(\mathbb{R}^2)^6 / \mathbf{u^0} \text{ verifies conditions (2.19)} \right\}. \tag{2.24}$$

2.3 Exact set of hyperbolicity

In the previous section, we proved the hyperbolicity of the *Cauchy* problem, associated with the system (2.4) and the initial data $\mathbf{u^0}$, if $\gamma \in]0,1[$ and $\mathbf{u^0} \in \mathcal{S}^s_\gamma$. However, it was just a sufficient condition of hyperbolicity. The purpose of this section is to characterize the exact set of hyperbolicity of the system (2.4): $\mathcal{H}_\gamma$, defined by

$$\mathcal{H}_\gamma := \left\{ \mathbf{u^0} : \mathbb{R}^2 \to \mathbb{R}^6 / \mathbf{u^0} \text{ verifies conditions (2.11)} \right\} \tag{2.25}$$

To do so, we reduce the analysis of the spectrum of $\mathsf{A}(\mathbf{u},\theta)$: $\sigma(\mathsf{A}(\mathbf{u},\theta))$, to the one of $\mathsf{A}_x(\mathsf{P}(\theta)\mathbf{u})$, using the rotational invariance (2.8). In this section, the study is performed onto the spectrum of $\mathsf{A}_x(\mathbf{u})$ and is deduced, afterwards, to $\mathsf{A}_x(\mathsf{P}(\theta)\mathbf{u})$. As the characteristic polynomial of $\mathsf{A}_x(\mathbf{u})$ is equal to $\det(\mathsf{A}_x(\mathbf{u}) - \mu \mathsf{I}_6) = (\mu - u_1)(\mu - u_2)Q(\mu)$, where $Q(\mu)$ is a quartic, it is necessary to get an exact real roots criterion for quartic equations

2.3.1 Real roots criterion for quartic equations

Considering a quartic equation

$$R(\lambda) := a_4\lambda^4 + a_3\lambda^3 + a_2\lambda^2 + a_1\lambda + a_0 = 0, \tag{2.26}$$

where $(a_0, a_1, a_2, a_3, a_4) \in \mathbb{R}^4$ and $a_4 > 0$. We define the *Sylvester*'s matrix $\mathsf{M} := [\mathsf{M}_{i,j}]_{(i,j)\in[\![1,4]\!]}$ by

$$\sum_{i,j} \mathsf{M}_{i,j} X^{4-i} Y^{4-j} = \frac{R(X)R'(Y) - R(Y)R'(X)}{X - Y}, \tag{2.27}$$

Then, according to *Sturm*'s theorem, the roots of (2.26) are all real if and only if the matrix M is positive-definite or negative-definite. Then, using the *Sylvester*'s criterion on M (*i.e.* $\mathsf{M} > 0$ if and only if all the leading principal minors are strictly positive), it provides an exact criterion of hyperbolicity of the system (2.4).

Proposition 2.3.1 *The roots of the quartic equation are all real if and only if*

$$\forall k \in [\![1,3]\!],\ m_{k+1} m_k > 0 \tag{2.28}$$

where m_k is the k^{th} leading principal minor of M.

Remark: This general criterion is exactly the same given in [51] and [65].

2.3.2 Scaling of the equation

In order to rescale the equation $Q(\mu)=0$, undimensioned quantities are considered, assuming $h_1>0$:

$$\lambda := \frac{\mu-u_1}{\sqrt{gh_1}},\ F_x := \frac{u_2-u_1}{\sqrt{gh_1}},\ F_y := \frac{v_2-v_1}{\sqrt{gh_1}},\ h := \frac{h_2}{h_1}. \tag{2.29}$$

It is straightforward $(\lambda,F_x,F_y,h)\in\mathbb{R}\times\mathbb{R}\times\mathbb{R}\times\mathbb{R}_+$. Consequently, the equation $Q(\mu)=0$ is equivalent to $P(\lambda)=0$ with

$$P(\lambda) := \left[\lambda^2-1\right]\left[(\lambda-F_x)^2-h\right]-\gamma h. \tag{2.30}$$

According to (2.27), the symmetric matrix $\mathsf{M} := [\mathsf{M}_{i,j}]_{(i,j)\in[\![1,4]\!]}$ is here defined by

$$\begin{cases} \mathsf{M}_{1,1}=4 \\ \mathsf{M}_{1,2}=-6F_x \\ \mathsf{M}_{1,3}=-2(1+h-F_x^2) \\ \mathsf{M}_{1,4}=2F_x \\ \mathsf{M}_{2,2}=2(1+h+5F_x^2) \\ \mathsf{M}_{2,3}=-2F_x(1-2h+2F_x^2) \\ \mathsf{M}_{2,4}=4h(\gamma-1) \\ \mathsf{M}_{3,3}=2(1+h^2+4F_x^2+F_x^4+2h(\gamma-F_x^2)) \\ \mathsf{M}_{3,4}=-2F_x(1+h(3\gamma-2)+2F_x^2) \\ \mathsf{M}_{4,4}=F_x^4+F_x^2+h(1-2F_x^2+\gamma(F_x^2-1)))+2(h^2(1-\gamma) \end{cases} \tag{2.31}$$

Remark: As $m_1=4$, it is impossible M negative-definite and all the leading principal minors of M have to be strictly positive.

2.3.3 Hyperbolicity in one dimension

In this subsection, we give the exact criterion of real solutions for $P(\lambda)=0$ and deduce a general criterion of hyperbolicity of the model (2.4), in one dimension.

Proposition 2.3.2 *There exist $(F_{crit}^+,F_{crit}^-)\in\mathbb{R}_+^2$, with $F_{crit}^+\geq F_{crit}^-\geq 0$, such that the roots of $P(\lambda)$ are all real if and only if*

$$\gamma\in]0,1[\text{ and } |F_x|\in[0,F_{crit}^-[\cup]F_{crit}^+,+\infty[. \tag{2.32}$$

In order to prove this proposition, we evaluate the exact conditions (2.28), to prove the proposition 2.3.1, which is an easy consequence of the following lemmata.

Lemma 2.3.3 *For all $(F_x,h,\gamma)\in\mathbb{R}\times\mathbb{R}_+^2$,*

$$m_1>0,\ m_2>0. \tag{2.33}$$

Proof According to the expression of M, $m_1 = 4$ and $m_2 = 8(1+h)+4F_x^2$. As h is assumed strictly positive, the lemma 2.3.3 is proved.

Lemma 2.3.4 *Let* $(F_x, h, \gamma) \in \mathbb{R} \times \mathbb{R}_+^2$. *Then* $\gamma \in]0,1[$ *if and only if*

$$m_3 > 0. \tag{2.34}$$

Proof As the expression of m_3 is

$$m_3 = 8(1+h)F_x^4 - 16(1-h(6+\gamma)+h^2)F_x^2 + 8(1+h)(1-2h(1-2\gamma)+h^2), \tag{2.35}$$

it is considered as a quadratic polynomial in $z := F_x^2$, with main coefficient positive

$$m_3 = p_3(z) := b_2 z^2 + b_1 z + b_0. \tag{2.36}$$

with $b_2 := 8(1+h)$, $b_1 := -16(1-h(6+\gamma)+h^2)$ and $b_3 := 8(1+h)(1-2h(1-2\gamma)+h^2)$. Then, it is strictly positive if and only if one of the two following assertions is verified

$$\begin{cases} p_3^1(h) < 0, \\ \text{the roots of } p_3(z) \text{ are all strictly negative.} \end{cases} \tag{2.37}$$

where p_3^1 is the discriminant of the quadratic p_3

$$m_3^1 := -256h(6h-\gamma-2)(h(2+\gamma)-6). \tag{2.38}$$

In the first case, noting that roots of $p_3^1(h)$ are 0, $\frac{6}{2+\gamma}$ and $\frac{2+\gamma}{6}$, and as h is assumed strictly positive, the discriminant is strictly negative if and only if $2+\gamma > 0$ and $h \notin [h_{crit}^-, h_{crit}^+]$ or if $2+\gamma < 0$ and $h \in [h_{crit}^-, h_{crit}^+]$, with

$$\begin{cases} h_{crit}^- := \min(\frac{6}{2+\gamma}, \frac{2+\gamma}{6}), \\ h_{crit}^+ := \max(\frac{6}{2+\gamma}, \frac{2+\gamma}{6}). \end{cases} \tag{2.39}$$

As γ is assumed positive, if $h \notin [h_{crit}^-, h_{crit}^+]$ then $m_3 > 0$, and if $h \in [h_{crit}^-, h_{crit}^+]$, the second assertion of (2.37) should be verified: the roots of $p_3(z) := b_2 z^2 + b_1 z + b_0$ are all strictly negative, which is equivalent to

$$b_2 b_0 > 0 \text{ and } \frac{b_1}{b_2} > 0. \tag{2.40}$$

As, $b_2 b_0 = (8(1+h))^2(1-2h(1-2\gamma)+h^2) > 0$ if and only if $4\gamma(1-\gamma) > 0$

$$b_2 b_0 > 0 \Leftrightarrow \gamma \in]0,1[. \tag{2.41}$$

Moreover, for all $(h, \gamma) \in [h_{crit}^-, h_{crit}^+] \times \mathbb{R}_+$, one can check $\frac{b_1}{b_2} > 0$. To conclude, $m_3 > 0$ if and only if $\gamma \in]0,1[$ and the lemma 2.3.4 is proved.

Lemma 2.3.5 *Let $(F_x, h, \gamma) \in \mathbb{R} \times \mathbb{R}_+^2$ such that $\gamma \in]0,1[$. Then, there exist two positive real, denoted by $F_{crit}^{\pm}$, such that $F_{crit}^{+} \geq F_{crit}^{-} \geq 0$ and*

$$m_4 > 0 \Leftrightarrow |F_x| \in [0, F_{crit}^{-}[\cup]F_{crit}^{+}, +\infty[. \tag{2.42}$$

Proof Considering $m_4 = 16hq(z)$ where

$$\begin{aligned} q(z) := \quad & z^4 + (h+1)(\gamma-4)z^3 - \left(3(h^2+1)(\gamma-2) - h(\gamma^2 - 26\gamma + 4)\right) z^2 \\ & + (1+h)\left((h^2+1)(3\gamma-4) + h(-20\gamma^2 + 10\gamma + 8)\right) z \\ & - (\gamma-1)\left((h-1)^2 + 4\gamma h\right)^2 \end{aligned} \tag{2.43}$$

We denote by $\{z_1, z_2, z_3, z_4\}$ the roots of q. If $\gamma \in]0,1[$, then it is obvious that

$$\begin{cases} q(0) > 0, \\ q\left((1+\sqrt{h})^2\right) < 0, \\ \lim_{z \to +\infty} q(z) = +\infty \end{cases} \tag{2.44}$$

and then, q has, at least, two positive real roots . Moreover, as $\lim_{z \to -\infty} q(z) = +\infty$ and the product of the roots is positive if $\gamma \in]0,1[$

$$z_1 z_2 z_3 z_4 = (1-\gamma)\left((h-1)^2 + 4\gamma h\right) > 0, \tag{2.45}$$

and the two other roots are complex or have the same sign. However, if all the roots are real, the *Sylvester*'s criterion is necessarily verified for the quartic q. Then, the *Sylvester*'s matrix associated to q is not positive-definite because n_k, the k^{th} leading principal minors, with $k \in [\![1,4]\!]$, are such that

$$\forall \gamma \in]0,1[, \ \begin{cases} n_1 = 4 > 0, \\ n_4 = -\left(\gamma h(h-1)\right)^2 \left(27\gamma^2(1+h^2) - 2h(2\gamma^3 + 3\gamma^2 + 96\gamma - 128)\right)^3 < 0 \end{cases} \tag{2.46}$$

Consequently, the proposition 2.3.1 is not verified and all the roots of q are not real. Then, there are exactly two positive roots of q, denoted by $F_{crit}^{\pm\,2}$. Finally, if $\gamma \notin]0,1[$, one can prove that $q(z)$ has only one positive root, but it is not vital for the exact criterion of hyperbolicity, as $m_3 > 0$ if and only if $\gamma \in]0,1[$.

Remark: The critical quantities $F_{crit}^{\pm\,2}$ are analytical functions of h and γ. The existence of these quantities has been noticed numerically in [30].

Theorem 2.3.6 *Let $\mathbf{u^0} : \mathbb{R}^2 \mapsto \mathbb{R}^6$. The system (2.4), in one dimension, with initial data $\mathbf{u^0}$, is hyperbolic if and only if*

$$\begin{cases} \gamma \in]0,1[\\ \inf_{x \in \mathbb{R}} h_1^0(x) > 0, \ \inf_{x \in \mathbb{R}} h_2^0(x) > 0, \\ \forall x \in \mathbb{R}, \ |F_x^0(x)| < F_{crit}^{-\,0}(x) \text{ or } |F_x^0(x)| > F_{crit}^{+\,0}(x), \end{cases} \tag{2.47}$$

with $F_{crit}^{\pm}$ defined in lemma 2.3.5.

Proof In the one dimension case, the matrix $\mathsf{A}(\mathbf{u}, \theta)$ is reduced to $\mathsf{A}_x(\mathbf{u})$. Consequently, applying directly proposition 2.3.2, the theorem 2.3.6 is proved.

2.3.4 Hyperbolicity in two dimensions

In this subsection, we can deduce from below an exact criterion of hyperbolicity of the model (2.4). The next theorem is a generlisation of the result mentioned in [9], for the one spatial dimensions case. In the following theorem we explain the case of two spatial dimensions with a full proof.

Theorem 2.3.7 *Let* $\mathbf{u^0} : \mathbb{R}^2 \to \mathbb{R}^6$. *The system* (2.4), *with initial data* $\mathbf{u^0}$, *is hyperbolic if and only if*

$$\begin{cases} \gamma \in]0,1[\\ \inf_{X\in\mathbb{R}^2} h_1^0(x) > 0,\ \inf_{X\in\mathbb{R}^2} h_2^0(x) > 0, \\ \inf_{X\in\mathbb{R}^2} F_{crit}^{-}{}^0(X)^2 - F_x^0(X)^2 - F_y^0(X)^2 > 0. \end{cases} \tag{2.48}$$

Proof As it was mentioned in proposition 2.2.1, the hyperbolicity is insured if and only if the spectrum of $\mathsf{A}(\mathbf{u^0},\theta)$ included in $\mathbb{R}$, for all $\theta \in [0,2\pi]$. Moreover, using the rotational invariance (2.8), it is equivalent with the spectrum of $\mathsf{A}_x(\mathsf{P}(\theta)\mathbf{u})$ is included in $\mathbb{R}$, for all $\theta \in [0,2\pi]$. Then, with proposition 2.3.2, it is obvious the system (2.4) is hyperbolic if and only if

$$\forall \theta \in [0,2\pi],\ \begin{cases} \gamma \in]0,1[, \\ |F(\theta)| \in [0, F_{crit}^{-}[\ \cup\ ]F_{crit}^{+}, +\infty[, \end{cases} \tag{2.49}$$

with $F(\theta) := \cos(\theta)F_x + \sin(\theta)F_y$. Because these conditions are needed for all $\theta \in [0,2\pi]$ and

$$\begin{cases} \min_{\theta\in[0,2\pi]} F(\theta)^2 = 0, \\ \max_{\theta\in[0,2\pi]} F(\theta)^2 = F_x^2 + F_y^2, \end{cases} \tag{2.50}$$

one can deduce the theorem 2.3.7.

Remark: The hyperbolicity of the two-layer shallow water model with free surface is very different depending on the dimension considered. This model remains stable in the one and two spatial dimensions, if the shear velocity remains small. When the shear velocity grows, the interface liquid/liquid becomes subject to *Kelvin-Helmholtz* instabilities (see [16] and [19]). Under a strong shear of velocity, such instabilities will arise with a disturbance and will generate mixing between layers: the assumptions of the model will no more be valid and mass exchanges between neighboring layers must be taken into account. However, although the two spatial dimension model is unstable under high shear velocity (the disturbance will grow with time), the one spatial dimension model remains stable because the disturbance is advected away from each other before it can grow (see [127]).
To conclude, considering $\gamma \in]0,1[$, the exact set of hyperbolicity, $\mathcal{H}_\gamma$, is defined by

$$\mathbf{u} \in \mathcal{H}_\gamma \Longleftrightarrow \begin{cases} \inf_{X\in\mathbb{R}^2} h_1(X) > 0,\ \inf_{X\in\mathbb{R}^2} h_2(X) > 0, \\ \inf_{X\in\mathbb{R}^2} F_{crit}^{-}(X)^2 - F_x(X)^2 - F_y(X)^2 > 0. \end{cases} \tag{2.51}$$

2.4 Hyperbolicity in the region $0 < 1-\gamma \ll 1$

In this section, in order to compare $\mathcal{S}^s_\gamma$ and $\mathcal{H}_\gamma \cap \mathcal{H}^s(\mathbb{R}^2)^6$, asymptotic expansions of $F^{\pm}_{crit}$ is performed. Then, to prove a criterion of local well-posedness, in $\mathcal{H}^s(\mathbb{R}^2)$, more general than (2.19), expansion of $\sigma(\mathsf{A}(\mathbf{u},\theta))$ is carried out and diagonalizability of $\mathsf{A}(\mathbf{u},\theta)$ is proved, under weak density-stratification.

2.4.1 Expansion of $F^{\pm}_{crit}$

We define the function $f : \mathbb{R}\times\mathbb{R}_+\times[0,1]\to\mathbb{R}$ such that $f(z,h,\gamma) := q(z)$. The next proposition compares $\mathcal{S}^s_\gamma$ and $\mathcal{H}_\gamma\cap\mathcal{H}^s(\mathbb{R}^2)^6$, under weak density-stratification.

Proposition 2.4.1 *Let $\gamma\in]0,1[$ such that $1-\gamma$ is small. Then*

$$\mathcal{S}^s_\gamma \subset \mathcal{H}_\gamma\cap\mathcal{H}^s(\mathbb{R}^2)^6 \tag{2.52}$$

Proof Around the state $z=0$ and $\gamma=1$, it is obvious that $f(0,h,1)=0$. The 1st order *Taylor* expansion of $f(z,h,\gamma)$ about this state is

$$\begin{aligned} f(z,h,\gamma) = \quad & f(0,h,1) + z\tfrac{\partial f}{\partial z}(0,h,1) \\ & +(\gamma-1)\tfrac{\partial f}{\partial \gamma}(0,h,1) + o(z,\gamma-1). \end{aligned} \tag{2.53}$$

Lemma 2.4.2 *Let $h\in\mathbb{R}_+$, then*

$$\frac{\partial f}{\partial z}(0,h,1) = -(1+h)^3,\ \frac{\partial f}{\partial \gamma}(0,h,1) = -(1+h)^4, \tag{2.54}$$

consequently, an expansion of F^-_{crit} is

$$\begin{aligned} {F^-_{crit}}^2 &= (1-\gamma)(1+h) + \mathcal{O}((1-\gamma)^2) \\ &= (1-\gamma)h + (1-\gamma)(1+o(1)). \end{aligned} \tag{2.55}$$

Then it is clear that for all $X\in\mathbb{R}^2$, ${F^-_{crit}}^2(X) > (1-\gamma)h(X)$. Therefore, if $\mathbf{u}\in\mathcal{S}^s_\gamma$, it verifies conditions (2.24), which imply conditions (2.51) and $\mathbf{u}\in\mathcal{H}_\gamma$.

Moreover, another interesting comparison is between the rigid lid model (see [80]) and the free surface one. The exact set of hyperbolicity of the 1st one is characterized by

$$F_x^2 + F_y^2 < {F^{rig}_{crit}}^2, \tag{2.56}$$

with ${F^{rig}_{crit}}^2 = (1-\gamma)(1+h)$. This is compatible with the expansion (2.55) but does not indicate which model gets the largest set of hyperbolicity. In the next proposition, the comparison of these critical quantities is made.

Proposition 2.4.3 *Let $\gamma \in]0,1[$ such that $1-\gamma$ is small. If the rigid lid model is hyperbolic, then the free surface one is also hyperbolic:*

$$F_{crit}^{-\,2} > F_{crit}^{rig\ 2}. \tag{2.57}$$

Proof With a 2nd order *Taylor* expansion of $f(z,h,\gamma)$ about the state $z=0$ and $\gamma=1$, one can check that

$$F_{crit}^{-\,2} - F_{crit}^{rig\ 2} = (1-\gamma)^2 \frac{h\left(1+27h+27h^2+9h^3\right)}{(1+h)^4} + \mathcal{O}((1-\gamma)^3), \tag{2.58}$$

then, if $1-\gamma$ is sufficiently small, the expansion (2.58) is true and we have

$$F_{crit}^{-\,2} - F_{crit}^{rig\ 2} > 0, \tag{2.59}$$

and the proposition 2.4.3 is straightforward proved.

Finally, even if the expansion of the quantity F_{crit}^{+} is not necessary, as we proved in the theorem 2.3.7, the hyperbolicity of the two-dimensional model does not depend of F_{crit}^{+}. It is interesting to know the behavior of the hyperbolicity of the one-dimensional model. We perform expansion about the state $\gamma=1$, because the roots of $q(z)=f(z,h,1)$ are explicit.

$$f(z,h,1) = z^4 - 3z^3(1+h) + 3z^2(h^2-7h+1) - z(1+h)^3. \tag{2.60}$$

Then, the expansion of $F_{crit}^{+\,2}$ is the only non-zero and real root of $f(z,h,1)$:

$$F_{crit}^{+} = \left[1+h^{\frac{1}{3}}\right]^{\frac{3}{2}} + O(1-\gamma), \tag{2.61}$$

The last expansions of $F_{crit}^{\pm}$ are similar to [79] in the case $\gamma=1$ and [127] in the case $h_1=h_2$.

2.4.2 Expansion of the spectrum of $\mathsf{A}(\mathbf{u},\boldsymbol{\theta})$

In this subsection, eigenvalues of $\mathsf{A}(u,\theta)$ are expanded, in order to prove the diagonalizability of this matrix in the next subsection. Using the rotational invariance, eigenvalues of $\mathsf{A}(\mathbf{u},\theta)$ are deduced from $\sigma(\mathsf{A}_x(\mathbf{u}))$. The spectrum $\mathsf{A}_x(\mathbf{u})$ is set as

$$\sigma(\mathsf{A}_x(\mathbf{u})) := \{\mu_1^{\pm},\mu_2^{\pm},\mu_3^{\pm}\}. \tag{2.62}$$

We define the undimensioned quantities:

$$\forall i \in [\![1,3]\!], \lambda_i^{\pm} := \frac{\mu_i^{\pm}-u_1}{\sqrt{gh_1}}. \tag{2.63}$$

Then, $\mu_i^{\pm}$ is an eigenvalue of $\mathsf{A}_x(\mathbf{u})$ if and only if $g(\lambda_i^{\pm}, F_x, h, \gamma) = 0$, where $g : \mathbb{R}^3 \times [0,1] \to \mathbb{R}$ is defined by

$$g(\lambda, F_x, h, \gamma) := P(\lambda) = \left[\lambda^2 - 1\right]\left[(\lambda - F_x)^2 - h\right] - \gamma h. \tag{2.64}$$

As we get the exact criterion of hyperbolicity (2.51), the main goal is to know the conditions to have $\mathsf{A}(\mathbf{u}, \theta)$ diagonalizable, not only to get an eigenbasis of $\mathbb{R}^6$ to provide the *Riemann* invariants but also to prove that the model is locally well-posed in $\mathcal{H}^s(\mathbb{R}^2)$ (see proposition 2.2.5).

In the next paragraphs, as there are two trivial eigenvalues: u_1 and u_2, we settle down $\mu_3^- = u_1$ and $\mu_3^+ = u_2$ and asymptotic expansions are performed on $\mu_1^{\pm}$ and $\mu_2^{\pm}$ (*i.e.* $\lambda_1^{\pm}$ and $\lambda_2^{\pm}$), in both subsets of $\mathcal{H}_\gamma$.

2.4.2.1 Asymptotic expansions in the subset $|\mathbf{F_x}| > \mathbf{F_{crit}^+}$

As we know $\{\lambda_1^{\pm}, \lambda_2^{\pm}\}$ in the case $\gamma = 1$ and $h = 0$

$$\lambda_1^{\pm} = F_x,\ \lambda_2^{\pm} = \pm 1, \tag{2.65}$$

we expand $\{\lambda_1^{\pm}, \lambda_2^{\pm}\}$ under assumptions $\gamma \to 1^-$ and $h \to 0$. Although the case $h \to 0$ is not an usual operational case, this assumption is necessary to apply the implicit functions theorem. Therefore, as λ_2^- and λ_2^+ are two distinct eigenvalues, the purpose of this subsection is to know the behavior of $\lambda_1^{\pm}$ when $\gamma \to 1^-$ and $h \to 0$, which implies $F_{crit}^+ \to 1$, according to the expansion (2.61). The main result is summed up in the next proposition

Proposition 2.4.4 *Let $(\gamma, \mathbf{u}) \in]0,1[\times\mathbb{R}^6$ such that $1-\gamma$ and h are small and $|F_x| > F_{crit}^+$. Then, $\sigma(\mathsf{A}_x(\mathbf{u})) \subset \mathbb{R}$ and*

$$\begin{cases} \lambda_1^{\pm} = F_x + \frac{F_x h}{F_x^2 - 1} \pm h^{\frac{1}{2}} \left[1 + \frac{h\gamma}{F_x^2 - 1} + \left(\frac{hF_x}{F_x^2 - 1}\right)^2\right]^{\frac{1}{2}} + \mathcal{O}(h^{\frac{3}{2}}, 1-\gamma), \\ \lambda_2^{\pm} = \pm\left[1 + \frac{h}{2(F_x - 1)^2}\right] + \mathcal{O}(h^2, 1-\gamma). \end{cases} \tag{2.66}$$

Proof The 2nd order *Taylor* expansion of $g(\lambda, F_x, h, \gamma)$ about the state $\lambda = F_x$, $h = 0$ and $\gamma = 1$ provides the expansion of $\lambda_1^{\pm}$: $g(\lambda, F_x, h, \gamma)$ is equal to

$$\begin{array}{l} g(F_x, F_x, 0, 1) \\ +(\lambda - F_x)\frac{\partial g}{\partial \lambda}(F_x, F_x, 0, 1) + h\frac{\partial g}{\partial h}(F_x, F_x, 0, 1) + (\gamma - 1)\frac{\partial g}{\partial \gamma}(F_x, F_x, 0, 1) \\ \frac{1}{2}\left[(\lambda - F_x)^2\frac{\partial^2 g}{\partial \lambda^2}(F_x, F_x, 0, 1) + h^2\frac{\partial^2 g}{\partial h^2}(F_x, F_x, 0, 1) + (\gamma - 1)^2\frac{\partial^2 g}{\partial \gamma^2}(F_x, F_x, 0, 1)\right] \\ +(\lambda - F_x)h\frac{\partial^2 g}{\partial \lambda \partial h}(F_x, F_x, 0, 1) + (\lambda - F_x)(\gamma - 1)\frac{\partial^2 g}{\partial \lambda \partial \gamma}(F_x, F_x, 0, 1) \\ +h(\gamma - 1)\frac{\partial^2 g}{\partial h \partial \gamma}(F_x, F_x, 0, 1) + o\left((\lambda - F_x)^2, h^2, (\gamma - 1)^2\right) \end{array} \tag{2.67}$$

Lemma 2.4.5 $\forall F_x \in \mathbb{R}$,

$$\begin{cases} g(F_x,F_x,0,1)=0 \\ \frac{\partial g}{\partial \lambda}(F_x,F_x,0,1)=0, \\ \frac{\partial g}{\partial \gamma}(F_x,F_x,0,1)=0, \\ \frac{\partial^2 g}{\partial h^2}(F_x,F_x,0,1)=0, \\ \frac{\partial^2 g}{\partial \gamma^2}(F_x,F_x,0,1)=0, \\ \frac{\partial^2 g}{\partial \lambda \gamma}(F_x,F_x,0,1)=0, \end{cases} \quad \begin{cases} \frac{\partial g}{\partial h}(F_x,F_x,0,1)=-F_x^2, \\ \frac{\partial^2 g}{\partial \lambda^2}(F_x,F_x,0,1)=2(F_x^2-1), \\ \frac{\partial^2 g}{\partial \lambda \partial h}(F_x,F_x,0,1)=-2F_x, \\ \frac{\partial^2 g}{\partial h \gamma}(F_x,F_x,0,1)=-1, \end{cases} \tag{2.68}$$

Consequently, using the implicit functions theorem, the expansion of $\lambda_1^{\pm}$ is deduced. Moreover, $\lambda_1^{\pm}$ is real if $|F_x| > F_{crit}^{+}$, because $F_{crit}^{+} > 1$ (see (2.61)). Moreover, with 1st order *Taylor* expansion of $g(\lambda,F_x,h,\gamma)$ about $(\lambda,F_x,h,\gamma)=(\pm 1,F_x,0,1)$ and implicit theorem, one can get the expansion of $\lambda_2^{\pm}$. Moreover, $\lambda_2^{\pm}$ is unconditionally real.

Remarks: 1) As it was mentioned before, the expansion of $\lambda_2^{\pm}$ is not necessary to prove the diagonalizability of $\mathsf{A}_x(\mathbf{u})$, but it is interesting to get a more precise expression. 2) We could perform an analysis more general than the one about the state $(h,\gamma)=(0,1)$ as all the calculs are explicit but it is much simpler in this particular case.

2.4.2.2 Asymptotic expansions in the subset $|\mathbf{F_x}| < \mathbf{F_{crit}^{-}}$

According to the expansion (2.55), $\gamma = 1$ implies $F_{crit}^{-} = 0$. Then, under the assumption $1-\gamma$ small, $|F_x| < F_{crit}^{-}$ is equivalent to $F_x = 0$. As we know exactly $\{\lambda_1^{\pm},\lambda_2^{\pm}\}$ in the particular case $\gamma = 1$ and $F_x = 0$

$$\lambda_1^{\pm} = \pm\sqrt{1+h},\ \lambda_2^{\pm} = 0, \tag{2.69}$$

we expand $\{\lambda_1^{\pm},\lambda_2^{\pm}\}$ under assumption $\gamma \to 1^{-}$ and $|F_x| < F_{crit}^{-}$ Therefore, $\lambda_1^{\pm}$ give two distinct eigenvalues, so the main purpose of this subsection is to know the behavior of $\lambda_2^{\pm}$ when and $\gamma \to 1^{-}$, which implies $F_{crit}^{-} \to 0$ according to (2.55), as it was noticed above, and consequently $|F_x| \to 0$.

Proposition 2.4.6 *Let* $(\gamma,\mathbf{u}) \in]0,1[\times\mathbb{R}^6$ *such that* $1-\gamma$ *is small and* $|F_x| < F_{crit}^{-}$. *Then,* $\sigma(\mathsf{A}_x(\mathbf{u})) \subset \mathbb{R}$ *and*

$$\begin{cases} \lambda_1^{\pm} = \frac{1}{(1+h)^{\frac{3}{2}}}\left[F_x h(1+h)^{\frac{1}{2}} \pm \left((1+h)^2 - \frac{1}{2}h(1-\gamma)\right)\right] + \mathcal{O}(1-\gamma), \\ \lambda_2^{\pm} = \frac{F_x}{1+h} \pm \left[\frac{h}{(1+h)^2}\left((1+h)(1-\gamma) - F_x^2\right)\right]^{\frac{1}{2}} + \mathcal{O}(1-\gamma). \end{cases} \tag{2.70}$$

Proof The 2nd order *Taylor* expansion of $g(\lambda, F_x, h, \gamma)$ about the state $\lambda = 0$, $F_x = 0$ and $\gamma = 1$ provides the expand of $\lambda_2^{\pm}$: $g(\lambda, F_x, h, \gamma)$ is equal to

$$\begin{array}{l} g(0,0,h,1) \\ +\lambda \frac{\partial g}{\partial \lambda}(0,0,h,1) + F_x \frac{\partial g}{\partial F_x}(0,0,h,1) + (\gamma-1)\frac{\partial g}{\partial \gamma}(0,0,h,1) \\ \frac{1}{2}\left[\lambda^2 \frac{\partial^2 g}{\partial \lambda^2}(0,0,h,1) + F_x^2 \frac{\partial^2 g}{\partial F_x^2}(0,0,h,1) + (\gamma-1)^2 \frac{\partial^2 g}{\partial \gamma^2}(0,0,h,1)\right] \\ +\lambda F_x \frac{\partial^2 g}{\partial \lambda \partial F_x}(0,0,h,1) + \lambda(\gamma-1)\frac{\partial^2 g}{\partial \lambda \partial \gamma}(0,0,h,1) \\ +F_x(\gamma-1)\frac{\partial^2 g}{\partial F_x \partial \gamma}(0,0,h,1) + o\left(\lambda^2, F_x^2, (\gamma-1)^2\right) \end{array} \tag{2.71}$$

Lemma 2.4.7 $\forall h \in \mathbb{R}_+^*$,

$$\left\{ \begin{array}{l} g(0,0,h,1) = 0 \\ \frac{\partial g}{\partial \lambda}(0,0,h,1) = 0, \\ \frac{\partial g}{\partial F_x}(0,0,h,1) = 0, \\ \frac{\partial^2 g}{\partial \gamma^2}(0,0,h,1) = 0, \\ \frac{\partial^2 g}{\partial \lambda \partial \gamma}(0,0,h,1) = 0, \\ \frac{\partial^2 g}{\partial F_x \partial \gamma}(0,0,h,1) = 0, \end{array} \right. \quad \left\{ \begin{array}{l} \frac{\partial g}{\partial \gamma}(0,0,h,1) = -h, \\ \frac{\partial^2 g}{\partial \lambda^2}(0,0,h,1) = -2(1+h), \\ \frac{\partial^2 g}{\partial F_x^2}(0,0,h,1) = -2, \\ \frac{\partial^2 g}{\partial \lambda \partial F_x}(0,0,h,1) = 2. \end{array} \right. \tag{2.72}$$

Consequently, if $|F_x| < F_{crit}^-$, $\lambda_2^{\pm}$ is real and using the implicit functions theorem, the expansion of $\lambda_2^{\pm}$ is insured. Moreover, with 1st order *Taylor* expansion of $g(\lambda, F_x, h, \gamma)$ about $(\lambda, F_x, h, \gamma) = (\pm\sqrt{1+h}, 0, h, 1)$ and the implicit theorem, one can get the expansion of $\lambda_1^{\pm}$. Moreover, $\lambda_1^{\pm}$ is unconditionally real.

In this set of hyperbolicity (*i.e.* $|F_x| < F_{crit}^-$), we have proved completely the expressions of the asymptotic expansions given in [114], [97], [67], [1] and [127].

Remarks: 1) Approximations (2.70) are precise in $\mathcal{O}(1-\gamma)$, and not $\mathcal{O}(F_x^2, (1-\gamma))$, because if $F_x^2 < {F_{crit}^-}^2$ then $F_x^2 = \mathcal{O}(1-\gamma)$, according to expansion (2.55). 2) The expansion of $\lambda_1^{\pm}$ is not necessary, but it is interesting to get a more precise expression.

2.4.3 The eigenstructure of $\mathsf{A}(\mathbf{u}, \theta)$

The description of the eigenstructure is a decisive point, as it permits to characterize exactly the *Riemann* invariants and the local well-posedness in $\mathcal{H}^s(\mathbb{R}^2)$ (see proposition 2.2.5).

Proposition 2.4.8 *There exists* $\delta > 0$ *such that if* $\gamma \in]1-\delta, 1[$ *and* $(\mathbf{u}, \theta) \in \mathcal{H}_\gamma \times [0, 2\pi]$, *the matrix* $\mathsf{A}(\mathbf{u}, \theta)$ *is diagonalizable.*

Proof With the rotational invariance (2.8), it is equivalent to prove the diagonalizability of $\mathsf{A}_x(\mathbf{u})$. By denoting $(\mathbf{e_i})_{i\in[\![1,6]\!]}$ the canonical basis of $\mathbb{R}^6$, one can prove the right eigenvectors $\boldsymbol{r}_x^\mu(\mathbf{u})$ of $\mathsf{A}_x(\mathbf{u})$, associated to the eigenvalue μ, are defined by

$$\begin{cases} \boldsymbol{r}_x^\mu(\mathbf{u}) = \mathbf{e_1} + \frac{\mu-u_1}{h_1}\mathbf{e_3} - c_\mu^r\left(\mathbf{e_2} + \frac{\mu-u_2}{h_2}\mathbf{e_4}\right), & \text{if } \mu \in \{\mu_1^\pm, \mu_2^\pm\}, \\ \boldsymbol{r}_x^\mu(\mathbf{u}) = \mathbf{e_5}, & \text{if } \mu = \mu_3^-, \\ \boldsymbol{r}_x^\mu(\mathbf{u}) = \mathbf{e_6}, & \text{if } \mu = \mu_3^+, \end{cases} \tag{2.73}$$

where $c_\mu^r := 1 - \frac{(\mu-u_1)^2}{gh_1}$. Then, the right eigenvectors $\boldsymbol{r}^\mu(\mathbf{u},\theta)$ of $\mathsf{A}(\mathbf{u},\theta)$ are defined by

$$\forall \mu \in \sigma(\mathsf{A}(\mathbf{u},\theta)),\ \boldsymbol{r}^\mu(\mathbf{u},\theta) = \mathsf{P}(\theta)^{-1}\boldsymbol{r}_x^\mu(\mathsf{P}(\theta)\mathbf{u}). \tag{2.74}$$

Moreover, if $1-\gamma$ is sufficiently small (*i.e.* $\gamma \in]1-\delta, 1[$), the eigenvalues $\mu_i^\pm$, with $i \in \{1,2\}$, are all distinct (the existence of $\delta > 0$ is guaranteed). Indeed, there is the next inequalities if $\gamma \in]1-\delta, 1[$

$$\mu_1^+ > \mu_2^+ > \mu_2^- > \mu_1^- \tag{2.75}$$

Consequently, as the eigenvalues are real, the right-eigenvectors (2.73) constitute an eigenbasis of $\mathbb{R}^6$ and $\mathsf{A}_x(\mathbf{u})$ is diagonalizable.

Remark: The left eigenvectors $\boldsymbol{l}_x^\mu(\mathbf{u})$ of $\mathsf{A}_x(\mathbf{u})$, associated to the eigenvalue $\mu \in \sigma(\mathsf{A}_x(\mathbf{u}))$, are also interesting for the treatment of open boundaries for instance (see [14]). They are defined by:

$$\begin{cases} {}^\top\boldsymbol{l}_x^\mu(\mathbf{u}) = -c_\mu^l\left(\frac{\mu-u_1}{h_1}\mathbf{e_1} + \mathbf{e_3}\right) + \frac{\mu-u_2}{h_2}\mathbf{e_2} + \mathbf{e_4}, & \text{if } \mu \in \{\mu_1^\pm, \mu_2^\pm\}, \\ {}^\top\boldsymbol{l}_x^\mu(\mathbf{u}) = \mathbf{e_5}, & \text{if } \mu = \mu_3^-, \\ {}^\top\boldsymbol{l}_x^\mu(\mathbf{u}) = \mathbf{e_6}, & \text{if } \mu = \mu_3^+, \end{cases} \tag{2.76}$$

where $c_\mu^l := 1 - \frac{(\mu-u_2)^2}{gh_2}$. And the left eigenvectors $\boldsymbol{l}^\mu(\mathbf{u},\theta)$ of $\mathsf{A}(\mathbf{u},\theta)$ are defined by

$$\forall \mu \in \sigma(\mathsf{A}(\mathbf{u},\theta)),\ \boldsymbol{l}^\mu(\mathbf{u},\theta) = \boldsymbol{l}_x^\mu(\mathsf{P}(\theta)\mathbf{u})\mathsf{P}(\theta). \tag{2.77}$$

Furthermore, in order to know the type of the wave associated to each eigenvalue – shock, contact or rarefaction wave – there is the next proposition

Proposition 2.4.9 *There exists $\delta > 0$ such that if $\gamma \in]1-\delta, 1[$, then*

$$\begin{cases} \text{the } \mu_i^\pm\text{−characteristic field is genuinely non} - \text{linear}, & \text{if } i \in \{1,2\}, \\ \text{the } \mu_i^\pm\text{−characteristic field is linearly degenerate}, & \text{if } i = 3. \end{cases} \tag{2.78}$$

This last proposition generalizes the results proved in [66] with $u_1 = u_2$.

Proof If γ is sufficiently close to 1 (*i.e.* $\gamma \in]1-\delta, 1[$, with $\delta > 0$) the expansions (2.70), when $|F_x| < F_{crit}^-$, are valid. Moreover, we remark that $\mu_i^\pm$ depends analytically of the parameters of the problem and we deduce that the $o(1-\gamma)$ still remains small after derivating. Then, with the expression of the right eigenvectors (2.73) of $\mathsf{A}_x(\mathbf{u})$, one can check

$$\begin{cases} \nabla\mu_i^\pm \cdot \boldsymbol{r}_x^\mu(\mathbf{u}) \neq 0, & \text{if } i \in \{1,2\}, \\ \nabla\mu_i^\pm \cdot \boldsymbol{r}_x^\mu(\mathbf{u}) = 0, & \text{if } i = 3, \end{cases} \tag{2.79}$$

then, the proposition 2.4.9 is proved.

Remark: when $u_2 - u_1$ and $1-\gamma$ are both equal to 0, the $\mu_1^\pm$-characteristic field remains genuinely non-linear but the $\mu_2^\pm$-characteristic field becomes linearly degenerate.
To conclude, under conditions of the proposition 2.4.9, for all $i \in \{1,2\}$, the $\mu_i^\pm$-wave is a shock wave or a rarefaction wave and the $\mu_3^\pm$-wave is a contact wave.
Finally, as a consequence, we deduce a criterion of local well-posedness in $\mathcal{H}^s(\mathbb{R}^2)$, more general than criterion (2.24).

Corollary 2.4.10 *There exists $\delta > 0$ such that if $\gamma \in]1-\delta, 1[$ and $\mathbf{u^0} \in \mathcal{H}_\gamma \cap \mathcal{H}^s(\mathbb{R}^2)^6$, then, the* Cauchy *problem, associated with* (2.4) *and initial data $\mathbf{u^0}$, is locally well-posed in $\mathcal{H}^s(\mathbb{R}^2)$, hyperbolic and the unique solution verifies conditions* (2.14).

Proof Let $\gamma \in]0,1[$. As it was proved in the proposition 2.4.8, there exists $\delta > 0$ such that if $\gamma \in]1-\delta, 1[$ then for all $(\mathbf{u}, \theta) \in \mathcal{H}_\gamma \times [0, 2\pi]$, $\mathsf{A}(\mathbf{u^0}, \theta)$ is diagonalizable. Then, by definition of $\mathcal{H}_\gamma$, the *Cauchy* problem is hyperbolic. Moreover, according to proposition 2.2.5, it is locally well-posed in $\mathcal{H}^s(\mathbb{R}^2)$ and the unique solution verifies conditions (2.14).

Remark: This criterion is less restrictive than (2.24), because as it was proved in proposition 2.4.1: if $1-\gamma$ is sufficiently small, $\mathcal{S}_\gamma^s \subset \mathcal{H}_\gamma$.

2.5 A *conservative* two-layer shallow water model

Even if the model (2.1–2.2) is conservative, in the one-dimensional case, with the unknowns (h_i, u_i), with $i \in \{1,2\}$. It is not anymore true in the two-dimensional case. This subsection will treat this lack of conservativity by an augmented model, with a different approach from [1]. In this last reference, the aim is to approach the two-layer model with another one for which it is possible to define exactly the eigenstructure. We remind that no assumption has been made concerning the horizontal vorticity, in each layer

$$w_i := curl(\boldsymbol{u_i}) = \frac{\partial v_i}{\partial x} - \frac{\partial u_i}{\partial y},\ i \in \{1,2\}. \tag{2.80}$$

2.5.1 Conservation laws

Using a *Frobenius* problem, it was proved in [8] that the one-dimensional two-layer shallow water model with free surface has a finite number of conservative quantities: the height and velocity in each layer, the total momentum and the total energy. Obviously, in the two spatial dimension case we can not have more classical conservation laws (depending only on unknowns) than in the one spatial dimension case. However, such additional conservation laws can exist, if we allow the dependence not only on the unknowns, but also on their derivatives. Nevertheless, introducing w_i, for $i \in \{1,2\}$, in equations (2.1–2.2), the conservation of mass (2.1) is unchanged

$$\frac{\partial h_i}{\partial t} + \nabla\cdot(h_i \boldsymbol{u_i}) = 0, \tag{2.81}$$

but the equation of depth-averaged horizontal velocity (2.2) becomes conservative

$$\frac{\partial \boldsymbol{u_i}}{\partial t} + \nabla\left(\frac{1}{2}(u_i^2+v_i^2)+P_i\right) - (f+w_i)\boldsymbol{u_i}^{\perp} = 0. \tag{2.82}$$

Moreover, the horizontal vorticity in each layer is also conservative

$$\frac{\partial w_i}{\partial t} + \nabla\cdot((w_i+f)\boldsymbol{u_i}) = 0. \tag{2.83}$$

Therefore, in the two-dimensional case, there are at least 8 conservative quantities: the height, the velocity and the horizontal vorticity in each layer, the total momentum and the energy e_2:

$$e_2 := \frac{1}{2}\gamma h_1\left(u_1^2+v_1^2+g(h_1+2h_2)\right) + \frac{1}{2}h_2\left(u_2^2+v_2^2+gh_2\right). \tag{2.84}$$

2.5.2 A new augmented model

From equations (2.1–2.2), it is possible to obtain a new model. We denote $(\mathbf{u},\mathbf{v}) \in \mathcal{H}^s(\mathbb{R}^2)^6 \times \mathcal{H}^s(\mathbb{R}^2)^8$, the vectors defined by

$$\begin{cases} \mathbf{u} := {}^{\top}(h_1,h_2,u_1,u_2,v_1,v_2), \\ \mathbf{v} := {}^{\top}(h_1,h_2,u_1,u_2,v_1,v_2,w_1,w_2). \end{cases} \tag{2.85}$$

If $\mathbf{u}$ is a classical solution of (2.4), then $\mathbf{v}$ is solution of the augmented system

$$\frac{\partial \mathbf{v}}{\partial t} + \mathsf{A}_x^{\mathsf{a}}(\mathbf{v})\frac{\partial \mathbf{v}}{\partial x} + \mathsf{A}_y^{\mathsf{a}}(\mathbf{v})\frac{\partial \mathbf{v}}{\partial y} + \mathbf{b}^{\mathbf{a}}(\mathbf{v}) = 0, \tag{2.86}$$

where $\mathsf{A}_x^{\mathsf{a}}(\mathbf{v})$, $\mathsf{A}_y^{\mathsf{a}}(\mathbf{v})$ and $\mathbf{b}^{\mathbf{a}}(\mathbf{v})$ are defined by

$$\mathsf{A}_x^{\mathsf{a}}(\mathbf{v}) := \begin{bmatrix} u_1 & 0 & h_1 & 0 & 0 & 0 & 0 & 0 \\ 0 & u_2 & 0 & h_2 & 0 & 0 & 0 & 0 \\ g & g & u_1 & 0 & v_1 & 0 & 0 & 0 \\ \gamma g & g & 0 & u_2 & 0 & v_2 & 0 & 0 \\ 0 & 0 & 0 & 0 & 0 & 0 & 0 & 0 \\ 0 & 0 & 0 & 0 & 0 & 0 & 0 & 0 \\ 0 & 0 & w_1+f & 0 & 0 & 0 & u_1 & 0 \\ 0 & 0 & 0 & w_2+f & 0 & 0 & 0 & u_2 \end{bmatrix}, \tag{2.87}$$

$$\mathsf{A}_y^{\mathsf{a}}(\mathbf{v}) := \begin{bmatrix} v_1 & 0 & 0 & 0 & h_1 & 0 & 0 & 0 \\ 0 & v_2 & 0 & 0 & 0 & h_2 & 0 & 0 \\ 0 & 0 & 0 & 0 & 0 & 0 & 0 & 0 \\ 0 & 0 & 0 & 0 & 0 & 0 & 0 & 0 \\ g & g & u_1 & 0 & v_1 & 0 & 0 & 0 \\ \gamma g & g & 0 & u_2 & 0 & v_2 & 0 & 0 \\ 0 & 0 & 0 & 0 & w_1+f & 0 & v_1 & 0 \\ 0 & 0 & 0 & 0 & 0 & w_2+f & 0 & v2 \end{bmatrix}, \tag{2.88}$$

$$\begin{aligned} \mathbf{b}^{\mathsf{a}}(\mathbf{v}) := \ & {}^{\top}(0,0,-(w_1+f)v_1,-(w_2+f)v_2,(w_1+f)u_1,(w_2+f)u_2) \\ & +{}^{\top}\left(0,0,g\tfrac{\partial b}{\partial x},g\tfrac{\partial b}{\partial x},g\tfrac{\partial b}{\partial y},g\tfrac{\partial b}{\partial y},0,0\right). \end{aligned} \tag{2.89}$$

Even if the model (2.1–2.2) is not conservative, the model (2.86) is always conservative. Then, there is no need to chose a conservative path in the numerical resolution. *Remarks:* e_2, defined in (2.84), is not an energy of the augmented model (2.86). Although e_2 is a conservative quantity of the augmented model, the function $\mathbf{v} \mapsto e_2(\mathbf{v})$ is never a convex function with the variables $\mathbf{v} := {}^{\top}(h_1,h_2,u_1,u_2,v_1,v_2,w_1,w_2)$ as it is independent of w_1 and w_2: the hessian of this function is never positive-definite.

Proposition 2.5.1 *The augmented model (2.86) verifies the rotational invariance.*

Proof We denote by $\mathsf{A}^{\mathsf{a}}(\mathbf{v},\theta)$ the matrix defined by $\cos(\theta)\mathsf{A}_x^{\mathsf{a}}(\mathbf{v}) + \sin(\theta)\mathsf{A}_y^{\mathsf{a}}(\mathbf{v})$. One can check the next equality, for all $(\mathbf{v},\theta) \in \mathbb{R}^8 \times [0,2\pi]$

$$\mathsf{A}^{\mathsf{a}}(\mathbf{v},\theta) = \mathsf{P}^{\mathsf{a}}(\theta)^{-1}\mathsf{A}_x(\mathsf{P}^{\mathsf{a}}(\theta)\mathbf{v})\mathsf{P}^{\mathsf{a}}(\theta), \tag{2.90}$$

where $\mathsf{P}^{\mathsf{a}}(\theta)$ is the 8×8 matrix defined by

$$\mathsf{P}^{\mathsf{a}}(\theta) := \begin{bmatrix} 1 & 0 & 0 & 0 & 0 & 0 & 0 & 0 \\ 0 & 1 & 0 & 0 & 0 & 0 & 0 & 0 \\ 0 & 0 & \cos(\theta) & 0 & \sin(\theta) & 0 & 0 & 0 \\ 0 & 0 & 0 & \cos(\theta) & 0 & \sin(\theta) & 0 & 0 \\ 0 & 0 & -\sin(\theta) & 0 & \cos(\theta) & 0 & 0 & 0 \\ 0 & 0 & 0 & -\sin(\theta) & 0 & \cos(\theta) & 0 & 0 \\ 0 & 0 & 0 & 0 & 0 & 0 & 1 & 0 \\ 0 & 0 & 0 & 0 & 0 & 0 & 0 & 1 \end{bmatrix}, \tag{2.91}$$

and, moreover, we notice $\mathsf{P}^{\mathsf{a}}(\theta)^{-1} = {}^{\top}\mathsf{P}^{\mathsf{a}}(\theta)$.

2.5.3 The eigenstructure of $\mathsf{A}^{\mathsf{a}}(\mathbf{v},\theta)$

As it was reminded before, the description of the eigenstructure of $\mathsf{A}^{\mathsf{a}}(\mathbf{v},\theta)$ is a decisive point, as it permits to characterize exactly its diagonalizability, for the local well-posedness, and also the *Riemann* invariants with the left eigenvectors, for the treatment of open boundaries for example (see

[14]). According to the rotational invariance (2.90), we restrict the analysis to the eigenstructure of $\mathsf{A}^{\mathsf{a}}_x(\mathbf{v})$. First of all, we define the spectrum of $\mathsf{A}^{\mathsf{a}}_x(\mathbf{v})$ by

$$\sigma(\mathsf{A}^{\mathsf{a}}_x(\mathbf{v})) := \{\nu_i^{\pm},\ i \in [\![1,4]\!]\}. \tag{2.92}$$

As the characteristic polynomial of $\mathsf{A}^{\mathsf{a}}_x(\mathbf{v})$ is equal to

$$\det(\mathsf{A}^{\mathsf{a}}_x(\mathbf{v}) - \mu \mathsf{I}_8) = \mu^2 \det(\mathsf{A}_x(\mathbf{u}) - \mu \mathsf{I}_6), \tag{2.93}$$

we settle down $\nu_4^{\pm} := 0$ and for all $i \in [\![1,3]\!]$ and $\nu_i^{\pm} := \mu_i^{\pm}$. Then, we define $\mathcal{H}^a_\gamma \subset \mathcal{L}^2(\mathbb{R}^2)^8$, the open subset of initial conditions, such that the system (2.86) is hyperbolic:

$$\mathcal{H}^a_\gamma := \left\{ \mathbf{v} : \mathbb{R}^2 \mapsto \mathbb{R}^8 / \mathbf{u} \in \mathcal{H}_\gamma \right\}. \tag{2.94}$$

Proposition 2.5.2 *There exists $\delta > 0$ such that if $\gamma \in]1-\delta, 1[$ and $(\mathbf{v}, \theta) \in \mathcal{H}^a_\gamma \times [0, 2\pi]$. Then, the matrix $\mathsf{A}^{\mathsf{a}}(\mathbf{v}, \theta)$ is diagonalizable.*

Proof With the rotational invariance (2.90), it is equivalent to prove the diagonalizability of $\mathsf{A}^{\mathsf{a}}_x(\mathbf{v})$. By denoting $(\mathbf{e}'_{\mathbf{i}})_{i \in [\![1,8]\!]}$ the canonical basis of $\mathbb{R}^8$, one can prove the right eigenvectors $\boldsymbol{r}^{\nu}_x(\mathbf{u})$ of $\mathsf{A}^{\mathsf{a}}_x(\mathbf{u})$, associated to the eigenvalue $\nu \in \sigma(\mathsf{A}^{\mathsf{a}}_x(\mathbf{u}))$, are defined by

$$\begin{cases} \boldsymbol{r}^{\nu}_x(\mathbf{u}) = & \mathbf{e}'_{\mathbf{1}} + \frac{1}{h_1}((\nu - u_1)\mathbf{e}'_{\mathbf{3}} + (w_1 + f)\mathbf{e}'_{\mathbf{7}}) \\ & -c^r_\nu \left(\mathbf{e}'_{\mathbf{2}} + \frac{1}{h_2}((\nu - u_2)\mathbf{e}'_{\mathbf{4}} + (w_2 + f)\mathbf{e}'_{\mathbf{8}}) \right), & \text{if } \nu \in \{\nu_1^{\pm}, \nu_2^{\pm}\}, \\ \boldsymbol{r}^{\nu}_x(\mathbf{u}) = \mathbf{e}'_{\mathbf{7}}, & & \text{if } \nu = \nu_3^{-}, \\ \boldsymbol{r}^{\nu}_x(\mathbf{u}) = \mathbf{e}'_{\mathbf{8}}, & & \text{if } \nu = \nu_3^{+}, \\ \boldsymbol{r}^{\nu}_x(\mathbf{u}) = & v_1 v_2 (h_2 \mathbf{e}'_{\mathbf{2}} - u_2 \mathbf{e}'_{\mathbf{4}} + (f + w_2)\mathbf{e}'_{\mathbf{8}}) \\ & -g h_2 v_2 \mathbf{e}'_{\mathbf{5}} + v_1 (u_2^2 - g h_2)\mathbf{e}'_{\mathbf{6}}, & \text{if } \nu = \nu_4^{-}, \\ \boldsymbol{r}^{\nu}_x(\mathbf{u}) = & v_1 v_2 (h_1 \mathbf{e}'_{\mathbf{1}} - u_1 \mathbf{e}'_{\mathbf{3}} + (f + w_1)\mathbf{e}'_{\mathbf{7}}) \\ & + v_2 (u_1^2 - g h_1)\mathbf{e}'_{\mathbf{5}} - \gamma g h_1 v_1 \mathbf{e}'_{\mathbf{6}}, & \text{if } \nu = \nu_4^{+}, \end{cases} \tag{2.95}$$

where $c^r_\nu := 1 - \frac{(\nu - u_1)^2}{g h_1}$. Then, the right eigenvectors $\boldsymbol{r}^{\nu}(\mathbf{v}, \theta)$ of $\mathsf{A}^{\mathsf{a}}(\mathbf{v}, \theta)$ are defined by

$$\forall \nu \in \sigma(\mathsf{A}^{\mathsf{a}}(\mathbf{v}, \theta)),\ \boldsymbol{r}^{\nu}(\mathbf{v}, \theta) = \mathsf{P}^{\mathsf{a}}(\theta)^{-1} \boldsymbol{r}^{\nu}_x(\mathsf{P}^{\mathsf{a}}(\theta)\mathbf{v}). \tag{2.96}$$

Moreover, according to the definition of δ, in inequalities (2.75), if $\gamma \in]1-\delta, 1[$, the eigenvalues $\nu_i^{\pm} := \mu_i^{\pm}$, with $i \in \{1,2\}$, are all distinct. A consequence is the right eigenvectors form an eigenbasis of $\mathbb{R}^8$ and $\mathsf{A}^{\mathsf{a}}_x(\mathbf{v})$ is diagonalizable.

Remark: As it was mentioned before, the left eigenvectors $\boldsymbol{l}_x^{\nu}(\mathbf{v})$ of $\mathsf{A}_x^{\mathsf{a}}(\mathbf{v})$, associated to the eigenvalue $\nu \in \sigma(\mathsf{A}_x^{\mathsf{a}}(\mathbf{v}))$, are also interesting. They are defined by:

$$\begin{cases} {}^{\top}\boldsymbol{l}_x^{\nu}(\mathbf{v}) = \begin{array}{l} \nu\frac{\nu-u_1}{h_1}\mathbf{e}_1' + \nu\mathbf{e}_3' + v_1\mathbf{e}_6' \\ -c_\nu^l\left(\nu\frac{\nu-u_2}{h_2}\mathbf{e}_2' - \nu\mathbf{e}_4' - v_2\mathbf{e}_7'\right), \end{array} & \text{if } \nu \in \{\nu_1^{\pm}, \nu_2^{\pm}\}, \\ {}^{\top}\boldsymbol{l}_x^{\nu}(\mathbf{v}) = \mathbf{e}_5', & \text{if } \nu = \nu_4^{-}, \\ {}^{\top}\boldsymbol{l}_x^{\nu}(\mathbf{v}) = \mathbf{e}_6', & \text{if } \nu = \nu_4^{+}, \\ {}^{\top}\boldsymbol{l}_x^{\nu}(\mathbf{v}) = -(f+w_1)\mathbf{e}_1' + h_1\mathbf{e}_7', & \text{if } \nu = \nu_3^{-}, \\ {}^{\top}\boldsymbol{l}_x^{\nu}(\mathbf{v}) = -(f+w_2)\mathbf{e}_2' + h_2\mathbf{e}_8', & \text{if } \nu = \nu_3^{+}, \end{cases} \tag{2.97}$$

where $c_\nu^l := 1 - \frac{(\nu-u_2)^2}{gh_2}$. And the left eigenvectors $\boldsymbol{l}^{\nu}(\mathbf{v},\theta)$ of $\mathsf{A}^{\mathsf{a}}(\mathbf{v},\theta)$ are also defined by

$$\forall \nu \in \sigma\left(\mathsf{A}^{\mathsf{a}}(\mathbf{v},\theta)\right),\ \boldsymbol{l}^{\nu}(\mathbf{v},\theta) = \boldsymbol{l}_x^{\nu}(\mathsf{P}^{\mathsf{a}}(\theta)\mathbf{v})\mathsf{P}^{\mathsf{a}}(\theta). \tag{2.98}$$

Furthermore, the type of the wave associated to each eigenvalue is described in the next proposition.

Proposition 2.5.3 *There exists* $\delta > 0$ *such that if* $\gamma \in]1-\delta, 1[$, *then*

$$\begin{cases} \text{the } \nu_i^{\pm}\text{−characteristic field is genuinely non} - \text{linear}, & \text{if } i \in \{1,2\}, \\ \text{the } \nu_i^{\pm}\text{−characteristic field is linearly degenerate}, & \text{if } i \in \{3,4\}. \end{cases} \tag{2.99}$$

Proof Using the same proof of proposition 2.4.9 and remarking that $\nu_4^{\pm} = 0$, it implies

$$\nabla\nu_4^{\pm} \cdot \boldsymbol{r}_x^{\nu}(\mathbf{v}) = 0, \tag{2.100}$$

and the proposition 2.5.3 is proved.

To conclude, under conditions of the proposition (2.5.3), for all $i \in \{1,2\}$, the $\nu_i^{\pm}$-wave is a shock wave or a rarefaction wave and for all $i \in \{3,4\}$, the $\nu_i^{\pm}$-wave is a contact wave.
Finally, the point is to know if this augmented system (2.86) is locally well-posed and if its solution provides the solution of the non-augmented system (2.4).

Theorem 2.5.4 *There exists* $\delta > 0$ *such that if* $\gamma \in]1-\delta, 1[$, $\mathbf{v}^{\mathbf{0}} \in \mathcal{H}_\gamma^a \cap \mathcal{H}^s(\mathbb{R}^2)^8$. *Then the* Cauchy *problem associated with system* (2.86) *and initial data* $\mathbf{v}^{\mathbf{0}}$, *is locally well-posed in* $\mathcal{H}^s(\mathbb{R}^2)$ *and hyperbolic: there exists* $T > 0$ *such that* $\mathbf{v}$, *the unique solution of the* Cauchy *problem, verifies*

$$\begin{cases} \mathbf{v} \in \mathcal{C}^1([0,T]\times\mathbb{R}^2)^8, \\ \mathbf{v} \in \mathcal{C}([0,T];\mathcal{H}^s(\mathbb{R}^2))^8 \cap \mathcal{C}^1([0,T];\mathcal{H}^{s-1}(\mathbb{R}^2))^8. \end{cases} \tag{2.101}$$

Furthermore, $\mathbf{u}$ *verifies conditions* (2.14) *and is the unique classical solution of the Cauchy problem, associated with* (2.4) *and initial data* $\mathbf{u}^{\mathbf{0}}$, *if and only if*

$$\forall i \in \{1,2\},\ w_i^0 = \frac{\partial v_i^0}{\partial x} - \frac{\partial u_i^0}{\partial y}. \tag{2.102}$$

Proof Using proposition 2.5.2, $\sigma(\mathsf{A}^{\mathsf{a}}(\mathbf{v},\theta)) \subset \mathbb{R}$ and $\mathsf{A}^{\mathsf{a}}(\mathbf{v},\theta)$ is diagonalizable. Then, the proposition 2.2.5 is verified: the hyperbolicity and the local well-posedness of the *Cauchy* problem, associated with system (2.86) and initial data $\mathbf{v^0}$, is insured and conditions (2.101) are verified. Moreover, it is obvious to prove that, for all $i \in \{1,2\}$, there exists $\phi_i : \mathbb{R}^2 \to \mathbb{R}$ such that

$$\forall (t,x,y) \in \mathbb{R}_+ \times \mathbb{R}^2,\ w_i(t,x,y) = \frac{\partial v_i}{\partial x}(t,x,y) - \frac{\partial u_i}{\partial y}(t,x,y) + \phi_i(x,y). \tag{2.103}$$

As ϕ_i does not depend of the time t: $\mathbf{u}$ – the 6^{th} first coordinates of $\mathbf{v}$ – is solution of the non-augmented system (2.4) if and only if $\phi_i = 0$, $\forall i \in \{1,2\}$, which is true if and only if it is verified at $t = 0$.

2.6 Discussions and perspectives

In this article, we proved the hyperbolicity and the local well-posedness, in $\mathcal{H}^s(\mathbb{R}^2)$, of the two-dimensional two-layer shallow water model with free surface with various techniques. All of them use the rotational invariance property (2.8), reducing the problem from two dimensions to one dimension. We gave, at first, a criterion of local well-posedness, in $\mathcal{H}^s(\mathbb{R}^2)$, using the symmetrizability of the system (2.4). Afterwards, the exact set of hyperbolicity of this system was explicitly characterized and compared with the set of symmetrizability. Then, after getting an asymptotic expansion of the eigenvalues, we characterized the type of wave associated to each element of the spectrum of $\mathsf{A}_x(\mathbf{u})$ – shock, rarefaction of contact wave – and we proved the local well-posedness, in $\mathcal{H}^s(\mathbb{R}^2)$, of the system (2.4) under conditions of hyperbolicity and weak density-stratification. Finally, we introduced an augmented model (2.86), adding the horizontal vorticity as a new unknown. We also characterized the type of the waves, proved the local well-posedness in $\mathcal{H}^s(\mathbb{R}^2)$ and explained the link of a solution of the model (2.4) and a solution of the augmented model (2.86).

As shown in this paper, most of the analysis of the two-dimensional two-layer model with free surface is performed explicitly. In the case of n fluids, with $n \geq 3$, it is not possible anymore. Very few results have been proved concerning the general multi-layer model. Most of them are in particular cases, such as [127] and [27] in the three-layer case; [4] in the case $\rho_1 = \ldots = \rho_n$. In the general case, [42] proved the local well-posedness, in one dimension, of the multi-layer model, under conditions of weak stratification in density and velocity. Though, there is no estimate of these stratifications.

Finally, the augmented model was introduced. The *conservativity* of this model avoid choosing a conservative path, introduced in [36], to solve the numerical problem.

I don't believe in mathematics.

A. Einstein discussing with G. Ferrié.

Conclusion

Dans ce chapitre, l'hyperbolicité et le caractère localement bien-posé, du modèle de *Saint-Venant* bi-couches a été démontré. À la différence du modèle à une couche, toutes les vitesses ne sont pas admissibles. En effet, dans le cas à une dimension d'espace, la différence de vitesse, entre les deux couches, doit vérifier certaines conditions, sans être nécessairement bornée. Au contraire, dans le cas à deux dimensions d'espace, ce saut de vitesse doit être borné et doit vérifié une condition similaire à celle rencontrée dans le cas d'un toit rigide.

Un nouveau modèle bi-couches, augmenté de la vorticité, a aussi été introduit. Il a été démontré que ce modèle est aussi hyperbolique et localement bien-posé, sous certaines conditions explicitées. De plus, le lien entre les solutions des modèles bi-couches augmenté et non-augmenté a été démontré : si les solutions sont initialement égales et suffisamment régulières, alors elles sont toujours égales.

Cependant, les résultats démontrés dans ce chapitre, pour le modèle bi-couches, ne sont pas directement déductibles au modèle multi-couches. En effet, les calculs qui ont été menés sont principalement explicite : les racine du polynôme caractéristique sont connues puisque ce n'est qu'un polynôme de degré 6, avec deux racines évidentes. Mais, dans le cas général à n couches, il n'existe pas d'expression simple de ce polynôme, ni de formule de récurrence. À partir des résultats du modèle à n couches, il n'est pas possible d'en déduire des résultats pour le modèle à $n+1$ couches.

Part II

The multi-layer model with free surface

Introduction

Dans ce chapitre, l'étude se focalise sur le modèle général de *Saint-Venant* multi-couches à surface libre. Le plan est le suivant :

- Premièrement, le modèle ainsi que les hypothèses supposées sont rappelées dans l'introduction. Une propriété, qui est à la base des développements de tous les résultats de ce chapitre, est justifiée : l'invariance par rotation. Cette caractéristique du modèle de *Saint-Venant* multi-couches à surface libre, et de nombreux autres modèles physiques, permet de réduire le problème à deux dimensions, à un problème à une dimension,
- Deuxièmement, les définitions d'hyperbolicité et de symétrisabilité sont rappelées, ainsi que leurs liens. Un critère de symétrisabilité du modèle multi-couches est alors déduit : il permet alors de vérifier l'existence de conditions initiales assurant l'hyperbolicité du modèle. Cependant, ce critère est implicite. Pour obtenir une estimation explicite de ce critère, un encadrement de cette condition est effectuée. Il est alors intéressant de savoir si ce critère est optimal ou s'il est possible d'en déduire un nouveau plus général,
- Troisièmement, l'hyperbolicité du modèle est analysée, dans des configurations particulières :
  - toutes les vitesses sont égales,
  - les vitesses de deux couches voisines sont égales,
  - le comportement asymptotique de la fusion de deux couches.

  Cette étude permet de dévoiler une première condition nécessaire à l'hyperbolicité,
- Quatrièmement, les développements asymptotiques des valeurs propres de l'opérateur différentiel, associé au modèle, sont prouvés. Pour les démontrer, il est nécessaire de se placer dans un régime asymptotique particulier :
  - la stratification en densité est supposée faible et représentée par une application injective,
  - la stratification en vitesse doit être en accord avec la condition nécessaire d'hyperbolicité prouvée dans la section précédente,
  - les hauteurs de chaque couche sont supposées du même ordre de grandeur.

Ces développements permettent de déduire un nouveau critère d'hyperbolicité du modèle de *Saint-Venant* multi-couches. Celui-ci est comparé avec le critère de symétrisabilité démontré en début de chapitre. De plus, ce critère général est remarquable : il est de même nature que le critère d'hyperbolicité démontré pour le modèle bi-couches,

- Cinquièmement, les développements asymptotiques des vecteurs propres de l'opérateur différentiel, associé au modèle, sont déterminés. Ils permettent d'en déduire le caractère localement bien-posé du modèle de *Saint-Venant* multi-couches à surface libre. De plus, il est alors possible de caractériser la nature de toutes les ondes associées au modèle,
- Sixièmement, les quantités conservés du modèle multi-couches sont étudiées. Puis, le modèle augmenté de la vorticité, introduit dans le chapitre précédent, est généralisé à n couches. Ce modèle conserve les propriétés du modèle de*Saint-Venant* multi-couches initial, et possède un atout en plus : il est conservatif. L'hyperbolicité et le caractère bien-posé de ce nouveau modèle sont démontrés. Les liens entre les solutions des modèles augmenté et non-augmenté sont démontrés,
- Enfin, la conclusion permet de souligner les résultats prouvés ainsi que les difficultés rencontrées lors de ce chapitre. De plus, l'existence d'invariants de *Riemann*, pour le modèle de *Saint-Venant* multi-couches à surface libre, est abordée.

Ce chapitre a été soumis à publication dans un journal international à comité de lecture. Par conséquent, il n'a pas été retouché et est à lecture indépendante.

3

Local well-posedness of the multi-layer shallow water model with free surface

Contents

3.1 Introduction

We consider n immiscible, homogeneous, inviscid and incompressible superposed fluids, with no surface tension and under the influence of gravity and the *Coriolis* forces; the pressure is assumed to be hydrostatic: Constant at the interface liquid/air (*i.e.* the free surface) and continuous at the interfaces liquid/liquid (*i.e.* the internal surfaces). Moreover, the shallow water assumption is considered in each fluid layer: There exist vertical and horizontal characteristic lengths, for each fluid, and the vertical one is assumed much smaller than the horizontal one.

For more details on the formal derivation of these equations, see [113], [100], [54] (the single-layer model), [80] (the two-layer model with rigid lid), [114], [97], [79] (the two-layer model with free surface). In the *curl*-free case, these models have been obtained rigorously with an asymptotic model of the three-dimensional *Euler* equations, under the shallow water assumption, in [3] for the single-layer model with free surface and in [41] for the two-layer one. This has been obtained in [26] for the single-layer case and without assumption on the vorticity.

Unlike the two-layer model — see [88] — the analysis of the hyperbolicity of the multi-layer model, with $n \geq 3$, cannot be performed explicitly. Very few results have been proved concerning the general multi-layer model. They are in particular cases: [127] and [27] in the three-layer case; [4] in the very particular case $\rho_1 = \ldots = \rho_n$; [6] and [5], where the interfaces between layers have no physical meaning. In the general case, it was proved only the local well-posedness of the model, in one dimension, under conditions of weak density-stratification and weak velocity-stratification (see [42]). Though, there is no explicit estimate of these stratifications, nor asymptotic one: we know there exists conditions such that the multi-layer model with free surface is locally well-posed but we do not know the characterization of these conditions.

The first aim of this paper is to obtain conditions of symmetrizability and hyperbolicity of the multi-layer shallow water model, in order to insure the local well-posedness of the associated *Cauchy* problem. The second aim is to characterize the eigenstructure of the space-differential operator, associated with the model, for the treatment of a well-posed open boundary problem with *characteristic* variables

— see full proof in [21], for the single-layer case. The third aim is to prove the local well-posedness of the new conservative model, and characterize its eigenstructure.
The main result of this paper is, under weak density-stratification and weak velocity-stratification, we obtained an asymptotic expansion of all the eigenvalues associated with the multi-layer model. The interpretation of these expressions is really interesting:

- the eigenvalues, related to the free surface, are asymptotically the same as the single-layer model.
- the eigenvalues, corresponding to an internal surface $i \in [\![1, n-1]\!]$, are asymptotically as the internal eigenvalues of a two-layer model, where the upper layer would be all the layers, directly above the interface i, where the corresponding interface has a density-gap smaller than the density-gap of the interface i, and the lower layer would be all the layers, directly below the interface i, where the corresponding interface has a density-gap smaller than the density-gap of the interface i.

Outline: In section 1, the model is introduced. In section 2, useful definitions are reminded and a sufficient condition of hyperbolicity and local well-posedness in $\mathcal{H}^s(\mathbb{R}^2)$, is given. In section 3, the hyperbolicity of the model is studied in particular cases. In sections 4 and 5, the asymptotic expansion of all the eigenvalues and all the eigenvecotrs is performed, in order to deduce a new necessary condition of local well-podeness in $\mathcal{H}^s(\mathbb{R}^2)$, which will be interpreted as the condition obtained in a two-layer model, and compared to the one proved in section 2. Finally, in the last section, after discussing the conservative quantities of the model and reminding the definition of the horizontal vorticity, a new model is introduced: Benefits of this model are explained, local well-posedness, in $\mathcal{H}^s(\mathbb{R}^2)$, is proved and links, with the multi-layer shallow water model, are fully justified.

3.1.1 Governing equations

Let us introduce ρ_i the constant density of the i^{th} fluid layer, $i \in [\![1, n]\!]$, $h_i(t,X)$ its height and $\boldsymbol{u_i}(t,X) := {}^{\top}(u_i(t,X), v_i(t,X))$ its depth-averaged horizontal velocity, where t denotes the time and $X := (x,y)$ the horizontal cartesian coordinates, as drawn in figure 3.1.
The governing equations of the multi-layer shallow water model with free surface, in two dimensions, is given by a system of $3n$ partial differential equations of 1^{st} order. For all $i \in [\![1, n]\!]$, there is the mass-conservation of the layer i:

$$\frac{\partial h_i}{\partial t} + \nabla \cdot (h_i \boldsymbol{u_i}) = 0, \tag{3.1}$$

whereas equations on the momentum of the layer i:

$$\frac{\partial \boldsymbol{u_i}}{\partial t} + (\boldsymbol{u_i} \cdot \nabla)\boldsymbol{u_i} + \nabla P_i - f \boldsymbol{u_i}^{\perp} = 0, \tag{3.2}$$

where $P_i := g\big(b + \sum_{k=1}^{n} \alpha_{i,k} h_k\big)$, $\boldsymbol{u_i^{\perp}} := {}^{\top}(v_i, -u_i)$, g is the gravitational acceleration, b is the bottom topography, f is the *Coriolis* parameter and

$$\alpha_{i,k} = \begin{cases} \frac{\rho_k}{\rho_i}, & k < i, \\ 1, & k \geq i. \end{cases} \tag{3.3}$$

A useful notation is introduced, for all $i \in [\![1, n-1]\!]$, γ_i is defined by:

$$\gamma_i := \frac{\rho_i}{\rho_{i+1}}, \tag{3.4}$$

and is the density ratio between the layer i and the layer $i+1$. Then, if $k \leq i-1$, the ratio $\frac{\rho_k}{\rho_i}$ is equal to

$$\frac{\rho_k}{\rho_i} = \prod_{j=k}^{i-1} \gamma_j, \tag{3.5}$$

the vector $\boldsymbol{\gamma}$ will denote ${}^{\top}(\gamma_1, \ldots, \gamma_{n-1}) \in \mathbb{R}_+^{n-1}$ and the vector $\mathbf{h}$ will be equal to ${}^{\top}(h_1, \ldots, h_n) \in \mathbb{R}_+^n$.
Remark: At this point, no assumption is made over the range of ρ_i and an interesting consequence of the expansion, made in this paper, will be to verify the *Rayleigh-Taylor* stability (*i.e.* $\rho_n > \rho_{n-1} > \ldots > \rho_1 > 0$).

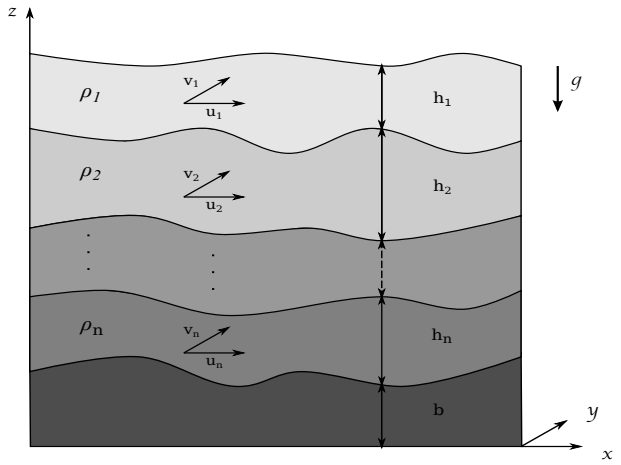

Figure 3.1: Configuration of the multi-layer shallow water model with free surface

Moreover, with $i \in [\![1, n]\!]$ and M a $n \times n$ matrix, we denote by $\mathrm{C}_i(\mathsf{M})$ and $\mathrm{L}_i(\mathsf{M})$ respectively the i^{th} column and the i^{th} line of M. We will denote the total depth by

$$H := \sum_{i=1}^{n} h_i, \tag{3.6}$$

and the average velocity in each direction by

$$\begin{cases} \bar{u} := \frac{1}{H} \sum_{i=1}^{n} h_i u_i, \\ \bar{v} := \frac{1}{H} \sum_{i=1}^{n} h_i v_i. \end{cases} \tag{3.7}$$

In order to get rid of the constant g, in the following analysis, we proceed the following rescaling:

$$\forall i \in [\![1, n-1]\!], \begin{cases} \hat{h}_i \leftarrow g h_i, \\ \hat{u}_i \leftarrow u_i, \\ \hat{v}_i \leftarrow v_i, \end{cases} \tag{3.8}$$

and in order to simplify the notations, $\hat{}$ will be removed. Then, with the vector

$$\mathbf{u} := {}^{\top}(h_1, \ldots, h_n, u_1, \ldots, u_n, v_1, \ldots, v_n), \tag{3.9}$$

the 1st order quasi-linear partial differential equations system (3.1-3.2) can be written as

$$\frac{\partial \mathbf{u}}{\partial t} + \mathsf{A}_x(\mathbf{u}, \boldsymbol{\gamma}) \frac{\partial \mathbf{u}}{\partial x} + \mathsf{A}_y(\mathbf{u}, \boldsymbol{\gamma}) \frac{\partial \mathbf{u}}{\partial y} + \mathbf{b}(\mathbf{u}) = 0, \tag{3.10}$$

where the $3n \times 3n$ block matrices $\mathsf{A}_x(\mathbf{u}, \boldsymbol{\gamma})$, $\mathsf{A}_y(\mathbf{u}, \boldsymbol{\gamma})$ and the vector $\mathbf{b}(\mathbf{u}) \in \mathbb{R}^{3n}$ are defined by

$$\mathsf{A}_x(\mathbf{u}, \boldsymbol{\gamma}) := \left[\begin{array}{c|c|c} \mathsf{V}_x & \mathsf{H} & 0 \\ \hline \Gamma & \mathsf{V}_x & 0 \\ \hline 0 & 0 & \mathsf{V}_x \end{array}\right], \mathsf{A}_y(\mathbf{u}, \boldsymbol{\gamma}) := \left[\begin{array}{c|c|c} \mathsf{V}_y & 0 & \mathsf{H} \\ \hline 0 & \mathsf{V}_y & 0 \\ \hline \Gamma & 0 & \mathsf{V}_y \end{array}\right], \tag{3.11}$$

$$\mathbf{b}(\mathbf{u}) := {}^{\top}\left(0, \ldots, 0, -f v_1 + \frac{\partial b}{\partial x}, \ldots, -f v_n + \frac{\partial b}{\partial x}, f u_1 + \frac{\partial b}{\partial y}, f u_n + \frac{\partial b}{\partial y}\right), \tag{3.12}$$

with the $n \times n$ block matrices

$$\begin{cases} \mathsf{V}_x & := \mathrm{diag}[u_i]_{i \in [\![1,n]\!]}, \\ \mathsf{V}_y & := \mathrm{diag}[v_i]_{i \in [\![1,n]\!]}, \\ \mathsf{H} & := \mathrm{diag}[h_i]_{i \in [\![1,n]\!]}, \\ \Gamma & := [\alpha_{i,k}]_{(i,k) \in [\![1,n]\!]^2}, \end{cases} \tag{3.13}$$

where $\mathrm{diag}[x_i]_{i \in [\![1,n]\!]}$ is the $n \times n$ diagonal matrix with $(x_1, \ldots, x_n)$ on the diagonal.

As it will be reminded in the next subsections, the hyperbolicity of the model is an interesting property to prove the local well-posedness. The study of the hyperbolicity of the model (3.10) is well-known in the case $n = 1$: there are 3 waves, in each direction, which are well-defined if the height remains strictly positive. In the case $n = 2$: if $\rho_1 > \rho_2$, the model is never hyperbolic, and if $\rho_1 = \rho_2$ the model is so if and only if $u_2 = u_1$, as proved in [4]. Moreover, in [88], an exact characterization of the domain of hyperbolicity of the model (3.10) was proved: unlike the one-dimensional model, the hyperbolicity of the two-dimensional model is verified if the shear velocity $|u_2 - u_1|^2 + |v_2 - v_1|^2$ is bounded by a positive parameter, ${F_{crit}^-}^2$, depending only on $\gamma_1 = \frac{\rho_1}{\rho_2}$, h_1 and h_2. In the *Boussinesq* approximation (*i.e.* $1 - \gamma_1 \ll 1$), the asymptotic expansion of this parameter is:

$${F_{crit}^-}^2 = (h_1 + h_2)(1 - \gamma_1) + o(1 - \gamma_1). \tag{3.14}$$

This condition, also explained in [30], [43], [127] and [136], can be interpreted as a physical instability condition — also known as *Kelvin-Helmoltz* stability — and if it is not verified, the equations have

exponential growing solutions. In the general case $n \geq 3$, appart from the formal study in [50] and the particular case in [34], there is no result of hyperbolicity. In order to treat this lack of hyperbolicity, several numerical methods have been proposed in [1], [17] and [48].

Remark: The multi-layer shallow water model, with free surface, describes fluids such as the ocean: the evolution of the density can be assumed piecewise-constant (which is verified), the horizontal characteristic length is much greater than the vertical one and the pressure can be expected only dependent of the height of fluid. This model is used by the *French Naval Hydrographic and Oceanographic Service*, with 40 layers, to provide the underwater weather forecast in the bay of Biscay, for example.

3.1.2 Rotational invariance

As the multi-layer shallow water model with free surface is based on physical partial differential equations, it verifies the so-called rotational invariance: the $3n \times 3n$ matrix

$$\mathsf{A}(\mathbf{u},\boldsymbol{\gamma},\theta) := \cos(\theta)\mathsf{A}_x(\mathbf{u},\boldsymbol{\gamma}) + \sin(\theta)\mathsf{A}_y(\mathbf{u},\boldsymbol{\gamma}) \tag{3.15}$$

depends only on the matrix $\mathsf{A}_x(\mathbf{u},\boldsymbol{\gamma})$ and the parameter θ. Indeed, there is the following relation:

$$\forall(\mathbf{u},\boldsymbol{\gamma},\theta) \in \mathbb{R}^{3n} \times {\mathbb{R}_+^*}^{n-1} \times [0,2\pi],\ \mathsf{A}(\mathbf{u},\boldsymbol{\gamma},\theta) = \mathsf{P}(\theta)^{-1}\mathsf{A}_x\left(\mathsf{P}(\theta)\mathbf{u},\boldsymbol{\gamma}\right)\mathsf{P}(\theta), \tag{3.16}$$

where the $3n \times 3n$ matrix $\mathsf{P}(\theta)$ is defined by

$$\mathsf{P}(\theta) := \left[\begin{array}{c|c|c} \mathsf{I_n} & 0 & 0 \\ \hline 0 & \cos(\theta)\mathsf{I_n} & \sin(\theta)\mathsf{I_n} \\ \hline 0 & -\sin(\theta)\mathsf{I_n} & \cos(\theta)\mathsf{I_n} \end{array}\right]. \tag{3.17}$$

Notice that $\mathsf{P}(\theta)^{-1} = {}^{\top}\mathsf{P}(\theta)$. The equality (3.16) will permit to simplify the analysis of $\mathsf{A}(\mathbf{u},\boldsymbol{\gamma},\theta)$ to the analysis of $\mathsf{A}_x(\mathbf{u},\boldsymbol{\gamma})$.

3.2 Well-posedness of the model: a first criterion

In this section, we remind useful criteria of local well-posedness in $\mathcal{L}^2(\mathbb{R}^2)^{3n}$, also called hyperbolicity, and in $\mathcal{H}^s(\mathbb{R}^2)^{3n}$. Connections between each one will be given and a 1st criterion of local well-posedness of the system (3.10) will be deduced.

3.2.1 Hyperbolicity

First, we give the definition of hyperbolicity, then a useful criterion of this property and an important property of hyperbolic problem. We will consider the euclidean space $(\mathcal{L}^2(\mathbb{R}^2)^{3n}, \|\cdot\|_{\mathcal{L}^2})$.

Definition (Hyperbolicity) Let $\mathbf{u} \in \mathcal{L}^2(\mathbb{R}^2)^{3n}$ and $\boldsymbol{\gamma} \in {\mathbb{R}_+^*}^{n-1}$. The system (3.10) is hyperbolic if and only if

$$\exists\, c > 0,\ \forall \theta \in [0, 2\pi],\ \sup_{\tau \in \mathbb{R}} \| \exp\left(-i\tau \mathsf{A}(\mathbf{u}, \boldsymbol{\gamma}, \theta)\right) \|_{\mathcal{L}^2} \leq c. \tag{3.18}$$

A useful criterion of hyperbolicity is in the next proposition:

Proposition 3.2.1 *Let* $\mathbf{u} \in \mathcal{L}^2(\mathbb{R}^2)^{3n}$ *and* $\boldsymbol{\gamma} \in {\mathbb{R}_+^*}^{n-1}$. *The system* (3.10) *is hyperbolic if and only if*

$$\forall (X, \theta) \in \mathbb{R}^2 \times [0, 2\pi],\ \sigma\left(\mathsf{A}(\mathbf{u}(X), \boldsymbol{\gamma}, \theta)\right) \subset \mathbb{R}. \tag{3.19}$$

Proof See in [117] in the case of a diagonalisable matrix. In the general case, considering $\mathsf{M} \in \mathcal{M}_n(\mathbb{R})$ a $n \times n$ matrix, then for all eigenvalue $\lambda \in \sigma(\mathsf{M})$, $\exp(\lambda)$ is an eigenvalue of the matrix $\exp(\mathsf{M})$ and we have also :

$$\rho(\mathsf{M}) \leq \|\mathsf{M}\|.$$

Then, for all $\lambda \in \sigma\left(\mathsf{A}(\mathbf{u}, \boldsymbol{\gamma}, \theta)\right)$, $\exp\left(-i\tau\lambda\right) \in \sigma\left(\exp\left(-i\tau \mathsf{A}(\mathbf{u}, \boldsymbol{\gamma}, \theta)\right)\right)$. Consequently, (3.19) is a necessary condition to ensure the existence of a constant number $c > 0$ such that

$$\forall \theta \in [0, 2\pi],\ \sup_{\tau \in \mathbb{R}} \| \exp\left(-i\tau \mathsf{A}(\mathbf{u}, \boldsymbol{\gamma}, \theta)\right) \|_{\mathcal{L}^2} \leq c,$$

Moreover, it is obvious that (3.19) is also a sufficient condition of hyperbolicity.

Remark: If the matrix $\mathsf{A}(\mathbf{u}, \boldsymbol{\gamma}, \theta)$ admits n distinct eigenvalues, the system (3.10) belongs to the strictly hyperbolic systems.

Proposition 3.2.2 *Let* $\mathbf{u} : \mathbb{R}^2 \to \mathbb{R}^{3n}$ *a constant function. If the system* (3.10) *is hyperbolic, then the* Cauchy *problem, associated with the linear system*

$$\frac{\partial \mathbf{v}}{\partial t} + \mathsf{A}_x(\mathbf{u}) \frac{\partial \mathbf{v}}{\partial x} + \mathsf{A}_y(\mathbf{u}) \frac{\partial \mathbf{v}}{\partial y} = 0, \tag{3.20}$$

and the initial data $\mathbf{v^0} \in \mathcal{L}^2(\mathbb{R}^2)^{3n}$, *is well-posed in* $\mathcal{L}^2(\mathbb{R}^2)^{3n}$ *and the unique solution* $\mathbf{v}$ *is such that*

$$\begin{cases} \forall\, T > 0,\ \exists\, c_T > 0,\ \sup_{t \in [0,T]} \|\mathbf{v}(t)\|_{\mathcal{L}^2} \leq c_T \|\mathbf{v^0}\|_{\mathcal{L}^2}, \\ \mathbf{v} \in \mathcal{C}(\mathbb{R}_+; \mathcal{L}^2(\mathbb{R}^2))^{3n}. \end{cases} \tag{3.21}$$

Remark: An interesting property of hyperbolic problems is the conservation of this property under $\mathcal{C}^1$ change of variables. More details about the main properties of hyperbolicity in [117].

3.2.2 Symmetrizability

In order to prove the local well-posedeness of the model (3.10), in $\mathcal{H}^s(\mathbb{R}^2)^{3n}$, we give below a useful criterion.

Definition (Symmetrizability) Let $\mathbf{u} \in \mathcal{H}^s(\mathbb{R}^2)^{3n}$. If there exists a $\mathcal{C}^\infty$ mapping $\mathsf{S} : \mathcal{H}^s(\mathbb{R}^2)^{3n} \times [0,2\pi] \to \mathcal{M}_{3n}(\mathbb{R})$ such that for all $\theta \in [0,2\pi]$,

1. $\mathsf{S}(\mathbf{u},\boldsymbol{\gamma},\theta)$ is symmetric,
2. $\mathsf{S}(\mathbf{u},\boldsymbol{\gamma},\theta)$ is positive-definite,
3. $\mathsf{S}(\mathbf{u},\boldsymbol{\gamma},\theta)\mathsf{A}(\mathbf{u},\theta)$ is symmetric.

Then, the model (3.10) is said symmetrizable and the mapping S is called a symbolic-symmetrizer.

Proposition 3.2.3 *Let $s > 2$ and $\mathbf{u^0} \in \mathcal{H}^s(\mathbb{R}^2)^{3n}$. If the model (3.10) is symmetrizable, then the* Cauchy *problem, associated with (3.10) and initial data $\mathbf{u^0}$, is locally well-posed in $\mathcal{H}^s(\mathbb{R}^2)^{3n}$. Furthermore, there exists $T > 0$ such that the unique solution $\mathbf{u}$ verifies*

$$\begin{cases} \mathbf{u} \in \mathcal{C}^1([0,T] \times \mathbb{R}^2)^{3n}, \\ \mathbf{u} \in \mathcal{C}([0,T];\mathcal{H}^s(\mathbb{R}^2))^{3n} \cap \mathcal{C}^1([0,T];\mathcal{H}^{s-1}(\mathbb{R}^2))^{3n}. \end{cases} \tag{3.22}$$

Remark: The proof of the last proposition is in [12], for instance.
In this paper, the model (3.1–3.2) is expressed with the variables $(h_i, \boldsymbol{u_i})$ with $i \in [\![1,n]\!]$. However, we could have worked with the unknowns h_i and $\boldsymbol{q_i} := h_i\boldsymbol{u_i}$, as it is well-known this quantities are conservative in the one-dimensional case. However, in the particular case of the multi-layer shallow water model with free surface, it is not true: The multi-layer model, in one space-dimension, is conservative with $(h_i, \boldsymbol{u_i})$ variables and not conservative with $(h_i, \boldsymbol{q_i})$ variables.
As it was noticed in [117], if the model is conservative and has a total energy, there exists a natural symmetrizer: the hessian of this total energy. In one dimension, the total energy of the model (3.10) is defined, modulo a constant, by

$$e_1(\mathbf{u},\boldsymbol{\gamma}) := \frac{1}{2}\sum_{i=1}^{n} \alpha_{n,i} h_i \left(u_i^2 + h_i\right) + \sum_{i=1}^{n-1}\sum_{j=i+1}^{n} \alpha_{n,i} h_i h_j. \tag{3.23}$$

As the model (3.1–3.2), in one space-dimension and variables $(h_i, \boldsymbol{u_i})$, is conservative, it is straightforward the hessian of e_1 is a symmetrizer of the one-dimensional model. However, it is not anymore a symmetrizer with the non-conservative variables $(h_i, \boldsymbol{q_i})$. This is another reason the analysis, in

this paper, is performed with variables $(h_i, \boldsymbol{u_i})$. Moreover, as the two-dimensional model is not conservative, the symmetrizer S, defined in definition 3.2.2, is not the hessian of the total energy of the two-dimensional model

$$e_2(\mathbf{u},\boldsymbol{\gamma}) := \frac{1}{2}\sum_{i=1}^{n} \alpha_{n,i} h_i \left(u_i^2 + v_i^2 + h_i\right) + \sum_{i=1}^{n-1}\sum_{j=i+1}^{n} \alpha_{n,i} h_i h_j. \tag{3.24}$$

This is why the symmetrizer is called symbolic: it will depend on θ. If it does not depend on (such as the irrotational model in two dimensions), the symmetrizer is called *Friedrichs*-symmetrizer.

Remarks: 1) In all this paper, the parameter $s \in \mathbb{R}$ is assumed such that

$$s > 1 + \frac{d}{2}, \tag{3.25}$$

where $d := 2$ is the space-dimension. 2) The criterion (3.19) is a necessary condition of hyperbolicity, whereas the symmetrizability is a sufficient condition of local well-posedness in $\mathcal{H}^s(\mathbb{R}^2)^{3n}$.

3.2.3 Connections between hyperbolicity and symmetrizability

In this subsection, we do not formulate all the connections between these two types of local well-posedness but only the useful ones for this paper.

Proposition 3.2.4 *If the system* (3.10) *is symmetrizable, then it is hyperbolic.*

Remark: This property is obvious in the linear case, with the change of variables $\tilde{\mathbf{u}} := \mathsf{S}(\mathbf{u^0},\boldsymbol{\gamma},\theta)\mathbf{u}$. See [12] and [117] for more details.

Proposition 3.2.5 *Let* $(\mathbf{u^0},\boldsymbol{\gamma}) \in \mathcal{H}^s(\mathbb{R}^2)^{3n} \times {\mathbb{R}_+^*}^{n-1}$ *such that the model is hyperbolic and for all* $\theta \in [0,2\pi]$*, the matrix* $\mathsf{A}(\mathbf{u^0},\boldsymbol{\gamma},\theta)$ *is diagonalizable. Then, the system* (3.10) *is symmetrizable and the unique solution verifies the conditions* (3.22)*.*

Proof Let $\mu \in \sigma(\mathsf{A}(\mathbf{u^0},\boldsymbol{\gamma},\theta))$, we denote $\mathsf{P}^\mu(\mathbf{u^0},\boldsymbol{\gamma},\theta)$ the projection onto the μ-eigenspace of $\mathsf{A}(\mathbf{u^0},\boldsymbol{\gamma},\theta)$. One can construct a symbolic-symmetrizer:

$$\mathsf{S}_1(\mathbf{u^0},\boldsymbol{\gamma},\theta) := \sum_{\mu\in\sigma(\mathsf{A}(\mathbf{u^0},\boldsymbol{\gamma},\theta))} {}^{\top}\mathsf{P}^\mu(\mathbf{u^0},\boldsymbol{\gamma},\theta)\mathsf{P}^\mu(\mathbf{u^0},\boldsymbol{\gamma},\theta). \tag{3.26}$$

Then, $\mathsf{S}_1(\mathbf{u^0},\boldsymbol{\gamma},\theta)$ verifies conditions of the proposition 3.2.3 because $\mathsf{A}(\mathbf{u^0},\boldsymbol{\gamma},\theta)$ is diagonalizable — which implies $\mathsf{S}_1(\mathbf{u^0},\boldsymbol{\gamma},\theta)$ induces a scalar product on $\mathbb{R}^{3n}$ — and the spectrum of $\mathsf{A}(\mathbf{u^0},\boldsymbol{\gamma},\theta)$ is a subset of $\mathbb{R}$. Then, proposition 3.2.3 implies the well-posedness of the system (3.10), in $\mathcal{H}^s(\mathbb{R}^2)^{3n}$, and there exists $T > 0$ such that conditions (3.22) are verified.

To conclude, the analysis of the eigenstrusture of $\mathsf{A}(\mathbf{u},\boldsymbol{\gamma},\theta)$ is a crucial point, in order to provide its diagonalizability. Moreover, it provides also the characterization of the *Riemann* invariants (see [118] and [133]), which is an important benefit for numerical resolution.

Remark: The proposition (3.2.5) was proved in [130], in the particular case of a strictly hyperbolic model (*i.e.* all the eigenvalues are real and distinct).

3.2.4 A first criterion of local well-posedness

According to the proposition 3.2.4, the symmetrizability implies the hyperbolicity. Then, we give a rough criterion of symmetrizability to insure the well-posedness in $\mathcal{H}^s(\mathbb{R}^2)^{3n}$ and $\mathcal{L}^2(\mathbb{R}^2)^{3n}$.

Theorem 3.2.6 *Let $s > 2$ and $(\mathbf{u^0},\boldsymbol{\gamma}) \in \mathcal{H}^s(\mathbb{R}^2)^{3n}\times]0,1[^{n-1}$. There exists a sequence $(\delta_i(\mathbf{h},\boldsymbol{\gamma}))_{i\in[\![1,n]\!]} \subset \mathbb{R}_+^*$ such that*

$$\forall\, i \in [\![1,n]\!],\ \begin{cases} \inf_{X\in\mathbb{R}^2} h_i^0(X) > 0, \\ \inf_{X\in\mathbb{R}^2} \delta_i(\mathbf{h^0}(X),\boldsymbol{\gamma}) - |u_i^0(X)-\bar{u}^0(X)|^2 - |v_i^0(X)-\bar{v}^0(X)|^2 > 0, \end{cases} \tag{3.27}$$

then, the Cauchy *problem, associated with the system* (3.10) *and the initial data $\mathbf{u^0}$, is hyperbolic, locally well-posed in $\mathcal{H}^s(\mathbb{R}^2)^{3n}$ and the unique solution verifies conditions* (3.22)*.*

Proof First, we prove the next lemma.

Lemma 3.2.7 *Let $\boldsymbol{\gamma}\in{\mathbb{R}_+^*}^{n-1}$, $\mathcal{S}$ an open subset of $\mathcal{H}^s(\mathbb{R}^2)^{3n}$ and $\mathsf{S}_x(\mathbf{u},\boldsymbol{\gamma})$ be a symmetric matrix such that $\mathsf{S}_x(\mathbf{u},\boldsymbol{\gamma})\mathsf{A}_x(\mathbf{u},\boldsymbol{\gamma})$ is symmetric. If there exists $\mathbf{u^0}\in\mathcal{S}$ such that*

$$\forall\theta\in[0,2\pi],\ \mathsf{S}_x(P(\theta)\mathbf{u^0},\boldsymbol{\gamma}) > 0, \tag{3.28}$$

then the Cauchy *problem, associated with system* (3.10) *and initial data $\mathbf{u^0}$, is hyperbolic, locally well-posed in $\mathcal{H}^s(\mathbb{R}^2)^{3n}$ and the unique solution verifies conditions* (3.22)*.*

Proof We consider $\mathbf{u^0}\in\mathcal{S}$ such that

$$\forall (X,\theta)\in\mathbb{R}^2\times[0,2\pi],\ \mathsf{S}_x(\mathsf{P}(\theta)\mathbf{u^0}(X),\boldsymbol{\gamma}) > 0. \tag{3.29}$$

We define the mapping

$$\mathsf{S} : (\mathbf{u},\boldsymbol{\gamma},\theta) \mapsto \mathsf{P}(\theta)^{-1}\mathsf{S}_x(\mathsf{P}(\theta)\mathbf{u},\boldsymbol{\gamma})\mathsf{P}(\theta). \tag{3.30}$$

Then, using the rotational invariance (3.16), the mapping S verifies assumptions of the definition 3.2.2, with $\mathbf{u^0}\in\mathcal{H}^s(\mathbb{R}^2)^{3n}$, and S is a symbolic-symmetrizer of the system (3.10).

As it was noticed before, the one-dimensional multi-layer model, with variables (h_i,u_i) is conservative: a natural symmetrizer of this model is the hessian of the total energy e_1. The next matrix defines

a symbolic-symmetrizer of the two-dimensional model — using the mapping (3.30) — and it has been constructed from the *Friedrichs*-symmetrizer of the one-dimensional model:

$$\mathsf{S}_x(\mathbf{u},\boldsymbol{\gamma},u_0) = \left[\begin{array}{c|c|c} \Delta\Gamma & \Delta(\mathsf{V}_x - u_0\mathsf{I}_\mathsf{n}) & 0 \\ \hline \Delta(\mathsf{V}_x - u_0\mathsf{I}_\mathsf{n}) & \Delta\mathsf{H} & 0 \\ \hline 0 & 0 & \Delta\mathsf{H} \end{array}\right], \tag{3.31}$$

where $\Delta := \mathrm{diag}(\alpha_{n,1},\dots,\alpha_{n,n-1},1)$ and $u_0 \in \mathbb{R}$ is a parameter, which will be chosen in order to simplify the calculus.

Remark: If $u_0 = 0$, the matrix

$$\left[\begin{array}{c|c} \Delta\Gamma & \Delta(\mathsf{V}_x - u_0\mathsf{I}_\mathsf{n}) \\ \hline \Delta(\mathsf{V}_x - u_0\mathsf{I}_\mathsf{n}) & \Delta\mathsf{H} \end{array}\right], \tag{3.32}$$

is exactly the hessian of the total energy e_1.

Moreover, we introduce the $3n \times 3n$ symmetric matrix $\mathsf{S}_x^0(\mathbf{h},\boldsymbol{\gamma})$ defined by

$$\mathsf{S}_x^0(\mathbf{h},\boldsymbol{\gamma}) := \left[\begin{array}{c|c|c} \Delta\Gamma & 0 & 0 \\ \hline 0 & \Delta\mathsf{H} & 0 \\ \hline 0 & 0 & \Delta\mathsf{H} \end{array}\right], \tag{3.33}$$

and prove the next lemma.

Lemma 3.2.8 *Let* $(\mathbf{h},\boldsymbol{\gamma}) \in \mathbb{R}_+^n \times \mathbb{R}_+^{*\,n-1}$. $\mathsf{S}_x^0(\mathbf{h},\boldsymbol{\gamma})$ *is positive-definite if and only if*

$$\left\{\begin{array}{ll} h_i > 0, & \forall\, i \in [\![1,n]\!], \\ 1 > \gamma_i > 0, & \forall\, i \in [\![1,n-1]\!]. \end{array}\right. \tag{3.34}$$

Proof First of all, it is clear $\mathsf{S}_x^0(\mathbf{h},\boldsymbol{\gamma})$ is positive-definite if and only if $\Delta\Gamma$ and $\Delta\mathsf{H}$ are positive-definite. Then, as $\Delta\mathsf{H} := \mathrm{diag}(\alpha_{n,i}h_i)$, it is positive-definite if and only if

$$\forall i \in [\![1,n]\!],\ \alpha_{n,i}h_i > 0. \tag{3.35}$$

Moreover, using the *Sylvester*'s criterion, $\Delta\Gamma := [\alpha_{n,\min(i,j)}]_{(i,j)\in[\![1,n]\!]^2}$ is positive-definite if and only if all the leading principal minors are strictly positive:

$$\forall k \in [\![1,n]\!],\ m_k := \det[\alpha_{n,\min(i,j)}]_{(i,j)\in[\![1,k]\!]^2} > 0. \tag{3.36}$$

Let $k \in [\![1,n]\!]$, performing the following elementary operations on the columns of $\det(\Delta\Gamma)$:

$$\forall\, i \in [\![1,n-1]\!],\ \mathrm{C}_i(\Delta\Gamma) \leftarrow \mathrm{C}_i(\Delta\Gamma) - \mathrm{C}_{i+1}(\Delta\Gamma), \tag{3.37}$$

and expanding this determinant along the 1^{st} line, we deduce the expression of m_k:

$$\left\{\begin{array}{ll} m_k = \alpha_{n,1}, & \text{if } k = 1, \\ m_k = \alpha_{n,1}\prod_{i=1}^{k-1}(\alpha_{n,i+1} - \alpha_{n,i}), & \text{if } k \in [\![2,n]\!]. \end{array}\right. \tag{3.38}$$

Consequently, it is obvious that

$$\forall k \in [\![1,n]\!],\ m_k > 0 \Longleftrightarrow \begin{cases} \alpha_{n,1} > 0, \\ \alpha_{n,k+1} - \alpha_{n,k} > 0, \quad \forall\, k \in [\![2,n]\!]. \end{cases} \tag{3.39}$$

As for all $k \in [\![1,n]\!]$, $\alpha_{n,k} := \frac{\rho_k}{\rho_n}$ and ρ_n is assumed strictly positive, S_x^0 is positive-definite if and only if conditions (3.34) are verified.

Finally, using lemmata 3.2.7–3.2.8, we can prove the theorem 3.2.6. One can check that $\mathsf{S}_x(\mathbf{u},\boldsymbol{\gamma},u_0)$ and $\mathsf{S}_x(\mathbf{u},\boldsymbol{\gamma},u_0)\mathsf{A}_x(\mathbf{u},\boldsymbol{\gamma})$ are unconditionally symmetric:

$$\mathsf{S}_x(\mathbf{u},\boldsymbol{\gamma},u_0)\mathsf{A}_x(\mathbf{u},\boldsymbol{\gamma}) := \left[\begin{array}{c|c|c} \Delta\Gamma(2\mathsf{V}_x - u_0\mathsf{I_n}) & \mathsf{S}_x^1(\mathbf{u},\boldsymbol{\gamma},u_0) & 0 \\ \hline \mathsf{S}_x^1(\mathbf{u},\boldsymbol{\gamma},u_0) & \Delta\mathsf{H}(2\mathsf{V}_x - u_0\mathsf{I_n}) & 0 \\ \hline 0 & 0 & \Delta\mathsf{H}\mathsf{V}_x \end{array}\right], \tag{3.40}$$

where $\mathsf{S}_x^1(\mathbf{u},\boldsymbol{\gamma},u_0) := \Delta(\Gamma\mathsf{H} + (\mathsf{V}_x - u_0\mathsf{I_n})\mathsf{V}_x)$. As we need to chose a reference velocity u_0, we decide to set $u_0 := \bar{u}$, the average velocity. Moreover, if $(\mathbf{u},\boldsymbol{\gamma}) \in \mathcal{H}^s(\mathbb{R}^2) \times {\mathbb{R}_+^*}^{n-1}$ are such that

$$\begin{cases} u_i(X) = \bar{u}(X), & \forall X \in \mathbb{R}^2,\ \forall i \in [\![1,n]\!], \\ \inf_{X\in\mathbb{R}^2} h_i(X) > 0, & \forall i \in [\![1,n]\!], \\ 1 > \gamma_i > 0, & \forall i \in [\![1,n-1]\!], \end{cases} \tag{3.41}$$

then, $\mathsf{S}_x(\mathbf{u},\boldsymbol{\gamma},\bar{u}) = \mathsf{S}_x^0(\mathbf{h},\boldsymbol{\gamma})$ and, according to the lemma 3.2.8,

$$\forall X \in \mathbb{R}^2,\ \mathsf{S}_x(\mathbf{u}(X),\boldsymbol{\gamma},\bar{u}(X)) > 0. \tag{3.42}$$

Then, if $(\mathbf{u},\boldsymbol{\gamma})$ verifies

$$\begin{cases} \inf_{X\in\mathbb{R}^2} h_i(X) > 0, & \forall\, i \in [\![1,n]\!], \\ 1 > \gamma_i > 0, & \forall\, i \in [\![1,n-1]\!], \end{cases} \tag{3.43}$$

as all the eigenvalues of $\mathsf{S}_x(\mathbf{u},\boldsymbol{\gamma},\bar{u})$ depend continuously on the parameter $\mathbf{u}$, the matrix $\mathsf{S}_x(\mathbf{u},\boldsymbol{\gamma},\bar{u})$ remains positive-definite if $u_i - \bar{u}$ is sufficiently small, for all $i \in [\![1,n]\!]$: this insures the existence of the sequence $(\delta_i(\mathbf{h},\boldsymbol{\gamma}))_{i\in[\![1,n]\!]} \subset \mathbb{R}_+^*$ such that

$$\forall i \in [\![1,n]\!],\ \inf_{X\in\mathbb{R}^2} \delta_i(\mathbf{h}(X),\boldsymbol{\gamma}) - |u_i(X) - \bar{u}(X)|^2 > 0 \Rightarrow \mathsf{S}_x(\mathbf{u}(X),\boldsymbol{\gamma},\bar{u}(X)) > 0. \tag{3.44}$$

Moreover, these quantities depend only on the parameters of $\mathsf{S}_x^0(\mathbf{h},\boldsymbol{\gamma})$: $\mathbf{h}$ and $\boldsymbol{\gamma}$. In order to use the lemma 3.2.7, we remark that if for all $\theta \in [0,2\pi]$,

$$\inf_{X\in\mathbb{R}^2} \delta_i(\mathbf{h}(X),\boldsymbol{\gamma}) - [\cos(\theta)(u_i(X) - \bar{u}(X)) - \sin(\theta)(v_i(X) - \bar{v}(X))]^2 > 0 \tag{3.45}$$

then,

$$\forall (X,\theta) \in \mathbb{R}^2 \times [0,2\pi],\ \mathsf{S}_x(\mathsf{P}(\theta)\mathbf{u}(X),\boldsymbol{\gamma},\mathsf{P}(\theta)\bar{u}(X)) > 0. \tag{3.46}$$

As this last condition must be verified for all $\theta \in [0, 2\pi]$ and

$$\forall (\alpha, \beta) \in \mathbb{R}^2, \max_{\theta \in [0,2\pi]} [\cos(\theta)\alpha + \sin(\theta)\beta]^2 = \alpha^2 + \beta^2, \tag{3.47}$$

then, if $(\mathbf{u^0}, \boldsymbol{\gamma})$ is such that

$$\inf_{X \in \mathbb{R}^2} \delta_i(\mathbf{h}(X), \boldsymbol{\gamma}) - |u_i(X) - \bar{u}(X)|^2 - |v_i(X) - \bar{v}(X)|^2 > 0, \tag{3.48}$$

then, $\mathsf{S}_x(\mathsf{P}(\theta)\mathbf{u}(X), \boldsymbol{\gamma}, \mathsf{P}(\theta)\bar{u}(X))$ is positive-definite for all $\theta \in [0, 2\pi]$.
Finally, using the lemma 3.2.7, if $(\mathbf{u^0}, \boldsymbol{\gamma}) \in \mathcal{H}^s(\mathbb{R}^2) \times]0,1[^{n-1}$ verifies conditions (3.27), the mapping

$$\mathsf{S} : (\mathbf{u}, \boldsymbol{\gamma}, \theta) \mapsto \mathsf{P}(\theta)^{-1} \mathsf{S}_x(\mathsf{P}(\theta)\mathbf{u}, \boldsymbol{\gamma}) \mathsf{P}(\theta) \tag{3.49}$$

is a symbolic-simmetrizer and, according to the proposition 3.2.3, the *Cauchy* problem, associated with (3.10) and the initial data $\mathbf{u^0}$, is hyperbolic, locally well-posed in $\mathcal{H}^s(\mathbb{R}^2)^{3n}$ and the unique solution verifies conditions (3.22).

To conclude, considering $\boldsymbol{\gamma} \in]0,1[^{n-1}$ and $s > 2$, we define $\mathcal{S}^s_{\boldsymbol{\gamma}} \subset \mathcal{H}^s(\mathbb{R}^2)^{3n}$, an open subset of intial conditions such that the model (3.10) is symmetrizable:

$$\mathcal{S}^s_{\gamma} := \left\{ \mathbf{u^0} \in \mathcal{H}^s(\mathbb{R}^2)^{3n} / \mathbf{u^0} \text{ verifies conditions (3.27)} \right\}. \tag{3.50}$$

Remark: The condition of symmetrizability expressed in [42], with the multi-layer shallow water model with free surface in one dimension, is a little different from (3.27). Indeed, there is no need of a velocity reference but even if it seems to be a more general criterion, it is not possible to insure it, as there is no explicit estimations of this criterion.

3.2.5 Lower bounds of δ_i

In this subsection, we do not estimate exactly the sequence $(\delta_i(\mathbf{h}, \boldsymbol{\gamma}))_{i \in [\![1,n]\!]} \subset \mathbb{R}^*_+$, but a lower bound of each element $\delta_i(\mathbf{h}, \boldsymbol{\gamma})$. The proof is based on the next propostion, where $\lambda^{\min}$ and $\lambda^{\max}$ denote rexpectivly the smallest and the largest eigenvalues.

Proposition 3.2.9 *Let $\mathcal{S}_n(\mathbb{R})$ the space-vector of $n \times n$ symmetric matrices, with real coefficients. Then, $\lambda^{\min} : \mathcal{S}_n(\mathbb{R}) \to \mathbb{R}$ is a concave function and $\lambda^{\max} : \mathcal{S}_n(\mathbb{R}) \to \mathbb{R}$ is a convex one:*

$$\forall (\mathsf{A}, \mathsf{B}) \in \mathcal{S}_n(\mathbb{R})^2, \begin{cases} \lambda^{\min}(\mathsf{A}+\mathsf{B}) \geq \lambda^{\min}(\mathsf{A}) + \lambda^{\min}(\mathsf{B}), \\ \lambda^{\max}(\mathsf{A}+\mathsf{B}) \leq \lambda^{\max}(\mathsf{A}) + \lambda^{\max}(\mathsf{B}), \end{cases} \tag{3.51}$$

Using this last proposition, we can extract conditions which maintain $\mathsf{S}_x(\mathbf{u}, \boldsymbol{\gamma}, \bar{u})$ positive-definite.

Proposition 3.2.10 *Let* $\boldsymbol{\gamma} \in]0,1[^{n-1}$ *and* $\mathbf{h} \in \mathbb{R}_+^{*\,n}$. *Then,* $\lambda^{\min}(\mathsf{S}_x^0(\mathbf{h},\boldsymbol{\gamma})) > 0$ *and a lower bound of* $\delta_i(\mathbf{h},\boldsymbol{\gamma})$, *for every* $i \in [\![1,n]\!]$, *is*

$$\delta_i(\mathbf{h},\boldsymbol{\gamma}) \geq \left(\frac{\lambda^{\min}(\mathsf{S}_x^0(\mathbf{h},\boldsymbol{\gamma}))}{\alpha_{n,i}} \right)^2 \tag{3.52}$$

Proof We remind that $(\delta_i(\mathbf{h},\boldsymbol{\gamma}))_{i\in[\![1,n]\!]}$ is the sequence that remains $\mathsf{S}_x(\mathbf{u},\boldsymbol{\gamma},\bar{u})$ positive-definite (*i.e.* $\lambda^{\min}(\mathsf{S}_x(\mathbf{u},\boldsymbol{\gamma},\bar{u})) > 0$). We decompose $\mathsf{S}_x(\mathbf{u},\boldsymbol{\gamma},\bar{u})$ as $\mathsf{S}_x^0(\mathbf{h},\boldsymbol{\gamma}) + \mathsf{S}_x(\mathbf{u},\boldsymbol{\gamma},\bar{u}) - \mathsf{S}_x^0(\mathbf{h},\boldsymbol{\gamma})$. Then, according to the proposition 3.2.9, a condition to insure $\mathsf{S}_x(\mathbf{u},\bar{u})$ positive-definite is

$$\lambda^{\min}(\mathsf{S}_x^0(\mathbf{h},\boldsymbol{\gamma})) + \lambda^{\min}(\mathsf{S}_x(\mathbf{u},\boldsymbol{\gamma},\bar{u}) - \mathsf{S}_x^0(\mathbf{h},\boldsymbol{\gamma})) > 0. \tag{3.53}$$

As the spectrum of $\mathsf{S}_x(\mathbf{u},\boldsymbol{\gamma},\bar{u}) - \mathsf{S}_x^0(\mathbf{h},\boldsymbol{\gamma})$ is explicit

$$\sigma\left(\mathsf{S}_x(\mathbf{u},\boldsymbol{\gamma},\bar{u}) - \mathsf{S}_x^0(\mathbf{h},\boldsymbol{\gamma})\right) = (\pm\alpha_{n,i}(u_i - \bar{u}))_{i\in[\![1,n]\!]}, \tag{3.54}$$

it is obvious that $\lambda^{\min}(\mathsf{S}_x(\mathbf{u},\boldsymbol{\gamma},\bar{u}) - \mathsf{S}_x^0(\mathbf{h},\boldsymbol{\gamma})) = -\max_{j\in[\![1,n]\!]}(\alpha_{n,j}|u_j - \bar{u}|)$ and the matrix $\mathsf{S}_x(\mathbf{u},\boldsymbol{\gamma},\bar{u})$ remains positive-definite if

$$\forall i \in [\![1,n]\!],\ \lambda^{\min}(\mathsf{S}_x^0(\mathbf{h},\boldsymbol{\gamma})) \geq \alpha_{n,i}|u_i - \bar{u}|. \tag{3.55}$$

Finally, the lower bound of $\delta_i(\mathbf{h},\boldsymbol{\gamma})$, for $i \in [\![1,n]\!]$, is straightforward obtained with the definition of $\delta_i(\mathbf{h},\boldsymbol{\gamma})$ in theorem 3.2.6.

As the lower bound (3.52) is not explicit in $\mathbf{h}$ and $\boldsymbol{\gamma}$, we give, in the next proposition, an explicit lower bound of $\delta_i(\mathbf{h},\boldsymbol{\gamma})$, for $i \in [\![1,n]\!]$.

Proposition 3.2.11 *Let* $\boldsymbol{\gamma} \in]0,1[^{n-1}$ *and* $\mathbf{h} \in \mathbb{R}_+^{*\,n}$. *A lower bound of* $\delta_i(\mathbf{h},\boldsymbol{\gamma})$, *for* $i \in [\![1,n]\!]$, *is*

$$\delta_i(\mathbf{h},\boldsymbol{\gamma}) \geq \frac{1}{(\alpha_{n,i}a(\mathbf{h},\boldsymbol{\gamma}))^2} \tag{3.56}$$

where

$$a(\mathbf{h},\boldsymbol{\gamma}) := \max\left(\left(\frac{\alpha_{n,2}}{\alpha_{n,1}} + 1 \right) p_1, 2 \max_{k\in[\![1,n-2]\!]} (p_k + p_{k+1}), \max_{i\in[\![1,n]\!]} \left(\alpha_{n,i}^{-1} h_i^{-1} \right) \right), \tag{3.57}$$

and for all $k \in [\![1,n-1]\!]$, $p_k := \frac{1}{\alpha_{n,k+1}-\alpha_{n,k}} = \frac{\rho_n}{\rho_{k+1}-\rho_k}$.

Proof First, in order to provide an explicit lower bound of $\lambda^{\min}(\mathsf{S}_x^0(\mathbf{h},\boldsymbol{\gamma}))$, an upper bound of the spectral radius of $\mathsf{S}_x^0(\mathbf{h},\boldsymbol{\gamma})^{-1}$ is sufficient and is proved in the next lemma.

Lemma 3.2.12 *Let* $\boldsymbol{\gamma} \in]0,1[^{n-1}$ *and* $\mathbf{h} \in \mathbb{R}_+^{*\,n}$. *Then, the next inequality is verified*

$$\lambda^{\max}(\mathsf{S}_x^0(\mathbf{h},\boldsymbol{\gamma})^{-1}) \leq a(\mathbf{h},\boldsymbol{\gamma}). \tag{3.58}$$

Proof We remind $\mathsf{S}_x^0(\mathbf{h},\boldsymbol{\gamma})$) is positive-definite under conditions (3.34). Then, the inverse of $\mathsf{S}_x^0(\mathbf{h},\boldsymbol{\gamma})$ is

$$\mathsf{S}_x^0(\mathbf{h},\boldsymbol{\gamma})^{-1} := \left[\begin{array}{c|c|c} \Delta^{-1}\Gamma^{-1} & 0 & 0 \\ \hline 0 & \Delta^{-1}\mathsf{H}^{-1} & 0 \\ \hline 0 & 0 & \Delta^{-1}\mathsf{H}^{-1} \end{array}\right], \tag{3.59}$$

where $\Delta^{-1}\mathsf{H}^{-1} = \mathrm{diag}(\alpha_{n,1}^{-1}h_1^{-1},\ldots,\alpha_{n,n-1}^{-1}h_{n-1}^{-1},h_n^{-1})$. Moreover, one can verified that $\Delta^{-1}\Gamma^{-1}$ is a *n-Toeplitz* symmetric matrix (*i.e.* a tridiagonal symmetric matrix), defined by $\boldsymbol{p_1}\in\mathbb{R}^n$ on the diagonal and $\boldsymbol{p_2}\in\mathbb{R}^{n-1}$ just above and below this diagonal, with

$$\left\{\begin{array}{l} \boldsymbol{p_1} := {}^\top\left(\frac{\alpha_{n,2}}{\alpha_{n,1}}p_1, p_1+p_2, p_2+p_3,\ldots,p_{n-2}+p_{n-1},p_{n-1}\right), \\ \boldsymbol{p_2} := {}^\top\left(-p_1,-p_2,p_3,\ldots,-p_{n-1}\right). \end{array}\right. \tag{3.60}$$

Then, using the *Gerschgorin*'s theorem, there exists $k\in[\![1,n]\!]$ such that

$$\lambda^{\max}(\Delta^{-1}\Gamma^{-1})\in\mathcal{D}_k(\Delta^{-1}\Gamma^{-1}), \tag{3.61}$$

with the subsets $(\mathcal{D}_k)_{k\in[\![1,n]\!]}\subset\mathbb{C}$ defined by

$$\forall k\in[\![1,n]\!],\ \forall \mathsf{A}:=[\mathsf{A}_{i,j}]_{(i,j)\in[\![1,n]\!]^2},\ \mathcal{D}_k(\mathsf{A}) := \left\{ z\in\mathbb{C},\ |z-\mathsf{A}_{k,k}|\le\sum_{j\neq k}|\mathsf{A}_{k,j}|\right\}. \tag{3.62}$$

Then, as $\Delta^{-1}\Gamma^{-1}$ is symmetric, real and positive-definite, $\lambda^{\max}(\Delta^{-1}\Gamma^{-1})\in\mathbb{R}_+^*$ and using the tridiagonal structure of $\Delta^{-1}\Gamma^{-1}$

$$\lambda^{\max}(\Delta^{-1}\Gamma^{-1})\le a_1(\mathbf{h},\boldsymbol{\gamma}), \tag{3.63}$$

with $a_1(\mathbf{h},\boldsymbol{\gamma}) := \max\left(\left(\frac{\alpha_{n,2}}{\alpha_{n,1}}+1\right)p_1, 2p_{n-1}, 2\max_{k\in[\![1,n-2]\!]}(p_i+p_{i+1})\right)$. Finally, as we have for all $i\in[\![1,n-1]\!]$, $\gamma_i\in]0,1[$, it implies that

$$\forall i\in[\![1,n-1]\!],\ p_i>0. \tag{3.64}$$

Consequently, the inequality (3.58) is proved, using the structure of $\mathsf{S}_x^0(\mathbf{h},\boldsymbol{\gamma})^{-1}$:

$$\lambda^{\max}(\mathsf{S}_x^0(\mathbf{h},\boldsymbol{\gamma})^{-1})\le\max\left(\left(\frac{\alpha_{n,2}}{\alpha_{n,1}}+1\right)p_1, 2\max_{k\in[\![1,n-2]\!]}(p_k+p_{k+1}), \max_{i\in[\![1,n]\!]}\left(\alpha_{n,i}^{-1}h_i^{-1}\right)\right), \tag{3.65}$$

and $a(\mathbf{h},\boldsymbol{\gamma})$ is an explicit upper bound of $\lambda^{\max}(\mathsf{S}_x^0(\mathbf{h},\boldsymbol{\gamma})^{-1})$.

Finally, we can prove the explicit lower bound (3.56). As $\mathsf{S}_x^0(\mathbf{h},\boldsymbol{\gamma})$ is positive-definite if $\boldsymbol{\gamma}\in]0,1[^{n-1}$ and $\mathbf{h}\in\mathbb{R}_+^{*\,n}$, its smallest eigenvalue is the inverse of the greatest eigenvalue of $\mathsf{S}_x^0(\mathbf{h},\boldsymbol{\gamma})^{-1}$. Then, according to the lemma 3.2.12,

$$\lambda^{\min}(\mathsf{S}_x^0(\mathbf{h},\boldsymbol{\gamma}))\ge\frac{1}{a(\mathbf{h},\boldsymbol{\gamma})}, \tag{3.66}$$

and using the proposition 3.2.10, the explicit lower bound (3.56) of $\delta_i(\mathbf{h},\boldsymbol{\gamma})$ is insured.

Remark: The lower bound (3.56) is explicit but rougher than the lower bound (3.52). However, the main loss was due to the concave-inequality (3.53).

3.3 Hyperbolicity of particular cases

According to the previous section, the system (3.10), with initial data $\mathbf{u^0} \in \mathcal{H}^s(\mathbb{R}^2)^{3n}$, $s>2$, is hyperbolic if $\mathbf{u^0} \in \mathcal{S}^s_{\boldsymbol{\gamma}}$. However, this was just a sufficient condition of hyperbolicity. The aim of this section is to analyse the eigenstructure of particular cases and to obtain an explicit and necessary condition of hyperbolicity. Then, it will insure the initial conditions to be in the set of hyperbolicity of the model (3.10): $\mathcal{H}_{\boldsymbol{\gamma}}$, defined by

$$\mathcal{H}_{\boldsymbol{\gamma}} := \left\{ \mathbf{u^0} \in \mathcal{L}^2(\mathbb{R}^2)^{3n} / \mathbf{u^0} \text{ verifies conditions (3.19)} \right\} \tag{3.67}$$

To succeed, $\boldsymbol{\gamma} \in]0,1[^{n-1}$ is set and only for one $i_0 \in [\![1,n]\!]$, the asymptotic case $1-\gamma_{i_0} \to 0$ is studied, in order to extract the necessary condition of hyperbolicity. The technique is based on the analysis performed for the two-layer model in [88].

3.3.1 Eigenstructure of the matrix A

Using the rotational invariance (3.16), the eigenstructure of $\mathsf{A}(\mathbf{u},\boldsymbol{\gamma},\theta)$ is deduced from the one of $\mathsf{A}_x(\mathbf{u},\boldsymbol{\gamma})$. Moreover, as the eigenstructure of $\mathsf{A}_x(\mathbf{u},\boldsymbol{\gamma})$ will be analyzed, the canonical basis of $\mathbb{R}^{3n}$ will be necessary and denoted by $(\boldsymbol{e_i})_{i\in[\![1,3n]\!]}$. For every eigenvalue $\lambda \in \sigma(\mathsf{A}_x(\mathbf{u},\boldsymbol{\gamma}))$, the associated eigenspace will be noted $\mathcal{E}_\lambda(\mathbf{u},\boldsymbol{\gamma}) := \ker(\mathsf{A}_x(\mathbf{u},\boldsymbol{\gamma}) - \lambda \mathsf{I}_{3n})$; the geometric multiplicity will be denoted by $\mu_\lambda(\mathbf{u},\boldsymbol{\gamma}) := \dim \mathcal{E}_\lambda(\mathbf{u},\boldsymbol{\gamma})$; the associated right eigenvector will be noted $\boldsymbol{r}^\lambda_{\boldsymbol{x}}(\mathbf{u},\boldsymbol{\gamma})$ and the left one $\boldsymbol{l}^\lambda_{\boldsymbol{x}}(\mathbf{u},\boldsymbol{\gamma})$. First, we prove the next proposition:

Proposition 3.3.1 *The characteristic polynomial of* $\mathsf{A}_x(\mathbf{u},\boldsymbol{\gamma})$ *is equal to*

$$\det(\mathsf{A}_x(\mathbf{u},\boldsymbol{\gamma}) - \lambda \mathsf{I}_{3n}) = \det(\mathsf{M}_x(\lambda,\mathbf{u},\boldsymbol{\gamma})) \prod_{i=1}^{n} (u_i - \lambda), \tag{3.68}$$

where the $n \times n$ *matrix* $\mathsf{M}_x(\lambda,\mathbf{u},\boldsymbol{\gamma}) := (\mathsf{V}_x - \lambda \mathsf{I}_n)^2 - \Gamma \mathsf{H}$

Proof First of all, according to the block-structure of $\mathsf{A}_x(\mathbf{u},\boldsymbol{\gamma})$, it is clear that

$$\det(\mathsf{A}_x(\mathbf{u},\boldsymbol{\gamma}) - \lambda \mathsf{I}_{3n}) = \det\left(\mathsf{A}^1_x(\mathbf{u},\boldsymbol{\gamma}) - \lambda \mathsf{I}_{2n}\right) \prod_{i=1}^{n} (u_i - \mu), \tag{3.69}$$

where the $2n \times 2n$ matrix $\mathsf{A}^1_x(\mathbf{u},\boldsymbol{\gamma})$ is defined by

$$\mathsf{A}^1_x(\mathbf{u},\boldsymbol{\gamma}) := \left[\begin{array}{c|c} \mathsf{V}_x & \mathsf{H} \\ \hline \Gamma & \mathsf{V}_x \end{array}\right]. \tag{3.70}$$

Then, as all the blocks of $\mathsf{A}^1_x(\mathbf{u},\boldsymbol{\gamma})$ commute, the characteristic polynomial of $\mathsf{A}^1_x(\mathbf{u},\boldsymbol{\gamma})$ is equal to $\det(\mathsf{M}_x(\lambda,\mathbf{u},\boldsymbol{\gamma}))$.

According to the expression of the characteristic polynomial of $\mathsf{A}_x(\mathbf{u},\boldsymbol{\gamma})$ in (3.68), we denote the spectrum of this matrix by

$$\sigma(\mathsf{A}_x(\mathbf{u},\boldsymbol{\gamma})) := \left(\lambda_i^{\pm}(\mathbf{u},\boldsymbol{\gamma})\right)_{i\in[\![1,n]\!]} \cup (\lambda_{2n+i}(\mathbf{u},\boldsymbol{\gamma}))_{i\in[\![1,n]\!]}, \tag{3.71}$$

where $\left(\lambda_i^{\pm}(\mathbf{u},\boldsymbol{\gamma})\right)_{i\in[\![1,n]\!]} =: \sigma(\mathsf{A}_x^1(\mathbf{u},\boldsymbol{\gamma}))$ and

$$\forall i \in [\![1,n]\!],\ \lambda_{2n+i}(\mathbf{u},\boldsymbol{\gamma}) := u_i. \tag{3.72}$$

Remarks: 1) Using the rotational invariance (3.16), the spectrum of $\mathsf{A}(\mathbf{u},\boldsymbol{\gamma},\theta)$ will be

$$\sigma\left(\mathsf{A}(\mathbf{u},\boldsymbol{\gamma},\theta)\right) = \left(\lambda_i^{\pm}(\mathsf{P}(\theta)\mathbf{u},\boldsymbol{\gamma})\right)_{i\in[\![1,n]\!]} \cup (\lambda_{2n+i}(\mathsf{P}(\theta)\mathbf{u},\boldsymbol{\gamma}))_{i\in[\![1,n]\!]}. \tag{3.73}$$

2) The eigenvalues $\left(\lambda_i^{\pm}(\mathbf{u},\boldsymbol{\gamma})\right)_{i\in[\![1,n-1]\!]}$ will be called the baroclinic eigenvalues and $\lambda_n^{\pm}(\mathbf{u},\boldsymbol{\gamma})$ will be called the barotropic eigenvalues.
As the eigenstructure associated to $(\lambda_{2n+i}(\mathbf{u},\boldsymbol{\gamma}))_{i\in[\![1,n]\!]}$ is entirely known

$$\forall i \in [\![1,n]\!],\ \begin{cases} \boldsymbol{r}_{\boldsymbol{x}}^{\lambda_{2n+i}}(\mathbf{u},\boldsymbol{\gamma}) = \boldsymbol{e}_{2n+i}, \\ \boldsymbol{l}_{\boldsymbol{x}}^{\lambda_{2n+i}}(\mathbf{u},\boldsymbol{\gamma}) = {}^{\top}\boldsymbol{e}_{2n+i}, \end{cases} \tag{3.74}$$

the following study is only focused on $\sigma(\mathsf{A}_x^1(\mathbf{u},\boldsymbol{\gamma}))$. Moreover, as

$$\mathsf{M}_x(\lambda,\mathbf{u},\boldsymbol{\gamma}) = (\mathsf{V}_x - \bar{u}\mathsf{I}_n - (\lambda-\bar{u})\mathsf{I}_n)^2 - \Gamma\mathsf{H}, \tag{3.75}$$

the analysis will be performed with the rescaling

$$\forall i \in [\![1,n]\!],\ \left\{\ \tilde{\lambda}_i^{\pm} := \lambda_i^{\pm} - \bar{u}, \tilde{u}_i := u_i - \bar{u}. \right. \tag{3.76}$$

In this part, we will remove the $\tilde{}$ and we consider $\mathbf{u}$ such that $\bar{u} = 0$. In the following study, we set $f_n : \mathbb{R}\times\mathbb{R}^{3n}\times\mathbb{R}^{n-1} \to \mathbb{R}$ such that

$$\forall (\lambda,\mathbf{u},\boldsymbol{\gamma}) \in \mathbb{R}\times\mathbb{R}^{3n}\times\mathbb{R}^{n-1},\ f_n(\lambda,\mathbf{u},\boldsymbol{\gamma}) := \det\left(\mathsf{M}_x(\lambda,\mathbf{u},\boldsymbol{\gamma})\right) \tag{3.77}$$

3.3.2 A first case: the single-layer model

The single-layer model with free surface is characterized by $(\mathbf{u},\boldsymbol{\gamma}) = (\mathbf{u}^{\mathbf{0}},\boldsymbol{\gamma}^{\mathbf{0}})$, where $\mathbf{u}^{\mathbf{0}}$ and $\boldsymbol{\gamma}^{\mathbf{0}}$ are defined by

$$\forall i \in [\![1,n-1]\!],\ \begin{cases} u_i = u_{i+1} = 0 \\ \gamma_i = 1. \end{cases} \tag{3.78}$$

In that case, the spectrum of $\mathsf{A}_x^1(\mathbf{u}^{\mathbf{0}},\boldsymbol{\gamma}^{\mathbf{0}})$ is always real and is such that

$$\begin{cases} \lambda_i^{\pm}(\mathbf{u}^{\mathbf{0}},\boldsymbol{\gamma}^{\mathbf{0}}) = \lambda_0, & \forall i \in [\![1,n-1]\!], \\ \lambda_n^{\pm}(\mathbf{u}^{\mathbf{0}},\boldsymbol{\gamma}^{\mathbf{0}}) = \pm\sqrt{H}, \end{cases} \tag{3.79}$$

where $\lambda_0 := 0$. The geometric multiplicity associated to λ_0 and $\lambda_n^\pm$ are respectively $\mu_{\lambda_0} = n-1$ and $\mu_{\lambda_n^\pm} = 1$. The eigenvectors associated to this spectrum are

$$\forall i \in [\![1, n-1]\!], \quad \begin{cases} \boldsymbol{r}_{\boldsymbol{x}}^{\lambda_i^\pm}(\mathbf{u}^{\mathbf{0}}, \boldsymbol{\gamma}^{\mathbf{0}}) = \boldsymbol{e_i} - \boldsymbol{e}_{i+1}, \\ \boldsymbol{l}_{\boldsymbol{x}}^{\lambda_i^\pm}(\mathbf{u}^{\mathbf{0}}, \boldsymbol{\gamma}^{\mathbf{0}}) = {}^\top \boldsymbol{e}_{n+i} - {}^\top \boldsymbol{e}_{n+i+1}, \end{cases} \tag{3.80}$$

$$\begin{cases} \boldsymbol{r}_{\boldsymbol{x}}^{\lambda_n^\pm}(\mathbf{u}^{\mathbf{0}}, \boldsymbol{\gamma}^{\mathbf{0}}) = \sum_{k=1}^n \boldsymbol{e}_{n+k} \pm \frac{h_k}{\sqrt{H}} \boldsymbol{e_k} \\ \boldsymbol{l}_{\boldsymbol{x}}^{\lambda_n^\pm}(\mathbf{u}^{\mathbf{0}}, \boldsymbol{\gamma}^{\mathbf{0}}) = \sum_{k=1}^n {}^\top \boldsymbol{e}_k \pm \frac{h_k}{\sqrt{H}} {}^\top \boldsymbol{e}_{n+k}. \end{cases} \tag{3.81}$$

To conclude, in the single-layer case, the model is hyperbolic but there is no eigenbasis of $\mathbb{R}^{3n}$.

3.3.3 A second case: the merger of two layers

The merger of two layers is characterized by the equality of the parameters of two neighboring layers: $i \in [\![1, n-1]\!]$ such that $(\mathbf{u}, \boldsymbol{\gamma}) = (\mathbf{u}^{\boldsymbol{i}}, \boldsymbol{\gamma}^{\boldsymbol{i}})$, where $\mathbf{u}^{\boldsymbol{i}}$ and $\boldsymbol{\gamma}^{\boldsymbol{i}}$ are defined by

$$\begin{cases} u_j^2 \leq \delta_j(\mathbf{h}, \boldsymbol{\gamma}), & \forall j \in [\![1, n]\!] \setminus \{i\}, \\ 0 < \gamma_j < 1, & \forall j \in [\![1, n-1]\!] \setminus \{i\}. \end{cases} \tag{3.82}$$

and for $i \in [\![1, n-1]\!]$,

$$\begin{cases} u_i = u_{i+1} \\ \gamma_i = 1. \end{cases} \tag{3.83}$$

Then, according to theorem 3.2.6, it is hyperbolic and the spectrum of $\mathsf{A}_x^1(\mathbf{u}^{\boldsymbol{i}}, \boldsymbol{\gamma}^{\boldsymbol{i}})$ is always a subset of $\mathbb{R}$. However there is no recursive method nor explicit expression to determine entirely this spectrum. Moreover, as the next equality on the columns is obvious,

$$\mathsf{C}_i \left(\mathsf{A}_x^1(\mathbf{u}^{\boldsymbol{i}}, \boldsymbol{\gamma}^{\boldsymbol{i}}) - u_i \mathsf{I}_{2\mathsf{n}} \right) = \mathsf{C}_{i+1} \left(\mathsf{A}_x^1(\mathbf{u}^{\boldsymbol{i}}, \boldsymbol{\gamma}^{\boldsymbol{i}}) - u_i \mathsf{I}_{2\mathsf{n}} \right), \tag{3.84}$$

there is only one trivial value for the eigenvalues $\lambda_i^\pm = u_i$. And for this eigenvalues, the eigenvectors associated are

$$\begin{cases} \boldsymbol{r}_{\boldsymbol{x}}^{\lambda_i^\pm}(\mathbf{u}^{\boldsymbol{i}}, \boldsymbol{\gamma}^{\boldsymbol{i}}) = \boldsymbol{e}_i - \boldsymbol{e}_{i+1}, \\ \boldsymbol{l}_{\boldsymbol{x}}^{\lambda_i^\pm}(\mathbf{u}^{\boldsymbol{i}}, \boldsymbol{\gamma}^{\boldsymbol{i}}) = {}^\top \boldsymbol{e}_{n+i} - {}^\top \boldsymbol{e}_{n+i+1}, \end{cases} \tag{3.85}$$

To conclude, as in the previous case, the model, with the merger of two layer, remains hyperbolic but there is no eigenbasis of $\mathbb{R}^{3n}$.

3.3.4 The asymptotic expansion of the merger of two layers

With the same notations as the previous subsection, we consider the merger of two layer: there exists $i \in [\![1, n-1]\!]$, such that conditions (3.82–3.83) are verified. As it was explained before, the eigenvalue $\lambda_i^\pm(\mathbf{u}, \boldsymbol{\gamma})$ is explicit but does not provide two distinct eigenvalues associated to the interface

i, in order to get two distinct right eigenvectors. Indeed, proving the existence of two distinct right eigenvectors would be a first step to prove the diagonalizability of the matrix $\mathsf{A}(\mathbf{u},\boldsymbol{\gamma},\theta)$, in order to apply proposition 3.2.5.

Proposition 3.3.2 *Let $i \in [\![1, n-1]\!]$, $(\mathbf{u},\boldsymbol{\gamma}) \in \mathbb{R}^{3n}\times]0,1[^{n-1}$ such that $1-\gamma_i$ and $(u_j)_{j\in[\![1,n]\!]}$ are sufficiently small. Then, an expansion of $\lambda_i^{\pm}(\mathbf{u},\boldsymbol{\gamma})$ is*

$$\begin{aligned}\lambda_i^{\pm}(\mathbf{u},\boldsymbol{\gamma}) = \quad & \tfrac{u_i h_{i+1}+u_{i+1}h_i}{h_i+h_{i+1}} \pm \left[\tfrac{h_i h_{i+1}}{h_i+h_{i+1}}\left(1-\gamma_i-\tfrac{(u_{i+1}-u_i)^2}{h_i+h_{i+1}}\right)\right]^{\frac{1}{2}} \\ & +\mathcal{O}((1-\gamma_i),(u_j^2)_{j\in[\![1,n]\!]}).\end{aligned} \tag{3.86}$$

Proof In order to obtain an asymptotic expansion of $\lambda_i^{\pm}$, we perform a 2^{nd} order *Taylor* expansion of f_n, about a state mixing the two cases analyzed in §3.3.2 and §3.3.3:

$$\begin{cases} \lambda = 0, \\ \mathbf{u} = \mathbf{u^0}, \\ \boldsymbol{\gamma} = \boldsymbol{\gamma^i} \end{cases} \tag{3.87}$$

Then, we have

$$\begin{aligned} f_n(\lambda,\boldsymbol{u},\boldsymbol{\gamma}) \quad & = f_n(0,\mathbf{u^0},\boldsymbol{\gamma^i}) + \lambda\frac{\partial f_n}{\partial\lambda}(0,\mathbf{u^0},\boldsymbol{\gamma^i}) + (\gamma_i-1)\frac{\partial f_n}{\partial\gamma_i}(0,\mathbf{u^0},\boldsymbol{\gamma^i}) \\ & + \sum_{j=1}^{n} u_j\frac{\partial f_n}{\partial u_j}(0,\mathbf{u^0},\boldsymbol{\gamma^i}) + \frac{1}{2}\lambda^2\frac{\partial^2 f_n}{\partial\lambda^2}(0,\mathbf{u^0},\boldsymbol{\gamma^i}) \\ & + \sum_{j=1}^{n}\frac{1}{2}u_j^2\frac{\partial^2 f_n}{\partial u_j^2}(0,\mathbf{u^0},\boldsymbol{\gamma^i}) + \frac{1}{2}(\gamma_i-1)^2\frac{\partial^2 f_n}{\partial\gamma_i^2}(0,\mathbf{u^0},\boldsymbol{\gamma^i}) \\ & + \sum_{j=1}^{n} u_j\left(\lambda\frac{\partial^2 f_n}{\partial u_j\partial\lambda}(0,\mathbf{u^0},\boldsymbol{\gamma^i}) + (\gamma_i-1)\frac{\partial^2 f_n}{\partial u_j\partial\gamma_i}(0,\mathbf{u^0},\boldsymbol{\gamma^i})\right) \\ & + \sum_{j\neq k} u_j u_k\frac{\partial^2 f_n}{\partial u_j\partial u_k}(0,\mathbf{u^0},\boldsymbol{\gamma^i}) + \lambda(\gamma_i-1)\frac{\partial^2 f_n}{\partial\lambda\partial\gamma_i}(0,\mathbf{u^0},\boldsymbol{\gamma^i}) \\ & + o(\lambda^2, 1-\gamma_i, (u_j^2)_{j\in[\![1,n]\!]}), \end{aligned}$$

To calculate all these derivatives, we use the following lemmata:

Lemma 3.3.3 *Let $\boldsymbol{\gamma}\in]0,1[^{n-1}$ and $\mathbf{h}\in\mathbb{R}_+^{*\,n}$, then*

$$f_n(0,\mathbf{u^0},\boldsymbol{\gamma}) = (-1)^n h_n\prod_{i=1}^{n-1} h_i(1-\gamma_i) \tag{3.88}$$

Proof First, we perform the next operations to the columns of $\mathsf{M}_x(\lambda,\mathbf{u^0},\boldsymbol{\gamma})$: for all $k\in[\![1,n-1]\!]$,

$$\mathsf{C}_k\left(\mathsf{M}_x(\lambda,\mathbf{u^0},\boldsymbol{\gamma})\right)\leftarrow\mathsf{C}_k\left(\mathsf{M}_x(\lambda,\mathbf{u^0},\boldsymbol{\gamma})\right)-\mathsf{C}_{k+1}\left(\mathsf{M}_x(\lambda,\mathbf{u^0},\boldsymbol{\gamma})\right) \tag{3.89}$$

Finally, with an expansion of the determinant obtained, about the 1st line, the lemma 3.3.3 is proved.

In the next lemma, for $k\in[\![1,n-1]\!]$, we denote by $\mathsf{M}_x^k(\lambda,\mathbf{u},\boldsymbol{\gamma})$, the $n-1\times n-1$ matrix obtained with $\mathsf{M}_x(\lambda,\mathbf{u},\boldsymbol{\gamma})$ with the k^{th} column and k^{th} line removed; and by $f_n^k:\mathbb{R}\times\mathbb{R}^{3n}\times\mathbb{R}^{n-1}\to\mathbb{R}$ such that $f_n^k(\lambda,\mathbf{u},\boldsymbol{\gamma})$ is the k^{th} first minor of $\mathsf{M}_x(\lambda,\mathbf{u},\boldsymbol{\gamma})$

$$f_n^k(\lambda,\mathbf{u},\boldsymbol{\gamma}):=\det\left(\mathsf{M}_x^k(\lambda,\mathbf{u},\boldsymbol{\gamma})\right). \tag{3.90}$$

Lemma 3.3.4 *Let $k\in[\![1,n]\!]$, $\boldsymbol{\gamma}\in]0,1[^{n-1}$ and $\mathbf{h}\in\mathbb{R}_+^{*\,n}$, then*

$$f_n^k(0,\mathbf{u^0},\boldsymbol{\gamma})=\begin{cases}(-1)^{n-1}\prod_{j=2}^n h_j\prod_{j=2}^{n-1}(1-\gamma_j), & \text{if } k=1,\\ (-1)^{n-1}\eta_k\prod_{j=1,j\neq k}^n h_j\prod_{j=1,j\notin\{k-1,k\}}^{n-1}(1-\gamma_j), & \text{if } k\in[\![2,n-1]\!],\\ (-1)^{n-1}\prod_{j=1}^{n-1}h_j\prod_{j=1}^{n-2}(1-\gamma_j), & \text{if } k=n,\end{cases} \tag{3.91}$$

where $\forall k\in[\![2,n-1]\!]$, $\eta_k:=1-\gamma_{k-1}\gamma_k$.

Proof First, we just remark that

$$f_n^k(0,\mathbf{u^0},\boldsymbol{\gamma})=f_{n-1}(0,\mathbf{u^0}(k),\boldsymbol{\gamma}(k)), \tag{3.92}$$

where $\mathbf{u^0}(k)\in\mathbb{R}^{3n-3}$ is the vector $\mathbf{u^0}$, where h_k, u_k and v_k have been removed; and $\boldsymbol{\gamma}(k)\in\mathbb{R}^{n-1}$ is defined by

$$\boldsymbol{\gamma}(k):=\begin{cases}{}^\top(\gamma_2,\dots,\gamma_{n-1}), & \text{if } k=1,\\ {}^\top(\gamma_1,\dots,\gamma_{k-2},\gamma_{k-1}\gamma_k,\gamma_{k+1},\dots,\gamma_{n-1}), & \text{if } k\in[\![2,n-1]\!],\\ {}^\top(\gamma_1,\dots,\gamma_{n-2}), & \text{if } k=n.\end{cases} \tag{3.93}$$

Then, the lemma 3.3.4 is straightforward deduced, as a direct application of the lemma 3.3.3.

Furthermore, using the lemma 3.3.3 and reminding that $\boldsymbol{\gamma^i}$ is defined such that $\gamma_i=1$, then it is clear that

$$f_n(0,\mathbf{u^0},\boldsymbol{\gamma^i})=0. \tag{3.94}$$

Consequently, all the derivatives of the 2nd order *Taylor* expansion of f_n, about the state $\lambda=0$, $\mathbf{u}=\mathbf{u^0}$ and $\boldsymbol{\gamma}=\boldsymbol{\gamma^i}$, are deduced from the particular structure of $\mathsf{M}_x(\lambda,\mathbf{u^0},\boldsymbol{\gamma})$ and lemmata 3.3.3–3.3.4.

Lemma 3.3.5 *The 1st order partial derivatives are such that*

$$\begin{cases}\frac{\partial f_n}{\partial\lambda}(0,\mathbf{u^0},\boldsymbol{\gamma^i}) &=0,\\ \frac{\partial f_n}{\partial u_j}(0,\mathbf{u^0},\boldsymbol{\gamma^i}) &=0, \qquad\qquad \forall j\in[\![1,n]\!]\\ \frac{\partial f_n}{\partial\gamma_i}(0,\mathbf{u^0},\boldsymbol{\gamma^i}) &=(-1)^{n+1}h_nh_i\prod_{j=1,j\neq i}^{n-1}h_j(1-\gamma_j).\end{cases} \tag{3.95}$$

Proof Remarking

$$\begin{cases} \frac{\partial f_n}{\partial \lambda}(\lambda,\mathbf{u},\boldsymbol{\gamma}) = \sum_{k=1}^{n} -2(u_k-\lambda) f_n^k(\lambda,\mathbf{u},\boldsymbol{\gamma}), \\ \frac{\partial f_n}{\partial u_j}(\lambda,\mathbf{u},\boldsymbol{\gamma}) = 2(u_j-\lambda) f_n^k(\lambda,\mathbf{u},\boldsymbol{\gamma}), \qquad \forall j \in [\![1,n]\!]. \end{cases} \tag{3.96}$$

and, according to the definition of $\mathbf{u^0}$ in (3.78): $\forall k \in [\![1,n]\!]$, $u_k = 0$, it is straightforward to prove the two 1st derivatives:

$$\begin{cases} \frac{\partial f_n}{\partial \lambda}(0,\mathbf{u^0},\boldsymbol{\gamma^i}) = 0, \\ \frac{\partial f_n}{\partial u_j}(0,\mathbf{u^0},\boldsymbol{\gamma^i}) = 0, \quad \forall j \in [\![1,n]\!]. \end{cases} \tag{3.97}$$

The 3rd one is obtained remarking that in each column of $\mathsf{M}_x(\lambda,\mathbf{u},\boldsymbol{\gamma})$, the terms in $\boldsymbol{\gamma}$ are not correlated with the terms in λ and $\mathbf{u}$. Then, the result is proved, applying the lemma 3.3.3.

Lemma 3.3.6 *The* 2nd *order partial derivatives are*

$$\begin{cases} \frac{\partial^2 f_n}{\partial \lambda \partial \gamma_i}(0,\mathbf{u^0},\boldsymbol{\gamma^i}) &= 0, \\ \frac{\partial^2 f_n}{\partial u_j \partial u_k}(0,\mathbf{u^0},\boldsymbol{\gamma^i}) &= 0, \qquad \forall j \neq k, \\ \frac{\partial^2 f_n}{\partial u_j \partial \gamma_i}(0,\mathbf{u^0},\boldsymbol{\gamma^i}) &= 0, \qquad \forall j \in [\![2,n]\!], \\ \frac{\partial^2 f_n}{\partial \gamma_i^2}(0,\mathbf{u^0},\boldsymbol{\gamma^i}) &= 0, \\ \frac{\partial^2 f_n}{\partial u_j^2}(0,\mathbf{u^0},\boldsymbol{\gamma^i}) &= 0, \quad \forall j \notin \{i,i+1\}, \\ \frac{\partial^2 f_n}{\partial \lambda \partial u_j}(0,\mathbf{u^0},\boldsymbol{\gamma^i}) &= 0, \quad \forall j \notin \{i,i+1\}, \end{cases} \tag{3.98}$$

$$\begin{cases} \frac{\partial^2 f_n}{\partial \lambda^2}(0,\mathbf{u^0},\boldsymbol{\gamma^i}) &= (h_i + h_{i+1})\kappa_i, \\ \frac{\partial^2 f_n}{\partial \lambda \partial u_{i+1}}(0,\mathbf{u^0},\boldsymbol{\gamma^i}) &= -h_i\kappa_i, \\ \frac{\partial^2 f_n}{\partial u_{i+1}^2}(0,\mathbf{u^0},\boldsymbol{\gamma^i}) &= h_i\kappa_i, \\ \frac{\partial^2 f_n}{\partial \lambda \partial u_i}(0,\mathbf{u^0},\boldsymbol{\gamma^i}) &= -h_{i+1}\kappa_i, \\ \frac{\partial^2 f_n}{\partial u_i^2}(0,\mathbf{u^0},\boldsymbol{\gamma^i}) &= h_{i+1}\kappa_i, \end{cases} \tag{3.99}$$

where $\kappa_i := 2(-1)^{n-1} \prod_{j=1, j\notin\{i,i+1\}}^{n} h_j \prod_{j=1, j\neq i}^{n-1} (1-\gamma_j)$.

Proof We note that

$$\begin{cases} \frac{\partial^2 f_n}{\partial \lambda^2}(\lambda,\mathbf{u},\boldsymbol{\gamma}) = \sum_{k=1}^{n} 2 f_n^k(\lambda,\mathbf{u},\boldsymbol{\gamma}), \\ \frac{\partial^2 f_n}{\partial u_j^2}(\lambda,\mathbf{u},\boldsymbol{\gamma}) = 2 f_n^j(\lambda,\mathbf{u},\boldsymbol{\gamma}), \qquad \forall j \in [\![1,n]\!], \\ \frac{\partial^2 f_n}{\partial \lambda \partial u_j}(\lambda,\mathbf{u},\boldsymbol{\gamma}) = -2 f_n^j(\lambda,\mathbf{u},\boldsymbol{\gamma}), \qquad \forall j \in [\![1,n]\!], \end{cases} \tag{3.100}$$

and as it was noticed before

$$\begin{cases} \frac{\partial^2 f_n}{\partial \gamma_i^2}(\lambda,\mathbf{u},\boldsymbol{\gamma}) = \frac{\partial^2 f_n}{\partial \gamma_i^2}(0,\mathbf{u^0},\boldsymbol{\gamma}), \\ \frac{\partial^2 f_n}{\partial \lambda \partial \gamma_i}(\lambda,\mathbf{u},\boldsymbol{\gamma}) = 0, \\ \frac{\partial^2 f_n}{\partial u_j \partial \gamma_i}(\lambda,\mathbf{u},\boldsymbol{\gamma}) = 0, \qquad \forall j \in [\![1,n]\!]. \end{cases} \tag{3.101}$$

Moreover, according to the definition of $\boldsymbol{\gamma}^{\boldsymbol{i}}$ in (3.82–3.83) and the expression of $f_n^j(0,\mathbf{u}^{\mathbf{0}},\boldsymbol{\gamma})$ in (3.91),

$$\forall j \in [\![1,n]\!],\ f_n^j(0,\mathbf{u}^{\mathbf{0}},\boldsymbol{\gamma}^{\boldsymbol{i}}) = \begin{cases} 0, & \text{if } j \neq i, i+1, \\ \frac{1}{2}\kappa_i h_{i+1}, & \text{if } j = i, \\ \frac{1}{2}\kappa_i h_i, & \text{if } j = i+1, \end{cases} \tag{3.102}$$

the other derivatives are directly calculated.

Using lemmata 3.3.3–3.3.6, the 2$^{\text{nd}}$ order *Taylor* expansion of f, about the state (3.87), becomes

$$\begin{aligned} 0 = \quad & \kappa_i \Big[\tfrac{1}{2}(\gamma_i - 1) h_i h_{i+1} + \tfrac{1}{2}\lambda^2 (h_i + h_{i+1}) + \tfrac{1}{2} u_i^2 h_{i+1} + \tfrac{1}{2} u_{i+1}^2 h_i \\ & - \lambda u_i h_{i+1} - \lambda u_{i+1} h_i \Big] + o(\lambda^2, 1-\gamma_i, \left(u_j^2\right)_{j\in[\![1,n]\!]}). \end{aligned} \tag{3.103}$$

Finally, as $\kappa_i \neq 0$, we apply the implicit function theorem and obtain the expression (3.86).

Theorem 3.3.7 *Let $i \in [\![1,n-1]\!]$, $(\mathbf{u},\boldsymbol{\gamma}) \in \mathbb{R}^{3n}\times]0,1[^{n-1}$ such that $\mathbf{h} > 0$, and $1-\gamma_i$, $(u_j)_{j\in[\![1,n]\!]}$ and $(v_j)_{j\in[\![1,n]\!]}$ are sufficiently small. Then, a necessary condition of hyperbolicity for the model (3.10) is*

$$(u_{i+1}-u_i)^2 + (v_{i+1}-v_i)^2 \leq (h_i + h_{i+1})(1-\gamma_i). \tag{3.104}$$

Proof To verify the hyperbolicity of the system (3.10), all the eigenvalues of $\mathsf{A}(\mathbf{u},\boldsymbol{\gamma},\theta)$ need to be real. According to the rotational invariance (3.16) and the proposition 3.3.2, if $1-\gamma_i$, $(u_j)_{j\in[\![1,n]\!]}$ and $(v_j)_{j\in[\![1,n]\!]}$ are sufficiently small, the asymptotic expansion of $\lambda_i^{\pm}(\mathsf{P}(\theta)\mathbf{u},\boldsymbol{\gamma}) \in \sigma(\mathsf{A}(\mathbf{u},\boldsymbol{\gamma},\theta)$ is

$$\begin{aligned} \lambda_i^{\pm}(\mathsf{P}(\theta)\mathbf{u},\boldsymbol{\gamma}) = \quad & \cos(\theta)\tfrac{u_i h_{i+1} + u_{i+1} h_i}{h_i + h_{i+1}} + \sin(\theta)\tfrac{v_i h_{i+1} + v_{i+1} h_i}{h_i + h_{i+1}} \\ & \pm \left[\tfrac{h_i h_{i+1}}{h_i + h_{i+1}} \left(1 - \gamma_i - \tfrac{(\cos(\theta)(u_{i+1}-u_i) + \sin(\theta)(v_{i+1}-v_i))^2}{h_i + h_{i+1}} \right) \right]^{\frac{1}{2}} \\ & + \mathcal{O}((1-\gamma_i), (u_j^2)_{j\in[\![1,n]\!]}). \end{aligned} \tag{3.105}$$

Then, as $h_i > 0$ for all $i \in [\![1,n]\!]$, a necessary condition to have $\lambda_i^{\pm}(\mathsf{P}(\theta)\mathbf{u},\boldsymbol{\gamma}) \in \mathbb{R}$, for all $\theta \in [0,2\pi]$ is

$$\forall \theta \in [0,2\pi],\ 1 - \gamma_i - \frac{(\cos(\theta)(u_{i+1}-u_i) + \sin(\theta)(v_{i+1}-v_i))^2}{h_i + h_{i+1}} \geq 0. \tag{3.106}$$

Finally, using (3.47), the necessary condition of hyperbolicity (3.104) is obtained.

With the asymptotic expansion (3.86), we can deduce an asymptotic expansion of the eigenvectors associated to $\lambda_i^{\pm}(\mathbf{u},\boldsymbol{\gamma})$.

Proposition 3.3.8 *Let $i \in [\![1,n-1]\!]$, $(\mathbf{u},\boldsymbol{\gamma}) \in \mathbb{R}^{3n}\times]0,1[^{n-1}$ such that $1-\gamma_i$ and $(|u_j|)_{j\in[\![1,n]\!]}$ are sufficiently small. Then, the asymptotic expansion of the right eigenvector associated to $\lambda_i^{\pm}(\mathbf{u},\boldsymbol{\gamma})$, with precision in $\mathcal{O}((1-\gamma_i),(u_j^2)_{j\in[\![1,n]\!]})$, is such that*

$$\begin{aligned} \boldsymbol{r}_{\boldsymbol{x}}^{\lambda_i^{\pm}}(\mathbf{u},\boldsymbol{\gamma}) = \quad & \boldsymbol{e}_i - \boldsymbol{e}_{i+1} + \tfrac{u_{i+1}-u_i}{h_i+h_{i+1}}(\boldsymbol{e}_{n+i}+\boldsymbol{e}_{n+i+1}) \\ & \pm \left[\tfrac{h_i h_{i+1}}{h_i+h_{i+1}}\left(1-\gamma_i-\tfrac{(u_{i+1}-u_i)^2}{h_i+h_{i+1}}\right)\right]^{\frac{1}{2}}(\tfrac{\boldsymbol{e}_{n+i}}{h_i}-\tfrac{\boldsymbol{e}_{n+i+1}}{h_{i+1}}) \\ & +\mathcal{O}((1-\gamma_i),(u_j^2)_{j\in[\![1,n]\!]}), \end{aligned} \tag{3.107}$$

and the asymptotic expansion of the left eigenvector associated to $\lambda_i^{\pm}(\mathbf{u},\boldsymbol{\gamma})$, with precision in $\mathcal{O}((1-\gamma_i),(u_j^2)_{j\in[\![1,n]\!]})$, is such that

$$\begin{aligned} \boldsymbol{l}_{\boldsymbol{x}}^{\lambda_i^{\pm}}(\mathbf{u},\boldsymbol{\gamma}) = \quad & {}^{\top}\boldsymbol{e}_{n+i} - {}^{\top}\boldsymbol{e}_{n+i+1} + \tfrac{u_{i+1}-u_i}{h_i+h_{i+1}}({}^{\top}\boldsymbol{e}_i + {}^{\top}\boldsymbol{e}_{i+1}) \\ & \pm \left[\tfrac{h_i h_{i+1}}{h_i+h_{i+1}}\left(1-\gamma_i-\tfrac{(u_{i+1}-u_i)^2}{h_i+h_{i+1}}\right)\right]^{\frac{1}{2}}(\tfrac{{}^{\top}\boldsymbol{e}_i}{h_i}-\tfrac{{}^{\top}\boldsymbol{e}_{i+1}}{h_{i+1}}) \\ & +\mathcal{O}((1-\gamma_i),(u_j^2)_{j\in[\![1,n]\!]}). \end{aligned} \tag{3.108}$$

Proof We consider $\lambda_i^{\pm}(\mathbf{u},\boldsymbol{\gamma}) \in \mathbb{R}$:

$$(u_{i+1}-u_i)^2 \leq (h_{i+1}+h_i)(1-\gamma_i). \tag{3.109}$$

Then, we define $\pi_i \in [-(h_{i+1}+h_i)^{\frac{1}{2}},(h_{i+1}+h_i)^{\frac{1}{2}}]$ such that

$$(u_{i+1}-u_i)^2 = \pi_i^2(1-\gamma_i), \tag{3.110}$$

$$\lambda_i^{\pm}(\mathbf{u},\boldsymbol{\gamma}) = u_i + \chi_i^{\pm}(1-\gamma_i)^{\frac{1}{2}} + o((1-\gamma_i)^{\frac{1}{2}},(u_j)_{j\in[\![1,n]\!]}), \tag{3.111}$$

where $\chi_i^{\pm} := \pi_i \frac{h_i}{h_i+h_{i+1}} \pm \left[\frac{h_i h_{i+1}}{h_i+h_{i+1}}\left(1-\frac{\pi_i^2}{h_i+h_{i+1}}\right)\right]^{\frac{1}{2}}$ and we will expand the eigenvectors $\boldsymbol{r}_{\boldsymbol{x}}^{\lambda_i^{\pm}}(\mathbf{u},\boldsymbol{\gamma})$ and $\boldsymbol{l}_{\boldsymbol{x}}^{\lambda_i^{\pm}}(\mathbf{u},\boldsymbol{\gamma})$ as

$$\forall i \in [\![1,n-1]\!], \begin{cases} \boldsymbol{r}_{\boldsymbol{x}}^{\lambda_i^{\pm}}(\mathbf{u},\boldsymbol{\gamma}) = \boldsymbol{r}_{i,0}(\mathbf{u},\boldsymbol{\gamma}) + (1-\gamma_i)^{\frac{1}{2}}\boldsymbol{r}_{i,1}^{\pm}(\mathbf{u},\boldsymbol{\gamma}), \\ \boldsymbol{l}_{\boldsymbol{x}}^{\lambda_i^{\pm}}(\mathbf{u},\boldsymbol{\gamma}) = \boldsymbol{l}_{i,0}(\mathbf{u},\boldsymbol{\gamma}) + (1-\gamma_i)^{\frac{1}{2}}\boldsymbol{l}_{i,1}^{\pm}(\mathbf{u},\boldsymbol{\gamma}), \end{cases} \tag{3.112}$$

where

$$\begin{cases} \boldsymbol{r}_{i,0}(\mathbf{u},\boldsymbol{\gamma}) := \boldsymbol{e_i} - \boldsymbol{e}_{i+1}, \\ \boldsymbol{l}_{i,0}(\mathbf{u},\boldsymbol{\gamma}) := {}^{\top}\boldsymbol{e}_{n+i} - {}^{\top}\boldsymbol{e}_{n+i+1}. \end{cases} \tag{3.113}$$

Moreover, we have

$$\mathsf{A}_x(\mathbf{u},\boldsymbol{\gamma}) = \mathsf{A}_x(\mathbf{u}^{\boldsymbol{i}},\boldsymbol{\gamma}^{\boldsymbol{i}}) + (u_{i+1}-u_i)\mathsf{A}_x^{i,1} + (1-\gamma_i)\mathsf{A}_x^{i,2}(\boldsymbol{\gamma}), \tag{3.114}$$

where the $3n \times 3n$ matrices, $\mathsf{A}_x^{i,1} := \left[\mathsf{A}_{l,k}^{i,1}\right]_{(l,k)\in[\![1,n]\!]^2}$ and $\mathsf{A}_x^{i,2}(\boldsymbol{\gamma}) := \left[\mathsf{A}_{l,k}^{i,2}\right]_{(l,k)\in[\![1,n]\!]^2}$, are defined by

$$\mathsf{A}_{l,k}^{i,1} := \begin{cases} 1, & \text{if } l = k \text{ and } l \in \{pn+i+1/p \in [\![0,2]\!]\}, \\ 0, & \text{otherwise}, \end{cases} \tag{3.115}$$

$$\mathsf{A}_{l,k}^{i,2} := \begin{cases} 0, & \text{if } l \leq n+i \text{ or } l \geq 2n+1, \\ 0, & \text{if } k \geq n+1, \\ 0, & \text{if } n+k \geq l, \\ -\alpha_{l-n-1,k}, & \text{otherwise}, \end{cases} \tag{3.116}$$

and

$$\mathsf{A}_x(\mathbf{u},\boldsymbol{\gamma}) = \mathsf{A}_x(\mathbf{u}^{\boldsymbol{i}},\boldsymbol{\gamma}^{\boldsymbol{i}}) + \pi_i(1-\gamma_i)^{\frac{1}{2}}\mathsf{A}_x^{i,1} + (1-\gamma_i)\mathsf{A}_x^{i,2}(\boldsymbol{\gamma}). \tag{3.117}$$

In the asymptotic regime $0 < 1-\gamma_i \ll 1$ and for every $j \in [\![1,n]\!], |u_j| \ll 1$, $\boldsymbol{r}_{\boldsymbol{x}}^{\lambda_i^\pm}(\mathbf{u},\boldsymbol{\gamma})$ and $\boldsymbol{l}_{\boldsymbol{x}}^{\lambda_i^\pm}(\mathbf{u},\boldsymbol{\gamma})$ are respectively the approximations of the right and left eigenvectors associated to $\lambda_x^\pm(\mathbf{u},\boldsymbol{\gamma})$, with precision $\mathcal{O}(1-\gamma_i)$ if and only if $\boldsymbol{r}_{i,1}^\pm(\mathbf{u},\boldsymbol{\gamma})$ and $\boldsymbol{l}_{i,1}^\pm(\mathbf{u},\boldsymbol{\gamma})$ verify

$$\begin{cases} \left(\pi_i\mathsf{A}_x^{i,1} - \chi_i^\pm \mathsf{I}_{3n}\right)\boldsymbol{r}_{i,0}(\mathbf{u},\boldsymbol{\gamma}) = -\left(\mathsf{A}_x(\mathbf{u}^{\boldsymbol{i}},\boldsymbol{\gamma}^{\boldsymbol{i}}) - u_i\mathsf{I}_{3n}\right)\boldsymbol{r}_{i,1}^\pm(\mathbf{u},\boldsymbol{\gamma}), \\ \boldsymbol{l}_{i,0}(\mathbf{u},\boldsymbol{\gamma})\left(\pi_i\mathsf{A}_x^{i,1} - \chi_i^\pm\mathsf{I}_{3n}\right) = -\boldsymbol{l}_{i,1}^\pm(\mathbf{u},\boldsymbol{\gamma})\left(\mathsf{A}_x(\mathbf{u}^{\boldsymbol{i}},\boldsymbol{\gamma}^{\boldsymbol{i}}) - u_i\mathsf{I}_{3n}\right), \end{cases} \tag{3.118}$$

Finally, a solution of (3.118) is

$$\begin{cases} \boldsymbol{r}_{i,1}^\pm(\mathbf{u},\boldsymbol{\gamma}) = \frac{\chi_i^\pm}{h_i}\boldsymbol{e}_{n+i} + \frac{\pi_i-\chi_i^\pm}{h_{i+1}}\boldsymbol{e}_{n+i+1}, \\ \boldsymbol{l}_{i,1}^\pm(\mathbf{u},\boldsymbol{\gamma}) = \frac{\chi_i^\pm}{h_i}{}^\top\boldsymbol{e}_i - + \frac{\pi_i-\chi_i^\pm}{h_{i+1}}{}^\top\boldsymbol{e}_{i+1}, \end{cases} \tag{3.119}$$

and the approximations of the eigenvectors given in proposition 3.3.8 are verified.

To sum this section up, we succeeded to split the eigenvalues $\lambda_i^\pm$ into two distinct ones, for one $i \in [\![1,n-1]\!]$, in the asymptotic $1-\gamma_i \ll 1$ and for all $j \in [\![1,n]\!], |u_j| \ll 1$. Moreover, we managed to get approximations of the corresponding left and right eigenvectors. However, this study was done just for one $i \in [\![1,n]\!]$ and need to be proved for each one to deduce the diagonalizability of $\mathsf{A}(\mathbf{u},\boldsymbol{\gamma},\theta)$ and the local well-posedness of the system (3.10).

3.4 Asymptotic expansion of all the eigenvalues

In the previous section, a bifurcation of one couple of eigenvalues (associated with one interface liquide/liquid) has been obtained, in the regime of the merger of two layers: for the interface where the density ratio is the closest to 1, we managed to prove there exist two distinct eigenvalues with distinct eigenvectors. However, this analysis is not possible anymore if all the density ratios tend to 1, without distinction on how they tend to. In this section, we will prove the expressions of the asymptotic expansions of all the eigenvalues of $\mathsf{A}(\mathbf{u},\boldsymbol{\gamma})$ and give a necessary condition of hyperbolicity of the system (3.10), under a regime which distinguish how these density ratios tend to 1.

3.4.1 The asymptotic regime

In order to get an asymptotic expansion of the eigenvalues and the eigenvectors, it is necessary to assume there exist a small parameter $\varepsilon > 0$ and an injective function $\sigma : [\![1, n-1]\!] \to \mathbb{R}_+^*$ such that for all $i \in [\![1, n-1]\!]$

$$1 - \gamma_i = \varepsilon^{\sigma(i)}. \tag{3.120}$$

Without loss of generality, we consider ε is such that

$$\min_{i \in [\![1,n-1]\!]} \sigma(i) = 1. \tag{3.121}$$

Moreover, we set the next notations:

$$\begin{cases} u_{i+1} - u_i := \pi_i \varepsilon^{\frac{\sigma(i)}{2}}, \\ h_i := \varpi_i h_{i+1}. \end{cases} \tag{3.122}$$

Another assumption will be made on the paramters $\boldsymbol{\pi} := (\pi_i)_{i \in [\![1,n-1]\!]} \in \mathbb{R}^{n-1}$ and $\boldsymbol{\varpi} := (\varpi_i)_{i \in [\![1,n-1]\!]} \in \mathbb{R}_+^{*\,n-1}$:

$$\forall j \in [\![1, n-1]\!], \begin{cases} \pi_j^2 = \mathcal{O}(h_{j+1} + h_j), \\ \varpi_j = \mathcal{O}(1). \end{cases} \tag{3.123}$$

Remark: The assumption on $\boldsymbol{\pi}$ is in agreement with the necessary condition of hyperbolicity (3.3.7): we expect to get this type of condition for the hyperbolicity of the complete model. However, the assumption on $\boldsymbol{\varpi}$ is a particular case, where there is no preponderant layer.

The density-stratification (3.120) will permit to consider the multi-layer system as the two-layer system. We explain in this section how we figure it out: That is why we define the next subsets of $\mathbb{N}^*$, which provide a partition of $[\![1, n]\!]$:

$$\begin{aligned}
\Sigma_i^- &:= \{1 \le j \le i \ / \sigma([\![j, i]\!]) \subset [\sigma(i), +\infty[\}, \\
\Sigma_i^+ &:= \{n \ge j > i \ / \sigma([\![i, j-1]\!]) \subset [\sigma(i), +\infty[\}, \\
\overline{\Sigma}_{i,1}^- &:= \{j \notin \Sigma_i^- \cup \Sigma_i^+ \ / \ \sigma(j) > \sigma(i) \text{ and } 1 \le j < i\}, \\
\overline{\Sigma}_{i,1}^+ &:= \{j \notin \Sigma_i^- \cup \Sigma_i^+ \ / \ \sigma(j) > \sigma(i) \text{ and } n \ge j > i\}, \\
\overline{\Sigma}_{i,2}^- &:= \{j \notin \Sigma_i^- \cup \Sigma_i^+ \ / \ \sigma(j) < \sigma(i) \text{ and } 1 \le j < i\}, \\
\overline{\Sigma}_{i,2}^+ &:= \{j \notin \Sigma_i^- \cup \Sigma_i^+ \ / \ \sigma(j) < \sigma(i) \text{ and } n \ge j > i\},
\end{aligned} \tag{3.124}$$

and

$$\begin{cases} m_i^- := \min \Sigma_i^-, \\ m_i^+ := \max \Sigma_i^+. \end{cases} \tag{3.125}$$

Using the implicit function theorem and assumption (3.120), we will prove the eigenvalues associated to the interface i, $\lambda_i^{\pm}$, are influenced just by the layers with indices in

$$\Sigma_i^- \cup \Sigma_i^+ = [\![m_i^-, m_i^+]\!]. \tag{3.126}$$

Remark: The interpretation of the indices m_i^- and m_i^+ is: coming from the interface i, the interface $m_i^- - 1$ is the first one, above the interface i, with a density ratio smaller than γ_i; the interface m_i^+ is the first one, below the interface i, with a density ratio smaller than γ_i:

$$\begin{aligned} m_i^- &:= \max\{1 \leq j \leq i / \gamma_j \geq \gamma_i\}, \\ m_i^+ &:= \min\{n \geq j > i / \gamma_{j-1} \geq \gamma_i\}. \end{aligned} \tag{3.127}$$

Then, in respect of the interface i, the interface $m_i^- - 1$ has the same behavior as a free-surface and the interface m_i^+ as a bathymetry.

3.4.2 The barotropic eigenvalues

When all the densities and the velocities are equal, the barotropic eigenvalues degenerate to eigenvalues with simple multiplicity, so the asymptotic expansion is not necessary to prove the diagonalizability of the matrix $\mathsf{A}(\mathbf{u}, \boldsymbol{\gamma}, \theta)$. However, using classical analysis, we can obtain more accurate expression of these eigenvalues, as it is proved in the next proposition. Thus, we may know the order of the perturbation under the asymtotic regime (3.120).

Proposition 3.4.1 *Let $(\mathbf{u}, \boldsymbol{\gamma}) \in \mathbb{R}^{3n} \times]0,1[^{n-1}$ such that $(1-\gamma_j)_{j \in [\![1,n-1]\!]}$ and $(u_j)_{j \in [\![1,n]\!]}$ are sufficiently small. Then, an asymptotic expansion of $\lambda_n^{\pm}(\mathbf{u}, \boldsymbol{\gamma})$ is*

$$\begin{aligned} \lambda_n^{\pm}(\mathbf{u}, \boldsymbol{\gamma}) = \quad & \bar{u} \pm \left[\sqrt{H} - \frac{1}{2H^{\frac{3}{2}}} \sum_{j=1}^{n-1} (1-\gamma_j) \left(\sum_{k=1}^{j} h_k \right) \left(\sum_{k=j+1}^{n} h_k \right) \right] \\ & + \mathcal{O}\left(\left((1-\gamma_j)^2 \right)_{j \in [\![1,n-1]\!]}, \left((1-\gamma_j) u_k \right)_{(j,k) \in [\![1,n-1]\!] \times [\![1,n]\!]}, \left(u_k^2 \right)_{k \in [\![1,n]\!]} \right). \end{aligned} \tag{3.128}$$

Proof First, we prove two useful lemmata.

Lemma 3.4.2 *Let $\boldsymbol{\alpha} := (\alpha_1, \ldots, \alpha_n) \in \mathbb{R}^n$ and $\lambda \in \mathbb{R}$. We consider the matrix*

$$\mathsf{N}(\boldsymbol{\alpha}, \lambda) := \left[\lambda^2 \delta_i^j - \alpha_j \right]_{(i,j) \in [\![1,n]\!]^2},$$

where δ_i^j is the Kronecker symbol. Then

$$det(\mathsf{N}(\boldsymbol{\alpha}, \lambda)) = \lambda^{2n-2} \left(\lambda^2 - \sum_{i=1}^{n} \alpha_i \right) \tag{3.129}$$

Proof We define $q(\boldsymbol{\alpha}, \lambda) := det(\mathsf{N}(\boldsymbol{\alpha}, \lambda))$, which is a polynomial in λ:

$$g(\boldsymbol{\alpha}, \lambda) := \sum_{i=1}^{n} a_i \lambda^{2i} \tag{3.130}$$

with for all $i \in [\![0,n]\!], a_i = \frac{\partial^{2i} g}{\partial \beta^{2i}}(\boldsymbol{\alpha},0)$. One can prove recursively that

$$a_i = \begin{cases} 0, & \text{if } i \in [\![0,n-2]\!], \\ -\sum_{i=1}^{n} \alpha_i, & \text{if } i = n-1, \\ 1, & \text{if } i = n, \end{cases}$$

and the lemma 3.4.2 is straightforward proved.

Lemma 3.4.3 *Let* $\lambda \in \mathbb{R}^*$, $\boldsymbol{\gamma} \in]0,1[^{n-1}$ *and* $\mathbf{h} \in \mathbb{R}_+^{*\,n}$, *then*

$$f_n(\lambda, \mathbf{u^0}, \boldsymbol{\gamma}) = -\lambda^{2n-2}(h_n \zeta_n - \lambda^2) \tag{3.131}$$

where the sequence $(\zeta_i)_{i\in\mathbb{N}^*}$ *is defined by*

$$\begin{cases} \zeta_1 = 1, \\ \zeta_{i+1} = \zeta_1 + \frac{h_i}{\lambda^2}\zeta_i(\gamma_i - 1 + \frac{\lambda^2}{h_{i+1}}) + \sum_{j=1}^{i-2} \frac{\rho_{j+1} h_j}{\rho_n \lambda^2}(\gamma_j - 1)\zeta_j. \end{cases} \tag{3.132}$$

Proof First, we factorize $f_n(\lambda, \mathbf{u^0}, \boldsymbol{\gamma})$ by $(-1)^n \prod_{i=1}^n h_i$ and then we perform the next operations on the columns of $\mathsf{M}_x(\pm\sqrt{H}, \mathbf{u^0}, \boldsymbol{\gamma})$, for every $k \in [\![1, n-1]\!]$:

$$\mathrm{C}_k \leftarrow \mathrm{C}_k - \mathrm{C}_{k+1}, \tag{3.133}$$

and then for $i \in [\![1, n-1]\!]$,

$$\mathrm{C}_n \leftarrow \mathrm{C}_n + \frac{h_i}{\lambda^2}\zeta_i \mathrm{C}_i, \tag{3.134}$$

To finish, as the determinant becomes lower triangular, the lemma 3.4.3 is proved.

Then, we verify the next lemma to apply the implicit function theorem:

Lemma 3.4.4 *The barotropic eigenvalues* $\lambda_n^{\pm}(\mathbf{u^0}, \boldsymbol{\gamma^0}) := \pm\sqrt{H}$ *verify*

$$\begin{cases} f_n(\lambda_n^{\pm}(\mathbf{u^0}, \boldsymbol{\gamma^0}), \mathbf{u^0}, \boldsymbol{\gamma^0}) = 0, \\ \frac{\partial f_n}{\partial \lambda}(\lambda_n^{\pm}(\mathbf{u^0}, \boldsymbol{\gamma^0}), \mathbf{u^0}, \boldsymbol{\gamma^0}) \neq 0, \end{cases} \tag{3.135}$$

Proof According to the lemma 3.4.2 and the definition of H in (3.6), it is clear that

$$f_n(\lambda_n^{\pm}(\mathbf{u^0}, \boldsymbol{\gamma^0}), \mathbf{u^0}, \boldsymbol{\gamma^0}) = 0. \tag{3.136}$$

Concerning the derivative, we have

$$\frac{\partial f_n}{\partial \lambda}(\lambda_n^{\pm}(\mathbf{u^0}, \boldsymbol{\gamma^0}), \mathbf{u^0}, \boldsymbol{\gamma^0}) = \sum_{k=1}^{n} 2\lambda_n^{\pm}(\mathbf{u^0}, \boldsymbol{\gamma^0}) f_n^k(\lambda_n^{\pm}(\mathbf{u^0}, \boldsymbol{\gamma^0}), \mathbf{u^0}, \boldsymbol{\gamma^0}). \tag{3.137}$$

Then, with the lemma 3.4.2 and using the same argument as in (3.92),

$$\frac{\partial f_n}{\partial \lambda}(\lambda_n^{\pm}(\mathbf{u^0}, \boldsymbol{\gamma^0}), \mathbf{u^0}, \boldsymbol{\gamma^0}) = \pm 2H^{n-\frac{1}{2}}, \tag{3.138}$$

and the lemma 3.4.4 is proved.

Then, as the lemma 3.4.4 is verified, it is possible to apply the implicit function theorem to get the approximation of $\lambda_n^{\pm}(\mathbf{u},\boldsymbol{\gamma})$:

$$\begin{aligned} 0 \quad = \quad & (\lambda_n^{\pm}(\mathbf{u},\boldsymbol{\gamma}) - \lambda_n^{\pm}(\mathbf{u^0},\boldsymbol{\gamma^0}))\frac{\partial f_n}{\partial \lambda}(\lambda_n^{\pm}(\mathbf{u^0},\boldsymbol{\gamma^0}),\mathbf{u^0},\boldsymbol{\gamma^0}) \\ & + \sum_{j=1}^{n-1}(\gamma_j - 1)\frac{\partial f_n}{\partial \gamma_j}(\lambda_n^{\pm}(\mathbf{u^0},\boldsymbol{\gamma^0}),\mathbf{u^0},\boldsymbol{\gamma^0}) \\ & + \sum_{j=1}^{n} u_j \frac{\partial f_n}{\partial u_j}(\lambda_n^{\pm}(\mathbf{u^0},\boldsymbol{\gamma^0}),\mathbf{u^0},\boldsymbol{\gamma^0}) \\ & + \mathcal{O}(\left((1-\gamma_j)^2\right)_{j\in[\![1,n-1]\!]}, \left((1-\gamma_j)u_k\right)_{(j,k)\in[\![1,n-1]\!]\times[\![1,n]\!]}, \left(u_k^2\right)_{k\in[\![1,n]\!]}), \end{aligned} \tag{3.139}$$

Lemma 3.4.5 *The* 1st *order partial derivatives are such that*

$$\begin{cases} \frac{\partial f_n}{\partial u_j}(\lambda_n^{\pm}(\mathbf{u^0},\boldsymbol{\gamma^0}),\mathbf{u^0},\boldsymbol{\gamma^0}) & = -2\left(\pm H^{\frac{1}{2}}\right)H^{n-2}h_j, \qquad \forall j \in [\![1,n]\!], \\ \frac{\partial f_n}{\partial \gamma_j}(\lambda_n^{\pm}(\mathbf{u^0},\boldsymbol{\gamma^0}),\mathbf{u^0},\boldsymbol{\gamma^0}) & = -H^{n-2}\left(\sum_{k=1}^{j}h_k\right)\left(\sum_{k=j+1}^{n}h_k\right), \quad \forall j \in [\![1,n-1]\!]. \end{cases} \tag{3.140}$$

Proof The expressions of the 1st ones come from

$$\frac{\partial f_n}{\partial u_j}(\lambda_n^{\pm}(\mathbf{u^0},\boldsymbol{\gamma^0}),\mathbf{u^0},\boldsymbol{\gamma^0}) = -2\lambda_n^{\pm}(\mathbf{u^0},\boldsymbol{\gamma^0})f_n^j(\mathbf{u^0},\boldsymbol{\gamma^0}),\mathbf{u^0},\boldsymbol{\gamma^0}), \tag{3.141}$$

the lemma 3.4.2 and using the same argument as in (3.92). For the 2nd ones, we define a new sequence:

$$\forall (i,j) \in [\![1,n]\!]\times[\![1,n-1]\!],\ \eta_i^j := \frac{\partial \zeta_i}{\partial \gamma_j}(\lambda_n^{\pm}(\mathbf{u^0},\boldsymbol{\gamma^0}),\mathbf{u^0},\boldsymbol{\gamma^0}). \tag{3.142}$$

Then, one can prove that for all $j \in [\![1,n-1]\!]$,

$$\eta_i^j = \begin{cases} \frac{h_{i-1}}{h_i}\eta_{i-1}^j, & i \in [\![1,k]\!], \\ \frac{h_k}{H}\zeta_j + \frac{h_{i-1}}{h_i}\eta_{i-1}^j, & i \in [\![k+1,n]\!]. \end{cases} \tag{3.143}$$

which implies that

$$\forall j \in [\![1,n-1]\!],\ \eta_n^j = \frac{1}{Hh_n}\Big(\sum_{k=1}^{j}h_k\Big)\Big(\sum_{k=j+1}^{n}h_k\Big). \tag{3.144}$$

According to the lemma 3.4.3,

$$\frac{\partial f_n}{\partial \gamma_j}(\lambda_n^{\pm}(\mathbf{u^0},\boldsymbol{\gamma^0}),\mathbf{u^0},\boldsymbol{\gamma^0}) = -H^{n-1}h_n\eta_n^j, \tag{3.145}$$

and the lemma 3.4.5 is proved.

Finally, using lemmata 3.4.4 and 3.4.5 in (3.139), we have

$$\begin{aligned} 0 \;=\; & \pm 2(\lambda_n^{\pm}(\mathbf{u},\boldsymbol{\gamma}) - \lambda_n^{\pm}(\mathbf{u^0},\boldsymbol{\gamma^0}))H^{n-\frac{1}{2}} \\ & + H^{n-2}\sum_{j=1}^{n-1}(1-\gamma_j)\Big(\sum_{k=1}^{j}h_k\Big)\Big(\sum_{k=j+1}^{n}h_k\Big) \\ & - 2\big(\pm H^{\frac{1}{2}}\big)H^{n-2}\sum_{j=1}^{n}u_j h_j \\ & + \mathcal{O}\Big(\big((1-\gamma_j)^2\big)_{j\in[\![1,n-1]\!]}, \big((1-\gamma_j)u_k\big)_{(j,k)\in[\![1,n-1]\!]\times[\![1,n]\!]}, \big(u_k^2\big)_{k\in[\![1,n]\!]}\Big), \end{aligned} \tag{3.146}$$

and the proposition 3.4.1 is proved.

Then, we can deduce the expressions of the asymptotic expansions of the barotropic eigenvalues, in the particular asymptotic regime (3.120).

Proposition 3.4.6 *Let* $(\mathbf{u},\boldsymbol{\gamma}) \in \mathbb{R}^{3n}\times]0,1[^{n-1}$, $\varepsilon > 0$ *and an injective function* $\sigma \in \mathbb{R}_+^{*\,[\![1,n-1]\!]}$ *such that* $\boldsymbol{\gamma}$ *verifies* (3.120), $\mathbf{u}$ *verifies* (3.123) *and*

$$\varepsilon \ll 1. \tag{3.147}$$

Then, an asymptotic expansion of $\lambda_n^{\pm}(\mathbf{u},\boldsymbol{\gamma})$ *is*

$$\begin{aligned} \lambda_n^{\pm}(\mathbf{u},\boldsymbol{\gamma}) = \; & u_{m_\sigma^-} \pm \sqrt{H} + (u_{m_\sigma^-+1} - u_{m_\sigma^-})\frac{\sum_{k=m_\sigma^++1}^{n} h_k}{H} \\ & + \mathcal{O}\left(1-\gamma_{m_\sigma^-}\right), \end{aligned} \tag{3.148}$$

where $m_\sigma^- \in [\![1,n-1]\!]$ *is defined by*

$$\sigma(m_\sigma^-) = \min_{j\in[\![1,n-1]\!]}\sigma(j) = 1, \tag{3.149}$$

or with other words, it is the indice of the interface liquid/liquid with the biggest density gap.

Proof According to the assumption (3.120), (3.123) and the proposition 3.4.1, the expression (3.148) is directly deduced,

$$\begin{aligned} \lambda_n^{\pm}(\mathbf{u},\boldsymbol{\gamma}) \; & = u_{m_\sigma^-} \pm \sqrt{H} + \psi_{m_\sigma^-}\varepsilon^{\frac{1}{2}} \pm \big(-h^-_{\sigma,m_\sigma^-}h^+_{\sigma,m_\sigma^-}\big)\varepsilon + \mathcal{O}(\varepsilon^{\frac{3}{2}}) \\ & = u_{m_\sigma^-} \pm \sqrt{H} + \psi_{m_\sigma^-}\varepsilon^{\frac{1}{2}} + \mathcal{O}(\varepsilon), \end{aligned} \tag{3.150}$$

where $\psi_{m_\sigma^-} := \pi_{m_\sigma^-}\frac{\sum_{k=m_\sigma^++1}^{n} h_k}{H}$. In conclusion, the approximations of the eigenvalues given in proposition 3.4.6 are verified.

Remark: The asymptotic expansion of $\lambda_n^{\pm}(\mathbf{u},\boldsymbol{\gamma})$ in proposition 3.4.1 corresponds to the asymptotic expansion of $\lambda_1^{\pm}$ in the set of hyperbolicity $|F_x| < F_{crit}^-$ in [88], in the two-layer case. Moreover, it is in accordance with the expression of the internal eigenvalues in [1], [9], [30], [67], [97], [114] and [127].

To sum this subsection up, we managed to obtain an asymptotic expansion of the barotropic eigenvalues, $\lambda_n^{\pm}(\mathbf{u},\boldsymbol{\gamma})$, with a precision in

$$\mathcal{O}\left((1-\gamma_j)^2\right)_{j\in[\![1,n-1]\!]}, ((1-\gamma_j)u_k)_{(j,k)\in[\![1,n-1]\!]\times[\![1,n]\!]}, \left(u_k^2\right)_{k\in[\![1,n]\!]}. \tag{3.151}$$

Moreover, we gave the asymptotic expansion, with the assumptions (3.120), (3.123) and (3.147), with a precision about $\mathcal{O}(\varepsilon)$.
In the next subsection, we prove the expression of asymptotic expansion of the baroclinic eigenvalues and give a necessary condition of hyperbolicity, in the asymptotic regime (3.120).

3.4.3 The baroclinic eigenvalues

In the proposition 3.3.2, we have proved the asymptotic expansion of the eigenvalues associated to an interface where the layers just above and below are almost merged. We prove, in this subsection, the asymptotic expansion of the baroclinic eigenvalues, for each interface.

Proposition 3.4.7 *Let* $(\mathbf{u},\boldsymbol{\gamma}) \in \mathbb{R}^{3n}\times]0,1[^{n-1}$, $\varepsilon > 0$ *and an injective function* $\sigma \in \mathbb{R}_+^{*\,[\![1,n-1]\!]}$ *such that* $\boldsymbol{\gamma}$ *verifies* (3.120), $\mathbf{u}$ *verifies* (3.123) *and*

$$\varepsilon \ll 1. \tag{3.152}$$

Then, for all $i \in [\![1,n-1]\!]$, *the asymptotic expansion of* $\lambda_i^{\pm}(\mathbf{u},\boldsymbol{\gamma})$ *is*

$$\begin{aligned}\lambda_i^{\pm}(\mathbf{u},\boldsymbol{\gamma}) = \ & \frac{u_{i+1}h_{\sigma,i}^- + u_i h_{\sigma,i}^+}{h_{\sigma,i}^- + h_{\sigma,i}^+} \pm \left[\frac{h_{\sigma,i}^- h_{\sigma,i}^+}{(h_{\sigma,i}^- + h_{\sigma,i}^+)}\left(1-\gamma_i - \frac{(u_{i+1}-u_i)^2}{h_{\sigma,i}^- + h_{\sigma,i}^+}\right)\right]^{\frac{1}{2}} \\ & + \mathcal{O}(\varepsilon^{\frac{\sigma(i)+1}{2}})\end{aligned} \tag{3.153}$$

where $h_{\sigma,i}^- := \sum_{k=m_i^-}^{i} h_k$ *and* $h_{\sigma,i}^+ := \sum_{k=i+1}^{m_i^+} h_k$.

Remark: $h_{\sigma,i}^{\pm}$ are the upper and lower layers influencing $\lambda_i^{\pm}$.

Proof Let $i \in [\![1,n-1]\!]$, according to the corollary 3.3.7, the eigenvalue $\lambda_i^{\pm}$ is assumed as

$$\begin{cases} \lambda_i^{\pm} - u_i := \tilde{\lambda}_i^{\pm}\varepsilon^{\frac{\sigma(i)}{2}}, \\ \tilde{\lambda}_i^{\pm} = \mathcal{O}(\varpi_i). \end{cases} \tag{3.154}$$

First of all, we need to evaluate the order of each term of $\det(\mathsf{M}_x(\lambda_i^{\pm},\mathbf{u},\boldsymbol{\gamma}))$. The next operations are performed to the columns of the determinant, without changing its value:

$$\forall j \in [\![1,n-1]\!],\ \mathrm{C}_j \leftarrow \mathrm{C}_j - \varpi_j \mathrm{C}_{j+1}. \tag{3.155}$$

Then, for all $j \in [\![1, n-1]\!]$, the new column C_j is expressed in $(\boldsymbol{f_i})_{i\in[|1,n|]}$, the canonical basis of $\mathbb{R}^n$

$$\begin{cases} C_j = & h_j(\lambda_i^{\pm} - u_j)^2 \boldsymbol{f_j} + [h_j(1-\gamma_j) - \varpi_j(\lambda_i^{\pm} - u_{j+1})^2]\boldsymbol{f}_{j+1} \\ & + h_j \sum_{k=j+2}^{n} \alpha_{k,j+1}(1-\gamma_j)\boldsymbol{f_k}, \\ C_n = & h_n(\lambda_i^{\pm} - u_n)^2 \boldsymbol{f_n} - h_n \sum_{k=1}^{n} \boldsymbol{f_k}. \end{cases} \tag{3.156}$$

Then, for all $j \in [\![1, n]\!]$, we denote by $o(i, j, \sigma)$, the order of the terms of the column C_j:

$$C_j = \mathcal{O}(\varepsilon^{o(i,j,\sigma)}). \tag{3.157}$$

We provide the expression of $o(i, j, \sigma)$ in the next lemma:

Lemma 3.4.8 *Let* $(i, j) \in [\![1, n]\!] \times [\![1, n-1]\!]$,

$$o(i,j,\sigma) = \begin{cases} \sigma(i), & \text{if } j \in \Sigma_i^- \cup \Sigma_i^+, \\ \sigma_{i,j}^-, & \text{if } j \in \overline{\Sigma}_{i,1}^- \cup \overline{\Sigma}_{i,2}^-, \\ \sigma_{i,j}^+, & \text{if } j \in \overline{\Sigma}_{i,1}^+ \cup \overline{\Sigma}_{i,2}^+, \end{cases} \tag{3.158}$$

and

$$o(i,n,\sigma) = 0, \tag{3.159}$$

where for all $j \leq i$,

$$\sigma_{i,j}^- := \min\{\sigma(k)/k \in [\![j, i]\!]\}, \tag{3.160}$$

and for all $j \geq i$,

$$\sigma_{i,j}^+ := \min\{\sigma(k)/k \in [\![i, j]\!]\}. \tag{3.161}$$

Proof According to the expression of C_n in (3.158), it is clear that the order of C_n is 1

$$o(i,n,\sigma) = 0, \tag{3.162}$$

Moreover, we analyse each term of C_j, for all $j \in [\![1, n-1]\!]$:

$$\forall k \geq j+2,\ h_j \alpha_{k,j+1}(1-\gamma_j) \sim h_j(1-\gamma_j), \tag{3.163}$$

$$\lambda_i^{\pm} - u_j \sim \begin{cases} \lambda_i^{\pm} - u_i, & \text{if } j \in \Sigma_i^-, \\ \lambda_i^{\pm} - u_{i+1}, & \text{if } j \in \Sigma_i^+, \\ u_{\beta_{i,j}^- + 1} - u_{\beta_{i,j}^-}, & \text{if } j \in \overline{\Sigma}_{i,1}^- \cup \overline{\Sigma}_{i,2}^-, \\ u_{\beta_{i,j}^+} - u_{\beta_{i,j}^+ + 1}, & \text{if } j \in \overline{\Sigma}_{i,1}^+ \cup \overline{\Sigma}_{i,2}^+, \end{cases} \tag{3.164}$$

$$s_{i,j} \sim \begin{cases} -\varpi_j(\lambda_i^{\pm} - u_i)^2, & \text{if } j \in \Sigma_i^- \backslash \{i\}, \\ -\varpi_j(\lambda_i^{\pm} - u_{i+1})^2, & \text{if } j \in \Sigma_i^+ \backslash \{m_i^+\}, \\ -\varpi_j(u_{\beta^-_{i,j+1}+1} - u_{\beta^-_{i,j+1}})^2, & \text{if } j \in \overline{\Sigma}^-_{i,1}, \\ -\varpi_j(u_{\beta^+_{i,j}+1} - u_{\beta^+_{i,j}})^2, & \text{if } j \in \overline{\Sigma}^+_{i,1}, \\ \delta^j_{\beta^-_{i,j}} h_j(1-\gamma_j) - \delta^{\beta^-_{i,j+1}}_{\beta^-_{i,j}} \varpi_j(u_{\beta^-_{i,j+1}+1} - u_{\beta^-_{i,j+1}})^2, & \text{if } j \in \overline{\Sigma}^-_{i,2}, \\ \delta^j_{\beta^+_{i,j}} h_j(1-\gamma_j) - \varpi_j(u_{\beta^+_{i,j}+1} - u_{\beta^+_{i,j}})^2, & \text{if } j \in \overline{\Sigma}^+_{i,2}, \\ h_j(1-\gamma_j) - \varpi_j(\lambda_i^{\pm} - u_{j+1})^2, & \text{if } j = i, \\ h_j(1-\gamma_j) - \varpi_j(u_j - u_{j+1})^2, & \text{if } j = m_i^+, \end{cases} \tag{3.165}$$

where δ^j_i is the Kronecker symbol, $s_{i,j}$ is defined by

$$s_{i,j} := h_j(1-\gamma_j) - \varpi_j(\lambda_i^{\pm} - u_{j+1})^2, \tag{3.166}$$

and $\beta^{\pm}_{i,j} \in [\![1,n]\!]$ are defined such that

$$\sigma(\beta^{\pm}_{i,j}) := \sigma^{\pm}_{i,j}. \tag{3.167}$$

Then, according to (3.120), (3.123) and (3.154),

$$\forall k \geq j+2,\ h_j \alpha_{k,j+1}(1-\gamma_j) \sim h_j \varepsilon^{\sigma(j)}, \tag{3.168}$$

$$\lambda_i^{\pm} - u_j \sim \begin{cases} \tilde{\lambda}_i^{\pm} \varepsilon^{\frac{\sigma(i)}{2}}, & \text{if } j \in \Sigma_i^-, \\ (\tilde{\lambda}_i^{\pm} - \pi_i)\varepsilon^{\frac{\sigma(i)}{2}}, & \text{if } j \in \Sigma_i^+, \\ \pi_{\beta^-_{i,j}} \varepsilon^{\frac{\sigma^-_{i,j}}{2}}, & \text{if } j \in \overline{\Sigma}^-_{i,1} \cup \overline{\Sigma}^-_{i,2}, \\ -\pi_{\beta^+_{i,j}} \varepsilon^{\frac{\sigma^+_{i,j}}{2}}, & \text{if } j \in \overline{\Sigma}^+_{i,1} \cup \overline{\Sigma}^+_{i,2}, \end{cases} \tag{3.169}$$

$$s_{i,j} \sim \begin{cases} -\varpi_j(\tilde{\lambda}_i^{\pm})^2 \varepsilon^{\sigma(i)}, & \text{if } j \in \Sigma_i^- \backslash \{i\}, \\ -\varpi_j(\tilde{\lambda}_i^{\pm} - \pi_i)^2 \varepsilon^{\sigma(i)} & \text{if } j \in \Sigma_i^+ \backslash \{m_i^+\}, \\ -\varpi_j \pi^2_{\beta^-_{i,j+1}} \varepsilon^{\sigma^-_{i,j}}, & \text{if } j \in \overline{\Sigma}^-_{i,1}, \\ -\varpi_j \pi^2_{\beta^+_{i,j}} \varepsilon^{\sigma^+_{i,j}}, & \text{if } j \in \overline{\Sigma}^+_{i,1}, \\ \delta^j_{\beta^-_{i,j}} h_j \varepsilon^{\sigma(j)} - \delta^{\beta^-_{i,j+1}}_{\beta^-_{i,j}} \varpi_j \pi^2_{\beta^-_{i,j+1}} \varepsilon^{\sigma^-_{i,j}}, & \text{if } j \in \overline{\Sigma}^-_{i,2}, \\ \delta^j_{\beta^+_{i,j}} h_j \varepsilon^{\sigma(j)} - \varpi_j \pi^2_{\beta^+_{i,j}} \varepsilon^{\sigma^+_{i,j}}, & \text{if } j \in \overline{\Sigma}^+_{i,2}, \\ (h_j - \varpi_j(\tilde{\lambda}_i^{\pm} - \pi_j)^2)\varepsilon^{\sigma(i)}, & \text{if } j = i, \\ (h_j - \varpi_j \pi_j^2)\varepsilon^{\sigma(j)}, & \text{if } j = m_i^+. \end{cases} \tag{3.170}$$

Finally, using that

$$\forall (i,j) \in [\![1,n-1]\!]^2, \begin{cases} \sigma^-_{i,j} \leq \sigma(j), \\ \sigma^+_{i,j} \leq \sigma(j), \\ \sigma^-_{i,m^-_i-1} = \sigma(m^-_i - 1), \end{cases} \tag{3.171}$$

the lemma 3.4.8 is proved.

Afterwards, we define for all $j \in [\![1,n]\!]$, $\tilde{C}_j := \frac{C_j}{\varepsilon^{o(i,j,\sigma)}}\big|_{\varepsilon=0}$. If $j \in [\![1,n-1]\!]$, $\tilde{C}_j$ is equal to

$$\begin{cases} (\tilde{\lambda}^{\pm}_i)^2(\boldsymbol{f_j} - \varpi_j \boldsymbol{f}_{j+1}), & \text{if } j \in \Sigma^-_i \backslash \{i\}, \\ (\tilde{\lambda}^{\pm}_i - \pi_i)^2(\boldsymbol{f_j} - \varpi_j \boldsymbol{f}_{j+1}), & \text{if } j \in \Sigma^+_i \backslash \{m^+_i\}, \\ (\pi_{\beta^-_{i,j}})^2 \boldsymbol{f_j} - \delta^{\sigma^-_{i,j+1}}_{\sigma^-_{i,j}} \varpi_j (\pi_{\beta^-_{i,j+1}})^2 \boldsymbol{f}_{j+1}, & \text{if } j \in \overline{\Sigma}^-_{i,1}, \\ \delta^{\sigma^+_{i,j+1}}_{\sigma^+_{i,j}} (\pi_{\beta^+_{i,j-1}})^2 \boldsymbol{f_j} - \varpi_j (\pi_{\beta^+_{i,j+1}})^2 \boldsymbol{f}_{j+1}, & \text{if } j \in \overline{\Sigma}^+_{i,1}, \\ (\pi_{\beta^-_{i,j}})^2 \boldsymbol{f_j} - \delta^{\sigma^-_{i,j+1}}_{\sigma^-_{i,j}} \varpi_j (\pi_{\beta^-_{i,j+1}})^2 \boldsymbol{f}_{j+1} + \delta^{\sigma(j)}_{\sigma^-_{i,j}} h_j \sum_{k=j+1}^n \boldsymbol{f_k}, & \text{if } j \in \overline{\Sigma}^-_{i,2}, \\ \delta^{\sigma^+_{i,j+1}}_{\sigma^+_{i,j}} (\pi_{\beta^+_{i,j}})^2 \boldsymbol{f_j} - \varpi_j (\pi_{\beta^+_{i,j+1}})^2 \boldsymbol{f}_{j+1} + \delta^{\sigma(j)}_{\sigma^+_{i,j}} h_j \sum_{k=j+1}^n \boldsymbol{f_k}, & \text{if } j \in \overline{\Sigma}^+_{i,2}, \\ (\tilde{\lambda}^{\pm}_i)^2 \boldsymbol{f_j} - \varpi_j (\tilde{\lambda}^{\pm}_i - \pi_i)^2 \boldsymbol{f}_{j+1} + h_j \sum_{k=j+1}^n \boldsymbol{f_k}, & \text{if } j = i, \\ -\varpi_j \pi_j^2 \boldsymbol{f}_{j+1} + h_j \sum_{k=j+1}^n \boldsymbol{f_k}, & \text{if } j = m^+_i, \end{cases} \tag{3.172}$$

and if $j = n$, $\tilde{C}_j$ is equal to

$$\tilde{C}_n = h_n \sum_{k=1}^n \boldsymbol{f_k}. \tag{3.173}$$

Then, to every the column $\tilde{C}_j$, with $j \in [\![1,n-1]\!]$ such that one of the following conditions is verified:

$$\begin{cases} j = i, \\ j = m^+_i, \\ j \in \overline{\Sigma}^-_{i,2} \text{ and } \sigma^-_{i,j} = \sigma(j), \end{cases} \tag{3.174}$$

we perform the next operations:

$$\tilde{C}_j \leftarrow \tilde{C}_j - \frac{h_j}{h_n} \tilde{C}_n. \tag{3.175}$$

We define

$$\begin{aligned} \tilde{g}(\tilde{\lambda}^{\pm}_i, \boldsymbol{\pi}, \boldsymbol{\varpi}, \sigma) &:= \frac{g(\lambda^{\pm}_i, \boldsymbol{u}, \boldsymbol{\gamma})}{\varepsilon^{\sigma_i}}\Big|_{\varepsilon=0} \\ &= \det((\tilde{C}_j)_{j \in [\![1,n]\!]}), \end{aligned} \tag{3.176}$$

where $\sigma_i := \sum_{j=1}^n o(i,j,\sigma)$, $\boldsymbol{\pi} := (\pi_i)_{i \in [\![1,n-1]\!]}$ and $\boldsymbol{\varpi} := (\varpi_i)_{i \in [\![1,n-1]\!]}$. Then, according to (3.172), (3.173) and (3.175), the determinant $\tilde{g}(\tilde{\lambda}^{\pm}_i, \boldsymbol{\pi}, \boldsymbol{\varpi}, \sigma)$ is under the following form:

$$\tilde{g}(\tilde{\lambda}^{\pm}_i, \boldsymbol{\pi}, \boldsymbol{\varpi}, \sigma) = \begin{vmatrix} \Delta^1(\boldsymbol{\pi}, \boldsymbol{\varpi}, \sigma) & \Omega^1(\boldsymbol{\pi}, \boldsymbol{\varpi}, \sigma) & 0 \\ 0 & \Lambda(\tilde{\lambda}^{\pm}_i, \pi_i, \boldsymbol{\varpi}, \sigma) & 0 \\ 0 & \Omega^2(\boldsymbol{\pi}, \boldsymbol{\varpi}, \sigma) & \Delta^2(\boldsymbol{\pi}, \boldsymbol{\varpi}, \sigma) \end{vmatrix},$$

where $\Lambda(\tilde{\lambda}_i^{\pm},\pi_i,\boldsymbol{\varpi},\sigma)$, $\Delta^1(\boldsymbol{\pi},\boldsymbol{\varpi},\sigma)$ and $\Delta^2(\boldsymbol{\pi},\boldsymbol{\varpi},\sigma)$ are square matrices with respective dimensions $m_i^+ - m_i^- + 1$, $m_i^- - 1$ and $n - m_i^+$; $\Omega^1(\boldsymbol{\pi},\boldsymbol{\varpi},\sigma)$ and $\Omega^2(\boldsymbol{\pi},\boldsymbol{\varpi},\sigma)$ are rectangular matrices with respective dimensions $m_i^- - 1 \times m_i^+ - m_i^- + 1$ and $n - m_i^+ \times m_i^+ - m_i^-$.
Then, it is clear that

$$\tilde{g}(\tilde{\lambda}_i^{\pm},\boldsymbol{\pi},\boldsymbol{\varpi},\sigma) = \det\left(\Delta^1(\boldsymbol{\pi},\boldsymbol{\varpi},\sigma)\right)\det\left(\Lambda(\tilde{\lambda}_i^{\pm},\pi_i,\boldsymbol{\varpi},\sigma)\right)\det\left(\Delta^2(\boldsymbol{\pi},\boldsymbol{\varpi},\sigma)\right). \tag{3.177}$$

The important point of this proof is there is just $\Lambda(\tilde{\lambda}_i^{\pm},\pi_i,\boldsymbol{\varpi},\sigma)$ which depends of $\tilde{\lambda}_i^{\pm}$, therefore it is necessary to find the solution, $\tilde{\lambda}_i^{\pm}$, such that

$$\det\left(\Lambda(\tilde{\lambda}_i^{\pm},\pi_i,\boldsymbol{\varpi},\sigma)\right) = 0. \tag{3.178}$$

where, according to the previous analysis, the columns of $\det\left(\Lambda(\tilde{\lambda}_i^{\pm},\pi_i,\boldsymbol{\varpi},\sigma)\right)$ are such that for all $j \in [\![1, m_i^+ - m_i^- + 1]\!]$,

$$\mathrm{C}_j(\Lambda) = \begin{cases} (\tilde{\lambda}_i^{\pm})^2(\boldsymbol{f_j} - \varpi_j \boldsymbol{f}_{j+1}), & \text{if } m_i^- \le j_i \le i-1, \\ (\tilde{\lambda}_i^{\pm} - \pi_i)^2(\boldsymbol{f_j} - \varpi_j \boldsymbol{f}_{j+1}), & \text{if } i+1 \le j_i \le m_i^+ - 1, \\ (\tilde{\lambda}_i^{\pm})^2 \boldsymbol{f_i} - \varpi_i(\tilde{\lambda}_i^{\pm} - \pi_i)^2 \boldsymbol{f}_{i+1} - h_i \sum_{k=m_i^-}^{i} \boldsymbol{f_k}, & \text{if } j_i = i, \\ -h_j \sum_{j=1}^{m_i^+} \boldsymbol{f}_k, & \text{if } j_i = m_i^+, \end{cases} \tag{3.179}$$

where $j_i := j + m_i^- - 1$.

Lemma 3.4.9 *Let $(\pi_i, \boldsymbol{h}) \in \mathbb{R} \times \mathbb{R}^n$ and an injective function $\sigma \in \mathbb{R}_+^{*\,[\![1,n-1]\!]}$. Then, $\tilde{\lambda} \in \mathbb{R}$ is solution of*

$$\det\left(\Lambda(\tilde{\lambda},\pi_i,\boldsymbol{\varpi},\sigma)\right) = 0. \tag{3.180}$$

if and only if

$$\tilde{\lambda} \in \left\{0, \pi_i, \frac{\pi_i h_{\sigma,i}^-}{h_{\sigma,i}^- + h_{\sigma,i}^+} \pm \left[\frac{h_{\sigma,i}^- h_{\sigma,i}^+}{(h_{\sigma,i}^- + h_{\sigma,i}^+)^2}\left(h_{\sigma,i}^- + h_{\sigma,i}^+ - \pi_i^2\right)\right]^{\frac{1}{2}}\right\}, \tag{3.181}$$

where $h_{\sigma,i}^- := h_i(1 + \sum_{k=m_i^-}^{i-1}\prod_{j=k}^{i-1}\varpi_j)$ and $h_{\sigma,i}^+ := h_{m_i^+}(1 + \sum_{k=i+1}^{m_i^+-1}\prod_{j=k}^{m_i^+-1}\varpi_j)$. Moreover, the respective multiplicities are $2(i-m_i^-)$, $2(m_i^+ - i - 1)$ and 1.

Proof As $\mathrm{C}_n\left(\Lambda(\tilde{\lambda},\pi_i,\boldsymbol{\varpi},\sigma)\right)$ does not depend of $\tilde{\lambda}$, $\det\left(\Lambda(\tilde{\lambda},\pi_i,\boldsymbol{\varpi},\sigma)\right)$ is a polynomial in $\tilde{\lambda}$, with a degree equal to $2(m_i^+ - m_i^-)$. According to (3.179), 0 and π_i are two roots, with respective multiplicity $2(i-m_i^-)$ and $2(m_i^+ - i - 1)$. To determine the expression of the other roots, it is sufficient to perform the next operations on two columns of $\det\left(\Lambda(\tilde{\lambda}_i^{\pm},\pi_i,\boldsymbol{\varpi},\sigma)\right)$, assuming that $\tilde{\lambda} \notin \{0,\pi_i\}$:

$$\forall j \in [\![m_i^-, i-1]\!], \begin{cases} \mathrm{C}_i \leftarrow \mathrm{C}_i + \frac{h_i\left(1+\sum_{k=1}^{j-1}\prod_{q=k}^{j-1}\varpi_q\right)}{\tilde{\lambda}^2}\mathrm{C}_j, \\ \mathrm{C}_{m_i^+} \leftarrow \mathrm{C}_{m_i^+} + \frac{h_n\left(1+\sum_{k=1}^{j-1}\prod_{q=k}^{j-1}\varpi_q\right)}{\tilde{\lambda}^2}\mathrm{C}_j, \end{cases} \tag{3.182}$$

and afterwards

$$\forall j \in [\![i+1, m_i^+ - 1]\!], \mathrm{C}_{m_i^+} \leftarrow \mathrm{C}_{m_i^+} + \frac{h_i\left(1+\sum_{k=1}^{j-1}\prod_{q=k}^{j-1}\varpi_q\right)}{(\tilde{\lambda}-\pi_i)^2}\mathrm{C}_j. \tag{3.183}$$

Therefore, for all $j \in [\![1, m_i^+ - m_i^- + 1]\!]$, the new column of $\det\left(\Lambda(\tilde{\lambda}_i^{\pm}, \pi_i, \boldsymbol{\varpi}, \sigma)\right)$, C_j, is equal to

$$\begin{cases} (\tilde{\lambda}_i^{\pm})^2(\boldsymbol{f_j} - \varpi_j \boldsymbol{f}_{j+1}), & \text{if } m_i^- \leq j_i \leq i-1, \\ (\tilde{\lambda}_i^{\pm} - \pi_i)^2(\boldsymbol{f_j} - \varpi_j \boldsymbol{f}_{j+1}), & \text{if } i+1 \leq j_i \leq m_i^+ - 1, \\ ((\tilde{\lambda}_i^{\pm})^2 - h_{\sigma,i}^- +)\boldsymbol{f_i} - \varpi_i(\tilde{\lambda}_i^{\pm} - \pi_i)^2 \boldsymbol{f}_{i+1}, & \text{if } j_i = i, \\ -\frac{h_{m_i^+}}{h_i} h_{\sigma,i}^- \boldsymbol{f}_i - h_{\sigma,i}^+ \boldsymbol{f}_{m_i^+}, & \text{if } j_i = m_i^+, \end{cases} \tag{3.184}$$

where $j_i := j + m_i^- - 1$. An expansion of the determinant about the last column, $\mathrm{C}_{m_i^+}$, provides

$$\det\left(\Lambda(\tilde{\lambda}, \pi_i, \boldsymbol{\varpi}, \sigma)\right) = -\tilde{\lambda}^{2i-2}(\tilde{\lambda} - \pi_i)^{2(m_i^+ - i - 1)}\left[h_{\sigma,i}^-(\tilde{\lambda} - \pi_i)^2 + h_{\sigma,i}^+(\tilde{\lambda}^2 - h_{\sigma,i}^-)\right]. \tag{3.185}$$

Finally, the only solutions of (3.180), different from 0 and π_i are:

$$\tilde{\lambda}_i^{\pm} = \frac{\pi_i h_{\sigma,i}^-}{h_{\sigma,i}^- + h_{\sigma,i}^+} \pm \left[\frac{h_{\sigma,i}^- h_{\sigma,i}^+}{(h_{\sigma,i}^- + h_{\sigma,i}^+)^2}\left(h_{\sigma,i}^- + h_{\sigma,i}^+ - \pi_i^2\right)\right]^{\frac{1}{2}}, \tag{3.186}$$

with multiplicity equal to 1.

Consequently, according to the lemma 3.181

$$\tilde{g}(\tilde{\lambda}, \boldsymbol{\pi}, \boldsymbol{\varpi}, \sigma) = 0, \tag{3.187}$$

if and only if

$$\tilde{\lambda} \in \left\{0, \pi_i, \frac{\pi_i h_{\sigma,i}^-}{h_{\sigma,i}^- + h_{\sigma,i}^+} \pm \left[\frac{h_{\sigma,i}^- h_{\sigma,i}^+}{(h_{\sigma,i}^- + h_{\sigma,i}^+)^2}\left(h_{\sigma,i}^- + h_{\sigma,i}^+ - \pi_i^2\right)\right]^{\frac{1}{2}}\right\}. \tag{3.188}$$

According to the implicit functions theorem,

$$g(\lambda, \boldsymbol{u}, \boldsymbol{\gamma}) = 0, \tag{3.189}$$

if and only if $\lambda - \mathcal{O}(\varepsilon^{\frac{\sigma(i)+1}{2}})$ is in

$$\begin{aligned} &\left\{u_i, u_i + \pi_i \varepsilon^{\frac{\sigma(i)}{2}}, u_i + \left(\frac{\pi_i h_{\sigma,i}^-}{h_{\sigma,i}^- + h_{\sigma,i}^+} \pm \left[\frac{h_{\sigma,i}^- h_{\sigma,i}^+}{(h_{\sigma,i}^- + h_{\sigma,i}^+)^2}\left(h_{\sigma,i}^- + h_{\sigma,i}^+ - \pi_i^2\right)\right]^{\frac{1}{2}}\right)\varepsilon^{\frac{\sigma(i)}{2}}\right\} \\ &= \left\{u_i, u_{i+1}, \frac{u_{i+1} h_{\sigma,i}^- + u_i h_{\sigma,i}^+}{h_{\sigma,i}^- + h_{\sigma,i}^+} \pm \left[\frac{h_{\sigma,i}^- h_{\sigma,i}^+}{h_{\sigma,i}^- + h_{\sigma,i}^+}\left(1 - \gamma_i - (u_{i+1} - u_i)^2\right)\right]^{\frac{1}{2}}\right\}. \end{aligned} \tag{3.190}$$

$\lambda \in \{u_i + \mathcal{O}(\varepsilon^{\frac{\sigma(i)+1}{2}}), u_{i+1} + \mathcal{O}(\varepsilon^{\frac{\sigma(i)+1}{2}})\}$ corresponds to the merger of layers and does not provide the correct roots because the multiplicities are not equal to 1. That is why we chose

$$\lambda = \lambda_i^{\pm} := \frac{u_{i+1}h_{\sigma,i}^{-} + u_i h_{\sigma,i}^{+}}{h_{\sigma,i}^{-} + h_{\sigma,i}^{+}} \pm \left[\frac{h_{\sigma,i}^{-} h_{\sigma,i}^{+}}{h_{\sigma,i}^{-} + h_{\sigma,i}^{+}} \left(1 - \gamma_i - (u_{i+1} - u_i)^2\right) \right]^{\frac{1}{2}} + \mathcal{O}(\varepsilon^{\frac{\sigma(i)+1}{2}}), \tag{3.191}$$

which provides two roots, with multiplicity equal to 1, and the proposition 3.4.7 is proved.

Remark: The asymptotic expansion of $\lambda_i^{\pm}(\mathbf{u}, \boldsymbol{\gamma})$ in proposition 3.4.1 corresponds to the asymptotic expansion of $\lambda_2^{\pm}$ in the set of hyperbolicity $|F_x| < F_{crit}^{-}$ in [88], in the two-layer case. Moreover, it is also in accordance with [1], [9], [30], [67], [97], [114] and [127]. 2) In the oceanographic applications, the *French Naval Hydrographic and Oceanographic Service* uses the multi-layer shallow water model with 40 layers. For instance, in the bay of Biscay, the assumption (3.120) is verified, with

$$\varepsilon \simeq 10^{-4}. \tag{3.192}$$

However, the matter is that

$$\forall i \in [\![1, n-1]\!],\ 1 \leq \sigma(i) \leq 2, \tag{3.193}$$

which implies that the baroclinic eigenvalues are not much separated. Moreover, the assumption on $\boldsymbol{\pi}$ is verified, but the one on $\boldsymbol{\varpi}$ can be contradicted. On the one hand, a part of the layers used to describe the deep sea are reduced with a thickness of the order of ε and then, there would exist $j_0 \in [\![1, n-1]\!]$ such that

$$1 \ll \varpi_{j_0}. \tag{3.194}$$

On the other hand, it can be interesting to increase the number of layers in a certain area where well-known phenomena occur, in order to provide more accurate results. Then, there would exist $k_0 \in [\![1, n-1]\!]$ such that

$$\varpi_{k_0} \ll 1. \tag{3.195}$$

On the figure 3.2, both of these cases occur. The first one concerns the layers near the bottom: these layers have high heights in the deep sea but, at the oceanic plateau, these heights tend to 0 and then (3.194) is verified for some $j_0 \in [\![1, n-1]\!]$. Moreover, the second case concerns the layers near the free surface: to describe well the mixing-zone, 20 layers are necessary — the black band just below the free surface — and therefore the assumption (3.195) is verified for some $k_0 \in [\![1, n-1]\!]$.

Remark: According to the figure 3.2, the assumption (3.195) would be verified for all $X \in \mathbb{R}^2$. However, this is not true in the case of (3.194).

As a consequence of the proposition 3.4.7, we can deduce the next theorem:

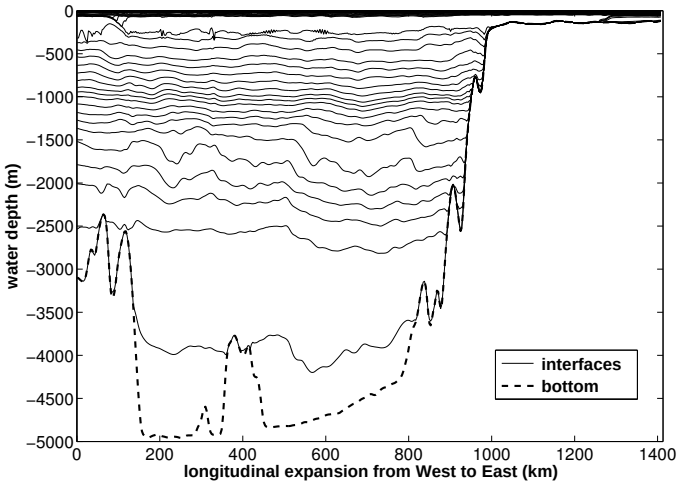

Figure 3.2: Configuration of 40 layers in the bay of Biscay

Theorem 3.4.10 *Let* $\mathbf{u^0} \in \mathcal{L}^2(\mathbb{R}^2)^{3n}$, $\boldsymbol{\gamma} \in]0,1[^{n-1}$, $\varepsilon > 0$ *and an injective function* $\sigma : [\![1, n-1]\!] \to \mathbb{R}_+^*$ *such that* $\boldsymbol{\gamma}$ *verifies* (3.120) *and for all* $X \in \mathbb{R}^2$, $\mathbf{u^0}(X)$ *verifies* (3.123).
If the system (3.10)*, with initial data* $\mathbf{u^0}$*, is hyperbolic and* ε *is sufficiently small :*

$$\exists \delta > 0 / \ \varepsilon \leq \delta. \tag{3.196}$$

Then,

$$\begin{cases} \inf_{X\in\mathbb{R}^2} h_i^0(X) > 0, & \forall i \in [\![1,n]\!], \\ \inf_{X\in\mathbb{R}^2} \phi_{\sigma,i}(\boldsymbol{h^0}(X)) - |u_{i+1}^0 - u_i^0|^2(X) - |v_{i+1}^0 - v_i^0|^2(X) > 0, & \forall i \in [\![1,n-1]\!], \end{cases} \tag{3.197}$$

where $\phi_{\sigma,i}(\boldsymbol{h}) := (h_{\sigma,i}^- + h_{\sigma,i}^+)(1-\gamma_i)$.

Remark: A direct consequence of this theorem is that if the model (3.10) is hyperbolic, then the *Rayleigh-Taylor* stability is verified (*i.e.* $\rho_n > \rho_{n-1} > \ldots > \rho_1 > 0$).

Proof To verify the hyperbolicity of the system (3.10), all the eigenvalues of $A(\mathbf{u}, \boldsymbol{\gamma}, \theta)$ need to be real. Let $i \in [\![1, n-1]\!]$, according to the rotational invariance (3.16) and the proposition 3.3.2, if $(\mathbf{u}, \boldsymbol{\gamma})$ verify (3.120), (3.123) and (3.196), the asymptotic expansion of $\lambda_i^{\pm}(P(\theta)\mathbf{u}, \boldsymbol{\gamma}) \in \sigma(A(\mathbf{u}, \boldsymbol{\gamma}, \theta)$ is

$$\begin{aligned} \lambda_i^{\pm}(P(\theta)\mathbf{u}, \boldsymbol{\gamma}) = \ & \cos(\theta)\frac{u_{i+1}h_{\sigma,i}^- + u_i h_{\sigma,i}^-}{h_{\sigma,i}^- + h_{\sigma,i}^+} + \sin(\theta)\frac{v_{i+1}h_{\sigma,i}^- + v_i h_{\sigma,i}^+}{h_{\sigma,i}^- + h_{\sigma,i}^+} \\ & \pm \left[\frac{h_{\sigma,i}^- h_{\sigma,i}^+}{h_{\sigma,i}^- + h_{\sigma,i}^+} \left(1 - \gamma_i - \frac{(\cos(\theta)(u_{i+1}-u_i) + \sin(\theta)(v_{i+1}-v_i))^2}{h_{\sigma,i}^- + h_{\sigma,i}^+} \right) \right]^{\frac{1}{2}} \\ & + \mathcal{O}(\varepsilon^{\frac{\sigma(i)+1}{2}}). \end{aligned} \tag{3.198}$$

Then, as $h^-_{\sigma,i} > 0$ and $h^+_{\sigma,i} > 0$, for all $i \in [\![1, n-1]\!]$, if $h_k > 0$ for all $k \in [\![1,n]\!]$, a necessary condition to have $\lambda^\pm_i(\mathsf{P}(\theta)\mathbf{u}, \boldsymbol{\gamma}) \in \mathbb{R}$, for all $\theta \in [0, 2\pi]$, is

$$\forall \theta \in [0,2\pi],\ 1 - \gamma_i - \frac{(\cos(\theta)(u_{i+1}-u_i) + \sin(\theta)(v_{i+1}-v_i))^2}{h^-_{\sigma,i} + h^+_{\sigma,i}} \geq 0. \tag{3.199}$$

Finally, using (3.47), the necessary condition of hyperbolicity (3.197) is obtained.

Then, the theorem 3.4.10 insures all the elements of the set of hyperbolicity (*i.e.* $\mathcal{H}_{\boldsymbol{\gamma}}$) verify the conditions (3.123) and (3.197), when $\boldsymbol{\gamma}$ verifies (3.120) and (3.196).

Remarks: 1) The theorem 3.4.10 is a generalization of the theorem 3.3.7, in the asymptotic regime (3.120) and (3.123): it provides a necessary condition of hyperbolicity. Moreover, the shape of the baroclinic eigenvalues, in the merged-layer case (3.86), is the same in the considered asymptotic regime, with the assumptions (3.196). 2) In [127], the numerical set of hyperbolicity of the three-layer model, in one dimension (see figure 4), seems that the difference of velocities $u_{i+1} - u_i$, for $i \in [\![1,2]\!]$, is allowed to be very large: this shows the condition (3.197) is very different from the entire set of hyperbolicity. However, as it was proved in [88] for the two-layer case, there is a gap between the one and the two dimensions sets of hyperbolicity. Indeed, the elements in the one dimension set have to be rotational invariant (*i.e.* remain in the one dimension set of hyperbolicity if a rotation is applied) to be in the two dimensions one. This is why it should not be far from the exact set of hyperbolicity, even if the condition (3.197) is a necessary condition of hyperbolicity of the multi-layer shallow water model, in two dimensions, and not a sufficient one.

In conclusion, we managed to obtain an asymptotic expansion of the baroclinic eigenvalues, $\left(\lambda^\pm_i(\mathbf{u}, \boldsymbol{\gamma})\right)_{i \in [\![1,n-1]\!]}$, considering the asymptotic regime (3.120) and assuming the heights of each layer have all the same range and the difference of velocity between an interface has the same order as the square root of the relative difference of density, at this interface. The expansions of $\lambda^\pm_i(\mathbf{u}, \boldsymbol{\gamma})$, for $i \in [\![1, n-1]\!]$, has been proved with a precision in $\mathcal{O}(\varepsilon^{\frac{\sigma(i)+1}{2}})$.

3.4.4 Comparison of the conditions of hyperbolicity

In this paper, we expressed an explicit criterion of symmetrizability — see (3.27) with (3.56) — and an explicit necessary condition of hyperbolicity — see theorem 3.4.10. As the symmetrizability implies the hyperbolicity, we need to veify that criterion of symmetrizability implies the necessary condition of hyperbolicity. The main difference between both of them is that the 1st one gives conditions on $|u_i - \bar{u}|^2$, for all $i \in [\![1,n]\!]$,while the 2nd one gives conditions on $|u_{i+1} - u_i|^2$, for all $i \in [\![1, n-1]\!]$. Then, to compare these two conditions, we need to know which one of the following assertions is

true, in the asymptotic regime (3.120) and (3.123):

$$\forall i \in [\![1,n-1]\!],\ \phi_{\sigma,i}(\boldsymbol{h}) \leq \left(\frac{\alpha_{n,i}+\alpha_{n,i+1}}{\alpha_{n,i}\alpha_{n,i+1}a(\mathbf{h},\boldsymbol{\gamma})}\right)^2, \tag{3.200}$$

or

$$\forall i \in [\![1,n-1]\!],\ \left(\frac{\alpha_{n,i}+\alpha_{n,i+1}}{\alpha_{n,i}\alpha_{n,i+1}a(\mathbf{h},\boldsymbol{\gamma})}\right)^2 \leq \phi_{\sigma,i}(\boldsymbol{h}). \tag{3.201}$$

Indeed, if for all $i \in [\![1,n-1]\!]$, u_i is sufficiently close to $\bar{u}$, then

$$\forall i \in [\![1,n]\!],\ \frac{1}{\left(\alpha_{n,i}a(\mathbf{h},\boldsymbol{\gamma})\right)^2} > |u_i-\bar{u}|^2. \tag{3.202}$$

Consequently,

$$\forall i \in [\![1,n-1]\!],\ \left(\frac{\alpha_{n,i}+\alpha_{n,i+1}}{\alpha_{n,i}\alpha_{n,i+1}a(\mathbf{h},\boldsymbol{\gamma})}\right)^2 > |u_{i+1}-u_i|^2. \tag{3.203}$$

Consequently, if (3.200) is verified, for instance, it implies the conditions of hyperbolicity:

$$\forall i \in [\![1,n-1]\!],\ \phi_{\sigma,i}(\boldsymbol{h}) > |u_{i+1}-u_i|^2. \tag{3.204}$$

Let $\boldsymbol{\gamma} \in]0,1[^{n-1}$, $\varepsilon > 0$ and an injective function $\sigma : [\![1,n-1]\!] \to \mathbb{R}_+^*$ such that $\boldsymbol{\gamma}$ verifies (3.120). We define the next subset of $\mathcal{L}^2(\mathbb{R}^2)^{3n}$

$$\mathcal{H}_{\sigma,\varepsilon} := \left\{\mathbf{u^0} \in \mathcal{L}^2(\mathbb{R}^2)^{3n} / \ \forall X \in \mathbb{R}^2,\ \mathbf{u^0}(X) \text{ verifies conditions (3.123) and (3.197)}\right\} \tag{3.205}$$

and the subset of $\mathcal{H}^s(\mathbb{R}^2)^{3n}$

$$\mathcal{S}^s_{\sigma,\varepsilon} := \left\{\mathbf{u^0} \in \mathcal{H}^s(\mathbb{R}^2)^{3n} / \ \forall X \in \mathbb{R}^2,\ \mathbf{u^0}(X) \text{ verifies conditions (3.123) and (3.202)}\right\} \tag{3.206}$$

According to the proposition 3.2.11, it is clear that

$$\mathcal{S}^s_{\sigma,\varepsilon} \subset \mathcal{S}^s_{\boldsymbol{\gamma}}, \tag{3.207}$$

and according to the theorem 3.4.10, it is clear that if $\varepsilon \leq \delta$,

$$\mathcal{H}_{\boldsymbol{\gamma}} \subset \mathcal{H}_{\sigma,\varepsilon}. \tag{3.208}$$

Moreover, there is the next proposition:

Proposition 3.4.11 *Let $s > 2$, $\mathbf{u^0} : \mathbb{R}^2 \to \mathbb{R}^{3n}$, $\boldsymbol{\gamma} \in]0,1[^{n-1}$, $\varepsilon > 0$ and an injective function $\sigma : [\![1,n-1]\!] \to \mathbb{R}_+^*$ such that $\boldsymbol{\gamma}$ verifies (3.120) and for all $X \in \mathbb{R}^2$, $\mathbf{u}(X)$ verifies (3.123).*
There exists $\delta > 0$ such that if

$$\varepsilon \leq \delta, \tag{3.209}$$

then,

$$\mathcal{S}^s_{\sigma,\varepsilon} \subset \mathcal{H}_{\sigma,\varepsilon} \cap \mathcal{H}^s(\mathbb{R}^2)^{3n}. \tag{3.210}$$

Proof As the symmetrizability implies the hyperbolicity, which implies the condition (3.197), the proof is trivial.

To conclude this section, we highlighted a necessary condition of hyperbolicity for the system (3.10), with initial data $\mathbf{u^0}$, in the asymptotic regime (3.120), (3.123) and (3.209). In the next section, we perform the asymptotic expansion of the eigenvectors, in order to specify the nature of the waves associated to each eigenvalues and to prove the diagonalizability of the matrix $\mathsf{A}(\mathbf{u},\boldsymbol{\gamma},\theta)$.

3.5 Asymptotic expansion of all the eigenvectors

In the previous section, the asymptotic expansion of all the eigenvalues associated to $\mathsf{A}_x(\mathbf{u},\boldsymbol{\gamma})$ were proved, in a particular regime, which enables to separate all the baroclinic eigenvalues. In this section, we will give the associated expressions of the asymptotic expansions of all the eigenvectors of $\mathsf{A}_x(\mathbf{u},\boldsymbol{\gamma})$. Moreover, we will deduce the diagonalizability of the matrix $\mathsf{A}(\mathbf{u},\boldsymbol{\gamma},\theta)$ and the local well-posedness of the model (3.10) in $\mathcal{H}^s(\mathbb{R}^2)^{3n}$, with $s>2$. Finally, the nature of the waves associated to each eigenvalues – shock, contact or rarefaction wave – in the asymptotic regime considered in the previous section, is deduced.

3.5.1 The barotropic eigenvectors

In the asymptotic regime (3.120) and (3.123), we can deduce the asymptotic expansions of the right and left eigenvectors associated to $\lambda_n^{\pm}(\mathbf{u},\boldsymbol{\gamma})$.

Proposition 3.5.1 *Let* $(\mathbf{u},\boldsymbol{\gamma})\in\mathbb{R}^{3n}\times]0,1[^{n-1}$, $\varepsilon>0$ *and an injective function* $\sigma\in\mathbb{R}_+^{*\,[\![1,n-1]\!]}$ *such that* $\boldsymbol{\gamma}$ *verifies* (3.120), $\mathbf{u}$ *verifies* (3.123) *and*

$$\varepsilon \ll 1. \tag{3.211}$$

Then, the asymptotic expansion of the right eigenvector associated to $\lambda_n^{\pm}(\mathbf{u},\boldsymbol{\gamma})$, *with precision about* $\mathcal{O}(1-\gamma_{m_\sigma^-})$, *is such that*

$$\begin{aligned} \boldsymbol{r}_{\boldsymbol{x}}^{\lambda_n^{\pm}}(\mathbf{u},\boldsymbol{\gamma}) = \;& \sum_{k=1}^{n}\boldsymbol{e}_{n+k}\pm\frac{h_k}{\sqrt{H}}\boldsymbol{e_k} \\ & -\sum_{k=1}^{m_\sigma^-}\frac{(u_{m_\sigma^-+1}-u_{m_\sigma^-})}{\sqrt{H}}\left(\frac{2h_k}{\sqrt{H}}\boldsymbol{e}_k\pm\boldsymbol{e}_{n+k}\right) \\ & +\sum_{k=m_\sigma^-+1}^{n}\frac{(u_{m_\sigma^-+1}-u_{m_\sigma^-})h^-_{\sigma,m_\sigma^-}}{\sqrt{H}h^+_{\sigma,m_\sigma^-}}\left(\frac{2h_k}{\sqrt{H}}\boldsymbol{e}_k\pm\boldsymbol{e}_{n+k}\right) \\ & +\mathcal{O}(1-\gamma_{m_\sigma^-}), \end{aligned} \tag{3.212}$$

and the asymptotic expansion of the left eigenvector associated to $\lambda_n^{\pm}(\mathbf{u},\boldsymbol{\gamma})$, *with precision about*

$\mathcal{O}(1-\gamma_{m_\sigma^-})$, *is such that*

$$\begin{aligned} \boldsymbol{l}_{\boldsymbol{x}}^{\lambda_n^\pm}(\mathbf{u},\boldsymbol{\gamma}) = \quad & \textstyle\sum_{k=1}^{n} {}^\top\boldsymbol{e}_k \pm \frac{h_k}{\sqrt{H}}{}^\top\boldsymbol{e}_{n+k} \\ & - \textstyle\sum_{k=1}^{m_\sigma^-} \frac{(u_{m_\sigma^-+1}-u_{m_\sigma^-})}{\sqrt{H}} \left(\frac{2h_k}{\sqrt{H}}{}^\top\boldsymbol{e}_{n+k} \pm {}^\top\boldsymbol{e}_k \right) \\ & + \textstyle\sum_{k=m_\sigma^-+1}^{n} \frac{(u_{m_\sigma^-+1}-u_{m_\sigma^-})h^-_{\sigma,m_\sigma^-}}{\sqrt{H}h^+_{\sigma,m_\sigma^-}} \left(\frac{2h_k}{\sqrt{H}}{}^\top\boldsymbol{e}_{n+k} \pm {}^\top\boldsymbol{e}_k \right) \\ & + \mathcal{O}(1-\gamma_{m_\sigma^-}). \end{aligned} \tag{3.213}$$

Proof According to the proposition 3.4.6,

$$\begin{aligned} \lambda_n^\pm(\mathbf{u},\boldsymbol{\gamma}) &= u_{m_\sigma^-} \pm \sqrt{H} + \psi_{m_\sigma^-}\varepsilon^{\frac{1}{2}} \pm \left(-h^-_{\sigma,m_\sigma^-}h^+_{\sigma,m_\sigma^-}\right)\varepsilon + \mathcal{O}(\varepsilon^{\frac{3}{2}}) \\ &= u_{m_\sigma^-} \pm \sqrt{H} + \psi_{m_\sigma^-}\varepsilon^{\frac{1}{2}} + \mathcal{O}(\varepsilon), \end{aligned} \tag{3.214}$$

where $\psi_{m_\sigma^-} := \pi_{m_\sigma^-}\frac{h^+_{\sigma,m_\sigma^-}}{h^-_{\sigma,m_\sigma^-}+h^+_{\sigma,m_\sigma^-}} = \pi_{m_\sigma^-}\frac{h^+_{\sigma,m_\sigma^-}}{H}$. We expand the eigenvectors $\boldsymbol{r}_{\boldsymbol{x}}^{\lambda_n^\pm}(\mathbf{u},\boldsymbol{\gamma})$ and $\boldsymbol{l}_{\boldsymbol{x}}^{\lambda_n^\pm}(\mathbf{u},\boldsymbol{\gamma})$ such that

$$\begin{cases} \boldsymbol{r}_{\boldsymbol{x}}^{\lambda_n^\pm}(\mathbf{u},\boldsymbol{\gamma}) = \boldsymbol{r}^\pm_{n,0}(\mathbf{u},\boldsymbol{\gamma}) + \varepsilon^{\frac{1}{2}}\boldsymbol{r}^\pm_{n,1}(\mathbf{u},\boldsymbol{\gamma}) + \mathcal{O}(\varepsilon), \\ \boldsymbol{l}_{\boldsymbol{x}}^{\lambda_n^\pm}(\mathbf{u},\boldsymbol{\gamma}) = \boldsymbol{l}^\pm_{n,0}(\mathbf{u},\boldsymbol{\gamma}) + \varepsilon^{\frac{1}{2}}\boldsymbol{l}^\pm_{n,1}(\mathbf{u},\boldsymbol{\gamma}) + \mathcal{O}(\varepsilon), \end{cases} \tag{3.215}$$

where

$$\begin{cases} \boldsymbol{r}^\pm_{n,0}(\mathbf{u},\boldsymbol{\gamma}) := \textstyle\sum_{k=1}^{n}\boldsymbol{e}_{n+k} \pm \frac{h_k}{\sqrt{H}}\boldsymbol{e}_{\boldsymbol{k}}, \\ \boldsymbol{l}^\pm_{n,0}(\mathbf{u},\boldsymbol{\gamma}) := \textstyle\sum_{k=1}^{n}{}^\top\boldsymbol{e}_k \pm \frac{h_k}{\sqrt{H}}{}^\top\boldsymbol{e}_{n+k}. \end{cases} \tag{3.216}$$

Moreover, we have

$$\begin{aligned} \mathsf{A}_x(\mathbf{u},\boldsymbol{\gamma}) = \quad & \mathsf{A}_x(\mathbf{u}_{\boldsymbol{\sigma}}^{\boldsymbol{m_\sigma^-}},\boldsymbol{\gamma}_{\boldsymbol{\sigma}}^{m_\sigma^-}) + \textstyle\sum_{k=1}^{n}(u_k-u_{m_\sigma^-})\mathsf{A}_x^{k-1,1}, \\ & + \textstyle\sum_{k=1}^{n-1}(1-\gamma_k)\mathsf{A}_x^{k,3}(\boldsymbol{\gamma}), \end{aligned} \tag{3.217}$$

where the $3n\times 3n$ matrices, $\mathsf{A}_x^{k-1,1}$ and $\mathsf{A}_x^{k,2}(\boldsymbol{\gamma})$, are defined respectively in (3.115–3.116), $\mathsf{A}_x^{k,3}(\boldsymbol{\gamma}) := \left[\mathsf{A}_{l,m}^{k,3}\right]_{(l,m)\in[\![1,n]\!]^2}$ is defined by

$$\mathsf{A}_{l,m}^{k,3} := \begin{cases} 0, & \text{if } m \neq k, \\ 0, & \text{if } l \leq n+k \text{ or } l \geq 2n+1, \\ -\alpha_{l-n-1,k}, & \text{otherwise}, \end{cases} \tag{3.218}$$

and for all $i \in [\![1;n-1]\!]$, $(\mathbf{u}_{\boldsymbol{\sigma}}^{\boldsymbol{i}},\boldsymbol{\gamma}_{\boldsymbol{\sigma}}^{\boldsymbol{i}})$ are defined by

$$\begin{cases} u_j = u_i, & \forall j \in [\![m_i^-, m_i^+]\!], \\ \gamma_j = 1, & \forall j \in [\![m_i^-, m_i^+ - 1]\!]. \end{cases} \tag{3.219}$$

Consequently, according to the assumptions (3.120), (3.123) and (3.211),

$$\begin{aligned}\mathsf{A}_x(\mathbf{u},\boldsymbol{\gamma}) &= \mathsf{A}_x(\mathbf{u}_{\boldsymbol{\sigma}}^{\boldsymbol{m}_{\sigma}^-},\boldsymbol{\gamma}_{\sigma}^{m_{\sigma}^-})+\sum_{k=m_{\sigma}^-+1}^{n}\pi_{m_{\sigma}^-}\varepsilon^{\frac{1}{2}}\mathsf{A}_x^{k-1,1}+\varepsilon\,\mathsf{A}_x^{m_{\sigma}^-,3}(\boldsymbol{\gamma})+\mathcal{O}(\varepsilon^{\frac{3}{2}}),\\ &= \mathsf{A}_x(\mathbf{u}_{\boldsymbol{\sigma}}^{\boldsymbol{m}_{\sigma}^-},\boldsymbol{\gamma}_{\sigma}^{m_{\sigma}^-})+\sum_{k=m_{\sigma}^-+1}^{n}\pi_{m_{\sigma}^-}\varepsilon^{\frac{1}{2}}\mathsf{A}_x^{k-1,1}+\mathcal{O}(\varepsilon).\end{aligned} \tag{3.220}$$

Therefore, $\boldsymbol{r}_{\boldsymbol{x}}^{\lambda_n^{\pm}}(\mathbf{u},\boldsymbol{\gamma})$ is the approximation of the right eigenvector associated to $\lambda_n^{\pm}(\mathbf{u},\boldsymbol{\gamma})$, with a precision about $\mathcal{O}(\varepsilon)$, if and only if $\boldsymbol{r}_{n,1}^{\pm}(\mathbf{u},\boldsymbol{\gamma})$ verifies:

$$\begin{aligned}&\big(\textstyle\sum_{k=m_{\sigma}^-+1}^{n}\pi_{m_{\sigma}^-}\mathsf{A}_x^{k-1,1}-\psi_{m_{\sigma}^-}\mathsf{I}_{3n}\big)\boldsymbol{r}_{n,0}^{\pm}(\mathbf{u},\boldsymbol{\gamma})\\ &=-\big(\mathsf{A}_x(\mathbf{u}_{\boldsymbol{\sigma}}^{\boldsymbol{m}_{\sigma}^-},\boldsymbol{\gamma}_{\sigma}^{m_{\sigma}^-})-(u_{m_{\sigma}^-}\pm\sqrt{H})\mathsf{I}_{3n}\big)\boldsymbol{r}_{n,1}^{\pm}(\mathbf{u},\boldsymbol{\gamma}),\end{aligned} \tag{3.221}$$

and $\boldsymbol{l}_{\boldsymbol{x}}^{\lambda_n^{\pm}}(\mathbf{u},\boldsymbol{\gamma})$ is the approximation of the left eigenvector associated to $\lambda_n^{\pm}(\mathbf{u},\boldsymbol{\gamma})$, with a precision about $\mathcal{O}(\varepsilon)$, if and only if $\boldsymbol{l}_{n,1}^{\pm}(\mathbf{u},\boldsymbol{\gamma})$ verifies:

$$\begin{aligned}&\boldsymbol{l}_{n,0}^{\pm}(\mathbf{u},\boldsymbol{\gamma})\big(\textstyle\sum_{k=m_{\sigma}^-+1}^{n}\pi_{m_{\sigma}^-}\mathsf{A}_x^{k-1,1}-\psi_{m_{\sigma}^-}\mathsf{I}_{3n}\big)\\ &=-\boldsymbol{l}_{n,1}^{\pm}(\mathbf{u},\boldsymbol{\gamma})\big(\mathsf{A}_x(\mathbf{u}_{\boldsymbol{\sigma}}^{\boldsymbol{m}_{\sigma}^-},\boldsymbol{\gamma}_{\sigma}^{m_{\sigma}^-})-(u_{m_{\sigma}^-}\pm\sqrt{H})\mathsf{I}_{3n}\big).\end{aligned} \tag{3.222}$$

Therefore, $\boldsymbol{r}_{n,1}^{\pm}(\mathbf{u},\boldsymbol{\gamma}) := {}^{\top}(r_{n,1}^{\pm,k})_{k\in[\![1,3n]\!]}$ is solution of (3.221) if and only if

$$r_{n,1}^{\pm,k}=\begin{cases}\frac{h_k}{H}(S_r-2\psi_{m_{\sigma}^-}), & \text{if } k\in[\![1,m_{\sigma}^-]\!],\\ \frac{h_k}{H}(S_r+2\frac{h_{\sigma,m_{\sigma}^-}^-}{h_{\sigma,m_{\sigma}^-}^+}\psi_{m_{\sigma}^-}), & \text{if } k\in[\![m_{\sigma}^-+1,n]\!],\\ \pm\frac{1}{\sqrt{H}}(S_r-\psi_{m_{\sigma}^-}), & \text{if } k\in[\![n+1,n+m_{\sigma}^-]\!],\\ \pm\frac{1}{\sqrt{H}}(S_r+\frac{h_{\sigma,m_{\sigma}^-}^-}{h_{\sigma,m_{\sigma}^-}^+}\psi_{m_{\sigma}^-}), & \text{if } k\in[\![n+m_{\sigma}^-+1,2n]\!],\\ 0, & \text{if } k\in[\![2n+1,3n]\!],\end{cases} \tag{3.223}$$

and $\boldsymbol{l}_{n,1}^{\pm}(\mathbf{u},\boldsymbol{\gamma}) := (l_{n,1}^{\pm,k})_{k\in[\![1,3n]\!]}$ is solution of (3.222) if and only if

$$l_{n,1}^{\pm,k}=\begin{cases}\pm\frac{1}{\sqrt{H}}(S_l-\psi_{m_{\sigma}^-}), & \text{if } k\in[\![1,m_{\sigma}^-]\!],\\ \pm\frac{1}{\sqrt{H}}(S_l+\frac{h_{\sigma,m_{\sigma}^-}^-}{h_{\sigma,m_{\sigma}^-}^+}\psi_{m_{\sigma}^-}), & \text{if } k\in[\![m_{\sigma}^-+1,n]\!],\\ \frac{h_k}{H}(S_l-2\psi_{m_{\sigma}^-}), & \text{if } k\in[\![n+1,n+m_{\sigma}^-]\!],\\ \frac{h_k}{H}(S_l+2\frac{h_{\sigma,m_{\sigma}^-}^-}{h_{\sigma,m_{\sigma}^-}^+}\psi_{m_{\sigma}^-}), & \text{if } k\in[\![n+m_{\sigma}^-+1,2n]\!],\\ 0, & \text{if } k\in[\![2n+1,3n]\!],\end{cases} \tag{3.224}$$

where $S_r := \sum_{k=1}^{n} r_{n,1}^{\pm,k}$ and $S_l := \sum_{k=1}^{n} l_{n,1}^{\pm,n+k}$. Finally, solutions of (3.221–3.222) are

$$\left\{\begin{array}{rl} \boldsymbol{r}_{n,1}^{\pm}(\mathbf{u},\boldsymbol{\gamma}) = & -\sum_{k=1}^{m_\sigma^-} \frac{\Psi_{m_\sigma^-}}{\sqrt{H}}\left(\frac{2h_k}{\sqrt{H}}\boldsymbol{e}_k \pm \boldsymbol{e}_{n+k}\right) \\ & +\sum_{k=m_\sigma^-+1}^{n} \frac{\Psi_{m_\sigma^-} h^-_{\sigma,m_\sigma^-}}{\sqrt{H} h^+_{\sigma,m_\sigma^-}}\left(\frac{2h_k}{\sqrt{H}}\boldsymbol{e}_k \pm \boldsymbol{e}_{n+k}\right), \\ \boldsymbol{l}_{n,1}^{\pm}(\mathbf{u},\boldsymbol{\gamma}) = & -\sum_{k=1}^{m_\sigma^-} \frac{\Psi_{m_\sigma^-}}{\sqrt{H}}\left(\frac{2h_k}{\sqrt{H}}{}^\top\boldsymbol{e}_{n+k} \pm {}^\top\boldsymbol{e}_k\right) \\ & +\sum_{k=m_\sigma^-+1}^{n} \frac{\Psi_{m_\sigma^-} h^-_{\sigma,m_\sigma^-}}{\sqrt{H} h^+_{\sigma,m_\sigma^-}}\left(\frac{2h_k}{\sqrt{H}}{}^\top\boldsymbol{e}_{n+k} \pm {}^\top\boldsymbol{e}_k\right), \end{array}\right. \tag{3.225}$$

and the approximations of the eigenvectors given in proposition 3.5.1 are verified.

Remark: The right eigenvectors of $\mathsf{A}(\mathbf{u},\boldsymbol{\gamma},\theta)$: $\boldsymbol{r}^{\lambda_n^\pm}(\mathbf{u},\boldsymbol{\gamma},\theta)$, associated to $\lambda_n^\pm(\mathbf{u},\boldsymbol{\gamma},\theta)$, are defined by

$$\boldsymbol{r}^{\lambda_n^\pm}(\mathbf{u},\boldsymbol{\gamma},\theta) = \mathsf{P}(\theta)^{-1}\boldsymbol{r}_{\boldsymbol{x}}^{\lambda_n^\pm}(\mathsf{P}(\theta)\mathbf{u},\boldsymbol{\gamma}), \tag{3.226}$$

and the left ones: $\boldsymbol{l}^{\lambda_n^\pm}(\mathbf{u},\boldsymbol{\gamma},\theta)$ are defined by

$$\boldsymbol{l}^{\lambda_n^\pm}(\mathbf{u},\boldsymbol{\gamma},\theta) = \boldsymbol{l}_{\boldsymbol{x}}^{\lambda_n^\pm}(\mathsf{P}(\theta)\mathbf{u},\boldsymbol{\gamma})\mathsf{P}(\theta). \tag{3.227}$$

To sum this subsection up, considering the asymptotic regime (3.120), (3.123) and assuming (3.211), we proved the expressions of the perturbations of the right and left eigenvectors associated to the barotropic eigenvalues, with a precision about $\mathcal{O}(\varepsilon)$.
In the next subsection, we give the asymptotic expansions of the right and left eigenvectors associated to the baroclinic eigenvalues.

3.5.2 The baroclinic eigenvectors

With the asymptotic expansions of the baroclinic eigenvalues in (3.153), we can deduce asymptotic expansions of the baroclinic eigenvectors.

Proposition 3.5.2 *Let* $(\mathbf{u},\boldsymbol{\gamma}) \in \mathbb{R}^{3n}\times]0,1[^{n-1}$, $\varepsilon > 0$ *and an injective function* $\sigma \in \mathbb{R}_+^{*\,[\![1,n-1]\!]}$ *such that* $\boldsymbol{\gamma}$ *verifies* (3.120), $\mathbf{u}$ *verifies* (3.123) *and*

$$\varepsilon \ll 1. \tag{3.228}$$

Then, for all $i \in [\![1,n-1]\!]$, *the asymptotic expansions of the right eigenvectors associated to* $\lambda_i^\pm(\mathbf{u},\boldsymbol{\gamma})$, *with precision about* $\mathcal{O}(\varepsilon^{\frac{\sigma(i)+1}{2}})$, *is such that*

$$\begin{array}{rl} \boldsymbol{r}_{\boldsymbol{x}}^{\lambda_i^\pm}(\mathbf{u},\boldsymbol{\gamma}) = & \sum_{j=m_i^-}^{i} \frac{\boldsymbol{e}_j}{i-m_i^-+1} - \sum_{j=i+1}^{m_i^+} \frac{\boldsymbol{e}_j}{m_i^+-i} \\ & + \frac{u_{i+1}-u_i}{h^-_{\sigma,i}+h^+_{\sigma,i}}\left(\sum_{j=m_i^-}^{i} \frac{h^-_{\sigma,i}\boldsymbol{e}_{n+j}}{(i-m_i^-+1)h_j} + \sum_{j=i+1}^{m_i^+} \frac{h^+_{\sigma,i}\boldsymbol{e}_{n+j}}{(m_i^+-i)h_j}\right) \\ & \pm \left[\frac{h^-_{\sigma,i}h^+_{\sigma,i}}{h^-_{\sigma,i}+h^+_{\sigma,i}}\left(1-\gamma_i-\frac{(u_{i+1}-u_i)^2}{h^-_{\sigma,i}+h^+_{\sigma,i}}\right)\right]^{\frac{1}{2}} \sum_{j=m_i^-}^{i} \frac{\boldsymbol{e}_{n+j}}{(i-m_i^-+1)h_j} \\ & \mp \left[\frac{h^-_{\sigma,i}h^+_{\sigma,i}}{h^-_{\sigma,i}+h^+_{\sigma,i}}\left(1-\gamma_i-\frac{(u_{i+1}-u_i)^2}{h^-_{\sigma,i}+h^+_{\sigma,i}}\right)\right]^{\frac{1}{2}} \sum_{j=i+1}^{m_i^+} \frac{\boldsymbol{e}_{n+j}}{(m_i^+-i)h_j} \\ & + \mathcal{O}(\varepsilon^{\frac{\sigma(i)+1}{2}}), \end{array} \tag{3.229}$$

and the asymptotic expansions of the left eigenvectors associated to $\lambda_i^{\pm}(\mathbf{u},\boldsymbol{\gamma})$*, with precision about* $\mathcal{O}(\varepsilon^{\frac{\sigma(i)+1}{2}})$*, is such that*

$$\begin{aligned}\boldsymbol{l}_{\boldsymbol{x}}^{\lambda_i^{\pm}}(\mathbf{u},\boldsymbol{\gamma}) = \;& \sum_{j=m_i^-}^{i} \frac{{}^{\top}\boldsymbol{e}_{n+j}}{i-m_i^-+1} - \sum_{j=i+1}^{m_i^+} \frac{{}^{\top}\boldsymbol{e}_{n+j}}{m_i^+-i} \\ & + \frac{u_{i+1}-u_i}{h_{\sigma,i}^- + h_{\sigma,i}^+}\left(\sum_{j=m_i^-}^{i} \frac{h_{\sigma,i}^-\,{}^{\top}\boldsymbol{e}_j}{(i-m_i^-+1)h_j} + \sum_{j=i+1}^{m_i^+} \frac{h_{\sigma,i}^+\,{}^{\top}\boldsymbol{e}_j}{(m_i^+-i)h_j}\right) \\ & \pm \left[\frac{h_{\sigma,i}^- h_{\sigma,i}^+}{h_{\sigma,i}^- + h_{\sigma,i}^+}\left(1-\gamma_i - \frac{(u_{i+1}-u_i)^2}{h_{\sigma,i}^- + h_{\sigma,i}^+}\right)\right]^{\frac{1}{2}} \sum_{j=m_i^-}^{i} \frac{{}^{\top}\boldsymbol{e}_j}{(i-m_i^-+1)h_j} \\ & \mp \left[\frac{h_{\sigma,i}^- h_{\sigma,i}^+}{h_{\sigma,i}^- + h_{\sigma,i}^+}\left(1-\gamma_i - \frac{(u_{i+1}-u_i)^2}{h_{\sigma,i}^- + h_{\sigma,i}^+}\right)\right]^{\frac{1}{2}} \sum_{j=i+1}^{m_i^+} \frac{{}^{\top}\boldsymbol{e}_j}{(m_i^+-i)h_j} \\ & + \mathcal{O}(\varepsilon^{\frac{\sigma(i)+1}{2}}).\end{aligned} \tag{3.230}$$

Proof We consider $\lambda_i^{\pm}(\mathbf{u},\boldsymbol{\gamma}) \in \mathbb{R}$, then, according to the asymptotic expansions of the proposition 3.4.7,

$$\lambda_i^{\pm}(\mathbf{u},\boldsymbol{\gamma}) = u_i + \chi_{\sigma,i}^{\pm}\varepsilon^{\frac{\sigma(i)}{2}} + \mathcal{O}(\varepsilon^{\frac{\sigma(i)+1}{2}}), \tag{3.231}$$

where $\chi_{\sigma,i}^{\pm} := \pi_i \frac{h_{\sigma,i}^-}{h_{\sigma,i}^- + h_{\sigma,i}^+} \pm \left[\frac{h_{\sigma,i}^- h_{\sigma,i}^+}{h_{\sigma,i}^- + h_{\sigma,i}^+}\left(1 - \frac{\pi_i^2}{h_{\sigma,i}^- + h_{\sigma,i}^+}\right)\right]^{\frac{1}{2}}$. We expand the eigenvectors $\boldsymbol{r}_{\boldsymbol{x}}^{\lambda_i^{\pm}}(\mathbf{u},\boldsymbol{\gamma})$ and $\boldsymbol{l}_{\boldsymbol{x}}^{\lambda_i^{\pm}}(\mathbf{u},\boldsymbol{\gamma})$ such that

$$\forall i \in [\![1,n-1]\!],\; \begin{cases} \boldsymbol{r}_{\boldsymbol{x}}^{\lambda_i^{\pm}}(\mathbf{u},\boldsymbol{\gamma}) = \boldsymbol{r}_{i,0}(\mathbf{u},\boldsymbol{\gamma}) + \varepsilon^{\frac{\sigma(i)}{2}}\boldsymbol{r}_{i,1}^{\pm}(\mathbf{u},\boldsymbol{\gamma}) + \mathcal{O}(\varepsilon^{\frac{\sigma(i)+1}{2}}), \\ \boldsymbol{l}_{\boldsymbol{x}}^{\lambda_i^{\pm}}(\mathbf{u},\boldsymbol{\gamma}) = \boldsymbol{l}_{i,0}(\mathbf{u},\boldsymbol{\gamma}) + \varepsilon^{\frac{\sigma(i)}{2}}\boldsymbol{l}_{i,1}^{\pm}(\mathbf{u},\boldsymbol{\gamma}) + \mathcal{O}(\varepsilon^{\frac{\sigma(i)+1}{2}}), \end{cases} \tag{3.232}$$

where $\boldsymbol{r}_{i,0}(\mathbf{u},\boldsymbol{\gamma})$ and $\boldsymbol{l}_{i,0}(\mathbf{u},\boldsymbol{\gamma})$ are right and left eigenvectors of the matrix $\mathsf{A}_x(\mathbf{u}_{\boldsymbol{\sigma}}^{\boldsymbol{i}},\boldsymbol{\gamma}_{\boldsymbol{\sigma}}^{\boldsymbol{i}})$, associated to the eigenvalue u_i:

$$\forall i \in [\![1,n-1]\!],\; \begin{cases} \boldsymbol{r}_{i,0}(\mathbf{u},\boldsymbol{\gamma}) := \sum_{j=m_i^-}^{i} \frac{\boldsymbol{e}_j}{i-m_i^-+1} - \sum_{j=i+1}^{m_i^+} \frac{\boldsymbol{e}_j}{m_i^+-i}, \\ \boldsymbol{l}_{i,0}(\mathbf{u},\boldsymbol{\gamma}) := \sum_{j=m_i^-}^{i} \frac{{}^{\top}\boldsymbol{e}_{n+j}}{i-m_i^-+1} - \sum_{j=i+1}^{m_i^+} \frac{{}^{\top}\boldsymbol{e}_{n+j}}{m_i^+-i}. \end{cases} \tag{3.233}$$

Moreover, we have

$$\begin{aligned}\mathsf{A}_x(\mathbf{u},\boldsymbol{\gamma}) = \;& \mathsf{A}_x(\mathbf{u}_{\boldsymbol{\sigma}}^{\boldsymbol{i}},\boldsymbol{\gamma}_{\boldsymbol{\sigma}}^{\boldsymbol{i}}) + \sum_{k=m_i^-}^{m_i^+}(u_k-u_i)\mathsf{A}_x^{k-1,1}, \\ & + (1-\gamma_{m_i^-})\mathsf{A}_x^{k,2}(\boldsymbol{\gamma}) + \sum_{k=m_i^-+1}^{m_i^+-1}(1-\gamma_k)\mathsf{A}_x^{k,3}(\boldsymbol{\gamma}),\end{aligned} \tag{3.234}$$

where the $3n \times 3n$ matrices, $\mathsf{A}_x^{k-1,1}$, $\mathsf{A}_x^{k,2}(\boldsymbol{\gamma})$ and $\mathsf{A}_x^{k,3}(\boldsymbol{\gamma})$ are defined respectively in (3.115–3.116) and (3.218), and $(\mathbf{u}_{\boldsymbol{\sigma}}^{\boldsymbol{i}},\boldsymbol{\gamma}_{\boldsymbol{\sigma}}^{\boldsymbol{i}})$ is defined in (3.219). Consequently,

$$\mathsf{A}_x(\mathbf{u},\boldsymbol{\gamma}) = \mathsf{A}_x(\mathbf{u}_{\boldsymbol{\sigma}}^{\boldsymbol{i}},\boldsymbol{\gamma}_{\boldsymbol{\sigma}}^{\boldsymbol{i}}) + \sum_{k=i+1}^{m_i^+} \pi_i \varepsilon^{\frac{\sigma(i)}{2}}\mathsf{A}_x^{k-1,1} + \mathcal{O}(\varepsilon^{\frac{\sigma(i)+1}{2}}) \tag{3.235}$$

Therefore, $\boldsymbol{r}_{\boldsymbol{x}}^{\lambda_i^{\pm}}(\mathbf{u},\boldsymbol{\gamma})$ and $\boldsymbol{l}_{\boldsymbol{x}}^{\lambda_i^{\pm}}(\mathbf{u},\boldsymbol{\gamma})$ are respectively the approximations of the right and left eigenvectors associated to $\lambda_i^{\pm}(\mathbf{u},\boldsymbol{\gamma})$, with a precision about $\mathcal{O}(\varepsilon^{\frac{\sigma(i)+1}{2}})$, if and only if $\boldsymbol{r}_{i,1}^{\pm}(\mathbf{u},\boldsymbol{\gamma})$ and $\boldsymbol{l}_{i,1}^{\pm}(\mathbf{u},\boldsymbol{\gamma})$ verify:

$$\begin{cases} \big(\sum_{k=i+1}^{m_i^+}\pi_i \mathsf{A}_x^{k-1,1}-\chi_{\sigma,i}^{\pm}\mathsf{I}_{3n}\big)\boldsymbol{r}_{i,0}(\mathbf{u},\boldsymbol{\gamma})=-\big(\mathsf{A}_x(\mathbf{u}_{\sigma}^{\boldsymbol{i}},\boldsymbol{\gamma}_{\sigma}^{\boldsymbol{i}})-u_i\mathsf{I}_{3n}\big)\boldsymbol{r}_{i,1}^{\pm}(\mathbf{u},\boldsymbol{\gamma}),\\ \boldsymbol{l}_{i,0}(\mathbf{u},\boldsymbol{\gamma})\big(\sum_{k=i+1}^{m_i^+}\pi_i \mathsf{A}_x^{k-1,1}-\chi_{\sigma,i}^{\pm}\mathsf{I}_{3n}\big)=-\boldsymbol{l}_{i,1}^{\pm}(\mathbf{u},\boldsymbol{\gamma})\big(\mathsf{A}_x(\mathbf{u}_{\sigma}^{\boldsymbol{i}},\boldsymbol{\gamma}_{\sigma}^{\boldsymbol{i}})-u_i\mathsf{I}_{3n}\big), \end{cases} \tag{3.236}$$

Finally, a solution of (3.236) is

$$\begin{cases} \boldsymbol{r}_{i,1}^{\pm}(\mathbf{u},\boldsymbol{\gamma})=\sum_{j=m_i^-}^{i}\frac{\chi_{\sigma,i}^{\pm}}{(i-m_i^-+1)h_j}\boldsymbol{e}_{n+j}-\sum_{j=i+1}^{m_i^+}\frac{\chi_{\sigma,i}^{\pm}-\pi_i}{(m_i^+-i)h_j}\boldsymbol{e}_{n+j},\\ \boldsymbol{l}_{i,1}^{\pm}(\mathbf{u},\boldsymbol{\gamma})=\sum_{j=m_i^-}^{i}\frac{\chi_{\sigma,i}^{\pm}}{(i-m_i^-+1)h_j}{}^{\top}\boldsymbol{e}_j-\sum_{j=i+1}^{m_i^+}\frac{\chi_{\sigma,i}^{\pm}-\pi_i}{(m_i^+-i)h_j}{}^{\top}\boldsymbol{e}_j, \end{cases} \tag{3.237}$$

and the approximations of the eigenvectors given in proposition 3.5.2 are verified.

Remark: 1) For all $i\in[\![1,n-1]\!]$, the right eigenvectors of $\mathsf{A}(\mathbf{u},\boldsymbol{\gamma},\theta)$, $\boldsymbol{r}^{\lambda_i^{\pm}}(\mathbf{u},\boldsymbol{\gamma},\theta)$, associated to the baroclinic eigenvalues, are defined by

$$\boldsymbol{r}^{\lambda_i^{\pm}}(\mathbf{u},\boldsymbol{\gamma},\theta)=\mathsf{P}^{-1}(\theta)\boldsymbol{r}_{\boldsymbol{x}}^{\lambda_i^{\pm}}(\mathsf{P}(\theta)\mathbf{u},\boldsymbol{\gamma}), \tag{3.238}$$

and the left eigenvectors of $\mathsf{A}(\mathbf{u},\boldsymbol{\gamma},\theta)$, $\boldsymbol{l}^{\lambda_i^{\pm}}(\mathbf{u},\boldsymbol{\gamma},\theta)$, associated to these eigenvalues, are defined by

$$\boldsymbol{l}^{\lambda_i^{\pm}}(\mathbf{u},\boldsymbol{\gamma},\theta)=\boldsymbol{l}_{\boldsymbol{x}}^{\lambda_i^{\pm}}(\mathsf{P}(\theta)\mathbf{u},\boldsymbol{\gamma})\mathsf{P}(\theta). \tag{3.239}$$

2) Note that the asymptotic expansions (3.213) for the barotropic eigenvectors and (3.230) for the baroclinic eigenvectors, are necessary to characterize the *Riemann* invariants, $r_{\lambda,x}(\mathbf{u},\boldsymbol{\gamma})$, for all $\lambda\in\sigma(\mathsf{A}_x(\mathbf{u},\boldsymbol{\gamma}))$, such that

$$\exists\,\alpha(\mathbf{u},\boldsymbol{\gamma})>0,\ ({}^{\top}\boldsymbol{l}_{\boldsymbol{x}}^{\lambda}(\mathbf{u},\boldsymbol{\gamma})\cdot\frac{\partial\mathbf{u}}{\partial t})=\alpha(\mathbf{u},\boldsymbol{\gamma})\frac{\partial r_{\lambda,x}(\mathbf{u},\boldsymbol{\gamma})}{\partial t}. \tag{3.240}$$

However, it is possible that this last equation has no explicit solution, $r_{\lambda,x}(\mathbf{u},\boldsymbol{\gamma})$, but the asymptotic expansion performed in this paper is still useful for a numerical resolution: we can approximately integrate the equation (3.240).

To conclude, we proved the expression of the asymptotic expansions of the baroclinic eigenvectors, considering the asymptotic regime (3.120) and assuming the heights of each layer have all the same range and the difference of velocity between an interface has the same order as the square root of the relative difference of density at this interface. Moreover, the expansions of these eigenvectors, $\boldsymbol{r}_{\boldsymbol{x}}^{\lambda_i^{\pm}}(\mathbf{u},\boldsymbol{\gamma})$ and $\boldsymbol{l}_{\boldsymbol{x}}^{\lambda_i^{\pm}}(\mathbf{u},\boldsymbol{\gamma})$, for $i\in[\![1,n-1]\!]$, have been performed with a precision about $\mathcal{O}(\varepsilon^{\frac{\sigma(i)+1}{2}})$.

In the next subsection, we deduce necessary condition of local well-posedness of the model (3.10), more general than (3.27).

3.5.3 Local well-posedness of the model

Using the previous asymptotic expansions, it is possible to prove the local well-posedness of the multi-layer shallow water model with free surface, in two space-dimensions.
First, we can prove the next proposition

Proposition 3.5.3 *Let* $(\mathbf{u},\boldsymbol{\gamma}) \in \mathbb{R}^{3n}\times]0,1[^{n-1}$, $\theta \in [0,2\pi]$, $\varepsilon > 0$ *and an injective function* $\sigma \in \mathbb{R}_+^{*\,[\![1,n-1]\!]}$ *such that* $\boldsymbol{\gamma}$ *verifies* (3.120), $\mathbf{u}$ *verifies* (3.123).
Then, there exists $\delta > 0$ *such that if*

$$\varepsilon \leq \delta, \tag{3.241}$$

the matrix $\mathsf{A}(\mathbf{u},\boldsymbol{\gamma},\theta)$ *is diagonalizable with real eigenvalues if*

$$\begin{cases} h_i > 0, & \forall i \in [\![1,n]\!], \\ \phi_{\sigma,i}(\boldsymbol{h}) - |u_{i+1}-u_i|^2 - |v_{i+1}-v_i|^2 > 0, & \forall i \in [\![1,n-1]\!], \end{cases} \tag{3.242}$$

where $\phi_{\sigma,i}(\boldsymbol{h}) := (h_{\sigma,i}^- + h_{\sigma,i}^+)(1-\gamma_i)$.

Proof With the rotational invariance (3.16), it is equivalent to prove the diagonalizability of $\mathsf{A}_x(\mathbf{u},\boldsymbol{\gamma})$. Assuming (3.120), (3.123) and (3.241), according to (3.74) and the propositions 3.5.1 and 3.5.2, the right eigenvectors

$$\left(\boldsymbol{r}_{\boldsymbol{x}}^{\lambda_i^\pm}(\mathbf{u},\boldsymbol{\gamma})\right)_{i\in[\![1,n]\!]} \cup \left(\boldsymbol{r}_{\boldsymbol{x}}^{\lambda_i}(\mathbf{u},\boldsymbol{\gamma})\right)_{i\in[\![2n+1,3n]\!]} \tag{3.243}$$

constitute an eigenbasis of $\mathbb{R}^{3n}$ if (3.242) is verified. Indeed, the conditions (3.242) are necessary to insure the eigenvectors are in $\mathbb{R}^{3n}$ and it is a basis of this vector-space because: for $i \in [\![2n+1,3n]\!]$, giving a vector $\boldsymbol{r}_{\boldsymbol{x}}^{\lambda_i}(\mathbf{u},\boldsymbol{\gamma})$, it is obvious to find back i; for $i \in [\![1,n]\!]$, giving $\boldsymbol{r}_{\boldsymbol{x}}^{\lambda_i^\pm}(\mathbf{u},\boldsymbol{\gamma})$ it is also easy to detect i — where the sign of the 1st coordinates changes — and, according to the strict inequalities (3.242),

$$\boldsymbol{r}_{\boldsymbol{x}}^{\lambda_i^+}(\mathbf{u},\boldsymbol{\gamma}) \neq \boldsymbol{r}_{\boldsymbol{x}}^{\lambda_i^-}(\mathbf{u},\boldsymbol{\gamma}). \tag{3.244}$$

Then, if the inequalities (3.242) are assumed, $\mathsf{A}_x(\mathbf{u},\boldsymbol{\gamma})$ is diagonalizable with real eigenvalues and the proposition 3.5.3 is proved.

Remark: According to the propositions 3.4.6 and 3.4.7, we would expect, in the asymptotic regime (3.120), (3.123) and $\varepsilon \leq \delta$, that

$$\lambda_n^- < \lambda_{m_\sigma^-}^- < \ldots < \lambda_{m_\sigma^+}^- < \lambda_{m_\sigma^+}^+ < \ldots < \lambda_{m_\sigma^-}^+ < \lambda_n^+. \tag{3.245}$$

In the particular case of two layers, these inequalities are true, in this asymptotic regime. Moreover, in the case of n layers, with $n \geq 3$, if we assume for all $i \in [\![1,n-2]\!]$, $\pi_i\pi_{i+1} > 0$ and

$$\left[\frac{h_{\sigma,i}^- h_{\sigma,i}^+}{h_{\sigma,i}^- + h_{\sigma,i}^+}\left(1-\gamma_i - \frac{(u_{i+1}-u_i)^2}{h_{\sigma,i}^- + h_{\sigma,i}^+}\right)\right]^{\frac{1}{2}} \ll \frac{|\pi_i| h_{\sigma,i}^-}{h_{\sigma,i}^- + h_{\sigma,i}^+}, \tag{3.246}$$

then (3.245) remains true, as we can deduce that

$$\forall i \in [\![1, n-1]\!],\ \min(u_i, u_{i+1}) < \lambda_i^{\pm} < \max(u_i, u_{i+1}), \tag{3.247}$$

and the diagonalizability of the matrix $\mathsf{A}(\mathbf{u}, \boldsymbol{\gamma}, \theta)$ is directly deduced. However, in the general case, (3.245) is not verified: to prove the diagonalizability of $\mathsf{A}(\mathbf{u}, \boldsymbol{\gamma}, \theta)$, we need the entirely eigenstructure of this matrix.

Finally, as a consequence of the previous proposition, we deduce a necessay condition of local well-posedness in $\mathcal{H}^s(\mathbb{R}^2)^{3n}$, more general than criterion (3.27).

Theorem 3.5.4 *Let $s > 2$, $\boldsymbol{\gamma} \in]0,1[^{n-1}$, $\varepsilon > 0$ and an injective function $\sigma : [\![1, n-1]\!] \to \mathbb{R}_+^*$ such that $\boldsymbol{\gamma}$ verifies* (3.120).
Then, there exists $\delta > 0$ such that if

$$\varepsilon \leq \delta, \tag{3.248}$$

the Cauchy *problem, associated with* (3.10) *and initial data $\mathbf{u^0} \in \mathcal{H}_{\sigma,\varepsilon} \cap \mathcal{H}^s(\mathbb{R}^2)^{3n}$, is hyperbolic, locally well-posed in $\mathcal{H}^s(\mathbb{R}^2)^{3n}$ and the unique solution verifies conditions* (3.22).

Proof Let $(\mathbf{u^0}, \boldsymbol{\gamma}) \in \mathcal{H}^s(\mathbb{R}^2)^{3n} \times]0,1[^{n-1}$ such that conditions (3.120), (3.123) and (3.248) are verified. As it was proved in the proposition 3.5.3, for all $(X, \theta) \in \mathbb{R}^2 \times [0, 2\pi]$, $\mathsf{A}(\mathbf{u^0}(X), \boldsymbol{\gamma}, \theta)$ is diagonalizable, with real eigenvalues, if $\mathbf{u} \in \mathcal{H}_{\sigma,\varepsilon}$. Then, the *Cauchy* problem is hyperbolic. Moreover, according to the proposition 3.2.5, it is locally well-posed in $\mathcal{H}^s(\mathbb{R}^2)^{3n}$ and the unique solution verifies conditions (3.22).

Remark: This necessary condition is less restrictive than (3.27), because, as it was proved in proposition 3.4.11, if $(\mathbf{u}, \boldsymbol{\gamma})$ verifies these conditions and ε is sufficiently small, $\mathcal{S}^s_{\boldsymbol{\gamma}} \subset \mathcal{H}_{\sigma,\varepsilon} \cap \mathcal{H}^s(\mathbb{R}^2)^{3n}$.

In conclusion, we proved the expression of the asymptotic expansions of the baroclinic eigenvectors, considering the asymptotic regime (3.120) and assuming the heights of each layer have all the same range and the difference of velocity between an interface has the same order as the square root of the relative difference of density at this interface. Moreover, the expansions of these eigenvectors, $\boldsymbol{r}_{\boldsymbol{x}}^{\lambda_i^{\pm}}(\mathbf{u}, \boldsymbol{\gamma})$ and $\boldsymbol{l}_{\boldsymbol{x}}^{\lambda_i^{\pm}}(\mathbf{u}, \boldsymbol{\gamma})$, for $i \in [\![1, n-1]\!]$, have been performed with a precision about $\mathcal{O}(\varepsilon^{\frac{\sigma(i)+1}{2}})$, permitting to give a condition of local well-posedness of the multi-layer shallow water model with free surface, in two dimensions.

In the next subsection, we deduce from the asymptotic expansions of the eigenstructure of $\mathsf{A}_x(\mathbf{u}, \boldsymbol{\gamma})$, the nature of the waves associated to each eigenvalues.

3.5.4 Nature of the waves

In order to know the type of the wave associated to each eigenvalue – shock, contact or rarefaction wave – there is the next proposition

Proposition 3.5.5 *Let* $\boldsymbol{\gamma} \in]0,1[^{n-1}$, $\varepsilon > 0$ *and an injective function* $\sigma \in \mathbb{R}_+^{*\,[\![1,n-1]\!]}$ *such that* $\boldsymbol{\gamma}$ *verifies* (3.120).
Then, there exists $\delta > 0$ *such that if*

$$\varepsilon \leq \delta, \tag{3.249}$$

and $\mathbf{u} \in \mathcal{H}_{\sigma,\varepsilon}$, *we have*

$$\begin{cases} \text{the } \lambda_i^{\pm}-\text{characteristic field is genuinely non} - \text{linear}, & \text{if } i \in [\![1,n]\!], \\ \text{the } \lambda_i-\text{characteristic field is linearly degenerate}, & \text{if } i \in [\![2n+1,3n]\!]. \end{cases} \tag{3.250}$$

Proof If $(\mathbf{u},\boldsymbol{\gamma})$ verify these assumptions, the asymptotic expansions (3.148) and (3.153) are valid. Moreover, we remark that for all $i \in [\![1,n]\!]$, $\lambda_i^{\pm}$ depends analytically of the parameters of the problem and we deduce that the error of the asymptotic expansions still remains small after derivating. Then, with the right eigenvectors (3.74) and the asymptotic expansions of the right eigenvectors (3.212) and (3.229) of $A_x(\mathbf{u},\boldsymbol{\gamma})$, one can check that

$$\begin{cases} \nabla\lambda_i^{\pm} \cdot \boldsymbol{r}_x^{\lambda_i^{\pm}}(\mathbf{u}) \neq 0, & \text{if } i \in [\![1,n]\!],, \\ \nabla\lambda_i \cdot \boldsymbol{r}_x^{\lambda}(\mathbf{u}) = 0, & \text{if } i \in [\![2n+1,3n]\!]. \end{cases} \tag{3.251}$$

Then, the proposition 3.5.5 is proved.

Remark: When for all $i \in [\![1,n-1]\!]$, $u_{i+1} - u_i$ and $1-\gamma_i$ are all equal to 0, the $\lambda_n^{\pm}$-characteristic field remains genuinely non-linear but the $\lambda_i^{\pm}$-characteristic field becomes linearly degenerate.
To conclude, under assumptions (3.120), (3.123) and (3.249), for all $i \in [\![1,n]\!]$, the $\lambda_i^{\pm}$-wave is a shock wave or a rarefaction wave and for all $i \in [\![2n+1,3n]\!]$ the λ_i-wave is a contact wave.

3.6 A *conservative* multi-layer shallow water model

Even if the model (3.1–3.2) is conservative, in the one-dimensional case, with the unknowns (h_i,u_i), $i \in [\![1,n]\!]$, it is not anymore true in the two-dimensional case. This section will treat this lack of conservativity by an augmented model, with a different approach from [1]. We remind that no assumption has been made concerning the horizontal vorticity, in each layer

$$\forall i \in [\![1,n]\!],\ w_i := curl(\boldsymbol{u_i}) = \frac{\partial v_i}{\partial x} - \frac{\partial u_i}{\partial y}. \tag{3.252}$$

3.6.1 Conservation laws

Using a *Frobenius* problem, it was proved in [8] that the one-dimensional two-layer shallow water model with free surface has a finite number of conservative quantities: the height and velocity in each layer, the total momentum and the total energy. However, in the two-dimensional case, it is still an open question.

Concerning the multi-layer model, in one dimension, we can also reduce the study of conservative quantities to the study of a *Frobenius* problem. Indeed, defining the new unknowns

$$\forall i \in [\![1,n]\!], \left\{ \begin{array}{l} \hat{h}_i := \alpha_{n,i} h_i, \\ \hat{u}_i := u_i, \end{array} \right. \tag{3.253}$$

and

$$\hat{\mathbf{u}} := {}^{\top}(\hat{h}_1, \ldots, \hat{h}_n, \hat{u}_n, \ldots, \hat{u}_n), \tag{3.254}$$

then, the model (3.10) is equivalent to

$$\frac{\partial \hat{\mathbf{u}}}{\partial t} + \hat{\mathsf{A}}_x(\hat{\mathbf{u}}, \boldsymbol{\gamma}) \frac{\partial \hat{\mathbf{u}}}{\partial x} + \hat{\mathbf{b}}(\hat{\mathbf{u}}) = 0, \tag{3.255}$$

with

$$\hat{\mathsf{A}}_x(\hat{\mathbf{u}}, \boldsymbol{\gamma}) := \left[\begin{array}{c|c} \Delta & 0 \\ \hline 0 & \mathsf{I_n} \end{array} \right] \left[\begin{array}{c|c} \mathsf{V}_x & \mathsf{H} \\ \hline \Gamma & \mathsf{V}_x \end{array} \right]. \tag{3.256}$$

Moreover, we have also

$$\hat{\mathsf{A}}_x(\hat{\mathbf{u}}, \boldsymbol{\gamma}) = \mathsf{P} \nabla^2 \hat{e}_1(\hat{\mathbf{u}}, \boldsymbol{\gamma}), \tag{3.257}$$

where $\hat{e}_1(\hat{\mathbf{u}}) := \frac{1}{2} \sum_{i=1}^{n} \hat{h}_i \left(\hat{u}_i^2 + \frac{\hat{h}_i}{\alpha_{n,i}} \right) + \sum_{i=1}^{n-1} \sum_{j=i+1}^{n} \hat{h}_i \frac{\hat{h}_j}{\alpha_{n,j}}$ and the $2n \times 2n$ block matrix P is defined by

$$\mathsf{P} := \left[\begin{array}{c|c} 0 & \mathsf{I_n} \\ \hline \mathsf{I_n} & 0 \end{array} \right], \tag{3.258}$$

Therefore, $\eta(\hat{\mathbf{u}})$ is a conservative quantity of the multi-layer model, in one dimension, if and only if the matrix $\nabla^2 \eta(\hat{\mathbf{u}})\ \hat{\mathsf{A}}_x(\hat{\mathbf{u}})$ is symmetric, which is equivalent to, according to (3.257),

$$(\mathsf{P} \nabla^2 \eta(\hat{\mathbf{u}})) \hat{\mathsf{A}}_x(\hat{\mathbf{u}}) = \hat{\mathsf{A}}_x(\hat{\mathbf{u}}) (\mathsf{P} \nabla^2 \eta(\hat{\mathbf{u}})). \tag{3.259}$$

Consequently, if we denote by $\mathsf{X} := \mathsf{P} \nabla^2 \eta(\hat{\mathbf{u}})$, the conservative quantities of (3.255) needs to verify the *Frobenius* problem:

$$\mathsf{X}\ \hat{\mathsf{A}}_x(\hat{\mathbf{u}}) = \hat{\mathsf{A}}_x(\hat{\mathbf{u}})\ \mathsf{X}. \tag{3.260}$$

Remark: The condition (3.260) is just necessary: the solution $\mathsf{X} := [\mathsf{X}_{i,j}]_{(i,j) \in [\![1,2n]\!]^2}$ needs to verify the compatibility conditions

$$\forall (i,j,k) \in [\![1,2n]\!]^3, \ \frac{\partial \mathsf{X}_{i,j}}{\partial \alpha_k} = \frac{\partial \mathsf{X}_{i,k}}{\partial \alpha_j}, \tag{3.261}$$

where for all $k \in [\![1,n]\!]$, $\alpha_k := \hat{h}_k$ and $\alpha_{n+k} := \hat{u}_k$, to insure that X is the hessian of a scalar field.
We remind a useful property of the set of the solutions of (3.260):

Proposition 3.6.1 *Let $\boldsymbol{\gamma} \in]0,1[^{n-1}$, $\varepsilon > 0$ and an injective function $\sigma \in \mathbb{R}_+^{*\,[\![1,n-1]\!]}$ such that $\boldsymbol{\gamma}$ verifies* (3.120).
Then, there exists $\delta > 0$ such that if

$$\varepsilon \leq \delta, \tag{3.262}$$

and $\mathbf{u} \in \mathcal{H}_{\sigma,\varepsilon}$, a matrix X is solution of the Frobenius *problem* (3.260) *if and only if*

$$\mathsf{X} \in \mathrm{Span}\big(\hat{\mathsf{A}}_x^k(\hat{\mathbf{u}}),\ k \in [\![0,2n-1]\!]\big). \tag{3.263}$$

Proof Under these conditions, as it was proved in propositions 3.4.6 and 3.4.7, the eigenvalues of $\hat{\mathsf{A}}_x(\hat{\mathbf{u}})$ are all distinct. Then, the characteristic polynomial of $\hat{\mathsf{A}}_x(\hat{\mathbf{u}})$ coincides with the minimal polynomial. Therefore, the set of solutions of (3.260) is equal to $\mathrm{Span}\big(\hat{\mathsf{A}}_x^k(\hat{\mathbf{u}}),\ k \in [\![0,2n-1]\!]\big)$.

Then, according to the last proposition, there exists $\big(x_i\big)_{i\in[\![1,2n-1]\!]} \subset \mathbb{R}$ such that

$$\nabla^2\eta(\hat{\mathbf{u}}) = \sum_{i=0}^{2n-1} x_i \mathsf{P}\hat{\mathsf{A}}_x^k(\hat{\mathbf{u}}). \tag{3.264}$$

Using the compatibility conditions (3.261), we should find conditions on $\big(x_i\big)_{i\in[\![1,2n-1]\!]}$, to insure $\eta(\hat{\mathbf{u}})$ to be a conservative quantity. However, the question is still open as the complexity of (3.261) is very high. However we would expect to find

$$\begin{cases} x_i \text{ is a constant}, & \forall i \in [\![0,1]\!], \\ x_i = 0, & \forall i \in [\![2,2n-1]\!], \end{cases} \tag{3.265}$$

to deduce that there exist $(x_0,x_1) \in \mathbb{R}^2$ and $(\mathbf{c},\mathbf{d}) \in \mathbb{R}^{2n}$ such that

$$\eta(\hat{\mathbf{u}}) = \frac{x_0}{2}\hat{\mathbf{u}}\cdot\mathsf{P}\hat{\mathbf{u}} + x_1\hat{e}_1(\hat{\mathbf{u}}) + \mathbf{c}\cdot\hat{\mathbf{u}} + \mathbf{d}, \tag{3.266}$$

as the only known conservative quantities, in one dimension, are the height, the velocity in each layer, the total momentum and the total energy of the system.
Concerning the conservative quantities of the multi-layer model, in two dimensions, the question is quite more complex and is also still open. Moreover, the study performed below does not remain possible — the structure (3.257) is not anymore verified.
Nevertheless, introducing w_i, for $i \in [\![1,n]\!]$, in equations (3.1–3.2), the conservation of mass (3.1) is unchanged

$$\frac{\partial h_i}{\partial t} + \nabla\cdot(h_i\boldsymbol{u_i}) = 0, \tag{3.267}$$

but the equation of depth-averaged horizontal velocity (3.2) becomes conservative

$$\frac{\partial \boldsymbol{u_i}}{\partial t} + \nabla\left(\frac{1}{2}(u_i^2+v_i^2)+P_i\right) - (f+w_i)\boldsymbol{u_i}^{\perp} = 0. \tag{3.268}$$

Moreover, the horizontal vorticity, in each layer, is also conservative:

$$\frac{\partial w_i}{\partial t} + \nabla\cdot((w_i+f)\boldsymbol{u_i}) = 0. \tag{3.269}$$

Therefore, in the two-dimensional case, there are at least $3n+2$ conservative quantities: the height, the velocity and the horizontal vorticity in each layer, the total momentum and the energy e_2:

$$e_2(\mathbf{v},\boldsymbol{\gamma}) := \frac{1}{2}\sum_{i=1}^{n}\alpha_{n,i}h_i\left(u_i^2+v_i^2+h_i\right) + \sum_{i=1}^{n-1}\sum_{j=i+1}^{n}\alpha_{n,i}h_ih_j. \tag{3.270}$$

3.6.2 A new augmented model

From equations (3.1–3.2), it is possible to obtain a new model. We denote $(\mathbf{u},\mathbf{v}) \in \mathcal{H}^s(\mathbb{R}^2)^{3n} \times \mathcal{H}^s(\mathbb{R}^2)^{4n}$, the vectors defined by

$$\left\{\begin{array}{l} \mathbf{u} := {}^{\top}(h_1,\dots,h_n,u_1,\dots,u_n,v_1,\dots,v_n), \\ \mathbf{v} := {}^{\top}(h_1,\dots,h_n,u_1,\dots,u_n,v_1,\dots,v_n,w_1,\dots,w_n). \end{array}\right. \tag{3.271}$$

If $\mathbf{u}$ is a classical solution of (3.10), then $\mathbf{v}$ is solution of the augmented system

$$\frac{\partial \mathbf{v}}{\partial t} + \mathsf{A}^{\mathsf{a}}_x(\mathbf{v},\boldsymbol{\gamma})\frac{\partial \mathbf{v}}{\partial x} + \mathsf{A}^{\mathsf{a}}_y(\mathbf{v},\boldsymbol{\gamma})\frac{\partial \mathbf{v}}{\partial y} + \mathbf{b}^{\mathbf{a}}(\mathbf{v}) = 0, \tag{3.272}$$

where the $4n\times 4n$ block matrices $\mathsf{A}^{\mathsf{a}}_x(\mathbf{v},\boldsymbol{\gamma})$ and $\mathsf{A}^{\mathsf{a}}_y(\mathbf{v},\boldsymbol{\gamma})$ are defined by

$$\mathsf{A}^{\mathsf{a}}_x(\mathbf{v},\boldsymbol{\gamma}) := \left[\begin{array}{c|c|c|c} \mathsf{V}_x & \mathsf{H} & 0 & 0 \\ \hline \Gamma & \mathsf{V}_x & \mathsf{V}_y & 0 \\ \hline 0 & 0 & 0 & 0 \\ \hline 0 & \mathsf{W} & 0 & \mathsf{V}_x \end{array}\right], \tag{3.273}$$

$$\mathsf{A}^{\mathsf{a}}_y(\mathbf{v},\boldsymbol{\gamma}) := \left[\begin{array}{c|c|c|c} \mathsf{V}_y & 0 & \mathsf{H} & 0 \\ \hline 0 & 0 & 0 & 0 \\ \hline \Gamma & \mathsf{V}_x & \mathsf{V}_y & 0 \\ \hline 0 & 0 & \mathsf{W} & \mathsf{V}_y \end{array}\right], \tag{3.274}$$

where $\mathsf{W} := \mathrm{diag}[w_i+f]_{i\in[\![1,n]\!]}$ and $\mathbf{b}^{\mathbf{a}}(\mathbf{v})$ is defined by

$$\mathbf{b}^{\mathbf{a}}(\mathbf{v}) := \sum_{k=1}^{n}\left(-(w_k+f)v_k + \frac{\partial b}{\partial x}\right)\boldsymbol{e'}_{n+k} + \left((w_k+f)u_k + \frac{\partial b}{\partial y}\right)\boldsymbol{e'}_{2n+k}, \tag{3.275}$$

where $(\boldsymbol{e'_i})_{i\in[\![1,4n]\!]}$ denotes the canonical basis of $\mathbb{R}^{4n}$.

Even if the model (3.1–3.2) is not conservative, the model (3.272) is always so. Then, there is no need to chose a conservative path in the numerical resolution.

Remark: 1) $e_2(\mathbf{v},\boldsymbol{\gamma})$ is not the total energy of the augmented model (3.272). Indeed, it is never a convex function with the variable $\mathbf{v}$ as it is independent of $(w_i)_{i\in[\![1,n]\!]}$. 2) Let $\mathbf{v}\in\mathbb{R}^{4n}$, the associated vector $\mathbf{u}\in\mathbb{R}^{3n}$ will be composed of the $3n$ first coordonates of the vector $\mathbf{v}$. All the quantities or functions with $\mathbf{u}$ as a variable will refer to the non-augmented model (3.10) and all the ones with $\mathbf{v}$, as a variable, will refer to the new augmented model (3.272).

Proposition 3.6.2 *The augmented model* (3.272) *verifies the rotational invariance.*

Proof We denote by $\mathsf{A}^{\mathsf{a}}(\mathbf{v},\boldsymbol{\gamma},\theta)$ the matrix defined by

$$\cos(\theta)\mathsf{A}^{\mathsf{a}}_x(\mathbf{v},\boldsymbol{\gamma})+\sin(\theta)\mathsf{A}^{\mathsf{a}}_y(\mathbf{v},\boldsymbol{\gamma}). \tag{3.276}$$

One can check the next equality, for all $(\mathbf{v},\boldsymbol{\gamma},\theta)\in\mathbb{R}^{4n}\times{\mathbb{R}_+^*}^{n-1}\times[0,2\pi]$

$$\mathsf{A}^{\mathsf{a}}(\mathbf{v},\boldsymbol{\gamma},\theta)=\mathsf{P}^{\mathsf{a}}(\theta)^{-1}\mathsf{A}^{\mathsf{a}}_x(\mathsf{P}^{\mathsf{a}}(\theta)\mathbf{v},\boldsymbol{\gamma})\mathsf{P}^{\mathsf{a}}(\theta), \tag{3.277}$$

where $\mathsf{P}^{\mathsf{a}}(\theta)$ is the $4n\times 4n$ block matrix defined by

$$\mathsf{P}^{\mathsf{a}}(\theta):=\left[\begin{array}{c|c|c|c} \mathsf{I_n} & 0 & 0 & 0\\ \hline 0 & \cos(\theta)\mathsf{I_n} & \sin(\theta)\mathsf{I_n} & 0\\ \hline 0 & -\sin(\theta)\mathsf{I_n} & \cos(\theta)\mathsf{I_n} & 0\\ \hline 0 & 0 & 0 & \mathsf{I_n}\end{array}\right], \tag{3.278}$$

and, moreover, we notice $\mathsf{P}^{\mathsf{a}}(\theta)^{-1}={}^{\top}\mathsf{P}^{\mathsf{a}}(\theta)$.

3.6.3 A rough criterion of local well-posedness

We give a 1st criterion of *Friedrichs*-symmetrizability to insure the local well-posedness in $\mathcal{H}^s(\mathbb{R}^2)^{4n}$ and $\mathcal{L}^2(\mathbb{R}^2)^{4n}$.

Theorem 3.6.3 *Let $s>2$ and $(\mathbf{v^0},\boldsymbol{\gamma})\in\mathcal{H}^s(\mathbb{R}^2)^{4n}\times]0,1[^{n-1}$ and $\boldsymbol{u_0}:=(u_0,v_0)\in\mathbb{R}^2$ such that*

$$\left\{\begin{array}{ll}\inf_{X\in\mathbb{R}^2}h_i^0(X)>0, & \forall\, i\in[\![1,n]\!],\\ \inf_{X\in\mathbb{R}^2}\delta^a(\mathbf{v^0}(X),\boldsymbol{\gamma},\boldsymbol{u_0})>0,\end{array}\right. \tag{3.279}$$

where for every $\mathbf{v}\in\mathbb{R}^{4n}$,

$$\begin{array}{rl}\delta^{\mathsf{a}}(\mathbf{v},\boldsymbol{\gamma},\boldsymbol{u_0}):= & \min\left(a(\mathbf{h},\boldsymbol{\gamma})^{-1},\min_{i\in[\![1,n]\!]}(h_i^2)\right)\\ & -\max_{i\in[\![1,n]\!]}\alpha_{n,i}|u_i-u_0|-\max_{i\in[\![1,n]\!]}\alpha_{n,i}|v_i-v_0|\\ & +\min\left(0,\min_{i\in[\![1,n]\!]}\frac{w_i+f}{2}\left(w_i+f-\sqrt{(w_i+f)^2+4h_i^2}\right)\right).\end{array} \tag{3.280}$$

Then, the Cauchy *problem, associated with the system* (3.272) *and the initial data $\mathbf{v^0}$, is hyperbolic, locally well-posed in $\mathcal{H}^s(\mathbb{R}^2)^{4n}$ and there exists $T>0$ such that $\mathbf{v}$, the unique solution of the* Cauchy *problem, verifies*

$$\left\{\begin{array}{l}\mathbf{v}\in\mathcal{C}^1([0,T]\times\mathbb{R}^2)^{4n},\\ \mathbf{v}\in\mathcal{C}([0,T];\mathcal{H}^s(\mathbb{R}^2))^{4n}\cap\mathcal{C}^1([0,T];\mathcal{H}^{s-1}(\mathbb{R}^2))^{4n}.\end{array}\right. \tag{3.281}$$

Proof We define the next $4n \times 4n$ symmetric matrix:

$$\mathsf{S}^{\mathsf{a}}(\mathbf{v},\boldsymbol{\gamma}) = \left[\begin{array}{c|c|c|c} \Delta\Gamma + \mathsf{W}^2 & \Delta\mathsf{V}_x & \Delta\mathsf{V}_y & -\mathsf{WH} \\ \hline \Delta\mathsf{V}_x & \Delta\mathsf{H} & 0 & 0 \\ \hline \Delta\mathsf{V}_y & 0 & \Delta\mathsf{H} & 0 \\ \hline -\mathsf{WH} & 0 & 0 & \mathsf{H}^2 \end{array}\right], \tag{3.282}$$

One can check that $\mathsf{S}^a(\mathbf{v},\boldsymbol{\gamma})$, $\mathsf{S}^a(\mathbf{v},\boldsymbol{\gamma})\mathsf{A}^a_x(\mathbf{v},\boldsymbol{\gamma})$ and $\mathsf{S}^a(\mathbf{v},\boldsymbol{\gamma})\mathsf{A}^a_y(\mathbf{v},\boldsymbol{\gamma})$ are unconditionally symmetric:

$$\mathsf{S}^{\mathsf{a}}(\mathbf{v},\boldsymbol{\gamma})\mathsf{A}^a_x = \left[\begin{array}{c|c|c|c} 2\Delta\Gamma\mathsf{V}_x + \mathsf{W}^2\mathsf{V}_x & \Delta\Gamma\mathsf{H} + \Delta\mathsf{V}_x^2 & \Delta\mathsf{V}_x\mathsf{V}_y & -\mathsf{WHV}_x \\ \hline \Delta\Gamma\mathsf{H} + \Delta\mathsf{V}_x^2 & 2\Delta\mathsf{HV}_x & \Delta\mathsf{HV}_y & 0 \\ \hline \Delta\mathsf{V}_x\mathsf{V}_y & \Delta\mathsf{HV}_y & 0 & 0 \\ \hline -\mathsf{WHV}_x & 0 & 0 & \mathsf{H}^2\mathsf{V}_x \end{array}\right], \tag{3.283}$$

$$\mathsf{S}^{\mathsf{a}}(\mathbf{v},\boldsymbol{\gamma})\mathsf{A}^a_y = \left[\begin{array}{c|c|c|c} 2\Delta\Gamma\mathsf{V}_y + \mathsf{W}^2\mathsf{V}_y & \Delta\mathsf{V}_x\mathsf{V}_y & \Delta\Gamma\mathsf{H} + \Delta\mathsf{V}_y^2 & -\mathsf{WHV}_y \\ \hline \Delta\mathsf{V}_x\mathsf{V}_y & 0 & \Delta\mathsf{HV}_x & 0 \\ \hline \Delta\Gamma\mathsf{H} + \Delta\mathsf{V}_y^2 & \Delta\mathsf{HV}_x & 2\Delta\mathsf{HV}_y & 0 \\ \hline -\mathsf{WHV}_y & 0 & 0 & \mathsf{H}^2\mathsf{V}_y \end{array}\right], \tag{3.284}$$

Then, we need to verify $\mathsf{S}^a(\mathbf{v},\boldsymbol{\gamma}) > 0$ (*i.e* $\lambda^{\min}\big(\mathsf{S}^a(\mathbf{v},\boldsymbol{\gamma})\big) > 0$), to insure that it is a *Friedrichs*-symmetrizer. We introduce the following decomposition of $\mathsf{S}^{\mathsf{a}}(\mathbf{v},\boldsymbol{\gamma})$:

$$\mathsf{S}^{\mathsf{a}}(\mathbf{v},\boldsymbol{\gamma}) = \mathsf{S}^{\mathsf{a}}_0(\mathbf{h},\boldsymbol{\gamma}) + \mathsf{S}^{\mathsf{a}}_1(\mathbf{v},\boldsymbol{\gamma}) + \mathsf{S}^a_2(\mathbf{v},\boldsymbol{\gamma}) + \mathsf{S}^a_3(\mathbf{v},\boldsymbol{\gamma}), \tag{3.285}$$

where the $4n \times 4n$ symmetric matrices are defined by

$$\mathsf{S}^a_0(\mathbf{h},\boldsymbol{\gamma}) = \left[\begin{array}{c|c|c|c} \Delta\Gamma & 0 & 0 & 0 \\ \hline 0 & \Delta\mathsf{H} & 0 & 0 \\ \hline 0 & 0 & \Delta\mathsf{H} & 0 \\ \hline 0 & 0 & 0 & \mathsf{H}^2 \end{array}\right], \tag{3.286}$$

$$\mathsf{S}^a_1(\mathbf{v},\boldsymbol{\gamma}) = \left[\begin{array}{c|c|c|c} 0 & \Delta\mathsf{V}_x & 0 & 0 \\ \hline \Delta\mathsf{V}_x & 0 & 0 & 0 \\ \hline 0 & 0 & 0 & 0 \\ \hline 0 & 0 & 0 & 0 \end{array}\right], \tag{3.287}$$

$$\mathsf{S}^{\mathsf{a}}_2(\mathbf{v},\boldsymbol{\gamma}) = \left[\begin{array}{c|c|c|c} 0 & 0 & \Delta\mathsf{V}_y & 0 \\ \hline 0 & 0 & 0 & 0 \\ \hline \Delta\mathsf{V}_y & 0 & 0 & 0 \\ \hline 0 & 0 & 0 & 0 \end{array}\right], \tag{3.288}$$

$$\mathsf{S}^a_3(\mathbf{v},\boldsymbol{\gamma}) = \left[\begin{array}{c|c|c|c} \mathsf{W}^2 & 0 & 0 & -\mathsf{WH} \\ \hline 0 & 0 & 0 & 0 \\ \hline 0 & 0 & 0 & 0 \\ \hline -\mathsf{WH} & 0 & 0 & 0 \end{array}\right]. \tag{3.289}$$

According to the inequality of convexity (3.51),

$$\lambda^{\min}\big(\mathsf{S}^a(\mathbf{v},\boldsymbol{\gamma})\big) \geq \lambda^{\min}\big(\mathsf{S}_0^a(\mathbf{h},\boldsymbol{\gamma})\big) + \lambda^{\min}\big(\mathsf{S}_1^a(\mathbf{v},\boldsymbol{\gamma})\big) + \lambda^{\min}\big(\mathsf{S}_2^a(\mathbf{v},\boldsymbol{\gamma})\big) + \lambda^{\min}\big(\mathsf{S}_2^a(\mathbf{v},\boldsymbol{\gamma})\big). \tag{3.290}$$

An analysis of each spectrum leads to

$$\left\{\begin{array}{l} \lambda^{\min}\big(\mathsf{S}_0^a(\mathbf{h},\boldsymbol{\gamma})\big) \geq \min\big(a(\mathbf{h},\boldsymbol{\gamma})^{-1}, \min_{i\in[\![1,n]\!]}(h_i^2)\big), \\ \lambda^{\min}\big(\mathsf{S}_1^a(\mathbf{v},\boldsymbol{\gamma})\big) = -\max_{i\in[\![1,n]\!]}\alpha_{n,i}|u_i|, \\ \lambda^{\min}\big(\mathsf{S}_1^a(\mathbf{v},\boldsymbol{\gamma})\big) = -\max_{i\in[\![1,n]\!]}\alpha_{n,i}|v_i|, \\ \lambda^{\min}\big(\mathsf{S}_1^a(\mathbf{v},\boldsymbol{\gamma})\big) = \min\left(0, \min_{i\in[\![1,n]\!]}\frac{w_i+f}{2}\big(w_i+f-\sqrt{(w_i+f)^2+4h_i^2}\big)\right). \end{array}\right. \tag{3.291}$$

Finally, with the rescaling

$$\forall i\in[\![1,n-1]\!],\ \left\{\begin{array}{l} h_i \leftarrow h_i, \\ u_i-u_0 \leftarrow u_i, \\ v_i-v_0 \leftarrow v_i, \end{array}\right. \tag{3.292}$$

and under conditions (3.279), the mapping

$$\mathsf{S}^{\mathsf{a}} : (\mathbf{v},\boldsymbol{\gamma}) \mapsto \mathsf{S}^{\mathsf{a}}(\mathbf{v},\boldsymbol{\gamma}) \tag{3.293}$$

is a *Friedrichs*-symmetrizer. Using the propositions 3.2.3 and 3.2.4, the *Cauchy* problem is hyperbolic, locally well-posed and the unique solution verifies (3.281), if the initial data verifies (3.279).

Remark: The non-augmeneted model (3.10) has a *symbolic*-symmetrizer if

$$a(\boldsymbol{h},\boldsymbol{\gamma})^{-1} - \alpha_{n,i}\big(|u_i-\bar{u}|+|v_i-\bar{v}|\big) > 0, \tag{3.294}$$

which is a more restrictive condition than the one of symmetrizability (3.279), for the augmented model (3.272), if for all $i\in[\![1,n]\!]$,

$$h_i^2 \geq a(\boldsymbol{h},\boldsymbol{\gamma})^{-1}, \tag{3.295}$$

and

$$\min\left(0, \min_{i\in[\![1,n]\!]}\frac{w_i+f}{2}\big(w_i+f-\sqrt{(w_i+f)^2+4h_i^2}\big)\right) > \max_{i\in[\![1,n]\!]}\alpha_{n,i}(|u_0|-|\bar{u}|+|v_0|-|\bar{v}|), \tag{3.296}$$

and less restrictive otherwise.

3.6.4 A necessary condition of local well-posedness

As it was reminded before, the description of the eigenstructure of $\mathsf{A}^{\mathsf{a}}(\mathbf{v},\boldsymbol{\gamma},\theta)$ is a decisive point, as it permits to characterize exactly its diagonalizability, the nature of the waves and also the *Riemann*

invariants. According to the rotational invariance (3.277), we restrict the analysis to the eigenstructure of $\mathsf{A}^{\mathsf{a}}_x(\mathbf{v},\boldsymbol{\gamma})$. First of all, as the characteristic polynomial of $\mathsf{A}^{\mathsf{a}}_x(\mathbf{v},\boldsymbol{\gamma})$ is equal to

$$\det(\mathsf{A}^{\mathsf{a}}_x(\mathbf{v},\boldsymbol{\gamma})-\lambda\mathsf{I}_{4\mathsf{n}})=\lambda^n\det(\mathsf{A}_x(\mathbf{u},\boldsymbol{\gamma})-\lambda\mathsf{I}_{3\mathsf{n}}), \tag{3.297}$$

we remark that the spectrum of $\mathsf{A}^{\mathsf{a}}_x(\mathbf{v},\boldsymbol{\gamma})$ is such that

$$\sigma(\mathsf{A}^{\mathsf{a}}_x(\mathbf{v},\boldsymbol{\gamma})):=\left(\lambda_i^{\pm}(\mathbf{v},\boldsymbol{\gamma})\right)_{i\in[\![1,n]\!]}\cup\left(\lambda_{2n+i}(\mathbf{v},\boldsymbol{\gamma})\right)_{i\in[\![1,2n]\!]}, \tag{3.298}$$

where $\left(\lambda_i^{\pm}(\mathbf{v},\boldsymbol{\gamma})\right)_{i\in[\![1,n]\!]}\cup\left(\lambda_{2n+i}(\mathbf{v},\boldsymbol{\gamma})\right)_{i\in[\![1,n]\!]}=:\sigma(\mathsf{A}_x(\mathbf{u},\boldsymbol{\gamma}))$ and

$$\forall i\in[\![1,n]\!],\ \lambda_{3n+i}(\mathbf{v},\boldsymbol{\gamma})=0. \tag{3.299}$$

Let $\boldsymbol{\gamma}\in]0,1[^{n-1}$, $\varepsilon>0$ and an injective function $\sigma:[\![1,n-1]\!]\to\mathbb{R}_+^*$ such that $\boldsymbol{\gamma}$ verifies (3.120). We define the next subset of $\mathcal{L}^2(\mathbb{R}^2)^{4n}$:

$$\mathcal{H}^a_{\sigma,\varepsilon}:=\left\{\mathbf{v}^{\mathbf{0}}\in\mathcal{L}^2(\mathbb{R}^2)^{4n}/\ \mathbf{u}^{\mathbf{0}}\in\mathcal{H}_{\sigma,\varepsilon}\right\} \tag{3.300}$$

Proposition 3.6.4 *Let* $(\mathbf{v},\boldsymbol{\gamma})\in\mathbb{R}^{4n}\times]0,1[^{n-1}$, $\theta\in[0,2\pi]$, $\varepsilon>0$ *and an injective function* $\sigma\in\mathbb{R}_+^{*\,[\![1,n-1]\!]}$ *such that* $\boldsymbol{\gamma}$ *verifies* (3.120) *and the associated vector* $\mathbf{u}$ *verifies* (3.123).
There exists $\delta>0$ *such that if*

$$\varepsilon\le\delta, \tag{3.301}$$

then the matrix $\mathsf{A}^{\mathsf{a}}(\mathbf{v},\boldsymbol{\gamma},\theta)$ *is diagonalizable with real eigenvalues if the associated vector,* $\mathbf{u}$*, verifies*

$$\begin{cases} h_i>0, & \forall i\in[\![1,n]\!],\\ \phi_{\sigma,i}(\boldsymbol{h})-|u_{i+1}-u_i|^2-|v_{i+1}-v_i|^2>0, & \forall i\in[\![1,n-1]\!]. \end{cases} \tag{3.302}$$

Proof With the rotational invariance (3.277), it is equivalent to prove the diagonalizability of $\mathsf{A}^{\mathsf{a}}_x(\mathbf{v},\boldsymbol{\gamma})$. By denoting $(\boldsymbol{e'_i})_{i\in[\![1,4n]\!]}$ the canonical basis of $\mathbb{R}^{4n}$, one can prove the expressions of the right eigenvectors $\boldsymbol{r}^{\lambda}_x(\mathbf{v},\boldsymbol{\gamma})$ of $\mathsf{A}^{\mathsf{a}}_x(\mathbf{v},\boldsymbol{\gamma})$, associated to the eigenvalue $\lambda\in\sigma(\mathsf{A}^{\mathsf{a}}_x(\mathbf{v},\boldsymbol{\gamma}))$, are, for all $i\in[\![1,n]\!]$, defined by

$$\boldsymbol{r}^{\lambda_i^{\pm}}_x(\mathbf{v},\boldsymbol{\gamma})=\boldsymbol{r}^{\lambda_i^{\pm}}_x(\mathbf{u},\boldsymbol{\gamma})+\sum_{k=1}^{n}\frac{w_k+f}{\lambda_i^{\pm}-u_k}(\boldsymbol{r}^{\lambda_i^{\pm}}_x(\mathbf{u},\boldsymbol{\gamma})\cdot\boldsymbol{e}_{n+k})\boldsymbol{e'}_{3n+k}, \tag{3.303}$$

$$\boldsymbol{r}^{\lambda_{2n+i}}_x(\mathbf{v},\boldsymbol{\gamma})=\boldsymbol{e'}_{3n+i}, \tag{3.304}$$

$$\boldsymbol{r}^{\lambda_{3n+i}}_x(\mathbf{v},\boldsymbol{\gamma})=\begin{cases} \begin{array}{l}(\Gamma\mathsf{V}_y\boldsymbol{e_i}\cdot\boldsymbol{e_i})\boldsymbol{e'_i}-(\mathsf{V}_x\mathsf{H}^{-1}\Gamma^{-1}\mathsf{V}_y\boldsymbol{e_i}\cdot\boldsymbol{e_i})\boldsymbol{e'}_{n+i}\\ -((\mathsf{I}_{\mathsf{n}}-\mathsf{V}_x^2\mathsf{H}^{-1}\Gamma^{-1})\mathsf{V}_y\boldsymbol{e_i}\cdot\boldsymbol{e_i})\boldsymbol{e'}_{2n+i}\\ +(\mathsf{W}\mathsf{H}^{-1}\Gamma^{-1}\mathsf{V}_y\boldsymbol{e_i}\cdot\boldsymbol{e_i})\boldsymbol{e'}_{3n+i}\end{array} & ,\quad \text{if } v_i\neq 0,\\ \boldsymbol{e'}_{2n+i}, & \text{if } v_i=0, \end{cases} \tag{3.305}$$

where $\boldsymbol{r}_x^{\lambda}(\mathbf{u},\boldsymbol{\gamma})$ are expressed in (3.212) and (3.229) and $(\cdot)$ is the inner product on $\mathbb{R}^{3n}$.
Consequently, the right eigenvectors $\boldsymbol{r}^{\lambda}(\mathbf{v},\boldsymbol{\gamma},\theta)$ of $\mathsf{A}^{\mathsf{a}}(\mathbf{v},\boldsymbol{\gamma},\theta)$ are defined by

$$\forall \lambda \in \sigma\left(\mathsf{A}^{\mathsf{a}}(\mathbf{v},\boldsymbol{\gamma},\theta)\right),\ \boldsymbol{r}^{\lambda}(\mathbf{v},\boldsymbol{\gamma},\theta) = \mathsf{P}^{\mathsf{r}}(\theta)^{-1}\boldsymbol{r}_x^{\lambda}(\mathsf{P}^{\mathsf{r}}(\theta)\mathbf{v},\boldsymbol{\gamma}). \tag{3.306}$$

Moreover, as it was proved in the diagonalizability of $\mathsf{A}_x(\mathbf{u},\boldsymbol{\gamma})$ in proposition 3.5.3, if $\varepsilon \leq \delta$, the right eigenvectors induced an eigenbasis of $\mathbb{R}^{4n}$. A consequence is the right eigenvectors form an eigenbasis of $\mathbb{R}^{4n}$ and $\mathsf{A}_x^{\mathsf{a}}(\mathbf{v},\boldsymbol{\gamma})$ is diagonalizable with real eigenvalues, if (3.302) is verified.

Remark: There is also the left eigenvectors $\boldsymbol{l}_x^{\lambda}(\mathbf{v},\boldsymbol{\gamma})$ of $\mathsf{A}_x^{\mathsf{a}}(\mathbf{v},\boldsymbol{\gamma})$, associated to the eigenvalue $\lambda \in \sigma(\mathsf{A}_x^{\mathsf{a}}(\mathbf{v},\boldsymbol{\gamma}))$: for all $i \in [\![1,n]\!]$,

$$\boldsymbol{l}_x^{\lambda_i^{\pm}}(\mathbf{v},\boldsymbol{\gamma}) = \boldsymbol{l}_x^{\lambda_i^{\pm}}(\mathbf{u},\boldsymbol{\gamma}) + \sum_{k=1}^{n} \frac{v_k}{\lambda_i^{\pm}} ({}^{\top}\boldsymbol{l}_x^{\lambda_i^{\pm}}(\mathbf{u},\boldsymbol{\gamma})\cdot \boldsymbol{e}_{n+k})^{\top}\boldsymbol{e}'_{2n+k}, \tag{3.307}$$

$$\boldsymbol{l}_x^{\lambda_{2n+i}}(\mathbf{v},\boldsymbol{\gamma}) = -(w_i+f)^{\top}\boldsymbol{e}'_i + h_i{}^{\top}\boldsymbol{e}'_{3n+i}, \tag{3.308}$$

$$\boldsymbol{l}_x^{\lambda_{3n+i}}(\mathbf{v},\boldsymbol{\gamma}) = {}^{\top}\boldsymbol{e}'_{2n+i}, \tag{3.309}$$

where $\boldsymbol{l}_x^{\lambda}(\mathbf{u},\boldsymbol{\gamma})$ are expressed in (3.213) and (3.230) and $(\cdot)$ is the inner product on $\mathbb{R}^{3n}$. Moreover, we made intentionally a mistake in (3.303) and (3.307), as we did not provide the expression of $\boldsymbol{r}_x^{\lambda_i^{\pm}}(\mathbf{u},\boldsymbol{\gamma})$ and $\boldsymbol{l}_x^{\lambda_i^{\pm}}(\mathbf{u},\boldsymbol{\gamma})$, but it is the natural expression coming from (3.212), (3.213), (3.229) and (3.230) and replacing $\boldsymbol{e}_i$ by $\boldsymbol{e}'_i$, for every $i \in [\![1,3n]\!]$.
Then, the left eigenvectors $\boldsymbol{l}^{\lambda}(\mathbf{v},\boldsymbol{\gamma},\theta)$ of $\mathsf{A}^{\mathsf{a}}(\mathbf{v},\boldsymbol{\gamma},\theta)$ are also defined by

$$\forall \lambda \in \sigma\left(\mathsf{A}^{\mathsf{a}}(\mathbf{v},\boldsymbol{\gamma},\theta)\right),\ \boldsymbol{l}^{\lambda}(\mathbf{v},\boldsymbol{\gamma},\theta) = \boldsymbol{l}_x^{\lambda}(\mathsf{P}^{\mathsf{r}}(\theta)\mathbf{v},\boldsymbol{\gamma})\mathsf{P}^{\mathsf{r}}(\theta). \tag{3.310}$$

Remark: According to the asymptotic expansions (3.213) and (3.230), in the general case, $\lambda_i^{\pm} \neq 0$ and $\lambda_i^{\pm} \neq u_i$; consequently, $\boldsymbol{r}_x^{\lambda_i^{\pm}}(\mathbf{v},\boldsymbol{\gamma})$ in (3.303) and $\boldsymbol{l}_x^{\lambda_i^{\pm}}(\mathbf{v},\boldsymbol{\gamma})$ in (3.307) are defined.
Furthermore, the type of the wave associated to each eigenvalue is described in the next proposition.

Proposition 3.6.5 *Let $\boldsymbol{\gamma} \in]0,1[^{n-1}$, $\varepsilon > 0$ and an injective function $\sigma \in \mathbb{R}_+^{*\,[\![1,n-1]\!]}$ such that $\boldsymbol{\gamma}$ verifies (3.120).*
Then, there exists $\delta > 0$ such that if

$$\varepsilon \leq \delta, \tag{3.311}$$

and $\mathbf{v} \in \mathcal{H}^a_{\sigma,\varepsilon}$, we have

$$\begin{cases} \text{the } \lambda_i^{\pm}\text{−characteristic field is genuinely non} - \text{linear}, & \text{if } i \in [\![1,n]\!], \\ \text{the } \lambda_i\text{−characteristic field is linearly degenerate}, & \text{if } i \in [\![2n+1,4n]\!]. \end{cases} \tag{3.312}$$

Proof Using the same proof of proposition 3.5.5, and remarking that for all $i \in [\![2n+1, 3n]\!]$, $\lambda_i = 0$, which implies

$$\nabla\lambda_i \cdot \boldsymbol{r}_x^{\lambda}(\mathbf{v}, \boldsymbol{\gamma}) = 0, \tag{3.313}$$

and the proof of the proposition 3.6.5.

To conclude, under conditions of the proposition 3.6.5, for all $i \in [\![1, n]\!]$, the $\lambda_i^{\pm}$-wave is a shock wave or a rarefaction wave and the $\lambda_{2n+i}^{\pm}$-wave and $\lambda_{3n+i}^{\pm}$-wave are contact waves.
Finally, the point is to know if this augmented system (3.272) is locally well-posed and if its solution provides the solution of the non-augmented system (3.10).

Theorem 3.6.6 *Let $s > 2$, $\boldsymbol{\gamma} \in]0,1[^{n-1}$, $\varepsilon > 0$ and an injective function $\sigma : [\![1, n-1]\!] \to \mathbb{R}_+^*$ such that $\boldsymbol{\gamma}$ verifies (3.120).*
Then, there exists $\delta > 0$ such that if

$$\varepsilon \leq \delta, \tag{3.314}$$

the Cauchy *problem, associated with (3.272) and initial data $\mathbf{v^0} \in \mathcal{H}^a_{\sigma,\varepsilon} \cap \mathcal{H}^s(\mathbb{R}^2)^{4n}$, is hyperbolic, locally well-posed in $\mathcal{H}^s(\mathbb{R}^2)^{4n}$ and the unique solution verifies conditions (3.281). Furthermore, $\mathbf{u}$, the associated vector field, verifies conditions (3.22) and is the unique classical solution of the* Cauchy *problem, associated with (3.10) and initial data $\mathbf{u^0} \in \mathcal{H}_{\sigma,\varepsilon} \cap \mathcal{H}^s(\mathbb{R}^2)^{3n}$, if and only if*

$$\forall i \in [\![1, n]\!],\ w_i^0 = \frac{\partial v_i^0}{\partial x} - \frac{\partial u_i^0}{\partial y}. \tag{3.315}$$

Proof Using proposition 3.6.4, $\sigma(\mathsf{A}^{\mathsf{a}}(\mathbf{v}, \boldsymbol{\gamma}, \theta)) \subset \mathbb{R}$ and $\mathsf{A}^{\mathsf{a}}(\mathbf{v}\boldsymbol{\gamma}, \theta)$ is diagonalizable. Then, the proposition 3.2.5 is verified: the hyperbolicity and the local well-posedness of the *Cauchy* problem, associated with system (3.272) and initial data $\mathbf{v^0}$, is insured and conditions (3.281) are verified. Moreover, it is obvious to prove that, for all $i \in [\![1, n]\!]$, there exists $\Phi_i : \mathbb{R}^2 \to \mathbb{R}$ such that

$$\forall (t, x, y) \in \mathbb{R}_+ \times \mathbb{R}^2,\ w_i(t, x, y) = \frac{\partial v_i}{\partial x}(t, x, y) - \frac{\partial u_i}{\partial y}(t, x, y) + \Phi_i(x, y). \tag{3.316}$$

As Φ_i does not depend on the time t, $\mathbf{u}$ – the vector associated to $\mathbf{v}$ – is solution of the non-augmented system (3.10) if and only if $\Phi_i = 0$, for all $i \in [\![1, n]\!]$, which is true if and only if it is verified at $t = 0$.

We deduce directly the next corollary.

Corollary 3.6.7 *Let $s > 2$, $\boldsymbol{\gamma} \in]0,1[^{n-1}$, $\varepsilon > 0$ and an injective function $\sigma : [\![1, n-1]\!] \to \mathbb{R}_+^*$ such that $\boldsymbol{\gamma}$ verifies (3.120).*
There exists $\delta > 0$ such that if we assume

$$\varepsilon \leq \delta, \tag{3.317}$$

and we consider $\mathbf{v}$*, the unique solution of the* Cauchy *problem, associated with* (3.272) *and initial data* $\mathbf{v^0} \in \mathcal{H}^a_{\sigma,\varepsilon} \cap \mathcal{H}^s(\mathbb{R}^2)^{4n}$*, then the associated vector field,* $u \in \mathcal{H}_{\sigma,\varepsilon} \cap \mathcal{H}^s(\mathbb{R}^2)^{3n}$ *is the unique solution of* (3.10) *and verifies* (3.22) *if and only if* $\mathbf{v^0}$ *verifies*

$$\forall i \in [\![1,n]\!],\ w_i^0 = \frac{\partial v_i^0}{\partial x} - \frac{\partial u_i^0}{\partial y}. \tag{3.318}$$

Proof If (σ,ε) verify these assumptions, then, according to the theorem 3.6.6, the unique solution of the *Cauchy* problem, associated with (3.272) and initial data $\mathbf{v^0} \in \mathcal{H}^a_{\sigma,\varepsilon} \cap \mathcal{H}^s(\mathbb{R}^2)^{4n}$ is such that the associated vector field, $\mathbf{u}$, verifies conditions (3.22) and is the unique classical solution of the Cauchy problem, associated with (3.10) and initial data $\mathbf{u^0} \in \mathcal{H}_{\sigma,\varepsilon} \cap \mathcal{H}^s(\mathbb{R}^2)^{3n}$, if and only if (3.318) is verified.

To cut a long story short, we introduced a new conservative multi-layer model, in two-dimensions, proved the *Friedrichs*-symmetrizability under conditions (3.279), proved its local well-posedness in $\mathcal{H}^s(\mathbb{R}^2)^{3n}$, with $s > 2$, under the same conditions expressed in the previous section. Moreover, we explained the link between the solutions of the augmented and the non-augmented models: they are the same if they verify the compatibility conditions (3.6.6), when $t = 0$. However, we did not address the treatment of non-conservative product with the new augmented model: a possible solution could be to generalize the results proved in [52] for the two-layer model.

3.7 Discussions and perspectives

In this paper, we proved, with various techniques, the hyperbolicity and the local well-posedness, in $\mathcal{H}^s(\mathbb{R}^2)^{3n}$, of the two-dimensional multi-layer shallow water model, with free surface. All of them use the rotational invariance property (3.16), reducing the problem from two dimensions to one dimension. We gave, at first, a criterion of local well-posedness, in $\mathcal{H}^s(\mathbb{R}^2)^{3n}$, using the symmetrizability of the system (3.10). Afterwards, we studied the hyperbolicity of different particular cases: the single-layer model, the merger of two layers and the asymptotic expansion of this last case. Then, we proved the asymptotic expansion of all the eigenvalues, in a particular asymptotic regime, and a new necessary condition of hyperbolicity of this system was explicitly characterized and compared with the set of symmetrizability. This condition is clearly similar with the criterion of hyperbolicity in the two-layer case. Moreover, we provided the asymptotic expansion of all the eigenvectors, in this regime, we characterized the nature of waves associated to each element of the spectrum of $\mathsf{A}_x(\mathbf{u},\boldsymbol{\gamma})$ – shock, rarefaction of contact wave – and we proved the local well-posedness, in $\mathcal{H}^s(\mathbb{R}^2)^{3n}$, of the system (3.10), under conditions of hyperbolicity and weak density-stratification. Finally, after

discussing about the conservative quantities of the system, we introduced a new augmented model (3.272), adding the horizontal vorticity, in each layer, as a new unknown. We also characterized the eigenstructure, the nature of the waves, proved the local well-posedness in $\mathcal{H}^s(\mathbb{R}^2)$ and explained the link of a solution of the non-augmented model (3.10) and a solution of the new model (3.272). The *conservativity* of the new augmented model avoid choosing a conservative path, introduced in [36], to solve the numerical problem.

However, the characterization of all the conservative quantities is still an open question, in the general case of n layers and in one and two dimensions. Moreover, we addressed the question of the hyperbolicity and the local well-posedness in a particular asymptotic regime. There are a lot of other possibilities which are not taken into account in this regime. Indeed, even if the assumption on the density-stratification seems to embrace most of the useful cases of the oceanography, the assumptions on the heights of each layer does clearly not. Then, other asymptotic expansions are needed to be performed, in order to characterize the other possibilities.

Finally, the characterization of the eigenstructure is a decisive point of the numerical treatment of the open boundary problem, in a limited domain Ω. Indeed, there are a lot of techniques to treat these kind of boundary conditions: the radiation methods as the *Sommerfeld* conditions from [122] or as the *Orlanski-type* conditions, for more complex hyperbolic flows, proposed in [96]; the absorbing conditions, explained in [47]; relaxation methods studied in [111]; or the *Flather* conditions proposed in [49]. As it was underlined in [14], the characteristic-based methods, such as *Flather* conditions — which is often seen as radiation conditions —, are natural and efficient open boundary conditions: the outgoing waves does not need any conditions, while conditions are imposed on the characteristic variables, for the incoming waves. However, the integration of the characteristics variables is not an issue when $n = 1$, the single-layer problem: the characteristics variables are exactly known, because the exact eigenvectors $\boldsymbol{l}^{\lambda_1^\pm} := {}^\top(1, \pm\sqrt{\frac{h}{g}}, 0)$, associated with the exact eigenvalue $\lambda_1^\pm := u \pm \sqrt{gh}$, is such that:

$$ {}^\top\boldsymbol{l}^{\lambda_1^\pm}\frac{\partial \mathbf{u}}{\partial t} = \sqrt{\frac{h}{g}}\frac{\partial}{\partial t}\left(u \pm 2\sqrt{gh}\right), \tag{3.319} $$

where we remind that $\mathbf{u} := {}^\top(h,u,v)$, when $n = 1$. Then, the characteristic variables of the single-layer model, at the surface $\partial\Omega$, are: $(\boldsymbol{u}\cdot\boldsymbol{n})$ and $(\boldsymbol{u}\cdot\boldsymbol{n}) \pm 2\sqrt{gh}$, where $\boldsymbol{n}$ is the outward pointing unit vector of $\partial\Omega$. In the case $n = 2$, [18] and [104] gave the 4 characteristic variables associated to the two-layer model and we will give it for an eastern surface: $\boldsymbol{n} = {}^\top(1,0)$. Two of them are associated to the total height of water (*i.e.* the barotropic waves):

$$ \frac{h_1u_1 + h_2u_2}{h_1 + h_2} \pm 2\sqrt{g(h_1 + h_2)}, \tag{3.320} $$

and two of them to the interface (*i.e.* the baroclinic waves):

$$\arcsin\left(\frac{h_1-h_2}{h_1+h_2}\right)\mp\arcsin\left(\frac{u_2-u_1}{\sqrt{g(1-\gamma_1)(h_1+h_2)}}\right). \tag{3.321}$$

Nevertheless, these expressions are formal approximations of the regime $\gamma_1 \approx 1$ in (3.320), and $\frac{\partial(h_1+h_2)}{\partial t} \approx 0$ in (3.321). They are not exact expressions of the characteristic variables. As far as we know, for the multi-layer problem, the question is still open about the existence of these non-linear characteristic variables.

Finally, as we have proved in this paper, the eigenstructure of the multi-layer model, with $n \geq 3$ and in the asymptotic regime considered, looks like different two-layer models, with different layers considered. Then, in the asymptotic regime (3.120) and (3.123), another open question is the efficiency of the treatment of open boundary conditions with the following formal characteristic variables:

$$\bar{u} \pm 2\sqrt{gH}, \tag{3.322}$$

and

$$\forall i \in [\![1, n-1]\!],\ \arcsin\left(\frac{h^-_{\sigma,i}-h^+_{\sigma,i}}{h^-_{\sigma,i}+h^+_{\sigma,i}}\right)\mp\arcsin\left(\frac{u_{i+1}-u_i}{\sqrt{g(1-\gamma_i)(h^-_{\sigma,i}+h^+_{\sigma,i})}}\right). \tag{3.323}$$

compared with a linearized treatment of the open boundary conditions, as *Flather* conditions for the single layer model. It would be interesting to compute these two kind of open boundary conditions in the two-layer case and a more general one, in a simple limited domain such as a rectangular, to address these open questions.

A mathematician is a blind man in a dark room
looking for a black cat which is not there.

C.R. Darwin.

Conclusion

Dans ce chapitre, l'hyperbolicité et le caractère localement bien-posé, du modèle de *Saint-Venant* multi-couches a été démontré. À la différence du modèle à une couche, toutes les vitesses ne sont pas admissibles. Cependant, le critère général d'hyperbolicité, démontré dans cette section, est semblable au critère d'hyperbolicité du modèle de *Saint-Venant* bi-couches.

Le modèle augmenté de la vorticité, introduit pour le modèle bi-couches, a été généralisé au modèle multi-couches. Ce modèle est aussi hyperbolique et localement bien-posé, sous certaines explicitées. De plus le lien entre les solutions des modèles augmenté et non-augmenté reste le même que dans le cas du modèle bi-couches : si les solutions sont initialement égales et suffisamment régulières, alors elles sont toujours égales.

Les développements asymptotiques des éléments propres démontrés dans ce chapitre vont permettre de caractériser les conditions limites à prescrire, pour le traitement des frontières artificielles, lors de la résolution numérique du modèle multi-couches. Cependant, ces conditions sont, *a priori*, valables pour le modèle linéarisé. Il serait intéressant de déterminer s'il est possible d'en déduire des invariants de *Riemann*, pour le modèle non-linéaire, et sous quelles hypothèses.

Part III

Numerical validation

Introduction

L'étude des modèles de *Saint-Venant* à surface libre effectuée dans les sections précédentes, dans le cas particulier bi-couches et dans le cas général multi-couches, a permis de mettre en exergue un critère général caractérisant l'hyperbolicité et le caractère bien-posé des modèles. Cette analyse a aussi permis d'obtenir un développement asymptotique des éléments propres associés à l'opérateur différentiel de ces modèles. Cependant, ces développement vont permettre de caractériser les conditions limites nécessaires au traitement des frontières ouvertes.

Pour les prévisions opérationnelles, une frontière artificielle est introduite, pour ne pas calculer la solution approchée sur tout l'océan mais sur une zone déterminée. Il est alors nécessaire d'imposer des conditions limites à cette frontière permettant de laisser entrer et sortir les ondes du domaine intérieur, sans altérer la solution approchée.

Plusieurs méthodes sont connues :

- radiative,
- absorbante,
- de relaxation,
- des caractéristiques.

Dans ce chapitre, il a été choisi d'utiliser la méthode des caractéristiques pour le traitement des frontières ouvertes. Cette méthode est fondamentalement liée à la structure du modèle et permet d'exploiter les développements effectués dans les chapitres précédents.

Le plan de ce chapitre est le suivant:

- Dans la première partie, les équations considérées sont rappelées, ainsi que les principaux résultats des chapitres précédents,

- La seconde partie est dédiée au caractère bien-posé du problème initial aux limites, associé aux modèle de *Saint-Venant* multi-couches. Les conditions limites à imposer aux frontières ouvertes seront expliciter pour un domaine quelconque et un domaine particulier : un rectangle,
- La troisième partie expose les choix effectués pour la résolution numérique du modèle multi-couches à surface libre,
- Enfin, dans la quatrième et dernière partie, les résultats numériques sont comparés entre les modèles à 1, 2 et 4 couches, avec deux cas tests: une onde de gravité et un vortex.

Ce chapitre est à lecture indépendante.

4

Numerical treatment of the open boundaries

Contents

4.1 Introduction

In the last decades, the computational capabilities have increased radically. This made possible the intensive calculus, such as the atmosphere or underwater meteorology. However, this capacity is not unlimited and the effort to improve the models and the numerical resolution still remain necessary.

Indeed, concerning the underwater forecasting for example, the scientists are much more interested in the behavior of the sea surface near the coasts than in the deep water. Consequently, it is necessary to focus the study on a finite domain, restricted to the goal area. This avoids any numerical resolution, on a part of the ocean, which will not be exploited.

Outline: In this section, the main properties of the multi-layer shallow water model with free surface, prove in the previous chapter are reminded. The results about the augmented model, with the vorticity, are also reminded. In section 2, the well-posedness of the initial-boundary value problem is proved, using the energy method. The boundary conditions are clarified in a general domain and in a particular on: a rectangle. In section 3, the numerical resolution is detailed. In the section 4, the numerical treatment of the open boundaries is performed with:

- two test cases: a gravity wave and a barotropic vortex,
- three models: 1, 2 and 4 layers,
- the linearized and non-linear models.

Finally, in section 5, the influence of various parameters is quantified, as the validity of the assumptions, made in the last chapter, to obtain the open boundary conditions.

The present numerical resolution uses basic tools to approximate the solution of the multi-layer shallow water model. More efficient methods of resolution of these equations are detailed in [11], [17], [28], [29], [35], [45], [101] and [136].

4.1.1 Governing equations and main properties

In this subsection, we give the equations of the multi-layer shallow water model, with free surface, and those of the augmented model. Moreover, we remind the main results of local well-posedness of these models, which will be useful to resolve the initial-boundary value problem.

The i^{th} layer of fluid, $i \in [\![1,n]\!]$, has a constant density ρ_i, a depth-averaged horizontal velocity $\boldsymbol{u_i}(t,X) := {}^{\top}(u_i(t,X),v_i(t,X))$ and a thickness designated by $h_i(t,X)$, where t denotes the time and $X := (x,y)$ the horizontal cartesian coordinates, as drawn in figure 4.1.

The governing equations of the multi-layer shallow water model with free surface, in two dimensions, is given by $3n$ partial differential equations of 1^{st} order: for all $i \in [\![1,n]\!]$ there is the mass-conservation of the layer i:

$$\frac{\partial h_i}{\partial t} + \nabla\cdot(h_i\boldsymbol{u_i}) = 0, \tag{4.1}$$

and equations on the depth-averaged horizontal momentum of the layer i:

$$\frac{\partial \boldsymbol{u_i}}{\partial t} + (\boldsymbol{u_i}\cdot\nabla)\boldsymbol{u_i} + \nabla P_i - f\boldsymbol{u_i}^{\perp} = 0, \tag{4.2}$$

where $P_i := g\left(b + \sum_{k=1}^{n} \alpha_{i,k} h_k\right)$, $\boldsymbol{u_i^\perp} := {}^\top(v_i, -u_i)$, g is the gravitational acceleration, b is the bottom topography, f is the *Coriolis* parameter and

$$\alpha_{i,k} = \begin{cases} \frac{\rho_k}{\rho_i}, & k < i \\ 1, & k \geq i. \end{cases} \tag{4.3}$$

A useful notation is introduced, for all $i \in [\![1, n-1]\!]$, γ_i is the density ratio between the layer i and the layer $i+1$:

$$\forall i \in [\![1, n-1]\!],\ \gamma_i := \frac{\rho_i}{\rho_{i+1}}. \tag{4.4}$$

Then, if $k \leq i-1$, the ratio $\frac{\rho_k}{\rho_i}$ is equal to

$$\frac{\rho_k}{\rho_i} = \prod_{j=k}^{i-1} \gamma_j, \tag{4.5}$$

the vector $\boldsymbol{\gamma}$ will denote ${}^\top(\gamma_1, \ldots, \gamma_{n-1}) \in \mathbb{R}_+^{n-1}$ and the vector $\mathbf{h}$ will be equal to ${}^\top(h_1, \ldots, h_n) \in \mathbb{R}_+^n$.

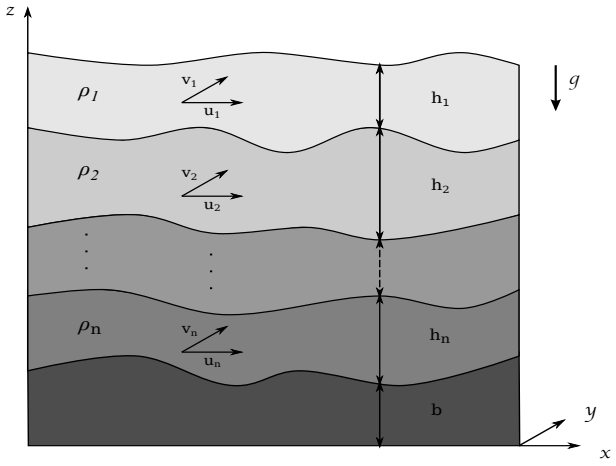

Figure 4.1: Configuration of the multi-layer shallow water model with free surface

We proceed the following rescaling:

$$\forall i \in [\![1, n-1]\!],\ \begin{cases} \hat{h}_i \leftarrow g h_i, \\ \hat{u}_i \leftarrow u_i, \\ \hat{v}_i \leftarrow v_i, \end{cases} \tag{4.6}$$

and in order to simplify the notations, $\hat{}$ will be removed. Then, with the vector

$$\mathbf{u} := {}^\top(h_1, \ldots, h_n, u_1, \ldots, u_n, v_1, \ldots, v_n), \tag{4.7}$$

the 1st order quasi-linear partial differential equations system (4.1-4.2) can be written as

$$\frac{\partial \mathbf{u}}{\partial t} + \mathsf{A}_x(\mathbf{u}, \boldsymbol{\gamma}) \frac{\partial \mathbf{u}}{\partial x} + \mathsf{A}_y(\mathbf{u}, \boldsymbol{\gamma}) \frac{\partial \mathbf{u}}{\partial y} + \mathbf{b}(\mathbf{u}) = 0, \tag{4.8}$$

where the $3n \times 3n$ block matrices $\mathsf{A}_x(\mathbf{u},\boldsymbol{\gamma})$, $\mathsf{A}_y(\mathbf{u},\boldsymbol{\gamma})$ and the vector $\mathbf{b}(\mathbf{u}) \in \mathbb{R}^{3n}$ are defined by

$$\mathsf{A}_x(\mathbf{u},\boldsymbol{\gamma}) := \left[\begin{array}{c|c|c} \mathsf{V}_x & \mathsf{H} & 0 \\ \hline \Gamma & \mathsf{V}_x & 0 \\ \hline 0 & 0 & \mathsf{V}_x \end{array}\right], \mathsf{A}_y(\mathbf{u},\boldsymbol{\gamma}) := \left[\begin{array}{c|c|c} \mathsf{V}_y & 0 & \mathsf{H} \\ \hline 0 & \mathsf{V}_y & 0 \\ \hline \Gamma & 0 & \mathsf{V}_y \end{array}\right], \tag{4.9}$$

$$\mathbf{b}(\mathbf{u}) := {}^{\top}\left(0,\dots,0,-fv_1+\frac{\partial b}{\partial x},\dots,-fv_n+\frac{\partial b}{\partial x},fu_1+\frac{\partial b}{\partial y},fu_n+\frac{\partial b}{\partial y}\right), \tag{4.10}$$

with the $n \times n$ block matrices

$$\left\{\begin{array}{ll} \mathsf{V}_x & := \mathrm{diag}[u_i]_{i\in[\![1,n]\!]}, \\ \mathsf{V}_y & := \mathrm{diag}[v_i]_{i\in[\![1,n]\!]}, \\ \mathsf{H} & := \mathrm{diag}[h_i]_{i\in[\![1,n]\!]}, \\ \Gamma & := [\alpha_{i,k}]_{(i,k)\in[\![1,n]\!]^2}, \end{array}\right. \tag{4.11}$$

where $\mathrm{diag}[x_i]_{i\in[\![1,n]\!]}$ is the $n \times n$ diagonal matrix with $(x_1,\dots,x_n)$ on the diagonal. Moreover, with $i \in [\![1,n]\!]$ and M a $n \times n$ matrix, we denote by $\mathrm{C}_i(\mathsf{M})$ and $\mathrm{L}_i(\mathsf{M})$ respectively the i^{th} column and the i^{th} line of M. We will denote the total depth by

$$H := \sum_{i=1}^{n} h_i, \tag{4.12}$$

and the average velocity in each direction by

$$\left\{\begin{array}{l} \bar{u} := \frac{1}{H}\sum_{i=1}^{n} h_i u_i, \\ \bar{v} := \frac{1}{H}\sum_{i=1}^{n} h_i v_i. \end{array}\right. \tag{4.13}$$

We remind that the model (4.8) verifies the rotational invariance: for all $(\mathbf{u},\boldsymbol{\gamma},\theta) \in \mathbb{R}^{3n} \times {\mathbb{R}_+^*}^{n-1} \times [0,2\pi]$, the $3n \times 3n$ matrix $\mathsf{A}(\mathbf{u},\boldsymbol{\gamma},\theta) := \cos(\theta)\mathsf{A}_x(\mathbf{u},\boldsymbol{\gamma}) + \sin(\theta)\mathsf{A}_y(\mathbf{u},\boldsymbol{\gamma})$ depends only on the matrix $\mathsf{A}_x(\mathbf{u},\boldsymbol{\gamma})$ and the parameter θ:

$$\forall(\mathbf{u},\boldsymbol{\gamma},\theta) \in \mathbb{R}^{3n} \times {\mathbb{R}_+^*}^{n-1} \times [0,2\pi],\ \mathsf{A}(\mathbf{u},\boldsymbol{\gamma},\theta) = \mathsf{P}(\theta)^{-1}\mathsf{A}_x\left(\mathsf{P}(\theta)\mathbf{u},\boldsymbol{\gamma}\right)\mathsf{P}(\theta), \tag{4.14}$$

where the $3n \times 3n$ matrix $\mathsf{P}(\theta)$ is defined by

$$\mathsf{P}(\theta) := \left[\begin{array}{c|c|c} \mathsf{I_n} & 0 & 0 \\ \hline 0 & \cos(\theta)\mathsf{I_n} & \sin(\theta)\mathsf{I_n} \\ \hline 0 & -\sin(\theta)\mathsf{I_n} & \cos(\theta)\mathsf{I_n} \end{array}\right]. \tag{4.15}$$

Then, assuming there exist an injective function $\sigma \in {\mathbb{R}_+^*}^{n-1}$ and a parameter $\varepsilon > 0$ such that

$$\left\{\begin{array}{ll} 1-\gamma_i = \varepsilon^{\sigma(i)}, & \forall i \in [\![1,n-1]\!], \\ \min_{i\in[\![1,n-1]\!]}\sigma(i) = 1. & \end{array}\right. \tag{4.16}$$

and

$$\forall i \in [\![1;,n-1]\!],\ \left\{\begin{array}{l} u_{i+1}-u_i := \pi_i \varepsilon^{\frac{\sigma(i)}{2}} = \mathcal{O}((h_i+h_{i+1})^{\frac{1}{2}}\varepsilon^{\frac{\sigma(i)}{2}}), \\ h_i := \varpi_i h_{i+1} = \mathcal{O}(h_{i+1}). \end{array}\right. \tag{4.17}$$

Moreover, we consider the function $\mathbf{u} \in \mathcal{L}^2(\mathbb{R}^2)^{3n}$ such that

$$\begin{cases} \inf_{X\in\mathbb{R}^2} h_i(X) > 0, & \forall i \in [\![1,n]\!], \\ \inf_{X\in\mathbb{R}^2} \phi_{\sigma,i}(\boldsymbol{h}(X)) - |u_{i+1}-u_i|^2(X) - |v_{i+1}-v_i|^2(X) > 0, & \forall i \in [\![1,n-1]\!], \end{cases} \tag{4.18}$$

where $h := {}^\top(h_1,\dots,h_n)$, for all $i \in [\![1,n-1]\!]$, $\phi_{\sigma,i}(\boldsymbol{h}) := (h^-_{\sigma,i}+h^+_{\sigma,i})(1-\gamma_i)$, $h^-_{\sigma,i} := \sum_{k=m_i^-}^{i} h_k$, $h^+_{\sigma,i} := \sum_{k=i+1}^{m_i^+} h_k$ and

$$\begin{cases} m_i^- := \max\{1 \le j \le i / \gamma_j \ge \gamma_i\}, \\ m_i^+ := \min\{n \ge j > i / \gamma_{j-1} \ge \gamma_i\}. \end{cases} \tag{4.19}$$

Defining the eigenvalues of $\mathsf{A}_x(\mathbf{u},\boldsymbol{\gamma})$ by

$$\sigma(\mathsf{A}_x(\mathbf{u},\boldsymbol{\gamma})) := \left(\lambda_i^{\pm}(\mathbf{u},\boldsymbol{\gamma})\right)_{i\in[\![1,n]\!]} \cup \left(\lambda_{2n+i}(\mathbf{u},\boldsymbol{\gamma})\right)_{i\in[\![1,n]\!]}, \tag{4.20}$$

the right and left eigenvectors of $\mathsf{A}_x(\mathbf{u},\boldsymbol{\gamma})$, associated with $\lambda \in \sigma(\mathsf{A}_x(\mathbf{u},\boldsymbol{\gamma}))$, are respectively denoted by $\boldsymbol{r}_{\boldsymbol{x}}^{\lambda}(\mathbf{u},\boldsymbol{\gamma})$ and $\boldsymbol{l}_{\boldsymbol{x}}^{\lambda}(\mathbf{u},\boldsymbol{\gamma})$. Then, according to the rotational invariance (4.14), the spectrum of $\mathsf{A}(\mathbf{u},\boldsymbol{\gamma},\theta)$ is such that

$$\forall (\mathbf{u},\boldsymbol{\gamma},\theta) \in \mathbb{R}^{3n} \times {\mathbb{R}_+^*}^{n-1} \times [0,2\pi],\ \sigma(\mathsf{A}(\mathbf{u},\boldsymbol{\gamma},\theta)) = \sigma(\mathsf{A}_x(\mathsf{P}(\theta)\mathbf{u},\boldsymbol{\gamma})) \tag{4.21}$$

and the right and left eigenvectors of $\mathsf{A}(\mathbf{u},\boldsymbol{\gamma},\theta)$, associated with the eigenvalue $\lambda \in \sigma(\mathsf{A}(\mathbf{u},\boldsymbol{\gamma},\theta))$, are consequently defined by

$$\begin{cases} \boldsymbol{r}^{\lambda}(\mathbf{u},\boldsymbol{\gamma},\theta) = \mathsf{P}^{-1}(\theta)\boldsymbol{r}_{\boldsymbol{x}}^{\lambda}(\mathsf{P}(\theta)\mathbf{u},\boldsymbol{\gamma}), \\ \boldsymbol{l}^{\lambda}(\mathbf{u},\boldsymbol{\gamma},\theta) = \boldsymbol{l}_{\boldsymbol{x}}^{\lambda}(\mathsf{P}(\theta)\mathbf{u},\boldsymbol{\gamma})\mathsf{P}(\theta). \end{cases} \tag{4.22}$$

According to (4.21) and (4.22), it is obvious that the eigenstructure of $\mathsf{A}(\mathbf{u},\boldsymbol{\gamma},\theta)$ is resumed in the one of $\mathsf{A}_x(\mathbf{u},\boldsymbol{\gamma})$. Moreover, a part of the eigenstructure of $\mathsf{A}_x(\mathbf{u},\boldsymbol{\gamma})$ is explicit, for all $(\mathbf{u},\boldsymbol{\gamma})\mathbb{R}^{3n} \times {\mathbb{R}_+^*}^{n-1}$:

$$\forall i \in [\![1,n]\!],\ \lambda_{2n+i}(\mathbf{u},\boldsymbol{\gamma}) := u_i. \tag{4.23}$$

and

$$\forall i \in [\![1,n]\!],\ \begin{cases} \boldsymbol{r}_{\boldsymbol{x}}^{\lambda_{2n+i}}(\mathbf{u},\boldsymbol{\gamma}) = \boldsymbol{e}_{2n+i}, \\ \boldsymbol{l}_{\boldsymbol{x}}^{\lambda_{2n+i}}(\mathbf{u},\boldsymbol{\gamma}) = {}^\top\boldsymbol{e}_{2n+i}, \end{cases} \tag{4.24}$$

where $(\boldsymbol{e_i})_{i\in[\![1,3n]\!]}$ is the canonical basis of $\mathbb{R}^{3n}$.
Furthermore, if $(\sigma,\varepsilon) \in \mathbb{R}^{[\![1,n-1]\!]} \times \mathbb{R}_+^*$ such that assumptions (4.16), (4.17) and ε sufficiently small, the other part of the eigenstructure of $\mathsf{A}(\mathbf{u},\boldsymbol{\gamma},\theta)$ is such that, for all $i \in [\![1,n-1]\!]$, the baroclinic eigenstructure is

$$\begin{aligned} \lambda_i^{\pm}(\mathbf{u},\boldsymbol{\gamma}) = \ & \frac{u_{i+1}h^-_{\sigma,i}+u_ih^+_{\sigma,i}}{h^-_{\sigma,i}+h^+_{\sigma,i}} \pm \left[\frac{h^-_{\sigma,i}h^+_{\sigma,i}}{(h^-_{\sigma,i}+h^+_{\sigma,i})}\left(1-\gamma_i-\frac{(u_{i+1}-u_i)^2}{h^-_{\sigma,i}+h^+_{\sigma,i}}\right)\right]^{\frac{1}{2}} \\ & +\mathcal{O}(\varepsilon^{\frac{\sigma(i)+1}{2}}), \end{aligned} \tag{4.25}$$

the asymptotic expansion of the associated right eigenvector is

$$\begin{aligned}
\boldsymbol{r}_{\boldsymbol{x}}^{\lambda_i^{\pm}}(\mathbf{u},\boldsymbol{\gamma}) = \;& \textstyle\sum_{j=m_i^-}^{i} \frac{\boldsymbol{e_j}}{i-m_i^-+1} - \sum_{j=i+1}^{m_i^+} \frac{\boldsymbol{e}_j}{m_i^+-i} \\
& + \frac{u_{i+1}-u_i}{h_{\sigma,i}^- + h_{\sigma,i}^+} \left(\sum_{j=m_i^-}^{i} \frac{h_{\sigma,i}^- \boldsymbol{e}_{n+j}}{(i-m_i^-+1)h_j} + \sum_{j=i+1}^{m_i^+} \frac{h_{\sigma,i}^+ \boldsymbol{e}_{n+j}}{(m_i^+-i)h_j} \right) \\
& \pm \left[\frac{h_{\sigma,i}^- h_{\sigma,i}^+}{h_{\sigma,i}^- + h_{\sigma,i}^+} \left(1 - \gamma_i - \frac{(u_{i+1}-u_i)^2}{h_{\sigma,i}^- + h_{\sigma,i}^+} \right) \right]^{\frac{1}{2}} \sum_{j=m_i^-}^{i} \frac{\boldsymbol{e}_{n+j}}{(i-m_i^-+1)h_j} \\
& \mp \left[\frac{h_{\sigma,i}^- h_{\sigma,i}^+}{h_{\sigma,i}^- + h_{\sigma,i}^+} \left(1 - \gamma_i - \frac{(u_{i+1}-u_i)^2}{h_{\sigma,i}^- + h_{\sigma,i}^+} \right) \right]^{\frac{1}{2}} \sum_{j=i+1}^{m_i^+} \frac{\boldsymbol{e}_{n+j}}{(m_i^+-i)h_j} \\
& + \mathcal{O}(\varepsilon^{\frac{\sigma(i)+1}{2}}),
\end{aligned} \tag{4.26}$$

and the one of the associated left eigenvector is such that

$$\begin{aligned}
\boldsymbol{l}_{\boldsymbol{x}}^{\lambda_i^{\pm}}(\mathbf{u},\boldsymbol{\gamma}) = \;& \textstyle\sum_{j=m_i^-}^{i} \frac{{}^{\top}\boldsymbol{e}_{n+j}}{i-m_i^-+1} - \sum_{j=i+1}^{m_i^+} \frac{{}^{\top}\boldsymbol{e}_{n+j}}{m_i^+-i} \\
& + \frac{u_{i+1}-u_i}{h_{\sigma,i}^- + h_{\sigma,i}^+} \left(\sum_{j=m_i^-}^{i} \frac{h_{\sigma,i}^- {}^{\top}\boldsymbol{e}_j}{(i-m_i^-+1)h_j} + \sum_{j=i+1}^{m_i^+} \frac{h_{\sigma,i}^+ {}^{\top}\boldsymbol{e}_j}{(m_i^+-i)h_j} \right) \\
& \pm \left[\frac{h_{\sigma,i}^- h_{\sigma,i}^+}{h_{\sigma,i}^- + h_{\sigma,i}^+} \left(1 - \gamma_i - \frac{(u_{i+1}-u_i)^2}{h_{\sigma,i}^- + h_{\sigma,i}^+} \right) \right]^{\frac{1}{2}} \sum_{j=m_i^-}^{i} \frac{{}^{\top}\boldsymbol{e}_j}{(i-m_i^-+1)h_j} \\
& \mp \left[\frac{h_{\sigma,i}^- h_{\sigma,i}^+}{h_{\sigma,i}^- + h_{\sigma,i}^+} \left(1 - \gamma_i - \frac{(u_{i+1}-u_i)^2}{h_{\sigma,i}^- + h_{\sigma,i}^+} \right) \right]^{\frac{1}{2}} \sum_{j=i+1}^{m_i^+} \frac{{}^{\top}\boldsymbol{e}_j}{(m_i^+-i)h_j} \\
& + \mathcal{O}(\varepsilon^{\frac{\sigma(i)+1}{2}}).
\end{aligned} \tag{4.27}$$

Furthermore, under the same assumptions, the barotropic eigenstructure is such that

$$\begin{aligned}
\lambda_n^{\pm}(\mathbf{u},\boldsymbol{\gamma}) = \;& u_{m_\sigma^-} \pm \sqrt{H} + (u_{m_\sigma^-+1} - u_{m_\sigma^-}) \frac{h_{\sigma,m_\sigma^-}^+}{h_{\sigma,m_\sigma^-}^- + h_{\sigma,m_\sigma^-}^+} \\
& + \mathcal{O}\left(1 - \gamma_{m_\sigma^-}\right),
\end{aligned} \tag{4.28}$$

where $m_\sigma^- \in [\![1, n-1]\!]$ is defined by

$$\sigma(m_\sigma^-) = \min_{j \in [\![1,n-1]\!]} \sigma(j) = 1. \tag{4.29}$$

the asymptotic expansion of the associated right eigenvector is

$$\begin{aligned}
\boldsymbol{r}_{\boldsymbol{x}}^{\lambda_n^{\pm}}(\mathbf{u},\boldsymbol{\gamma}) = \;& \textstyle\sum_{k=1}^{n} \boldsymbol{e}_{n+k} \pm \frac{h_k}{\sqrt{H}} \boldsymbol{e_k} \\
& - \sum_{k=1}^{m_\sigma^-} \frac{(u_{m_\sigma^-+1} - u_{m_\sigma^-})}{\sqrt{H}} \left(\frac{2h_k}{\sqrt{H}} \boldsymbol{e}_k \pm \boldsymbol{e}_{n+k} \right) \\
& + \sum_{k=m_\sigma^-+1}^{n} \frac{(u_{m_\sigma^-+1} - u_{m_\sigma^-}) h_{\sigma,m_\sigma^-}^-}{\sqrt{H} h_{\sigma,m_\sigma^-}^+} \left(\frac{2h_k}{\sqrt{H}} \boldsymbol{e}_k \pm \boldsymbol{e}_{n+k} \right) \\
& + \mathcal{O}(1 - \gamma_{m_\sigma^-}),
\end{aligned} \tag{4.30}$$

and the asymptotic expansion of the associated right eigenvector is such that

$$\begin{aligned} \boldsymbol{l}_{\boldsymbol{x}}^{\lambda_n^{\pm}}(\mathbf{u},\boldsymbol{\gamma}) = \quad & \sum_{k=1}^{n} {}^{\top}\boldsymbol{e}_k \pm \frac{h_k}{\sqrt{H}}{}^{\top}\boldsymbol{e}_{n+k} \\ & - \sum_{k=1}^{m_\sigma^-} \frac{(u_{m_\sigma^-+1}-u_{m_\sigma^-})}{\sqrt{H}} \left(\frac{2h_k}{\sqrt{H}}{}^{\top}\boldsymbol{e}_{n+k} \pm {}^{\top}\boldsymbol{e}_k \right) \\ & + \sum_{k=m_\sigma^-+1}^{n} \frac{(u_{m_\sigma^-+1}-u_{m_\sigma^-})h^-_{\sigma,m_\sigma^-}}{\sqrt{H}h^+_{\sigma,m_\sigma^-}} \left(\frac{2h_k}{\sqrt{H}}{}^{\top}\boldsymbol{e}_{n+k} \pm {}^{\top}\boldsymbol{e}_k \right) \\ & + \mathcal{O}(1-\gamma_{m_\sigma^-}). \end{aligned} \tag{4.31}$$

Proposition 4.1.1 *Let* $(\mathbf{u},\boldsymbol{\gamma}) \in \mathbb{R}^{3n}\times]0,1[^{n-1}$, $\theta \in [0,2\pi]$, $\varepsilon > 0$ *and an injective function* $\sigma \in \mathbb{R}_+^{*\,[\![1,n-1]\!]}$ *such that* $\boldsymbol{\gamma}$ *verifies* (4.16) *and* $\mathbf{u}$ *verifies* (4.17).
Then, there exists $\delta > 0$ *such that if*

$$\varepsilon \leq \delta, \tag{4.32}$$

the matrix $\mathsf{A}(\mathbf{u},\boldsymbol{\gamma},\theta)$ *is diagonalizable with real eigenvalues if*

$$\begin{cases} h_i > 0, & \forall i \in [\![1,n]\!], \\ \phi_{\sigma,i}(\boldsymbol{h}) - |u_{i+1}-u_i|^2 - |v_{i+1}-v_i|^2 > 0, & \forall i \in [\![1,n-1]\!]. \end{cases} \tag{4.33}$$

Consequently, let $\boldsymbol{\gamma} \in]0,1[^{n-1}$, $\varepsilon > 0$ and an injective function $\sigma : [\![1,n-1]\!] \to \mathbb{R}_+^*$ such that $\boldsymbol{\gamma}$ verifies (4.16) and ε verifies (4.32). It was proved in the last chapter that the following subset contains hyperbolic initial condition:

$$\mathcal{H}_{\sigma,\varepsilon} := \left\{ \mathbf{u}^{\mathbf{0}} \in \mathcal{L}^2(\mathbb{R}^2)^{3n} / \ \forall X \in \mathbb{R}^2,\ \mathbf{u}^{\mathbf{0}}(X) \text{ verifies conditions (4.17) and (4.18)} \right\}, \tag{4.34}$$

and

Theorem 4.1.2 *Let* $s > 2$, $\boldsymbol{\gamma} \in]0,1[^{n-1}$, $\varepsilon > 0$ *and an injective function* $\sigma : [\![1,n-1]\!] \to \mathbb{R}_+^*$ *such that* $\boldsymbol{\gamma}$ *verifies* (4.16).
Then, there exists $\delta > 0$ *such that if*

$$\varepsilon \leq \delta, \tag{4.35}$$

the Cauchy *problem, associated with* (4.8) *and initial data* $\mathbf{u}^{\mathbf{0}} \in \mathcal{H}_{\sigma,\varepsilon} \cap \mathcal{H}^s(\mathbb{R}^2)^{3n}$, *is hyperbolic, locally well-posed in* $\mathcal{H}^s(\mathbb{R}^2)^{3n}$ *and the unique solution verifies*

$$\begin{cases} \mathbf{u} \in \mathcal{C}^1([0,T]\times\mathbb{R}^2)^{3n}, \\ \mathbf{u} \in \mathcal{C}([0,T];\mathcal{H}^s(\mathbb{R}^2))^{3n} \cap \mathcal{C}^1([0,T];\mathcal{H}^{s-1}(\mathbb{R}^2))^{3n}. \end{cases} \tag{4.36}$$

4.1.2 The augmented-model

Because of the non-conservative form of the system of equations (4.8), a new conservative model is introduced in the previous chapter. We denote $\mathbf{v} \in \mathcal{H}^s(\mathbb{R}^2)^{4n}$, the vectors defined by

$$\mathbf{v} := {}^{\top}(h_1,\dots,h_n,u_1,\dots,u_n,v_1,\dots,v_n,w_1,\dots,w_n), \tag{4.37}$$

where

$$\forall i \in [\![1,n-1]\!],\ w_i := \frac{\partial v_i}{\partial x} - \frac{\partial u_i}{\partial y} \tag{4.38}$$

is the horizontal vorticity of each layer.

If $\mathbf{u}$ is a classical solution of (4.8), then $\mathbf{v}$ is solution of the augmented system of equations

$$\frac{\partial \mathbf{v}}{\partial t} + \mathsf{A}^{\mathsf{a}}_x(\mathbf{v},\boldsymbol{\gamma})\frac{\partial \mathbf{v}}{\partial x} + \mathsf{A}^{\mathsf{a}}_y(\mathbf{v},\boldsymbol{\gamma})\frac{\partial \mathbf{v}}{\partial y} + \mathbf{b}^{\mathbf{a}}(\mathbf{v}) = 0, \tag{4.39}$$

where the $4n \times 4n$ block matrices $\mathsf{A}^{\mathsf{a}}_x(\mathbf{v},\boldsymbol{\gamma})$ and $\mathsf{A}^{\mathsf{a}}_y(\mathbf{v},\boldsymbol{\gamma})$ are defined by

$$\mathsf{A}^{\mathsf{a}}_x(\mathbf{v},\boldsymbol{\gamma}) := \left[\begin{array}{c|c|c|c} \mathsf{V}_x & \mathsf{H} & 0 & 0 \\ \hline \Gamma & \mathsf{V}_x & \mathsf{V}_y & 0 \\ \hline 0 & 0 & 0 & 0 \\ \hline 0 & \mathsf{W} & 0 & \mathsf{V}_x \end{array}\right], \tag{4.40}$$

$$\mathsf{A}^{\mathsf{a}}_y(\mathbf{v},\boldsymbol{\gamma}) := \left[\begin{array}{c|c|c|c} \mathsf{V}_y & 0 & \mathsf{H} & 0 \\ \hline 0 & 0 & 0 & 0 \\ \hline \Gamma & \mathsf{V}_x & \mathsf{V}_y & 0 \\ \hline 0 & 0 & \mathsf{W} & \mathsf{V}_y \end{array}\right], \tag{4.41}$$

with $\mathsf{W} := \mathrm{diag}[w_i + f]_{i\in[\![1,n]\!]}$; and $\mathbf{b}^{\mathbf{a}}(\mathbf{v})$ is defined by

$$\mathbf{b}^{\mathbf{a}}(\mathbf{v}) := \sum_{k=n+1}^{2n} \Big(-(w_k+f)v_k + \frac{\partial b}{\partial x}\Big)\boldsymbol{e}'_{\boldsymbol{k}} + \Big((w_k+f)u_k + \frac{\partial b}{\partial y}\Big)\boldsymbol{e}'_{n+k}, \tag{4.42}$$

where $(\boldsymbol{e}'_{\boldsymbol{i}})_{i\in[\![1,4n]\!]}$ denotes the canonical basis of $\mathbb{R}^{4n}$.

Remark: The quasi-linear system of partial differential equations (4.8) will be called the non-augmented model and the system (4.39) will be called the augmented model. In this paper, $\mathbf{u}$ will be always associated with the system (4.8) and $\mathbf{v}$ will be always associated with (4.39).

The augmented model (4.39) verifies also the rotational invariance: for all $(\mathbf{v},\boldsymbol{\gamma},\theta) \in \mathbb{R}^{4n} \times {\mathbb{R}^*_+}^{n-1} \times [0,2\pi]$, the $4n \times 4n$ matrix $\mathsf{A}^{\mathsf{a}}(\mathbf{v},\boldsymbol{\gamma},\theta) := \cos(\theta)\mathsf{A}^{\mathsf{a}}_x(\mathbf{v},\boldsymbol{\gamma}) + \sin(\theta)\mathsf{A}^{\mathsf{a}}_y(\mathbf{v},\boldsymbol{\gamma})$ verifies

$$\mathsf{A}^{\mathsf{a}}(\mathbf{v},\boldsymbol{\gamma},\theta) = \mathsf{P}^{\mathsf{a}}(\theta)^{-1}\mathsf{A}^{\mathsf{a}}_x(\mathsf{P}^{\mathsf{a}}(\theta)\mathbf{v},\boldsymbol{\gamma})\mathsf{P}^{\mathsf{a}}(\theta), \tag{4.43}$$

where $\mathsf{P}^{\mathsf{a}}(\theta)$ is the $4n \times 4n$ block matrix defined by

$$\mathsf{P}^{\mathsf{a}}(\theta) := \left[\begin{array}{c|c|c|c} \mathsf{I_n} & 0 & 0 & 0 \\ \hline 0 & \cos(\theta)\mathsf{I_n} & \sin(\theta)\mathsf{I_n} & 0 \\ \hline 0 & -\sin(\theta)\mathsf{I_n} & \cos(\theta)\mathsf{I_n} & 0 \\ \hline 0 & 0 & 0 & \mathsf{I_n} \end{array}\right]. \tag{4.44}$$

The augmented model has a *Friedrichs*-symmetrizer:

Theorem 4.1.3 *Let $s > 2$ and $(\mathbf{v}^{\mathbf{0}}, \boldsymbol{\gamma}) \in \mathcal{H}^s(\mathbb{R}^2)^{4n} \times]0,1[^{n-1}$ and $\boldsymbol{u_0} := (u_0, v_0) \in \mathbb{R}^2$ such that*

$$\begin{cases} \inf_{X\in\mathbb{R}^2} h_i^0(X) > 0, & \forall\, i \in [\![1,n]\!], \\ \inf_{X\in\mathbb{R}^2} \delta^a(\mathbf{v}^{\mathbf{0}}(X), \boldsymbol{\gamma}, \boldsymbol{u_0}) > 0, \end{cases} \tag{4.45}$$

where

$$\begin{aligned} \delta^a(\mathbf{v}, \boldsymbol{\gamma}, \boldsymbol{u_0}) := \quad & \min\left(a(\boldsymbol{h}, \boldsymbol{\gamma})^{-1}, \min_{i\in[\![1,n]\!]} h_i^2\right) \\ & - \max_{i\in[\![1,n]\!]} \alpha_{n,i}|u_i - u_0| - \max_{i\in[\![1,n]\!]} \alpha_{n,i}|v_i - v_0| \\ & + \min\left(0, \min_{i\in[\![1,n]\!]} \tfrac{w_i+f}{2}\left(w_i + f - \sqrt{(w_i+f)^2 + 4h_i^2}\right)\right), \end{aligned} \tag{4.46}$$

then, the mapping

$$\mathsf{S}^{\mathsf{a}} : (\mathbf{v}, \boldsymbol{\gamma}) \mapsto \mathsf{S}^{\mathsf{a}}(\mathbf{v}, \boldsymbol{\gamma}) := \left[\begin{array}{c|c|c|c} \Delta\Gamma + \mathsf{W}^2 & \Delta\mathsf{V}_x & \Delta\mathsf{V}_y & -\mathsf{WH} \\ \hline \Delta\mathsf{V}_x & \Delta\mathsf{H} & 0 & 0 \\ \hline \Delta\mathsf{V}_y & 0 & \Delta\mathsf{H} & 0 \\ \hline -\mathsf{WH} & 0 & 0 & \mathsf{H}^2 \end{array}\right], \tag{4.47}$$

is a Friedrichs-*symmetrizer around $\mathbf{v}^{\mathbf{0}}$; the* Cauchy *problem, associated with the system* (4.39) *and the initial data $\mathbf{v}^{\mathbf{0}}$, is hyperbolic, locally well-posed in $\mathcal{H}^s(\mathbb{R}^2)^{4n}$ and there exists $T > 0$ such that $\mathbf{v}$, the unique solution of the* Cauchy *problem, verifies*

$$\begin{cases} \mathbf{v} \in \mathcal{C}^1([0,T] \times \mathbb{R}^2)^{4n}, \\ \mathbf{v} \in \mathcal{C}([0,T]; \mathcal{H}^s(\mathbb{R}^2))^{4n} \cap \mathcal{C}^1([0,T]; \mathcal{H}^{s-1}(\mathbb{R}^2))^{4n}. \end{cases} \tag{4.48}$$

Moreover, we define the spectrum of $\mathsf{A}_x^{\mathsf{a}}(\mathbf{v}, \boldsymbol{\gamma})$ by

$$\sigma(\mathsf{A}_x^{\mathsf{a}}(\mathbf{v}, \boldsymbol{\gamma})) := \left(\lambda_i^{\pm}(\mathbf{v}, \boldsymbol{\gamma})\right)_{i\in[\![1,n]\!]} \cup \left(\lambda_{2n+i}(\mathbf{v}, \boldsymbol{\gamma})\right)_{i\in[\![1,2n]\!]}, \tag{4.49}$$

and the right and left eigenvectors of $\mathsf{A}_x^{\mathsf{a}}(\mathbf{v}, \boldsymbol{\gamma})$, associated with the eigenvalue $\lambda \in \sigma(\mathsf{A}_x^{\mathsf{a}}(\mathbf{v}, \boldsymbol{\gamma}))$, are respectively defined by $\boldsymbol{r}_{\boldsymbol{x}}^{\lambda}(\mathbf{v}, \boldsymbol{\gamma})$ and $\boldsymbol{l}_{\boldsymbol{x}}^{\lambda}(\mathbf{v}, \boldsymbol{\gamma})$. Then, according to the structure of $\mathsf{A}_x^{\mathsf{a}}(\mathbf{v}, \boldsymbol{\gamma})$, it is obvious that

$$\left(\lambda_i^{\pm}(\mathbf{v}, \boldsymbol{\gamma})\right)_{i\in[\![1,n]\!]} \cup \left(\lambda_{2n+i}(\mathbf{v}, \boldsymbol{\gamma})\right)_{i\in[\![1,n]\!]} = \sigma(\mathsf{A}_x(\mathbf{u}, \boldsymbol{\gamma})) \tag{4.50}$$

and

$$\forall i \in [\![1,n]\!],\ \lambda_{3n+i}(\mathbf{v}, \boldsymbol{\gamma}) = 0. \tag{4.51}$$

Moreover, according to the rotational invariance (4.43), the spectrum of $\mathsf{A}^{\mathsf{a}}(\mathbf{v}, \boldsymbol{\gamma}, \theta)$ is such that for all $(\mathbf{v}, \boldsymbol{\gamma}, \theta) \in \mathbb{R}^{4n} \times \mathbb{R}_+^{*\,n-1} \times [0, 2\pi]$,

$$\begin{aligned} \sigma(\mathsf{A}^{\mathsf{a}}(\mathbf{v}, \boldsymbol{\gamma}, \theta)) \quad & = \sigma(\mathsf{A}_x^{\mathsf{a}}(\mathsf{P}(\theta)\mathbf{v}, \boldsymbol{\gamma})) \\ & = \sigma(\mathsf{A}_x(\mathsf{P}(\theta)\mathbf{v}, \boldsymbol{\gamma})) \cup \{0\}. \end{aligned} \tag{4.52}$$

and the right and left eigenvectors of $\mathsf{A}(\mathbf{v},\boldsymbol{\gamma},\theta)$, associated with the eigenvalue $\lambda \in \sigma(\mathsf{A}^{\mathsf{a}}(\mathbf{v},\boldsymbol{\gamma},\theta))$, are consequently defined by

$$\begin{cases} \boldsymbol{r}^{\lambda}(\mathbf{v},\boldsymbol{\gamma},\theta) = \mathsf{P}^{\mathsf{a}\,-1}(\theta)\boldsymbol{r}_{\boldsymbol{x}}^{\lambda}(\mathsf{P}^{\mathsf{a}}(\theta)\mathbf{v},\boldsymbol{\gamma}), \\ \boldsymbol{l}^{\lambda}(\mathbf{v},\boldsymbol{\gamma},\theta) = \boldsymbol{l}_{\boldsymbol{x}}^{\lambda}(\mathsf{P}^{\mathsf{a}}(\theta)\mathbf{v},\boldsymbol{\gamma})\mathsf{P}^{\mathsf{a}}(\theta). \end{cases} \tag{4.53}$$

Moreover, a part of the eigenstructure of $\mathsf{A}_x^a(\mathbf{v},\boldsymbol{\gamma})$ is explicit: for all $(\mathbf{v},\boldsymbol{\gamma})\mathbb{R}^{4n} \times \mathbb{R}_+^{*\,n-1}$ and for all $i \in [\![1,n]\!]$,:

$$\begin{cases} \boldsymbol{r}_{\boldsymbol{x}}^{\lambda_{2n+i}}(\mathbf{v},\boldsymbol{\gamma}) = \boldsymbol{e}'_{3n+i}, \\ \boldsymbol{l}_{\boldsymbol{x}}^{\lambda_{2n+i}}(\mathbf{v},\boldsymbol{\gamma}) = -(w_i+f)^{\top}\boldsymbol{e}'_i + h_i{}^{\top}\boldsymbol{e}'_{3n+i}, \end{cases} \tag{4.54}$$

$$\boldsymbol{r}_x^{\lambda_{3n+i}}(\mathbf{v},\boldsymbol{\gamma}) = \begin{cases} (\Gamma \mathsf{V}_y \boldsymbol{e_i}\cdot\boldsymbol{e_i})\boldsymbol{e}'_i - (\mathsf{V}_x\mathsf{H}^{-1}\Gamma^{-1}\mathsf{V}_y\boldsymbol{e_i}\cdot\boldsymbol{e_i})\boldsymbol{e}'_{n+i} \\ -((\mathsf{I_n} - \mathsf{V}_x^2\mathsf{H}^{-1}\Gamma^{-1})\mathsf{V}_y\boldsymbol{e_i}\cdot\boldsymbol{e_i})\boldsymbol{e}'_{2n+i} \\ +(\mathsf{W}\mathsf{H}^{-1}\Gamma^{-1}\mathsf{V}_y\boldsymbol{e_i}\cdot\boldsymbol{e_i})\boldsymbol{e}'_{3n+i} \end{cases}, \quad \text{if } v_i \neq 0, \\ \boldsymbol{e}'_{2n+i}, \qquad \text{if } v_i = 0, \tag{4.55}$$

and

$$\boldsymbol{l}_x^{\lambda_{3n+i}}(\mathbf{v},\boldsymbol{\gamma}) = {}^{\top}\boldsymbol{e}'_{2n+i}. \tag{4.56}$$

Moreover, for all $i \in [\![1,n]\!]$, the right eigenvector, associated with $\lambda \in \sigma(\mathsf{A}_x^{\mathsf{a}}(\mathbf{v},\boldsymbol{\gamma}))$, is such that

$$\boldsymbol{r}_x^{\lambda_i^{\pm}}(\mathbf{v},\boldsymbol{\gamma}) = \boldsymbol{r}_x^{\lambda_i^{\pm}}(\mathbf{u},\boldsymbol{\gamma}) + \sum_{k=1}^{n} \frac{w_k+f}{\lambda_i^{\pm}-u_k}(\boldsymbol{r}_x^{\lambda_i^{\pm}}(\mathbf{u},\boldsymbol{\gamma})\cdot\boldsymbol{e}_{n+k})\boldsymbol{e}'_{3n+k}, \tag{4.57}$$

and the left one is such that

$$\boldsymbol{l}_x^{\lambda_i^{\pm}}(\mathbf{v},\boldsymbol{\gamma}) = \boldsymbol{l}_x^{\lambda_i^{\pm}}(\mathbf{u},\boldsymbol{\gamma}) + \sum_{k=1}^{n} \frac{v_k}{\lambda_i^{\pm}}({}^{\top}\boldsymbol{l}_x^{\lambda_i^{\pm}}(\mathbf{u},\boldsymbol{\gamma})\cdot\boldsymbol{e}_{n+k})^{\top}\boldsymbol{e}'_{2n+k}. \tag{4.58}$$

Remark: We made intentionally a mistake in (4.57) and (4.58), as we did not provide the expression of $\boldsymbol{r}_x^{\lambda_i^{\pm}}(\mathbf{u},\boldsymbol{\gamma})$ and $\boldsymbol{l}_x^{\lambda_i^{\pm}}(\mathbf{u},\boldsymbol{\gamma})$, but it is the natural expression coming from (4.30), (4.31), (4.26) and (4.27) and replacing $\boldsymbol{e}_i$ by $\boldsymbol{e}'_i$, for every $i \in [\![1,3n]\!]$.

Finally, under assumptions (4.16–4.17) and (4.62), the other part of the eigenstructure is known: the eigenvalues of $\mathsf{A}^{\mathsf{a}}(\mathbf{v},\boldsymbol{\gamma},\theta)$ are given by (4.25) and (4.28) and the eigenvectors (4.57–4.58) are characterized, using (4.26–4.30).

Finally, there is the next proposition, about the diagonalizability of $\mathsf{A}^{\mathsf{a}}(\mathbf{v},\boldsymbol{\gamma},\theta)$:

Proposition 4.1.4 *Let* $(\mathbf{v},\boldsymbol{\gamma}) \in \mathbb{R}^{4n}\times]0,1[^{n-1}$, $\theta \in [0,2\pi]$, $\varepsilon > 0$ *and an injective function* $\sigma \in \mathbb{R}_+^{*\,[\![1,n-1]\!]}$ *such that* $\boldsymbol{\gamma}$ *verifies* (4.16) *and the associated vector* $\mathbf{u}$ *verifies* (4.17).
There exists $\delta > 0$ *such that if*

$$\varepsilon \leq \delta, \tag{4.59}$$

then the matrix $\mathsf{A}^{\mathsf{a}}(\mathbf{v},\boldsymbol{\gamma},\theta)$ *is diagonalizable with real eigenvalues if the associated vector,* $\mathbf{u}$*, verifies*

$$\begin{cases} h_i > 0, & \forall i \in [\![1,n]\!], \\ \phi_{\sigma,i}(\boldsymbol{h}) - |u_{i+1}-u_i|^2 - |v_{i+1}-v_i|^2 > 0, & \forall i \in [\![1,n-1]\!]. \end{cases} \tag{4.60}$$

where $\phi_{\sigma,i}(\boldsymbol{h}) := (h_{\sigma,i}^- + h_{\sigma,i}^+)(1-\gamma_i)$.

As it was proved in the last chapter, defining the next subset of $\mathcal{L}^2(\mathbb{R}^2)^{4n}$:

$$\mathcal{H}^a_{\sigma,\varepsilon} := \left\{ \mathbf{v^0} \in \mathcal{L}^2(\mathbb{R}^2)^{4n} / \ \mathbf{u^0} \in \mathcal{H}_{\sigma,\varepsilon} \right\} \tag{4.61}$$

Theorem 4.1.5 *Let $s > 2$, $\boldsymbol{\gamma} \in]0,1[^{n-1}$, $\varepsilon > 0$ and an injective function $\sigma : [\![1, n-1]\!] \to \mathbb{R}^*_+$ such that $\boldsymbol{\gamma}$ verifies (4.16).*
Then, there exists $\delta > 0$ such that if

$$\varepsilon \leq \delta, \tag{4.62}$$

the Cauchy *problem, associated with (4.39) and initial data $\mathbf{v^0} \in \mathcal{H}^a_{\sigma,\varepsilon} \cap \mathcal{H}^s(\mathbb{R}^2)^{4n}$, is hyperbolic, locally well-posed in $\mathcal{H}^s(\mathbb{R}^2)^{4n}$ and there exists $T > 0$ such that $\mathbf{v}$, the unique solution of the* Cauchy *problem, verifies*

$$\begin{cases} \mathbf{v} \in \mathcal{C}^1([0,T] \times \mathbb{R}^2)^{4n}, \\ \mathbf{v} \in \mathcal{C}([0,T]; \mathcal{H}^s(\mathbb{R}^2))^{4n} \cap \mathcal{C}^1([0,T]; \mathcal{H}^{s-1}(\mathbb{R}^2))^{4n}. \end{cases} \tag{4.63}$$

Furthermore, $\mathbf{u}$, the associated vector field, verifies conditions (4.36) and is the unique classical solution of the Cauchy *problem, associated with (4.8) and initial data $\mathbf{u^0} \in \mathcal{H}_{\sigma,\varepsilon} \cap \mathcal{H}^s(\mathbb{R}^2)^{3n}$, if and only if*

$$\forall i \in [\![1,n]\!], \ w_i^0 = \frac{\partial v_i^0}{\partial x} - \frac{\partial u_i^0}{\partial y}. \tag{4.64}$$

To sum up, the new augmented model has the same properties of local well-posedness as the non-augmented one, plus the *Friedrichs*-symmetrizer; the two solutions are equal, if the compatibility condition (4.64) is verified. Therefore, as the conservativity is a very interesting property for numerical approximation, we will work, in this paper, mostly with the augmented model (4.39).

4.2 Well-posedness of the initial-boundary value problem

In this section, we remind useful definitions in order to prove a theorem which provides well-posed boundary conditions to the augmented multi-layer shallow water model. First, we give criterion of strong well-posedness, based on the energy method. Then, we bring out the right boundary conditions to provide on the augmented model, in a general limited domain. Finally, we explain it in a particular domain: a rectangular domain.

4.2.1 The energy method

In order to derive well-posed boundary conditions, we need to define the well-posedness of an initial-boundary value problem such as the augmented multi-layer shallow water problem (4.39), in a limited

domain $\mathcal{D}$. First, we consider a linear initial-boundary value problem on the domain $\mathcal{D}$, with smooth boundary $\partial\mathcal{D}$:

$$\begin{cases} \frac{\partial \mathbf{w}}{\partial t}(t,X) + \mathsf{L}\mathbf{w}(t,X) + \mathsf{C}\mathbf{w}(t,X) = 0, & \forall X \in \mathcal{D}, \quad \forall t \geq 0, \\ \mathsf{B}(X)\mathbf{w}(t,X) = \mathbf{g}(t,X), & \forall X \in \partial\mathcal{D}, \quad \forall t \geq 0, \\ \mathbf{w}(t,X) = \mathbf{w^0}(X), & \forall X \in \mathcal{D}, \quad t = 0, \end{cases} \tag{4.65}$$

where $\mathbf{w} : \mathbb{R}_+^* \times \mathbb{R}^2 \to \mathbb{R}^m$ is the solution, $\mathsf{L} := \mathsf{A}_x \frac{\partial}{\partial x} + \mathsf{A}_y \frac{\partial}{\partial y} \in \mathcal{M}_m(\mathbb{R})$ is a symmetric spatial differential operator, $\mathsf{B} \in \mathcal{M}_{p\times m}(\mathbb{R})$ is the boundary operator — with $p := \text{rank } \mathsf{B}$ — and $\mathsf{C} \in \mathcal{M}_m(\mathbb{R})$ is a constant operator such that

$$\forall \mathbf{w} \in \mathbb{R}^m, \ {}^\top\mathbf{w}\mathsf{C}\mathbf{w} = 0. \tag{4.66}$$

Moreover, $\mathbf{g} \in \mathcal{L}^2(\mathbb{R}_+ \times \partial\mathcal{D})^m$ is the boundary function and $\mathbf{w^0} \in \mathcal{L}^2(\mathcal{D})^m$ is the initial function; these two functions are the known data of the problem (4.65). In this paper, L, C and B are assumed linear operators.

We denote by $(\,\cdot\,)$ and $||\,||$, respectively, the canonical inner product and canonical norm on the space of functions in $\mathcal{L}^2(\mathcal{D})^m$:

$$\forall (\mathbf{v_1}, \mathbf{v_2}), \ \begin{cases} (\mathbf{v_1} \cdot \mathbf{v_2}) := \int_{\mathcal{D}} {}^\top\mathbf{v_1}\mathbf{v_2} dxdy, \\ ||\mathbf{v_1}|| := (\mathbf{v_1} \cdot \mathbf{v_1})^{\frac{1}{2}}. \end{cases} \tag{4.67}$$

The energy method is a technique which consists in bounding $\frac{\partial ||\mathbf{w}(t,\cdot)||}{\partial t}$ and consequently $||\mathbf{w}(t,\cdot)||$, for all $t \geq 0$. Hereinafter, we give definitions to get a practical characterization of the well-posedness of (4.65) — see more details in [108], [56], [57] or more generally in [12].

Definition The boundary operator B is onto if and only if

$$\forall \mathbf{g} \in \mathcal{L}^2(\mathbb{R}_+ \times \partial\mathcal{D})^p, \ \exists \mathbf{w} \in \mathcal{L}^2(\mathbb{R}_+ \times \mathcal{D})^m, \ \mathsf{B}\mathbf{w} = \mathbf{g}. \tag{4.68}$$

We define for all $X \in \partial\mathcal{D}$,

$$\mathsf{L}(\theta) := \cos(\theta)\mathsf{A}_x + \sin(\theta)\mathsf{A}_y, \tag{4.69}$$

where

$$\mathbf{n}(X) := {}^\top(\cos(\theta), \sin(\theta)) \tag{4.70}$$

is the outward unit normal vector field to $\partial\mathcal{D}$ at X. In the following study, we will always associate $\theta \in [0, 2\pi]$ with the vector $\mathbf{n}(X)$, defined in (4.70).

Definition Assuming, for every $X \in \partial\mathcal{D}$, $\mathsf{L}(\theta)$ is symmetric non-singular and C verifies (4.66); we say the boundary operator B is strictly dissipative if the three properties below hold:

1. $\mathsf{L}(\theta)$ is positive-definite on $\ker \mathsf{B}$:

$$\forall X \in \partial\mathcal{D}, \forall \mathbf{w} \in \ker \mathsf{B}(X) \setminus \{0\},\ (\mathsf{L}(\theta)\mathbf{w}\cdot\mathbf{w}) > 0,$$

2. $\ker \mathsf{B}$ is maximal for the above property,

3. B is onto.

If B is strictly dissipative, the dimension of $\ker \mathsf{B}(X)$ equals the number of positive eigenvalues of $\mathsf{L}(\theta)$, and since $\mathsf{B}(X)$ is onto, it implies that $p(X)$, the rank of $\mathsf{B}(X)$, equals the number of negative eigenvalues of $\mathsf{L}(\theta)$.

Remark: The interpretation of this last assertion is quite easy because to evaluate the characteristics quantity q on $\partial\mathcal{D}$, the value just above $\partial\mathcal{D}$ is necessary if the characteristics is incoming, while it is not when it is going out.

Then, we have the next theorem — see in [12] for more details:

Theorem 4.2.1 *We assume* L *is symmetric and* B *is strictly dissipative. Then, for every data* $\mathbf{w^0} \in \mathcal{L}^2(\mathcal{D})^m$ *and* $\mathbf{g} \in \mathcal{L}^2((0,T)\times\partial\mathcal{D})^m$*, there exists a unique solution of the initial-boundary value problem* (4.65) $\mathbf{w} \in \mathcal{L}^2((0,T)\times\mathcal{D})^m \cap \mathcal{C}\big([0,T];\mathcal{L}^2(\mathcal{D})\big)^m$

Remark: In the more general case of a non-linear problem, the proof of the well-posedness of the initial-boundary value problem is based on the well-posedness of the associated linearized problem with constant coefficients, as it is detailed in [70] and [128]: using the localization principle, it can be proved that if all frozen coefficient problems are well-posed then the associate variable-coefficient problem is also well-posed; using the linearization principle one can state that if all the linear problems — which are obtained by linearizing around a solution $\mathbf{v}$ — are well-posed, then the associate non-linear problem is well-posed at $\mathbf{v}$. This is why we study, in this paper, the well-posedness of the linear initial-boundary value problem (4.65), with constant coefficients.

4.2.2 Well-posed boundary conditions for the augmented model

We consider the linearized augmented multi-layer shallow water model, with constant coefficients, and give conditions of well-posedness of the initial-boundary value problem associated.

Let $(\mathbf{v},\boldsymbol{\gamma}) \in \mathbb{R}^{4n} \times \mathbb{R}_+^{n-1}$ such that there exist $(\sigma,\varepsilon) \in \mathbb{R}^{[\![1,n-1]\!]} \times \mathbb{R}_+^*$, assumptions (4.16–4.17) are verified, ε sufficiently small and

$$\begin{cases} h_i > 0, & \forall i \in [\![1,n]\!], \\ \phi_{\sigma,i}(\boldsymbol{h}) - |u_{i+1}-u_i|^2 - |v_{i+1}-v_i|^2 > 0, & \forall i \in [\![1,n-1]\!], \\ \delta^a(\mathbf{v},\boldsymbol{\gamma},\boldsymbol{u_0}) > 0, \end{cases} \tag{4.71}$$

where $\boldsymbol{u_0} := \frac{1}{H}\sum_{i=1}^{n} h_i{}^{\top}(u_i, v_i)$. Then, we consider the following problem:

$$\begin{cases} \frac{\partial \tilde{\mathbf{v}}}{\partial t} + \mathsf{A}^{\mathsf{a}}_x(\mathbf{v},\boldsymbol{\gamma})\frac{\partial \tilde{\mathbf{v}}}{\partial x} + \mathsf{A}^{\mathsf{a}}_y(\mathbf{v},\boldsymbol{\gamma})\frac{\partial \tilde{\mathbf{v}}}{\partial y} + \mathsf{C}^{\mathsf{a}}(\mathbf{v})\tilde{\mathbf{v}} = 0, & \forall X \in \mathcal{D}, \quad \forall t \geq 0, \\ \mathsf{B}^{\mathsf{a}}(\mathbf{v},\boldsymbol{\gamma},\theta)\tilde{\mathbf{v}} = \mathbf{g}, & \forall X \in \partial\mathcal{D}, \quad \forall t \geq 0, \\ \tilde{\mathbf{v}} = \tilde{\mathbf{v}}^{\mathbf{0}}, & \forall X \in \mathcal{D}, \quad t = 0, \end{cases} \tag{4.72}$$

where $\mathsf{A}^{\mathsf{a}}_x(\mathbf{v},\boldsymbol{\gamma})$ and $\mathsf{A}^{\mathsf{a}}_y(\mathbf{v},\boldsymbol{\gamma})$ are defined in (4.40–4.41), $\mathsf{C}^{\mathsf{a}}(\mathbf{v})$ is defined by

$$\forall \mathbf{v} \in \mathbb{R}^{4n}, \ \mathsf{C}^{\mathsf{a}}(\mathbf{v}) := \left[\begin{array}{c|c|c|c} 0 & 0 & 0 & 0 \\ \hline 0 & 0 & -\mathsf{W} & -\mathsf{V}_y \\ \hline 0 & \mathsf{W} & 0 & \mathsf{V}_x \\ \hline 0 & 0 & 0 & 0 \end{array}\right], \tag{4.73}$$

$\mathbf{g} \in \mathcal{L}^2((0,T)\times\partial\mathcal{D})^{4n}$ and $\tilde{\mathbf{v}}^{\mathbf{0}} \in \mathcal{L}^2(\mathcal{D})^{4n}$. Moreover, $\mathsf{B}^{\mathsf{a}}(\mathbf{v},\boldsymbol{\gamma},\theta)$ is the boundary operator and will be defined below, in order to obtain a well-posed initial-boundary value problem. We denote by $p(\theta)$ the number of negative eigenvalues of the matrix $\mathsf{A}^{\mathsf{a}}(\mathbf{v},\boldsymbol{\gamma},\theta) =: \mathsf{L}(\theta)$.

Theorem 4.2.2 *Let $(\mathbf{v},\boldsymbol{\gamma},\sigma,\varepsilon) \in \mathbb{R}^{4n}\times\mathbb{R}^{n-1}_{+}\times\mathbb{R}^{[\![1,n-1]\!]}\times\mathbb{R}^{*}_{+}$ such that ε is sufficiently small and assumptions (4.16–4.17) and (4.71) are verified. For every $\mathbf{v}^{\mathbf{0}} \in \mathcal{L}^2((0,T)\times\mathcal{D})^{4n}$ and $\mathbf{g} \in \mathcal{L}^2((0,T)\times\partial\mathcal{D})^{4n}$, then the initial-boundary value problem (4.72), with $\mathsf{B}^{\mathsf{a}}(\mathbf{v},\boldsymbol{\gamma},\theta)$ such that*

$$\mathsf{B}^{\mathsf{a}}(\mathbf{v},\boldsymbol{\gamma},\theta) := [\boldsymbol{l}^{\lambda}(\mathbf{v},\boldsymbol{\gamma},\theta)]_{\lambda\in\sigma(\mathsf{A}^{\mathsf{a}}(\mathbf{v},\boldsymbol{\gamma},\theta))\cap\mathbb{R}^{*}_{-}}, \tag{4.74}$$

is well-posed in $\mathcal{L}^2((0,T)\times\mathcal{D})^{4n}$.

Proof Let $(\mathbf{v},\boldsymbol{\gamma},\sigma,\varepsilon,\mathbf{v}^{\mathbf{0}},\mathbf{g}) \in \mathbb{R}^{4n}\times\mathbb{R}^{n-1}_{+}\times\mathbb{R}^{[\![1,n-1]\!]}\times\mathbb{R}^{*}_{+}\times\mathcal{L}^2((0,T)\times\mathcal{D})^{4n}\times\mathcal{L}^2((0,T)\times\partial\mathcal{D})^{4n}$ such that ε is sufficiently small and assumptions (4.16–4.17) and (4.71) are verified. As the augmented model is *Friedrichs*-symmetrizable, we multiply the 1st equation of (4.72) by $\mathsf{S}^{\mathsf{a}}(\mathbf{v}^{\mathbf{0}},\boldsymbol{\gamma})^{\frac{1}{2}}$ to obtain a symmetric problem, as (4.65), with $m = 4n$ and

$$\begin{cases} \tilde{\mathbf{w}} & := \mathsf{S}^{\mathsf{a}}(\mathbf{v},\boldsymbol{\gamma})^{\frac{1}{2}}\tilde{\mathbf{v}}, \\ \mathsf{L} & := \mathsf{S}^{\mathsf{a}}(\mathbf{v},\boldsymbol{\gamma})^{\frac{1}{2}}\big(\mathsf{A}^{\mathsf{a}}_x(\mathbf{v},\boldsymbol{\gamma})\frac{\partial}{\partial x} + \mathsf{A}^{\mathsf{a}}_y(\mathbf{v},\boldsymbol{\gamma})\frac{\partial}{\partial y}\big)\mathsf{S}^{\mathsf{a}}(\mathbf{v},\boldsymbol{\gamma})^{-\frac{1}{2}}, \\ \mathsf{C} & := \mathsf{S}^{\mathsf{a}}(\mathbf{v},\boldsymbol{\gamma})^{\frac{1}{2}}\mathsf{C}^{\mathsf{a}}(\mathbf{v})\mathsf{S}^{\mathsf{a}}(\mathbf{v},\boldsymbol{\gamma})^{-\frac{1}{2}}. \end{cases} \tag{4.75}$$

According to the proposition 4.1.4, the matrix $\mathsf{A}^{\mathsf{a}}(\mathbf{v},\boldsymbol{\gamma},\theta)$ is diagonalizable with real eigenvalues and the vectors $({}^{\top}\boldsymbol{l}^{\lambda}(\mathbf{v},\boldsymbol{\gamma},\theta))_{\lambda\in\sigma(\mathsf{A}^{\mathsf{a}}(\mathbf{v},\boldsymbol{\gamma},\theta))}$ constitute an eigenbasis of $\mathbb{R}^{4n}$. Moreover, as the matrix $\mathsf{S}^{\mathsf{a}}(\mathbf{v},\boldsymbol{\gamma})\mathsf{A}^{\mathsf{a}}(\mathbf{v},\boldsymbol{\gamma},\theta))$ is real symmetric, then the matrix

$$\mathsf{R}(\mathbf{v},\boldsymbol{\gamma},\theta) := [\boldsymbol{l}^{\lambda}(\mathbf{v},\boldsymbol{\gamma},\theta)\mathsf{S}^{\mathsf{a}}(\mathbf{v},\boldsymbol{\gamma})^{-\frac{1}{2}}]_{\lambda\in\sigma(\mathsf{A}^{\mathsf{a}}(\mathbf{v},\boldsymbol{\gamma},\theta))}, \tag{4.76}$$

is reversible in $\mathcal{M}_{4n}(\mathbb{R})$ and

$$\mathsf{R}(\mathbf{v},\boldsymbol{\gamma},\theta)^{-1} = {}^{\top}\mathsf{R}(\mathbf{v},\boldsymbol{\gamma},\theta). \tag{4.77}$$

Consequently, it is clear the boundary operator (4.74) is onto. Moreover, one can verify that it is also strictly dissipative and

$$\forall \tilde{\mathbf{w}} \in \mathbb{R}^{4n},\ {}^{\top}\tilde{\mathbf{w}}\mathsf{S}^{\mathsf{a}}(\mathbf{v},\boldsymbol{\gamma})^{\frac{1}{2}}\mathsf{C}^{\mathsf{a}}(\mathbf{v})\mathsf{S}^{\mathsf{a}}(\mathbf{v},\boldsymbol{\gamma})^{-\frac{1}{2}}\tilde{\mathbf{w}} = 0. \tag{4.78}$$

Then, applying the theorem 4.2.1, to get a well-posed initial-boundary value problem, we need to require conditions for all the incoming characteristics of the linear spatial differential operator L, defined in (4.75):

$$\forall \lambda \in \sigma(\mathsf{A}^{\mathsf{a}}(\mathbf{v},\boldsymbol{\gamma},\theta)) \cap \mathbb{R}^{*}_{-},\ \boldsymbol{l}^{\lambda}(\mathbf{v},\boldsymbol{\gamma},\theta)\mathsf{S}^{\mathsf{a}}(\mathbf{v},\boldsymbol{\gamma})^{-\frac{1}{2}}\tilde{\mathbf{w}} = \mathbf{g_i}, \tag{4.79}$$

and according to the expression of $\mathbf{w}$ in (4.75), it is equivalent to

$$\forall \lambda \in \sigma(\mathsf{A}^{\mathsf{a}}(\mathbf{v},\boldsymbol{\gamma},\theta)) \cap \mathbb{R}^{*}_{-},\ \boldsymbol{l}^{\lambda}(\tilde{\mathbf{v}},\boldsymbol{\gamma},\theta)\tilde{\mathbf{v}} = \mathbf{g_i}, \tag{4.80}$$

and the theorem is proved.

Remark: For every eigenvalue $\lambda \in \sigma(\mathsf{A}^{\mathsf{a}}(\mathbf{v},\boldsymbol{\gamma},\theta))$, the quantity $\boldsymbol{l}^{\lambda}(\mathbf{v},\boldsymbol{\gamma},\theta)\tilde{\mathbf{v}}$ is called the *Riemann* invariant associated with λ.
In order to get a more convenient characterization, we give new definitions on the type of flows at the boundary, for each surface. First we give the definition for the free surface:

Definition Let $\mathbf{v} \in \mathbb{R}^{4n}$, $t \geq 0$ and $X \in \partial\mathcal{D}$. The free surface is called inflow type at (t,X) if

$$\bar{u}(\theta) := \cos(\theta)\bar{u} + \sin(\theta)\bar{v} < 0, \tag{4.81}$$

and outflow type otherwise. Moreover, it is called subcritical at (t,X) if

$$\bar{u}(\theta)^2 < gH, \tag{4.82}$$

and supercritical otherwise.

Then, we give the definition for the interfaces:

Definition Let $\mathbf{v} \in \mathbb{R}^{4n}$, $i \in [\![1, n-1]\!]$, $t \geq 0$ and $X \in \partial\mathcal{D}$. The interface i is called inflow type at (t,X) if

$$u_i(\theta) := \cos(\theta)u_i + \sin(\theta)v_i < 0, \tag{4.83}$$

and outflow type otherwise. Moreover, it is called subcritical at (t,X) if

$$u_i(\theta)^2 h^{+}_{\sigma,i} + u_{i+1}(\theta)^2 h^{-}_{\sigma,i} < h^{+}_{\sigma,i} h^{-}_{\sigma,i}(1-\gamma_i), \tag{4.84}$$

and supercritical otherwise.

The definition of the type of flow, for the free surface, is similar to the one given in the single-layer model. The definition of the inflow type (4.83), at the interface $i \in [\![1, n-1]\!]$, is also natural as it characterizes if the eigenvalue $u_i(\theta)$ is negative or not, at the boundary. However, it is important to understand the condition (4.84). According to (4.50) and the asymptotic expansions of the spectrum of $\mathsf{A}(\mathbf{u}, \boldsymbol{\gamma}, \theta)$, in (4.25), we have for every $i \in [\![1, n-1]\!]$, the eigenvalues associated with the interface i are 0, $u_i(\theta)$ and

$$\begin{aligned}\lambda_i^{\pm}(\mathbf{v}, \boldsymbol{\gamma}, \theta) = \quad & \cos(\theta)\tfrac{u_{i+1}h^-_{\sigma,i}+u_i h^+_{\sigma,i}}{h^-_{\sigma,i}+h^+_{\sigma,i}} + \sin(\theta)\tfrac{v_{i+1}h^-_{\sigma,i}+v_i h^+_{\sigma,i}}{h^-_{\sigma,i}+h^+_{\sigma,i}} \\ & \pm \left[\tfrac{h^-_{\sigma,i}h^+_{\sigma,i}}{(h^-_{\sigma,i}+h^+_{\sigma,i})}\left(1-\gamma_i - \tfrac{(\cos(\theta)(u_{i+1}-u_i)+\sin(\theta)(v_{i+1}-v_i))^2}{h^-_{\sigma,i}+h^+_{\sigma,i}}\right)\right]^{\frac{1}{2}} \\ & + \mathcal{O}(\varepsilon^{\frac{\sigma(i)+1}{2}}).\end{aligned} \tag{4.85}$$

Then, if we forget the term $\mathcal{O}(\varepsilon^{\frac{\sigma(i)+1}{2}})$, one can prove that the condition (4.84) is verified if and only if

$$\lambda_i^+(\mathbf{v}, \boldsymbol{\gamma}, \theta)\lambda_i^-(\mathbf{v}, \boldsymbol{\gamma}, \theta) < 0. \tag{4.86}$$

Remarks: 1) It is clear that if the free surface is inflow type, then it is subcritical. However, an interface which is inflow type, is possibly subcritical or supercritical, as there is no simple correlation between the inequalities (4.83) and (4.84). 2) We could have defined the inflow or outflow type on the layer i, instead of the interface i, as it could appear more natural to characterize the fluid instead of the surface; however, we preferred to define it on the interface i, as the condition (4.84) is deeply attached to this interface, as it takes into account the parameters of the layer i and $i+1$ — and not just the layer i.

We deduce the next corollary from the theorem 4.2.2,

Corollary 4.2.3 *Let $(\mathbf{v}, \boldsymbol{\gamma}, \sigma, \varepsilon) \in \mathbb{R}^{4n} \times \mathbb{R}_+^{n-1} \times \mathbb{R}^{[\![1,n-1]\!]} \times \mathbb{R}_+^*$ such that ε is sufficiently small and assumptions (4.16–4.17) and (4.71) are verified. For every $\mathbf{v}^{\mathbf{0}} \in \mathcal{L}^2((0,T)\times\mathcal{D})^{4n}$ and $\mathbf{g} \in \mathcal{L}^2((0,T)\times\partial\mathcal{D})^{4n}$, the initial-boundary value problem (4.72) is $\mathcal{L}^2$-well-posed if we provide the following number of boundary conditions at $(t, X) \in \mathbb{R}_+ \times \partial\mathcal{D}$:*

- 3 *conditions if the free surface is a supercritical inflow,* 2 *conditions if it is a subcritical inflow,* 1 *condition if it is a subcritical outflow and* 0 *condition if it is a supercritical outflow*
- *for every $i \in [\![1, n-1]\!]$,* 3 *conditions if the interface i is a supercritical inflow with $\lambda_i^+(\mathbf{v}, \boldsymbol{\gamma}, \theta) < 0$,* 2 *conditions if it is a subcritical inflow or if it is a supercritical outflow with $\lambda_i^+(\mathbf{v}, \boldsymbol{\gamma}, \theta) < 0$,* 1 *condition if it is a supercritical inflow with $\lambda_i^+(\mathbf{v}, \boldsymbol{\gamma}, \theta) > 0$ and* 0 *condition if it is a supercritical outflow with $\lambda_i^+(\mathbf{v}, \boldsymbol{\gamma}, \theta) > 0$.*

Proof According to the theorem 4.2.2 and the definitions of inflow/outflow and subcritical/supercritical, as we have to require one boundary condition for each incoming characteristics (*i.e.* negative eigenvalue of $\mathsf{A}^{\mathsf{a}}(\mathbf{v}, \boldsymbol{\gamma}, \theta)$), the corollary is directly deduced.

Remark: We could have given the conditions of well-posedness of the initial-boundary value problem associated with the non-augmented multi-layer shallow water model but, as it is not conservative, we will not use it in numerical tests — we will just compare the solutions of these two models. Moreover, the number of necessary boundary conditions for the non-augmented model is exactly the same as the augmented model, as the spectrum of the 2nd one is exactly the spectrum of the 1st one, plus 0, as it is explained in (4.52). The difference between both model is in the condition itself, as the eigenvectors differ from one model to the other one.

To conclude, we have obtained a characterization of the boundary conditions we need to provide, on a general domain $\mathcal{D}$. Moreover, according to the type of flow we have at the free surface and the interfaces, we gave the exact number of conditions, in order to get the $\mathcal{L}^2$-well-posedness.

4.2.3 A particular domain: a rectangle

In the particular case of a rectangle $\mathcal{D} := [-L_x, L_x] \times [-L_y, L_y]$, we can clarify the boundary conditions derived in the previous subsection. We consider $(\mathbf{v}, \boldsymbol{\gamma}, \sigma, \varepsilon, \mathbf{v}^{\mathbf{0}}, \mathbf{g}) \in \mathbb{R}^{4n} \times \mathbb{R}_+^{n-1} \times \mathbb{R}^{[\![1,n-1]\!]} \times \mathbb{R}_+^* \times \mathcal{L}^2((0,T) \times \mathcal{D})^{4n} \times \mathcal{L}^2((0,T) \times \partial\mathcal{D})^{4n}$ and the initial boundary-value problem (4.72), such that ε is sufficiently small and assumptions (4.16–4.17) and (4.71) are verified. In order to give explicitly the boundary conditions, we consider a particular flow: $\mathbf{v}$ is such that

$$\begin{cases} \bar{u}, \bar{v} > 0, \\ \bar{u}, \bar{v} < \sqrt{gH}, \end{cases} \tag{4.87}$$

and

$$\forall i \in [\![1, n-1]\!], \begin{cases} u_i, v_i > 0, \\ u_i^2 h_{\sigma,i}^+ + u_{i+1}^2 h_{\sigma,i}^- < h_{\sigma,i}^+ h_{\sigma,i}^- (1 - \gamma_i), \\ v_i^2 h_{\sigma,i}^+ + v_{i+1}^2 h_{\sigma,i}^- < h_{\sigma,i}^+ h_{\sigma,i}^- (1 - \gamma_i), \end{cases} \tag{4.88}$$

Moreover, $\tilde{\mathbf{v}} := {}^\top(\tilde{h}_1, \dots, \tilde{h}_n, \tilde{u}_1, \dots, \tilde{u}_n, \tilde{v}_1, \dots, \tilde{v}_n, \tilde{w}_1, \dots, \tilde{w}_n) \in \mathcal{L}^2((0,T) \times \mathcal{D})^{4n}$ will denote the solution of the problem (4.72). We will expand below the boundary conditions it is necessary to provide for the North, South, East and West boundaries, in that particular case (4.87–4.88).

4.2.3.1 Northern boundary conditions

The normal of the domain $\mathcal{D}$ is constant on this boundary and defined by

$$\mathbf{n} = {}^\top(0, 1), \tag{4.89}$$

or with $\theta = \frac{\pi}{2}$. According to the conditions (4.87–4.88), we can deduce, at the North boundary, the free surface and each internal surface are subcritical outflow type:

$$\begin{cases} \lambda_n^+(\mathbf{v},\boldsymbol{\gamma},\frac{\pi}{2}) > 0, & \\ \lambda_i^+(\mathbf{v},\boldsymbol{\gamma},\frac{\pi}{2}) > 0, & \forall i \in [\![1,n-1]\!], \\ \lambda_{2n+i}(\mathbf{v},\boldsymbol{\gamma},\frac{\pi}{2}) > 0, & \forall i \in [\![1,n]\!], \\ \lambda_{3n+i}(\mathbf{v},\boldsymbol{\gamma},\frac{\pi}{2}) = 0, & \forall i \in [\![1,n]\!], \end{cases} \tag{4.90}$$

and

$$\begin{cases} \lambda_n^-(\mathbf{v},\boldsymbol{\gamma},\frac{\pi}{2}) < 0, & \\ \lambda_i^-(\mathbf{v},\boldsymbol{\gamma},\frac{\pi}{2}) < 0, & \forall i \in [\![1,n-1]\!]. \end{cases} \tag{4.91}$$

Consequently, according to the theorem 4.2.2, we need to impose n conditions, at the North boundary. Using the expression of $\boldsymbol{l}^{\lambda}(\mathbf{v},\boldsymbol{\gamma},\frac{\pi}{2})$ in (4.53–4.58), for every $i \in [\![1,n-1]\!]$, the condition for the interface i is reduced to

$$\boldsymbol{l}^{\lambda_i^-}(\mathbf{v},\boldsymbol{\gamma},\frac{\pi}{2})\tilde{\mathbf{v}} = \mathbf{g}_i, \tag{4.92}$$

which is equivalent to the next equality, using the asymptotic expansion of $\boldsymbol{l}_{\boldsymbol{x}}^{\lambda_i^-}(\mathbf{u},\boldsymbol{\gamma})$ in (4.27):

$$\begin{aligned} &\textstyle\sum_{j=m_i^-}^{i} \frac{\lambda_i^-\tilde{v}_j+u_j\tilde{u}_j}{\lambda_i^-(i-m_i^-+1)} - \sum_{j=i+1}^{m_i^+} \frac{\lambda_i^-\tilde{v}_j+u_j\tilde{u}_j}{\lambda_i^-(m_i^+-i)} \\ &+\frac{v_{i+1}-v_i}{h_{\sigma,i}^-+h_{\sigma,i}^+}\left(\textstyle\sum_{j=m_i^-}^{i} \frac{h_{\sigma,i}^-\tilde{h}_j}{(i-m_i^-+1)h_j} + \sum_{j=i+1}^{m_i^+} \frac{h_{\sigma,i}^+\tilde{h}_j}{(m_i^+-i)h_j}\right) \\ &-\left[\frac{h_{\sigma,i}^-h_{\sigma,i}^+}{h_{\sigma,i}^-+h_{\sigma,i}^+}\left(1-\gamma_i-\frac{(v_{i+1}-v_i)^2}{h_{\sigma,i}^-+h_{\sigma,i}^+}\right)\right]^{\frac{1}{2}} \textstyle\sum_{j=m_i^-}^{i} \frac{\tilde{h}_j}{(i-m_i^-+1)h_j} \\ &+\left[\frac{h_{\sigma,i}^-h_{\sigma,i}^+}{h_{\sigma,i}^-+h_{\sigma,i}^+}\left(1-\gamma_i-\frac{(v_{i+1}-v_i)^2}{h_{\sigma,i}^-+h_{\sigma,i}^+}\right)\right]^{\frac{1}{2}} \textstyle\sum_{j=i+1}^{m_i^+} \frac{\tilde{h}_j}{(m_i^+-i)h_j} = \quad \mathbf{g}_i, \end{aligned} \tag{4.93}$$

where $\lambda_i^- := \lambda_i^-(\mathbf{v},\boldsymbol{\gamma},\frac{\pi}{2})$. The condition concerning the free surface is reduced to

$$\boldsymbol{l}^{\lambda_n^-}(\mathbf{v},\boldsymbol{\gamma},\frac{\pi}{2})\tilde{\mathbf{v}} = \mathbf{g}_n, \tag{4.94}$$

which is equivalent to the next equality, using the asymptotic expansion of $\boldsymbol{l}_{\boldsymbol{x}}^{\lambda_n^-}(\mathbf{u},\boldsymbol{\gamma})$ in (4.31):

$$\begin{aligned} &\textstyle\sum_{k=1}^{n} \tilde{h}_k - \frac{h_k(\lambda_n^-\tilde{v}_k+u_k\tilde{u}_k)}{\lambda_n^-\sqrt{H}} \\ &-\textstyle\sum_{k=1}^{m_\sigma^-} \frac{(v_{m_\sigma^-+1}-v_{m_\sigma^-})}{\sqrt{H}}\left(\frac{2h_k}{\sqrt{H}}(\tilde{v}_k+\frac{u_k}{\lambda_n^-}\tilde{u}_k)-\tilde{h}_k\right) \\ &+\textstyle\sum_{k=m_\sigma^-+1}^{n} \frac{(v_{m_\sigma^-+1}-v_{m_\sigma^-})h_{\sigma,m_\sigma^-}^-}{\sqrt{H}h_{\sigma,m_\sigma^-}^+}\left(\frac{2h_k}{\sqrt{H}}(\tilde{v}_k+\frac{u_k}{\lambda_n^-}\tilde{u}_k)-\tilde{h}_k\right) = \quad \mathbf{g}_n, \end{aligned} \tag{4.95}$$

where $\lambda_n^- := \lambda_n^-(\mathbf{v},\boldsymbol{\gamma},\frac{\pi}{2})$.

Remark: The condition (4.93) is the generalization, to n layers, of the famous *Flather* condition, introduced in [49].

4.2.3.2 Southern boundary conditions

The normal of the domain $\mathcal{D}$ is constant on this boundary and defined by

$$\mathbf{n} = {}^{\top}(0,-1), \tag{4.96}$$

or with $\theta = \frac{3\pi}{2}$. According to the conditions (4.87–4.88), we can deduce, at the South boundary, the free surface and each internal surface are subcritical inflow type:

$$\begin{cases} \lambda_n^+(\mathbf{v},\boldsymbol{\gamma},\frac{3\pi}{2}) > 0, & \\ \lambda_i^+(\mathbf{v},\boldsymbol{\gamma},\frac{3\pi}{2}) > 0, & \forall i \in [\![1,n-1]\!], \\ \lambda_{3n+i}(\mathbf{v},\boldsymbol{\gamma},\frac{3\pi}{2}) = 0, & \forall i \in [\![1,n]\!], \end{cases} \tag{4.97}$$

and

$$\begin{cases} \lambda_n^-(\mathbf{v},\boldsymbol{\gamma},\frac{3\pi}{2}) < 0, & \\ \lambda_i^-(\mathbf{v},\boldsymbol{\gamma},\frac{3\pi}{2}) < 0, & \forall i \in [\![1,n-1]\!]. \\ \lambda_{2n+i}(\mathbf{v},\boldsymbol{\gamma},\frac{3\pi}{2}) < 0, & \forall i \in [\![1,n]\!]. \end{cases} \tag{4.98}$$

Consequently, according to the theorem 4.2.2, we need to impose $2n$ conditions, at the South boundary. Using the expression of $\boldsymbol{l}^{\lambda}(\mathbf{v},\boldsymbol{\gamma},\frac{3\pi}{2})$ in (4.53–4.58), for every $i \in [\![1,n-1]\!]$, the condition for the interface i is reduced to

$$\begin{cases} \boldsymbol{l}^{\lambda_i^-}(\mathbf{v},\boldsymbol{\gamma},\frac{3\pi}{2})\tilde{\mathbf{v}} = \mathbf{g}_i, \\ \boldsymbol{l}^{\lambda_{2n+i}}(\mathbf{v},\boldsymbol{\gamma},\frac{3\pi}{2})\tilde{\mathbf{v}} = \mathbf{g}_{2n+i}, \end{cases} \tag{4.99}$$

which is equivalent to the next system of equations:

$$\begin{cases} \sum_{j=i+1}^{m_i^+} \frac{\lambda_i^+\tilde{v}_j + u_j\tilde{u}_j}{\lambda_i^+(m_i^+ - i)} - \sum_{j=m_i^-}^{i} \frac{\lambda_i^+\tilde{v}_j + u_j\tilde{u}_j}{\lambda_i^+(i-m_i^-+1)} \\ -\frac{v_{i+1}-v_i}{h_{\sigma,i}^- + h_{\sigma,i}^+}\left(\sum_{j=m_i^-}^{i} \frac{h_{\sigma,i}^-\tilde{h}_j}{(i-m_i^-+1)h_j} + \sum_{j=i+1}^{m_i^+} \frac{h_{\sigma,i}^+\tilde{h}_j}{(m_i^+ - i)h_j}\right) \\ -\left[\frac{h_{\sigma,i}^- h_{\sigma,i}^+}{h_{\sigma,i}^- + h_{\sigma,i}^+}\left(1 - \gamma_i - \frac{(v_{i+1}-v_i)^2}{h_{\sigma,i}^- + h_{\sigma,i}^+}\right)\right]^{\frac{1}{2}} \sum_{j=m_i^-}^{i} \frac{\tilde{h}_j}{(i-m_i^-+1)h_j} \\ +\left[\frac{h_{\sigma,i}^- h_{\sigma,i}^+}{h_{\sigma,i}^- + h_{\sigma,i}^+}\left(1 - \gamma_i - \frac{(v_{i+1}-v_i)^2}{h_{\sigma,i}^- + h_{\sigma,i}^+}\right)\right]^{\frac{1}{2}} \sum_{j=i+1}^{m_i^+} \frac{\tilde{h}_j}{(m_i^+ - i)h_j} = \quad \mathbf{g}_i, \\ -(w_i + f)\tilde{h}_i + h_i\tilde{w}_i = \mathbf{g}_{2n+i}, \end{cases} \tag{4.100}$$

where $\lambda_i^+ := \lambda_i^+(\mathbf{v},\boldsymbol{\gamma},\frac{\pi}{2})$. The conditions concerning the free surface are reduced to

$$\begin{cases} \boldsymbol{l}^{\lambda_n^-}(\mathbf{v},\boldsymbol{\gamma},\frac{3\pi}{2})\tilde{\mathbf{v}} = \mathbf{g}_n, \\ \boldsymbol{l}^{\lambda_{3n}}(\mathbf{v},\boldsymbol{\gamma},\frac{3\pi}{2})\tilde{\mathbf{v}} = \mathbf{g}_{3n}, \end{cases} \tag{4.101}$$

which is equivalent to the next system of equations, using the asymptotic expansion of $\boldsymbol{l}_{\boldsymbol{x}}^{\lambda_n^-}(\mathbf{u},\boldsymbol{\gamma})$ in (4.31):

$$\begin{cases} \sum_{k=1}^{n}\tilde{h}_k+\frac{h_k(\lambda_n^+\tilde{v}_k+u_k\tilde{u}_k)}{\lambda_n^+\sqrt{H}} \\ -\sum_{k=1}^{m_\sigma^-}\frac{(v_{m_\sigma^-+1}-v_{m_\sigma^-})}{\sqrt{H}}\left(\frac{2h_k}{\sqrt{H}}(\tilde{v}_k+\frac{u_k}{\lambda_n^+}\tilde{u}_k)+\tilde{h}_k\right) \\ +\sum_{k=m_\sigma^-+1}^{n}\frac{(v_{m_\sigma^-+1}-v_{m_\sigma^-})h^-_{\sigma,m_\sigma^-}}{\sqrt{H}h^+_{\sigma,m_\sigma^-}}\left(\frac{2h_k}{\sqrt{H}}(\tilde{v}_k+\frac{u_k}{\lambda_n^+}\tilde{u}_k)+\tilde{h}_k\right)= \quad \mathbf{g}_n, \\ -(w_n+f)\tilde{h}_n+h_n\tilde{w}_n=\mathbf{g}_{3n}, \end{cases} \tag{4.102}$$

where $\lambda_n^+ := \lambda_n^+(\mathbf{v},\boldsymbol{\gamma},\frac{\pi}{2})$.

4.2.3.3 Eastern boundary conditions

The normal of the domain $\mathcal{D}$ is constant on this boundary and defined by

$$\mathbf{n} = {}^{\top}(1,0), \tag{4.103}$$

or with $\theta = 0$. According to the conditions (4.87–4.88), we can deduce, at the East boundary, the free surface and each internal surface are subcritical outflow type:

$$\begin{cases} \lambda_n^+(\mathbf{v},\boldsymbol{\gamma},0)>0, \\ \lambda_i^+(\mathbf{v},\boldsymbol{\gamma},0)>0, \qquad \forall i\in[\![1,n-1]\!], \\ \lambda_{2n+i}(\mathbf{v},\boldsymbol{\gamma},0)>0, \qquad \forall i\in[\![1,n]\!], \\ \lambda_{3n+i}(\mathbf{v},\boldsymbol{\gamma},0)=0, \qquad \forall i\in[\![1,n]\!], \end{cases} \tag{4.104}$$

and

$$\begin{cases} \lambda_n^-(\mathbf{v},\boldsymbol{\gamma},0)<0, \\ \lambda_i^-(\mathbf{v},\boldsymbol{\gamma},0)<0, \quad \forall i\in[\![1,n-1]\!]. \end{cases} \tag{4.105}$$

Consequently, according to the theorem 4.2.2, we need to impose n conditions, at the East boundary. Using the expression of $\boldsymbol{l}^{\lambda}(\mathbf{v},\boldsymbol{\gamma},\frac{\pi}{2})$ in (4.53–4.58), for every $i\in[\![1,n-1]\!]$, the condition for the interface i is reduced to

$$\boldsymbol{l}^{\lambda_i^-}(\mathbf{v},\boldsymbol{\gamma},0)\tilde{\mathbf{v}}=\mathbf{g}_i, \tag{4.106}$$

which is equivalent to the next equality, using the asymptotic expansion of $\boldsymbol{l}_{\boldsymbol{x}}^{\lambda_i^-}(\mathbf{u},\boldsymbol{\gamma})$ in (4.27):

$$\begin{aligned} &\sum_{j=m_i^-}^{i}\frac{\lambda_i^-\tilde{u}_j+v_j\tilde{v}_j}{\lambda_i^-(i-m_i^-+1)}-\sum_{j=i+1}^{m_i^+}\frac{\lambda_i^-\tilde{u}_j+v_j\tilde{v}_j}{\lambda_i^-(m_i^+-i)} \\ &+\frac{u_{i+1}-u_i}{h^-_{\sigma,i}+h^+_{\sigma,i}}\left(\sum_{j=m_i^-}^{i}\frac{h^-_{\sigma,i}\tilde{h}_j}{(i-m_i^-+1)h_j}+\sum_{j=i+1}^{m_i^+}\frac{h^+_{\sigma,i}\tilde{h}_j}{(m_i^+-i)h_j}\right) \\ &-\left[\frac{h^-_{\sigma,i}h^+_{\sigma,i}}{h^-_{\sigma,i}+h^+_{\sigma,i}}\left(1-\gamma_i-\frac{(u_{i+1}-u_i)^2}{h^-_{\sigma,i}+h^+_{\sigma,i}}\right)\right]^{\frac{1}{2}}\sum_{j=m_i^-}^{i}\frac{\tilde{h}_j}{(i-m_i^-+1)h_j} \\ &+\left[\frac{h^-_{\sigma,i}h^+_{\sigma,i}}{h^-_{\sigma,i}+h^+_{\sigma,i}}\left(1-\gamma_i-\frac{(u_{i+1}-u_i)^2}{h^-_{\sigma,i}+h^+_{\sigma,i}}\right)\right]^{\frac{1}{2}}\sum_{j=i+1}^{m_i^+}\frac{\tilde{h}_j}{(m_i^+-i)h_j}= \quad \mathbf{g}_i, \end{aligned} \tag{4.107}$$

where $\lambda_i^- := \lambda_i^-(\mathbf{v},\boldsymbol{\gamma},0)$. The condition concerning the free surface is reduced to

$$\boldsymbol{l}^{\lambda_n^-}(\mathbf{v},\boldsymbol{\gamma},0)\tilde{\mathbf{v}} = \mathbf{g}_n, \tag{4.108}$$

which is equivalent to the next equality, using the asymptotic expansion of $\boldsymbol{l}_{\boldsymbol{x}}^{\lambda_n^-}(\mathbf{u},\boldsymbol{\gamma})$ in (4.31):

$$\begin{aligned}
&\textstyle\sum_{k=1}^{n}\tilde{h}_k - \frac{h_k(\lambda_n^-\tilde{u}_k+v_k\tilde{v}_k)}{\lambda_n^-\sqrt{H}}\\
&\textstyle-\sum_{k=1}^{m_\sigma^-}\frac{(u_{m_\sigma^-+1}-u_{m_\sigma^-})}{\sqrt{H}}\left(\frac{2h_k}{\sqrt{H}}(\tilde{u}_k+\frac{v_k}{\lambda_n^-}\tilde{v}_k)-\tilde{h}_k\right)\\
&\textstyle+\sum_{k=m_\sigma^-+1}^{n}\frac{(u_{m_\sigma^-+1}-u_{m_\sigma^-})h^-_{\sigma,m_\sigma^-}}{\sqrt{H}h^+_{\sigma,m_\sigma^-}}\left(\frac{2h_k}{\sqrt{H}}(\tilde{u}_k+\frac{v_k}{\lambda_n^-}\tilde{v}_k)-\tilde{h}_k\right) = \quad \mathbf{g}_n,
\end{aligned} \tag{4.109}$$

where $\lambda_n^- := \lambda_n^-(\mathbf{v},\boldsymbol{\gamma},0)$.

4.2.3.4 Western boundary conditions

The normal of the domain $\mathcal{D}$ is constant on this boundary and defined by

$$\mathbf{n} = {}^{\top}(-1,0), \tag{4.110}$$

or with $\theta = \pi$. According to the conditions (4.87–4.88), we can deduce, at the West boundary, the free surface and each internal surface are subcritical inflow type:

$$\begin{cases}
\lambda_n^+(\mathbf{v},\boldsymbol{\gamma},\pi) > 0,\\
\lambda_i^+(\mathbf{v},\boldsymbol{\gamma},\pi) > 0, \qquad \forall i \in [\![1,n-1]\!],\\
\lambda_{3n+i}(\mathbf{v},\boldsymbol{\gamma},\pi) = 0, \qquad \forall i \in [\![1,n]\!],
\end{cases} \tag{4.111}$$

and

$$\begin{cases}
\lambda_n^-(\mathbf{v},\boldsymbol{\gamma},\pi) < 0,\\
\lambda_i^-(\mathbf{v},\boldsymbol{\gamma},\pi) < 0, \qquad \forall i \in [\![1,n-1]\!].\\
\lambda_{2n+i}(\mathbf{v},\boldsymbol{\gamma},\pi) < 0, \qquad \forall i \in [\![1,n]\!].
\end{cases} \tag{4.112}$$

Consequently, according to the theorem 4.2.2, we need to impose $2n$ conditions, at the West boundary. Using the expression of $\boldsymbol{l}^{\lambda}(\mathbf{v},\boldsymbol{\gamma},\pi)$ in (4.53–4.58), for every $i \in [\![1,n-1]\!]$, the condition for the interface i is reduced to

$$\begin{cases}
\boldsymbol{l}^{\lambda_i^-}(\mathbf{v},\boldsymbol{\gamma},\pi)\tilde{\mathbf{v}} = \mathbf{g}_i,\\
\boldsymbol{l}^{\lambda_{2n+i}}(\mathbf{v},\boldsymbol{\gamma},\pi)\tilde{\mathbf{v}} = \mathbf{g}_{2n+i},
\end{cases} \tag{4.113}$$

which is equivalent to the next system of equations:

$$\begin{cases}
\textstyle\sum_{j=i+1}^{m_i^+}\frac{\lambda_i^+\tilde{u}_j+v_j\tilde{v}_j}{\lambda_i^+(m_i^+-i)} - \sum_{j=m_i^-}^{i}\frac{\lambda_i^+\tilde{u}_j+v_j\tilde{v}_j}{\lambda_i^+(i-m_i^-+1)}\\
\textstyle-\frac{u_{i+1}-u_i}{h^-_{\sigma,i}+h^+_{\sigma,i}}\left(\sum_{j=m_i^-}^{i}\frac{h^-_{\sigma,i}\tilde{h}_j}{(i-m_i^-+1)h_j}+\sum_{j=i+1}^{m_i^+}\frac{h^+_{\sigma,i}\tilde{h}_j}{(m_i^+-i)h_j}\right)\\
\textstyle-\left[\frac{h^-_{\sigma,i}h^+_{\sigma,i}}{h^-_{\sigma,i}+h^+_{\sigma,i}}\left(1-\gamma_i-\frac{(u_{i+1}-u_i)^2}{h^-_{\sigma,i}+h^+_{\sigma,i}}\right)\right]^{\frac{1}{2}}\sum_{j=m_i^-}^{i}\frac{\tilde{h}_j}{(i-m_i^-+1)h_j}\\
\textstyle+\left[\frac{h^-_{\sigma,i}h^+_{\sigma,i}}{h^-_{\sigma,i}+h^+_{\sigma,i}}\left(1-\gamma_i-\frac{(u_{i+1}-u_i)^2}{h^-_{\sigma,i}+h^+_{\sigma,i}}\right)\right]^{\frac{1}{2}}\sum_{j=i+1}^{m_i^+}\frac{\tilde{h}_j}{(m_i^+-i)h_j} = \quad \mathbf{g}_i,\\
-(w_i+f)\tilde{h}_i + h_i\tilde{w}_i = \mathbf{g}_{2n+i},
\end{cases} \tag{4.114}$$

where $\lambda_i^+ := \lambda_i^+(\mathbf{v},\boldsymbol{\gamma},0)$. The conditions concerning the free surface are reduced to

$$\begin{cases} \boldsymbol{l}^{\lambda_n^-}(\mathbf{v},\boldsymbol{\gamma},\pi)\tilde{\mathbf{v}} = \mathbf{g}_n, \\ \boldsymbol{l}^{\lambda_{3n}}(\mathbf{v},\boldsymbol{\gamma},\pi)\tilde{\mathbf{v}} = \mathbf{g}_{3n}, \end{cases} \tag{4.115}$$

which is equivalent to the next system of equations, using the asymptotic expansion of $\boldsymbol{l}_{\boldsymbol{x}}^{\lambda_n^-}(\mathbf{u},\boldsymbol{\gamma})$ in (4.31):

$$\begin{cases} \sum_{k=1}^{n}\tilde{h}_k + \frac{h_k(\lambda_n^+\tilde{u}_k+v_k\tilde{v}_k)}{\lambda_n^+\sqrt{H}} \\ -\sum_{k=1}^{m_\sigma^-}\frac{(u_{m_\sigma^-+1}-u_{m_\sigma^-})}{\sqrt{H}}\left(\frac{2h_k}{\sqrt{H}}(\tilde{u}_k+\frac{v_k}{\lambda_n^+}\tilde{v}_k)+\tilde{h}_k\right) \\ +\sum_{k=m_\sigma^-+1}^{n}\frac{(u_{m_\sigma^-+1}-u_{m_\sigma^-})h^-_{\sigma,m_\sigma^-}}{\sqrt{H}h^+_{\sigma,m_\sigma^-}}\left(\frac{2h_k}{\sqrt{H}}(\tilde{u}_k+\frac{v_k}{\lambda_n^+}\tilde{v}_k)+\tilde{h}_k\right) = \quad \mathbf{g}_n, \\ -(w_n+f)\tilde{h}_n + h_n\tilde{w}_n = \mathbf{g}_{3n}, \end{cases} \tag{4.116}$$

where $\lambda_n^+ := \lambda_n^+(\mathbf{v},\boldsymbol{\gamma},0)$.

Remark: If $\mathbf{v}$ verifies the conditions (4.87–4.88), then, n conditions are necessary at the North and East boundaries, while $2n$ conditions a the South and West boundaries. This is really important as we know that these conditions come usually with measurement in the real world, which is very expensive: the fewer conditions are necessary, the better it is. For example, it is possible with the satellites to measure the layer-heights, while the measure of the velocities is much more complicated, then, it is interesting to know if the boundaries, in a real case, are such as the North/East type seen before, or the South/west type.

4.3 Numerical resolution

In this section, we explain the choices we have made concerning the numerical resolution of the multi-layer shallow water model with free surface. First, we precise the type of mesh, a uniform structured grid. Then, the second order accurate numerical scheme is detailed. Afterwards, the time-splitting is explained. And finally, the effective numerical boundary conditions are expressed, in the case of an Eastern boundary.

In this part, we do not consider the linear initial-boundary value problem but the non-linear one. Let $\boldsymbol{\gamma} \in \mathbb{R}_+^{n-1}$ such that there exist $(\sigma,\varepsilon) \in \mathbb{R}^{[\![1,n-1]\!]} \times \mathbb{R}_+^*$, assumptions (4.16–4.17) are verified and ε sufficiently small; let $\mathbf{v}^{\mathbf{0}} \in \mathcal{L}^2(\mathcal{D})^{4n}$ such that conditions (4.71) is verified; let $\mathbf{g} \in \mathcal{L}^2(\mathbb{R}_+ \times \partial\mathcal{D})^{4n}$; then, we consider the following problem:

$$\begin{cases} \frac{\partial \mathbf{v}}{\partial t} + \mathsf{A}_x^{\mathsf{a}}(\mathbf{v},\boldsymbol{\gamma})\frac{\partial \mathbf{v}}{\partial x} + \mathsf{A}_y^{\mathsf{a}}(\mathbf{v},\boldsymbol{\gamma})\frac{\partial \mathbf{v}}{\partial y} + \mathbf{b}^{\mathbf{a}}(\mathbf{v}) = 0, & \forall X \in \mathcal{D}, \quad \forall t \geq 0, \\ \mathsf{B}^{\mathsf{a}}(\mathbf{v},\boldsymbol{\gamma},\theta)\mathbf{v} = \mathbf{g}, & \forall X \in \partial\mathcal{D}, \quad \forall t \geq 0, \\ \mathbf{v} = \mathbf{v}^{\mathbf{0}}, & \forall X \in \mathcal{D}, \quad t = 0, \end{cases} \tag{4.117}$$

where $\mathsf{A}^{\mathsf{a}}_x(\mathbf{v},\boldsymbol{\gamma})$ and $\mathsf{A}^{\mathsf{a}}_y(\mathbf{v},\boldsymbol{\gamma})$ are defined in (4.40–4.41) and $\mathbf{b}^{\mathbf{a}}(\mathbf{v})$ is defined in (4.42).
However, for every $\lambda \in \sigma\big(\mathsf{A}^{\mathsf{a}}(\mathbf{v},\boldsymbol{\gamma},\theta)\big)$, as the exact integration of the quantity

$$\boldsymbol{l}^{\lambda}(\mathbf{v},\boldsymbol{\gamma},\theta)\frac{\partial \mathbf{v}}{\partial t}, \tag{4.118}$$

is not possible, there is no *Riemann* invariant and we cannot precise the boundary operator $\mathsf{B}^{\mathsf{a}}(\mathbf{v},\boldsymbol{\gamma},\theta)$ to obtain a well-posed initial-boundary value problem in (4.117). We will explain, in the next subsection, the way we solve this problem.

4.3.1 The type of mesh

As the numerical resolution will be computed in a particular rectangle: a square $\mathcal{D} := [-L,L]\times[-L,L]$, with $L>0$, we take a structured grid with equal space discretization step, denoted by Δx, in both directions — see figure 4.2. We denote the number of cells by $N \in \mathbb{N}$:

$$N := \frac{2L}{\Delta x}. \tag{4.119}$$

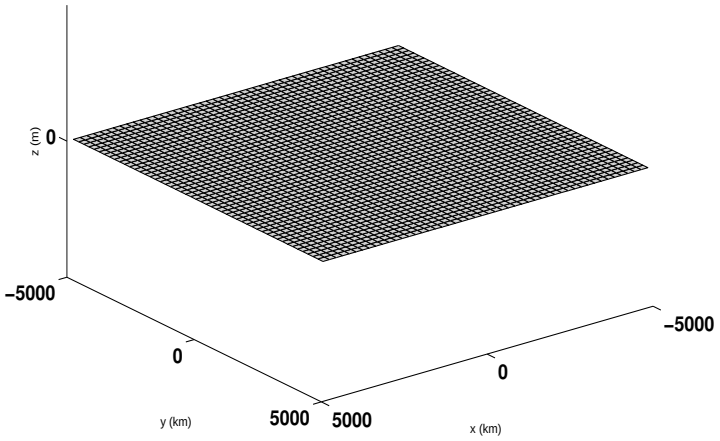

Figure 4.2: The structured grid in the domain $\mathcal{D}$

4.3.2 The numerical scheme

We decide to use a finite-volume method to solve numerically the hyperbolic initial-boundary value problem (4.72). In order to avoid any unknown behavior from the numerical scheme, we chose the well-known two-step *Lax-Wendroff* method, introduced in [73], [74] and [110]. This finite differences

method is generally sufficiently accurate, as it is second-order accurate in the particular case of the advection equation. We consider the augmented model (4.39) under the conservative form:

$$\frac{\partial \mathbf{v}}{\partial t} + \frac{\partial \mathbf{F}^{\mathbf{a}}_{\mathbf{x}}}{\partial x}(\mathbf{v},\boldsymbol{\gamma}) + \frac{\partial \mathbf{F}^{\mathbf{a}}_{\mathbf{y}}}{\partial y}(\mathbf{v},\boldsymbol{\gamma}) + \mathbf{b}^{\mathbf{a}}(\mathbf{v}) = 0, \tag{4.120}$$

where the flux-vectors $\mathbf{F}^{\mathbf{a}}_{\mathbf{x}}(\mathbf{v},\boldsymbol{\gamma}) \in \mathbb{R}^{4n}$ and $\mathbf{F}^{\mathbf{a}}_{\mathbf{y}}(\mathbf{v},\boldsymbol{\gamma}) \in \mathbb{R}^{4n}$ are defined by

$$\mathbf{F}^{\mathbf{a}}_{\mathbf{x}}(\mathbf{v},\boldsymbol{\gamma}) := \sum_{k=1}^{n} h_k u_k \boldsymbol{e'_k} + (\frac{1}{2}(u_k^2 + v_k^2 + \sum_{j=1}^{n} \alpha_{k,j} h_j)\boldsymbol{e'}_{n+k} + u_k(w_k + f)\boldsymbol{e'}_{3n+k}, \tag{4.121}$$

and

$$\mathbf{F}^{\mathbf{a}}_{\mathbf{y}}(\mathbf{v},\boldsymbol{\gamma}) := \sum_{k=1}^{n} h_k v_k \boldsymbol{e'_k} + (\frac{1}{2}(u_k^2 + v_k^2 + \sum_{j=1}^{n} \alpha_{k,j} h_j)\boldsymbol{e'}_{2n+k} + v_k(w_k + f)\boldsymbol{e'}_{3n+k}, \tag{4.122}$$

with $(\boldsymbol{e'_i})_{i\in[\![1,4n]\!]}$, the canonical basis of $\mathbb{R}^{4n}$.

First, we consider the system (4.120) in one space-dimension. Then, we can easily detail the two-step *Lax-Wendroff* method. Let $\Delta t > 0$ be the time-step and for every $(i,k) \in [\![0,N-1]\!] \times \mathbb{N}$, we denote by $\mathbf{V}_i^k$, the quantity

$$\mathbf{V}_i^k := \mathbf{v}(k\Delta t, i\Delta x - L), \tag{4.123}$$

using the two-step *Lax-Wendroff* method. We initialize the method with $\mathbf{v^0}$ and for each time-step, we perform the following proceeding: for every $(i,k) \in [\![0,N-1]\!] \times \mathbb{N}$, the first step of the *Lax-Wendroff* method is

$$\mathbf{V}_{i+\frac{1}{2}}^{k+\frac{1}{2}} = \frac{1}{2}\left(\mathbf{V}_{i+1}^k + \mathbf{V}_i^k\right) + \frac{\Delta t}{2\Delta x}\left(\mathbf{F}^{\mathbf{a}}_{\mathbf{x}}(\mathbf{V}_{i+1}^k,\boldsymbol{\gamma}) - \mathbf{F}^{\mathbf{a}}_{\mathbf{x}}(\mathbf{V}_i^k,\boldsymbol{\gamma})\right), \tag{4.124}$$

and the second step is such as

$$\mathbf{V}_i^{k+1} = \mathbf{V}_i^k + \frac{\Delta t}{\Delta x}\left(\mathbf{F}^{\mathbf{a}}_{\mathbf{x}}(\mathbf{V}_{i+\frac{1}{2}}^{k+\frac{1}{2}},\boldsymbol{\gamma}) - \mathbf{F}^{\mathbf{a}}_{\mathbf{x}}(\mathbf{V}_{i-\frac{1}{2}}^{k+\frac{1}{2}},\boldsymbol{\gamma})\right). \tag{4.125}$$

In the case of two dimensions, we will detail in the following subsection the treatment we perform to approximate the solution, using a time-splitting method.

In the following analysis, for every $(i,j,k) \in [\![0,N-1]\!]^2 \times \mathbb{N}$, we denote by $\mathbf{V}_{i,j}^k$ the approximation of the solution of the initial-boundary value problem (4.72), using the two-step *Lax-Wendroff* method. This quantity is defined by

$$\mathbf{V}_{i,j}^k := \mathbf{v}(k\Delta t, i\Delta x - L, j\Delta y - L). \tag{4.126}$$

This method is stable under the *CFL*-condition

$$\max_{(i,j,\theta)\in[\![0,N-1]\!]^2\times[0,2\pi]} \sigma(\mathsf{A}^{\mathsf{a}}(\mathbf{V}_{i,j}^0,\boldsymbol{\gamma},\theta))\frac{\Delta t}{\Delta x} < 1, \tag{4.127}$$

where $\mathbf{V}_{i,j}^0$ is the discretization of the initial condition :

$$\begin{aligned} \mathbf{V}_{i,j}^0 :=& \quad \mathbf{v}(0, i\Delta x - L, j\Delta y - L) \\ =& \quad \mathbf{v}^0(i\Delta x - L, j\Delta y - L). \end{aligned} \tag{4.128}$$

Remark: The two-step *Lax-Wendroff* method has also a formulation based on the finite-volume methods. One can find more details about this method, and about the general finite-volume methods, in [76].

4.3.3 The time-splitting method

In order to use the two-step *Lax-Wendroff* method, as it was presented before, in (4.124–4.125), we split the system (4.120) into three steps: for every time-step $k \in \mathbb{N}$,

1. the x-flux part:
$$\begin{cases} \frac{\partial \mathbf{v_1}}{\partial t} + \frac{\partial \mathbf{F_x^a}}{\partial x}(\mathbf{v_1}, \boldsymbol{\gamma}) = 0, \\ \mathbf{v_1}(t=0) = \mathbf{V}^k, \end{cases}$$

2. the y-flux part:
$$\begin{cases} \frac{\partial \mathbf{v_2}}{\partial t} + \frac{\partial \mathbf{F_y^a}}{\partial y}(\mathbf{v_2}, \boldsymbol{\gamma}) = 0, \\ \mathbf{v_2}(t=0) = \mathbf{v_1}(t=\frac{\Delta t}{2}) + \text{b.c.}, \end{cases}$$

3. the source-terms part:
$$\begin{cases} \frac{\partial \mathbf{v_3}}{\partial t} + \mathbf{b^a}(\mathbf{v_3}) = 0, \\ \mathbf{v_3}(t=0) = \mathbf{v_2}(t=\frac{\Delta t}{2}), \end{cases}$$

4. the y-flux part:
$$\begin{cases} \frac{\partial \mathbf{v_4}}{\partial t} + \frac{\partial \mathbf{F_y^a}}{\partial y}(\mathbf{v_4}, \boldsymbol{\gamma}) = 0, \\ \mathbf{v_4}(t=0) = \mathbf{v_3}(t=\Delta t), \end{cases}$$

5. the x-flux part:
$$\begin{cases} \frac{\partial \mathbf{v_5}}{\partial t} + \frac{\partial \mathbf{F_x^a}}{\partial x}(\mathbf{v_5}, \boldsymbol{\gamma}) = 0, \\ \mathbf{v_5}(t=0) = \mathbf{v_4}(t=\frac{\Delta t}{2}) + \text{b.c.}. \end{cases}$$

Then, we set $\mathbf{V}^{k+1} = \mathbf{v_5}(t=\frac{\Delta t}{2})$, and according to [63], this is a second-order accurate method (see also [78] for general time-splitting methods). Note that the boundary conditions are performed in steps 2 and 5 of this time-splitting (see [75]).
Moreover, we improve this time-splitting method, in order to treat equally the x-direction as the y-direction. The improvement is made by performing the following steps:

- 1.-2.-3.-4.-5. every even time-step,
- 2.-1.-3.-5.-4. every odd time-step.

This splitting method is a *Strang* splitting type, introduced in [129]. Moreover, it is possible to prove the following proposition:

Proposition 4.3.1 *The time-splitting described above is second-order accurate.*

Proof The proof is based on two assertions: the two-step *Lax-Wendroff* method is second-order accurate and considering $(\mathsf{A},\mathsf{B}) \in \mathcal{M}_m(\mathbb{R})^2$, the quantity $err(\mathsf{A},\mathsf{B})$, defined by

$$err(\mathsf{A},\mathsf{B}) := ||\exp\left(\frac{\Delta t}{2}\mathsf{A}\right)\exp\left(\Delta t\mathsf{B}\right)\exp\left(\frac{\Delta t}{2}\mathsf{A}\right) - \exp\left(\Delta t(\mathsf{A}+\mathsf{B})\right)||, \tag{4.129}$$

where $||\cdot||$ is a matrix-norm, $err(\mathsf{A},\mathsf{B})$ verifies the following inequality:

$$err(\mathsf{A},\mathsf{B}) \leq \Delta t^3\left(\frac{1}{12}[\mathsf{B},[\mathsf{B},\mathsf{A}]] - \frac{1}{24}[\mathsf{A},[\mathsf{A},\mathsf{B}]]\right) + \mathcal{O}(\Delta t^4), \tag{4.130}$$

where $[\mathsf{A},\mathsf{B}]$ is equal to

$$[\mathsf{A},\mathsf{B}] := \mathsf{AB} - \mathsf{BA}, \tag{4.131}$$

and is the commutator of these matrices.

Remark: More details about the time-splitting methods in [72] and [85]. Moreover, in the case of the multi-layer shallow water model, the source-terms may be stiff, as the bathymetry is not necessarily smooth. Then, semi-implicit methods have been developed, in order to block these kind of troubles. See for example [77] or [124]. However, in our particular case, we will perform the numerical tests with a flat bottom so stiffness of the source-terms vanishes.

4.3.4 The numerical boundary conditions

It was proved, in subsection 4.2.2, the open boundary conditions (4.74) insure the well-posedness of the linear initial-boundary value problem (4.72), associated with the augmented model (4.8). However there are two questions we need to answer:

- how do we chose the function $\mathbf{g} \in \mathcal{L}^2((0,T)\times\partial\mathcal{D})^{4n}$?
- what are the corresponding open boundary conditions of the non-linear problem?

Firstly, we address the question about the function $\mathbf{g}$. As it is explained in [53] and [12], the homogeneous initial-boundary value problem: (4.72) with

$$\mathbf{g} = 0, \tag{4.132}$$

is well-posed. Moreover, it is possible to derive a boundary operator a little bit more general than the one we gave in (4.74). However, the accuracy of such problem is quite poor. As it is explained in [14] and [21], It is more reasonable to take the external quantities. Indeed, if we consider $\tilde{\mathbf{v}}_{ext}$ the value of $\tilde{\mathbf{v}}$, solution of the linear problem associated with (4.39), just beyond the boundary of $\mathcal{D}$. Then, a good choice for $\mathbf{g}$ is

$$\mathbf{g} := \mathsf{B}^{\mathsf{a}}(\mathbf{v},\boldsymbol{\gamma},\theta)\tilde{\mathbf{v}}_{ext}. \tag{4.133}$$

This choice makes sense. We consider an interface $i \in [\![1, n-1]\!]$, at a boundary point $X \in \partial\mathcal{D}$. For instance, if it is a subcritical inflow interface at the time-step $k \in \mathbb{N}$, then the *Riemann* invariant associated with λ_i^- and λ_{2n+i} are coming in the domain $\mathcal{D}$. Consequently, to compute these quantities at time $k+1$, their values just beyond $\partial\mathcal{D}$ are necessary. Though, the characteristic unknown associated with λ_i^+ is going out. Therefore, the external value of this characteristic is not necessary at the time-step $k+1$.

The choice of $\mathbf{g}$, in (4.133), induces that we know $\tilde{\mathbf{v}}_e xt$. To know it, we need to know the

Remark: The function $\mathbf{g}$ defined in (4.133) is not rigorously defined in $\mathcal{L}^2((0,T)\times\partial\mathcal{D})^{4n}$ but in $\mathcal{L}^2((0,T)\times\partial\mathcal{D})^m$, where m is the number of strictly negative eigenvalues of $\mathsf{A}^{\mathsf{a}}(\mathbf{v},\boldsymbol{\gamma},\theta)$. One can augment $\mathbf{g}$ with zero-function to be more meticulous.

Secondly, the question about the corresponding boundary conditions for the non-linear problem is more complicated. Indeed, there is no *Riemann* invariant, in the general multi-layer shallow water model, as the quantity

$$\boldsymbol{l}^{\lambda}(\mathbf{v},\boldsymbol{\gamma},\theta)\frac{\partial \mathbf{v}}{\partial t} \tag{4.134}$$

is not exactly integrable. However, as it was proved before, the associated linear problem does have *Riemann* invariants. Then, we do not give boundary conditions we chose to perform, in the numerical resolution, a local linearization of the problem. To explain it, we concentrate the analysis on an Eastern boundary and we expand the method for this particular case — the other boundaries are easily deduced. For every $(j,k) \in [\![1,N]\!]\times\mathbb{N}$, we consider an Eastern cell $C_{N,j}$, at the time-step k. Below, we explain the value we impose to $\mathbf{V}_{N,j}^k$. We consider the following linear initial-boundary value problem:

$$\begin{cases} \frac{\partial \tilde{\mathbf{v}}}{\partial t} + \mathsf{A}_x^{\mathsf{a}}(\mathbf{v},\boldsymbol{\gamma})\frac{\partial \tilde{\mathbf{v}}}{\partial x} + \mathsf{A}_y^{\mathsf{a}}(\mathbf{v},\boldsymbol{\gamma})\frac{\partial \tilde{\mathbf{v}}}{\partial y} + \mathsf{C}^{\mathsf{a}}(\mathbf{v})\tilde{\mathbf{v}} = 0, & \forall X \in \mathcal{D}, \quad \forall t \geq 0, \\ \mathsf{B}^{\mathsf{a}}(\mathbf{v},\boldsymbol{\gamma},\theta)\tilde{\mathbf{v}} = \mathsf{B}^{\mathsf{a}}(\mathbf{v},\boldsymbol{\gamma},\theta)\tilde{\mathbf{v}}_{ext}, & \forall X \in \partial\mathcal{D}, \quad \forall t \geq 0, \\ \tilde{\mathbf{v}} = \tilde{\mathbf{v}}^{\mathbf{0}}, & \forall X \in \mathcal{D}, \quad t = 0, \end{cases} \tag{4.135}$$

where $\tilde{\mathbf{v}}_{ext}$ is the value of $\tilde{\mathbf{v}}$ just beyond the boundary $\partial\mathcal{D}$; and $\mathbf{v}$ is equal to

$$\mathbf{v} := \mathbf{V}_{N-1,j}^k. \tag{4.136}$$

The initial-boundary value problem (4.135) is the linearization of (4.117), about the constant value $\mathbf{V}_{N-1,j}^k$. Consequently, we already explicitly explained the boundary necessary boundary conditions in theorem 4.2.2, for such a linear problem. At the Eastern boundary, for every strictly negative eigenvalue

$$\lambda \in \sigma(\mathsf{A}^{\mathsf{a}}(\mathbf{V}_{N-1,j}^k,\boldsymbol{\gamma},0)) \cap \mathbb{R}_-^*, \tag{4.137}$$

we impose the condition:

$$\boldsymbol{l}^{\lambda}(\mathbf{V}_{N-1,j}^k,\boldsymbol{\gamma},0)\mathbf{V}_{N,j}^k = \boldsymbol{l}^{\lambda}(\mathbf{V}_{N-1,j}^k,\boldsymbol{\gamma},0)(\mathbf{V}_{ext})_{N,j}^k \tag{4.138}$$

Even if these boundary conditions are not theoretically exact, for non-linear problem, the resolution of this kind of problem is really efficient, because it is linear.

Remark: The numerical resolution needs $4n$ values to determine the vector $\mathbf{V}_{i,j}^k \in \mathbb{R}^{4n}$. To do so, we complete the boundary conditions (4.138) with homogeneous *Neumann* conditions. For every $i \in [\![1,n]\!]$, we associate the unknowns h_i with λ_i^-, u_i with λ_i^+, v_i with λ_{3n+i} and w_i with λ_{2n+i}:

$$\forall i \in [\![1,n]\!], \begin{cases} h_i \leftrightarrow \lambda_i^-, \\ u_i \leftrightarrow \lambda_i^+, \\ v_i \leftrightarrow \lambda_{3n+i}, \\ w_i \leftrightarrow \lambda_{2n+i}. \end{cases} \tag{4.139}$$

This association means that if $\lambda \in \sigma(\mathsf{A}^{\mathsf{a}}(\mathbf{V}_{N-1,j}^k, \boldsymbol{\gamma}, \theta))$ is strictly negative, then we impose the boundary conditions explained above. Nevertheless, if λ is positive, we impose an homogeneous *Neumann* condition to the associated variable, given by (4.139). For example, if the interface i is a subcritical inflow, we will impose, at the Eastern boundary of the interface i, the following conditions:

$$\begin{cases} \boldsymbol{l}^{\lambda_i^-}(\mathbf{V}_{N-1,j}^k, \boldsymbol{\gamma}, 0)\mathbf{V}_{N,j}^k = \boldsymbol{l}^{\lambda_i^-}(\mathbf{V}_{N-1,j}^k, \boldsymbol{\gamma}, 0)(\mathbf{V}_{ext})_{N,j}^k, \\ (u_i)_{N,j}^k = (u_i)_{N-1,j}^k, \\ (v_i)_{N,j}^k = (v_i)_{N-1,j}^k, \\ \boldsymbol{l}^{\lambda_{2n+i}}(\mathbf{V}_{N-1,j}^k, \boldsymbol{\gamma}, 0)\mathbf{V}_{N,j}^k = \boldsymbol{l}^{\lambda_{2n+i}}(\mathbf{V}_{N-1,j}^k, \boldsymbol{\gamma}, 0)(\mathbf{V}_{ext})_{N,j}^k, \end{cases} \tag{4.140}$$

Though, if the interface i is a subcritical outflow, we will impose, at the Eastern boundary of the interface i, the following conditions:

$$\begin{cases} \boldsymbol{l}^{\lambda_i^-}(\mathbf{V}_{N-1,j}^k, \boldsymbol{\gamma}, 0)\mathbf{V}_{N,j}^k = \boldsymbol{l}^{\lambda_i^-}(\mathbf{V}_{N-1,j}^k, \boldsymbol{\gamma}, 0)(\mathbf{V}_{ext})_{N,j}^k, \\ (u_i)_{N,j}^k = (u_i)_{N-1,j}^k, \\ (v_i)_{N,j}^k = (v_i)_{N-1,j}^k, \\ (w_i)_{N,j}^k = (w_i)_{N-1,j}^k, \end{cases} \tag{4.141}$$

In conclusion, we detailed, in this subsection, the open boundary conditions we performed in the numerical resolution of the augmented multi-layer shallow water model with free surface.

4.4 Numerical treatment of the open boundary conditions

In the previous section, we explained the choices we have made to solve numerically the open boundary problem. The main objective was to use well-known techniques (mesh type, numerical scheme, time-splitting), to focus on the behavior of the treatment of the open boundaries. Moreover, the external data $\mathbf{V}_{ext}$ are necessary to perform those conditions. Consequently, in our numerical test cases,

we compute the numerical resolution of the same initial problem, in a domain $\mathcal{D}_{ext}$, two times greater than $\mathcal{D}$:

$$\mathcal{D}_{ext} = 2\mathcal{D}. \tag{4.142}$$

Moreover, the boundary conditions, at $\partial\mathcal{D}_{ext}$, are two different types, depending on the test case:

- non-permeability conditions

$$\forall i \in [\![1,n]\!],\ \forall X\ \in \partial\mathcal{D}_{ext},\ \begin{cases} \frac{\partial h_i}{\partial \boldsymbol{n}} = 0, \\ \boldsymbol{u_i} \cdot \boldsymbol{n} = 0, \\ \frac{\partial w_i}{\partial \boldsymbol{n}} = 0. \end{cases}$$

- outgoing flow conditions

$$\forall i \in [\![1,n]\!],\ \forall X\ \in \partial\mathcal{D}_{ext},\ \frac{\partial \mathbf{u}}{\partial \boldsymbol{n}} = 0,$$

The domain $\mathcal{D}$ is centered in $\mathcal{D}_{ext}$ and at each time-step, we save the values of the solution $\mathbf{V}_{ext}$, just beyond the boundary $\partial\mathcal{D}$. For every test case, the length L, which defines $\mathcal{D}$ and $\mathcal{D}_{ext}$, will be equal to $L := 5000$km. The space and time discretizations will be constant and specified in each case.
We perform various test cases, in order to validate the previous theoretical results. First, we provide, in this section, the two different test cases we have chosen to perform the numerical resolutions. Then, we compare the solutions of the augmented and non-augmented models, with non-permeability conditions. Afterwards, we check the accuracy of the method to treat the open boundary problem, for the single-layer model. Finally, we evaluate the accuracy of the open boundary problem with different models and test cases (see table 4.1).

	1 layer	**2 layers**	**4 layers**
Test case 1	✓ linear	✓ linear	✓ linear
	✓ non-linear	✓ non-linear	✓ non-linear
Test case 2	✓ linear	✓ linear	✓ linear
	✓ non-linear	✓ non-linear	✓ non-linear

Table 4.1: Numerical validation plan of the boundary conditions.

Remark: The numerical approximation of the solution is performed on the exterior domain $\mathcal{D}_{ext}$, which is four times greater than the interior domain $\mathcal{D}$. This method would not be efficient if it would need such a large exterior domain to evaluate the approximation of the solution, in the interior domain. Indeed, in the reality, the solution of the exterior domain is not calculated but measured (with satellite for example) just at the boundary between $\mathcal{D}$ and $\mathcal{D}_{ext}$.

4.4.1 The different test cases

We initialize the numerical resolution with two different test cases:

- test case 1: The gravity wave,
- test case 2: The barotropic vortex.

They are performed with an interior domain and an exterior domain respectively defined by

$$\begin{cases} \mathcal{D} & := [-5000, 5000] \times [-5000, 5000](\text{km}), \\ \mathcal{D}_{ext} & := [-10000, 10000] \times [-10000, 10000](\text{km}). \end{cases} \tag{4.143}$$

Each test case is used with 3 models : 1, 2 and 4 layers (each one with a linear and non-linear version). Moreover, the diagnostic quantities are

- the normalized RMS error of the sea surface elevation,
- the normalized error of the energy,
- the RMS error of the vorticity,
- the mean absolute divergence.

These quantities are averaged over the total height. The RMS error of the sea surface quantifies the difference between the sea surface of the small domain $\mathcal{D}$, calculated just in this small domain, and the sea surface of the small domain $\mathcal{D}$, calculated in the large domain $\mathcal{D}_{ext}$. The RMS error of the vorticity is not normalized because the vorticity values are very small, especially in the test case 2, when the vortex goes out the interior domain $\mathcal{D}$. The divergence is even smaller than the vorticity so we chose to analyse the mean absolute divergence, as it is done in [92] for example. Finally, the normalized error of the energy quantifies is normalized by the energy in the interior domain, from the computation of the large domain $\mathcal{D}_{ext}$.
Furthermore, the gravitational acceleration is assumed equal to

$$g = 9.806, \tag{4.144}$$

and the *Coriolis* parameter is assumed constant (f-plane approximation) for the linear models

$$f = f_0, \tag{4.145}$$

or linearly dependent of y (β-plane approximation) for the non-linear models

$$f = f_0 + \beta y. \tag{4.146}$$

See more details about these approximations in [54], [59] and [100]. The parameter f is expanded around the latitude 38.5 North. Then, these two constants are equal to

$$\begin{cases} f_0 = 9.054 \times 10^{-5} (\text{rad.s}^{-1}), \\ \beta = 1.7876 \times 10^{-11} (\text{rad.m}^{-1}.\text{s}^{-1}). \end{cases} \tag{4.147}$$

Finally, we consider, for every test case and every model, a flat bottom

$$\frac{\partial b}{\partial x} = \frac{\partial b}{\partial y} = 0. \tag{4.148}$$

Remark: The following initial conditions verify the condition of local well-posedness (4.71), with $u_0 = v_0 = 0$.

4.4.1.1 Test case 1: The gravity wave

This initial condition is characterized by

$$\forall i \in [\![1,n]\!], \begin{cases} h_i = \frac{H_0}{n} + \frac{\hat{H}_0}{n} exp\left(-\frac{(x-L/2)^2+(y-L/2)^2}{(L/10)^2}\right), \\ u_i = 0, \\ v_i = 0, \end{cases} \tag{4.149}$$

We chose the following depth values

$$\begin{cases} H_0 = 5000\text{m}, \\ \hat{H}_0 = 500\text{m}. \end{cases} \tag{4.150}$$

The density ratios will be chosen such that

$$\forall i \in [\![1,n-1]\!], \begin{cases} \gamma_i = 1 - \varepsilon^{\sigma(i)}, \\ \varepsilon = 10^{-3}, \end{cases} \tag{4.151}$$

with σ defined by

$$\begin{cases} \sigma(1) = 1, \\ \sigma(2) = 3, \\ \sigma(3) = 2. \end{cases} \tag{4.152}$$

As this initial condition, expressed in (4.149), does not verify the condition

$$\nabla P_i = f \boldsymbol{u_i}^{\perp}, \tag{4.153}$$

where we remind that P_i is defined by

$$P_i := \sum_{k=1}^{n} \alpha_{i,k} g h_k. \tag{4.154}$$

Then, it will not be in geostrophic balance. For this test case, the boundary conditions at $\partial\mathcal{D}_{ext}$ are non-permeability conditions

$$\forall i \in [\![1,n]\!],\ \forall X\ \in \partial\mathcal{D}_{ext},\ \begin{cases} \frac{\partial h_i}{\partial \boldsymbol{n}} = 0, \\ \boldsymbol{u_i} \cdot \boldsymbol{n} = 0, \\ \frac{\partial w_i}{\partial \boldsymbol{n}} = 0. \end{cases} \tag{4.155}$$

As it is explained in [54] and [83], the system will radiate adjustment waves as it adjusts to a balance state. The figure 4.3 represents the sea surface elevation of this test case, in the domain $\mathcal{D}$, with $\Delta x = 100$km.

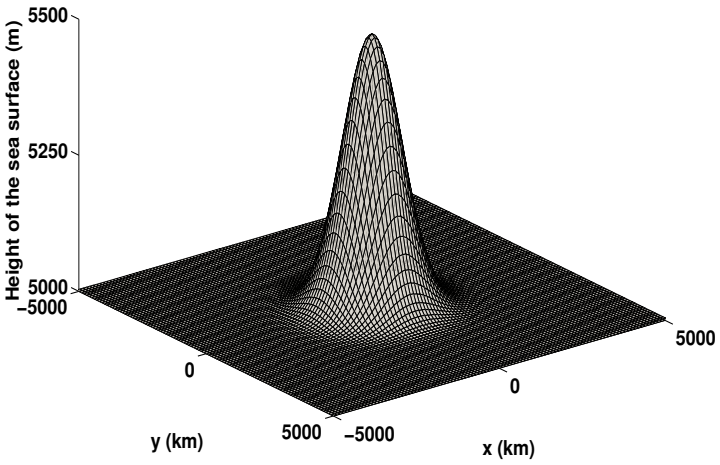

Figure 4.3: The initial sea surface, in the test case 1.

4.4.1.2 Test case 2: The barotropic vortex

The other test case is detailed in [92] for the one layer case. The multi-layer case is adapted from the single-layer one, in order to compare the results. It is defined by

$$\forall i \in [\![1,n]\!],\ \begin{cases} h_i = \frac{H_0}{n} + \frac{\hat{H}_0}{n} exp\left(-\frac{(x-L/2)^2+(y-L/2)^2}{(L/10)^2}\right), \\ u_i = -\frac{g}{f}\frac{\partial P_i}{\partial y}, \\ v_i = \frac{g}{f}\frac{\partial P_i}{\partial x}. \end{cases} \tag{4.156}$$

Moreover, $(H_0, \hat{H}_0)$ and the density ratios are equal to the values of the previous test case, respectively defined in (4.150) and (4.151). For this test case, the boundary conditions at $\partial\mathcal{D}_{ext}$ are outgoing flow conditions

$$\forall i \in [\![1,n]\!],\ \forall X\ \in \partial\mathcal{D}_{ext},\ \frac{\partial \mathbf{u}}{\partial \boldsymbol{n}} = 0.$$

The figure 4.3 shows also the initial sea surface of the single layer model, in the test case 2, with $\Delta x = 100$km. Moreover, figures 4.4 and 4.5 shows respectively the initial velocity u_1 and the initial vorticity w_1 of the upper layer, in the test case 2, with $\Delta x = 100$km.

Remark: The linearization of the single-layer and the two and four-layer models will be tested with this test case: they will permit the validation of the numerical resolution and the augmented model. Indeed, in the second test case, the linearized models have an explicit solution under the f-plane approximation, as it was noticed in [83] and [92] for the single-layer model.

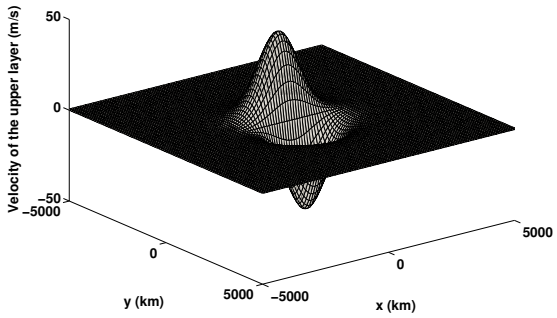

Figure 4.4: The initial velocity of the upper layer u_1, in the test case 2.

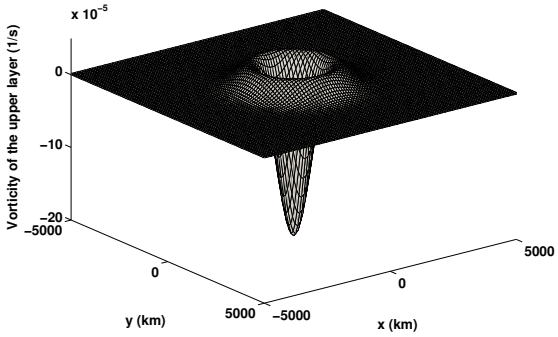

Figure 4.5: Initial vorticity of the upper layer w_1, in the test case 2.

4.4.2 The linear models

In this subsection, we consider a linearization of the multi-layer model, about the constant state

$$\mathbf{V} := {}^{\top}(H_1,\dots,H_n,U_1,\dots,U_n,V_1,\dots,V_n,W_1,\dots,W_n), \tag{4.157}$$

where ${}^{\top}(H_1,\dots,H_n,U_1,\dots,U_n,V_1,\dots,V_n,W_1,\dots,W_n) \in \mathbb{R}^{4n}$ is specified for each test case. Then, the linear model, under the f-plane assumption, is

$$\frac{\partial \tilde{\mathbf{v}}}{\partial t} + \mathsf{A}^{\mathsf{a}}_x(\mathbf{V},\boldsymbol{\gamma})\frac{\partial \tilde{\mathbf{v}}}{\partial x} + \mathsf{A}^{\mathsf{a}}_y(\mathbf{V},\boldsymbol{\gamma})\frac{\partial \tilde{\mathbf{v}}}{\partial y} + \mathsf{C}^{\mathsf{a}}(f_0)\tilde{\mathbf{v}} = 0, \tag{4.158}$$

where the new unknown vector $\tilde{\mathbf{v}}$ is defined by

$$\tilde{\mathbf{v}} := \mathbf{v} - \mathbf{V}, \tag{4.159}$$

the $4n \times 4n$ block matrices $\mathsf{A}^{\mathsf{a}}_x(\mathbf{V},\boldsymbol{\gamma})$ and $\mathsf{A}^{\mathsf{a}}_y(\mathbf{V},\boldsymbol{\gamma})$ are respectively defined in (4.40) and (4.41), and

the $4n \times 4n$ block matrix $\mathsf{C}^{\mathsf{a}}(f_0)$ is defined by

$$\mathsf{C}^{\mathsf{a}}(f_0) := \left[\begin{array}{c|c|c|c} 0 & 0 & 0 & 0 \\ \hline 0 & 0 & f_0 \mathsf{I_n} & 0 \\ \hline 0 & -f_0 \mathsf{I_n} & 0 & 0 \\ \hline 0 & 0 & 0 & 0 \end{array}\right]. \tag{4.160}$$

Remark: This linear model is not exactly the linearization of the multi-layer model. Although the differential operator is the right one, the source term is not. However, this linear model is still interesting, for the treatment of the open boundaries, as the asymptotic expansions of the eigenvalues and eigenvectors performed in the previous chapter, remain equal for this model. Moreover, if the constant state $\mathbf{V}$ verifies

$$\forall i \in [\![1,n]\!], \begin{cases} H_i > 0, \\ U_i = 0, \\ V_i = 0, \\ W_i = 0, \end{cases} \tag{4.161}$$

then, the linear model (4.158) is exactly the linearization of the multi-layer shallow water model. However, if the constant state $\mathbf{V}$ verifies

$$\forall i \in [\![1,n]\!], \begin{cases} H_i > 0, \\ U_i \neq 0, \\ V_i \neq 0, \\ W_i = 0, \end{cases} \tag{4.162}$$

the linear model (4.158) is not the linearization of the multi-layer model, but it is possible to obtain an explicit solution, as we explain it in the test case 2.

As these numerical tests are performed to validate the method, the single-layer case is compared to the studies performed in [92], [84], [102], [123] and [86]. Then, the two and four-layer cases are compared to the single-layer case.

4.4.2.1 Test case 1: The gravity wave

In this test case, we consider the propagation of a gravity wave, initialized on all the layers. The linear model is considered around the constant state $\mathbf{V}$, defined by

$$\forall i \in [\![1,n]\!], \begin{cases} H_i = \frac{H_0}{n}, \\ U_i = 0 \text{ m.s}^{-1}, \\ V_i = 0 \text{ m.s}^{-1}, \\ W_i = 0 \text{ s}^{-1}. \end{cases} \tag{4.163}$$

We compute the numerical approximation on the external domain $\mathcal{D}_{ext}$, where we assume non-permeability conditions at the boundaries

$$\forall i \in [\![1,n]\!],\ \forall X\ \in \partial\mathcal{D}_{ext},\ \begin{cases} \frac{\partial h_i}{\partial \boldsymbol{n}} = 0, \\ \boldsymbol{u_i} \cdot \boldsymbol{n} = 0, \\ \frac{\partial w_i}{\partial \boldsymbol{n}} = 0. \end{cases} \tag{4.164}$$

Consequently, the gravity wave reflects on the boundaries of $\mathcal{D}_{ext}$ to go back in the domain $\mathcal{D}$. Then, each interface is subcritical outflow, at the beginning, and becomes subcritical inflow, after the wave reflects on the boundaries of $\mathcal{D}_{ext}$.

We consider the following time and space-discretization

$$\begin{cases} \Delta t = 10 \text{ min}, \\ \Delta x = 100 \text{ km}, \end{cases} \tag{4.165}$$

and the numerical test is performed during 1 day.

In the figures 4.6–4.9, the evolution of the sea surface over the time is represented, for the single-layer model. We remind that the gravity wave goes out the interior domain $\mathcal{D}$, reflects on the walls of the exterior domain $\mathcal{D}_{ext}$ and comes back in $\mathcal{D}$.

In the figure 4.10, the evolution of the four diagnostic quantities are shown, for the linear models and in the first test case. The major part of the error is generated by the gravity wave going out the interior domain (from 6hrs to 10hrs) and by the same gravity wave going back in the interior domain, after reflecting on the walls of the large domain (from 18hrs to 24hrs). The errors on the sea surface, the energy and the vorticity prove the incoming wave generates greater errors than the outgoing one. However, even if this is already true for the single-layer model, the incoming wave generates a greater error for the two and four-layer models.

Moreover, it is clear that the treatment of the open boundaries for the two and four-layer models is not as efficient as the treatment for the single-layer. This is due to the exact expression of the eigenvalues and eigenvectors for the single-layer, and the approximation of these quantities for the multi-layer models. As we do not know the exact eigenstructure of the multi-layer models, the lack of exact expression generates a greater error than in the single-layer case. However, even if there is a gap between the single-layer model and the multi-layer ones, the behavior of the two and four-layer models are very close.

Remarks: 1) The behavior of the mean divergence are very close for each models. Moreover, this behavior is coherent with the numerical results presented in [92]. 2) We performed computation with boundary conditions as simple as possible, in order to quantify the gain of our work. These simple boundary conditions are such that we impose on the velocities the interior field and to the heights the

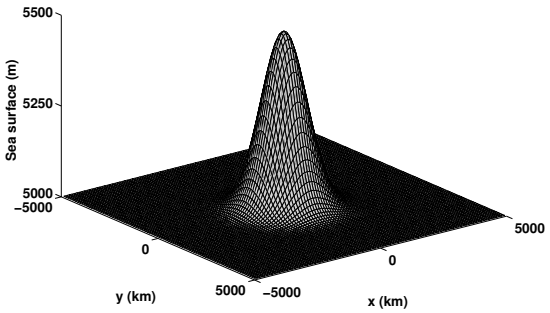

Figure 4.6: Sea surface at $t = 0$h.

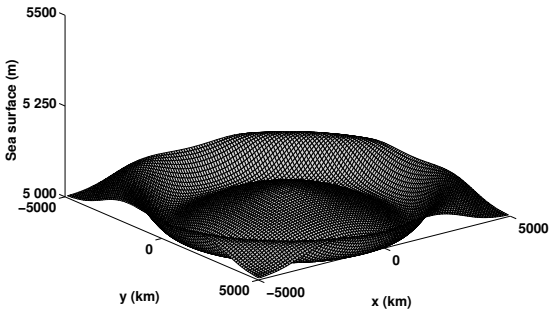

Figure 4.7: Sea surface at $t = 6$h.

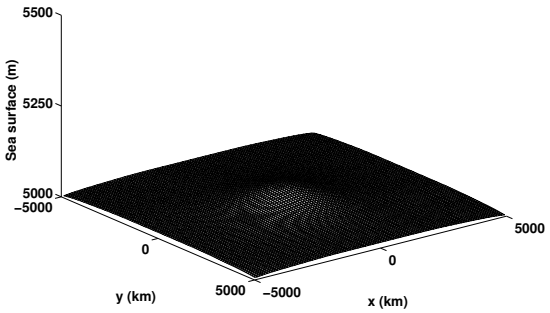

Figure 4.8: Sea surface at $t = 12$h.

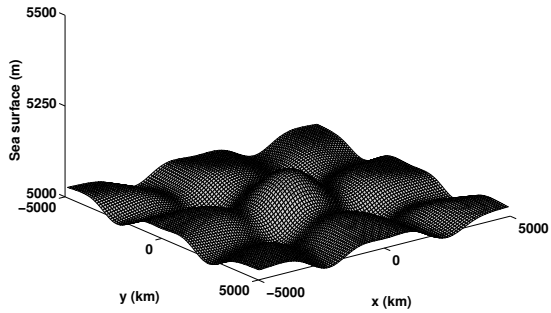

Figure 4.9: Sea surface at $t = 24$h.

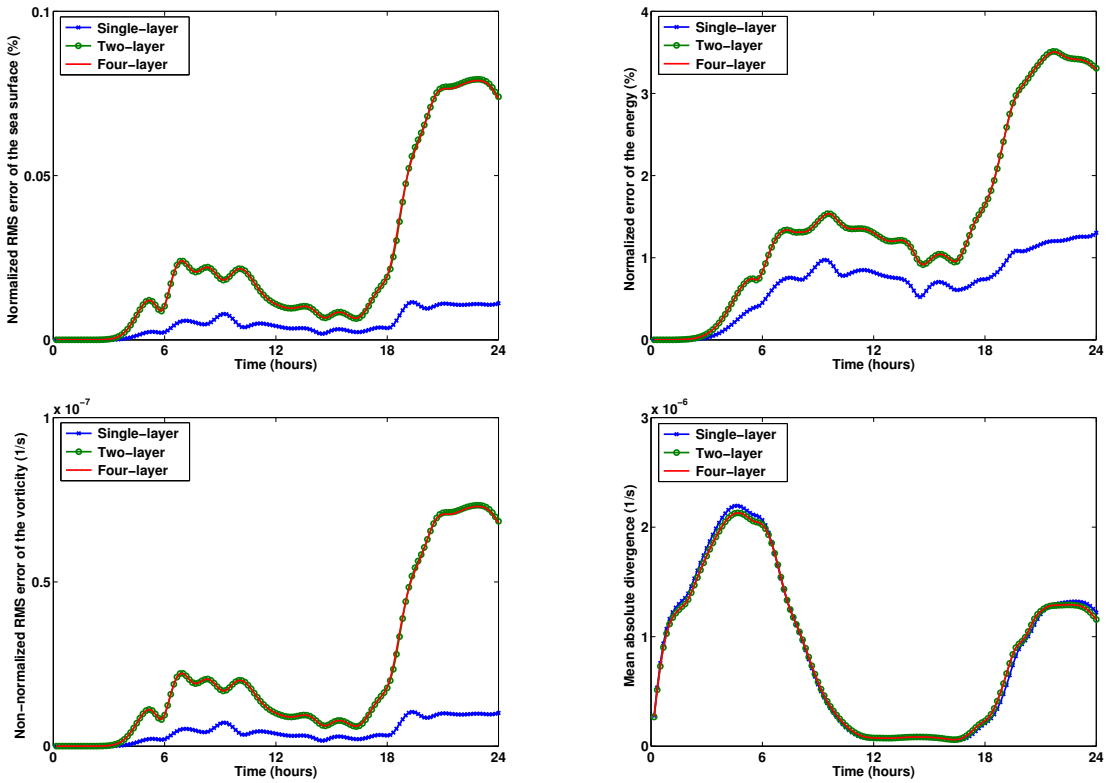

Figure 4.10: Evolution of the diagnostic quantities (linear models and test case 1)

exterior field (with no condition on the sign on the eigenvalues). It appears that our method generates an error twice as small as these simple boundary conditions.

4.4.2.2 The barotropic vortex

In this test case, we consider the propagation of a barotropic vortex. The linear model is considered around the constant state $\mathbf{V}$, defined by

$$\forall i \in [\![1,n]\!], \begin{cases} H_i = \frac{H_0}{n}, \\ U_i = -50 \text{ m.s}^{-1}, \\ V_i = -50 \text{ m.s}^{-1}, \\ W_i = 0 \text{ s}^{-1}. \end{cases} \tag{4.166}$$

We compute the numerical approximation on the external domain $\mathcal{D}_{ext}$, where we assume outgoing flow conditions at the boundaries

$$\forall i \in [\![1,n]\!], \ \forall X \ \in \partial\mathcal{D}_{ext}, \ \frac{\partial \mathbf{u}}{\partial \boldsymbol{n}} = 0. \tag{4.167}$$

Consequently, the vortex goes out the large domain $\mathcal{D}_{ext}$. In this test case, when the vortex arrives at the boundaries of the small domain $\mathcal{D}$, the free surface is in

- a subcritical outflow regime at the Southern and Western boundaries,
- a subcritical inflow regime at the Northern and Eastern boundaries,

and the interfaces liquid/liquid are in

- a supercritical outflow regime at the Southern and Western boundaries,
- a supercritical inflow regime at the Northern and Eastern boundaries.

We consider the following time and space-discretization

$$\begin{cases} \Delta t = 5 \text{ min}, \\ \Delta x = 100 \text{ km}, \end{cases} \tag{4.168}$$

and the numerical test is performed during 2 days, in order to get the barotropic vortex completely out the interior domain.
In the figures 4.11–4.13, the evolution of the sea surface over the time is represented, for the single-layer model. We remind that the barotropic vortex goes out the interior domain $\mathcal{D}$ and then out the exterior domain $\mathcal{D}_{ext}$. It does not come back in $\mathcal{D}$.
In the figure 4.15, the evolution of the four diagnostic quantities are shown, for the linear models and in the second test case. Compared with the gravity wave, this test case generates a greater error on the

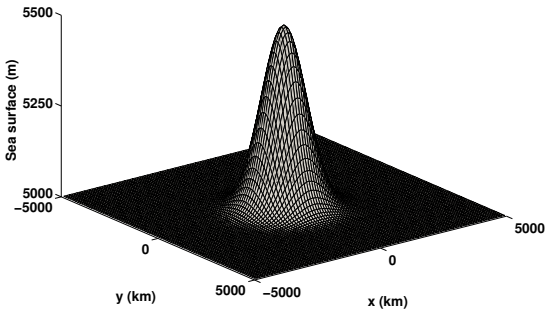

Figure 4.11: Sea surface at $t = 0$h.

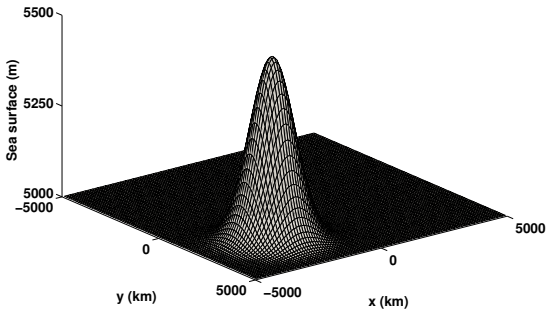

Figure 4.12: Sea surface at $t = 12$h.

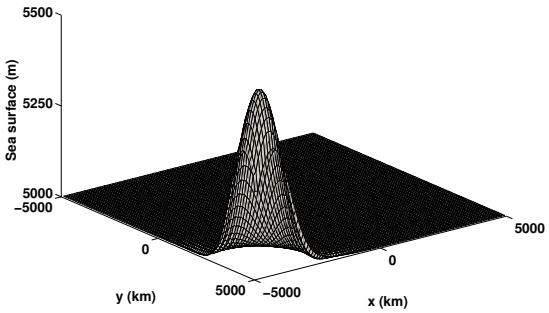

Figure 4.13: Sea surface at $t = 24$h.

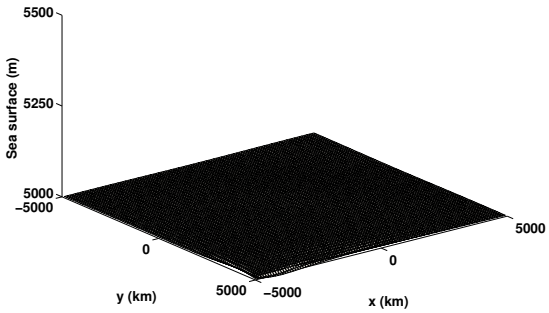

Figure 4.14: Sea surface at $t = 48$h.

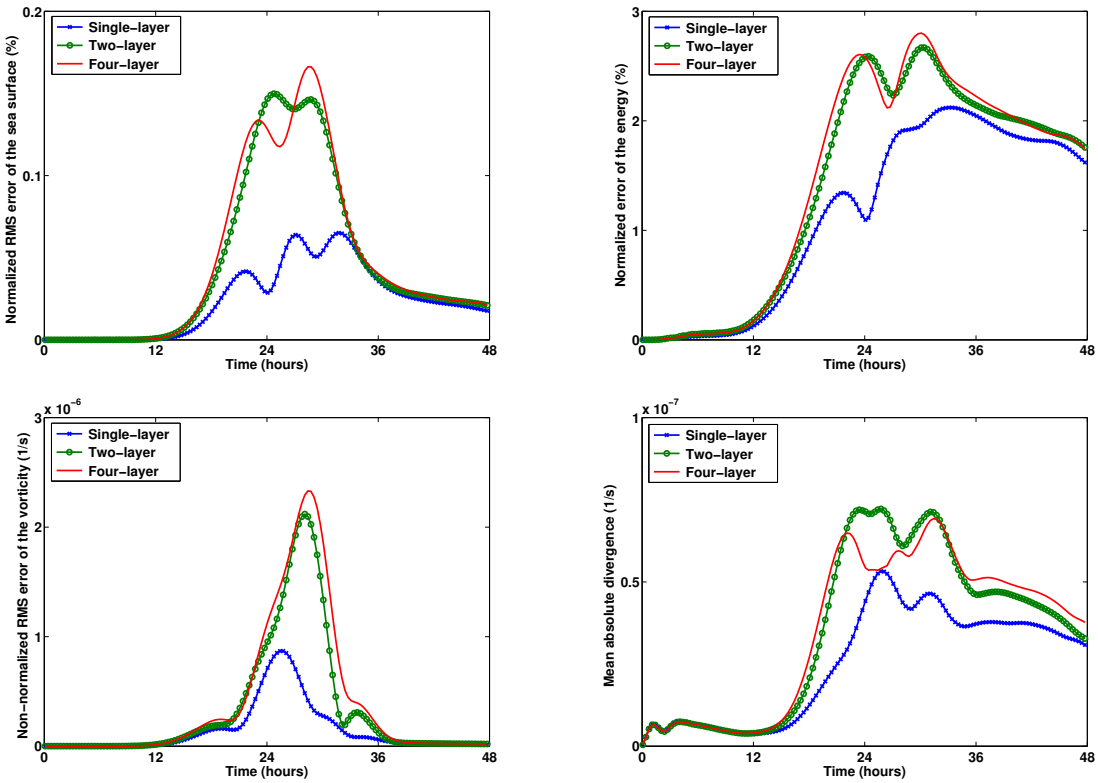

Figure 4.15: Evolution of the diagnostic quantities (linear models and test case 2)

sea surface but not on the total energy. Moreover, there is still a gap between the single-layer model and the multi-layer ones, but the two and four-layer models does not get the exact same behavior.
This simulation is particularly interesting because there exists an explicit solution of the associated *Cauchy* problem:

$$\forall i \in [\![1,n]\!],\ \begin{cases} h_i = \frac{H_0}{n} + \frac{\hat{H}_0}{n} exp\left(-\frac{(x-L/2-U_i t)^2+(y-L/2-V_i t)^2}{(L/10)^2}\right), \\ u_i = -\frac{g}{f_0}\frac{\partial P_i}{\partial y}, \\ v_i = \frac{g}{f_0}\frac{\partial P_i}{\partial x}. \end{cases} \tag{4.169}$$

where we remind that P_i is defined by

$$P_i := \sum_{k=1}^{n} g\alpha_{i,k} h_k. \tag{4.170}$$

At time $t = 48$ hrs, the errors between the approximated and the exact solutions are, for the four-layer model,

- 0.4 % for the normalized RMS error of the sea surface,
- 0.02 m.s^{-1} for the non-normalized RMS error of the velocity in x-direction, averaged over the total height,
- 0.02 m.s^{-1} for the non-normalized RMS error of the velocity in y-direction, averaged over the total height,
- 1.6×10^{-6} s^{-1} for the non-normalized RMS error of the vorticity, averaged over the total height.

To sum up, this confirms that for every layer $i \in [\![1,n]\!]$, the unknown w_i in the augmented models corresponds to the vorticity of the non-augmented model, in this layer.

4.4.3 The non-linear models

In this subsection, the general non-linear models are considered. As in the previous subsection, the same test cases are considered, under the approximation of β-plane.

4.4.3.1 The gravity wave

We consider the propagation of a gravity wave, going out the small domain, reflecting on the walls of the large domain and then coming back in the small domain. The numerical simulations are performed with non-permeability conditions on the boundaries of the domain $\mathcal{D}_{ext}$, the following time and space-discretization

$$\begin{cases} \Delta t = 10 \text{ min}, \\ \Delta x = 100 \text{ km}, \end{cases} \tag{4.171}$$

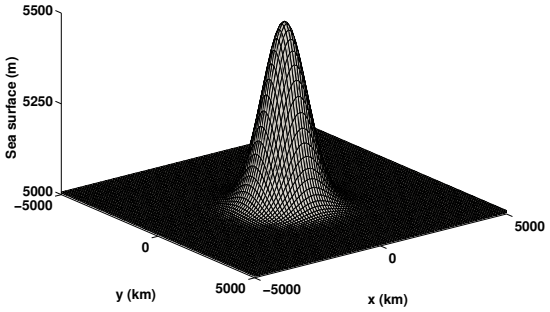

Figure 4.16: Sea surface at $t = 0$h.

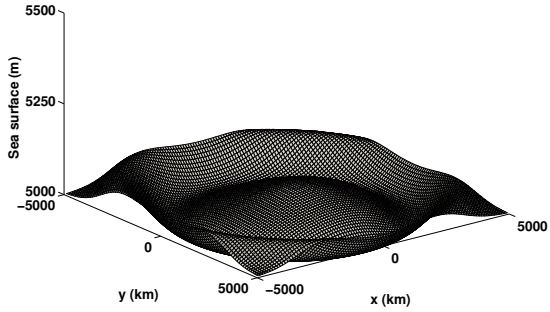

Figure 4.17: Sea surface at $t = 6$h.

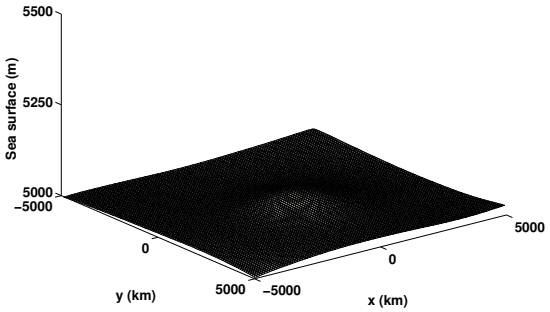

Figure 4.18: Sea surface at $t = 12$h.

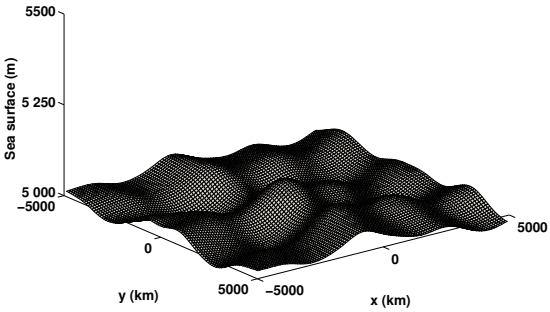

Figure 4.19: Sea surface at $t = 24$h.

and during 1 day.

In the figures 4.16–4.19, the evolution of the sea surface over the time is represented, for the single-layer model. The behavior is a little bit different from the linear case, because of the β-plane approximation: there is no symmetry anymore.

In the figure 4.20, the evolution of the four diagnostic quantities are shown, for the non-linear models and in the first test case. As with the linear models, the major part of the error is generated by the gravity wave going out the interior domain (from 6hrs to 10hrs) and by the same gravity wave going back in the interior domain, after reflecting on the walls of the large domain (from 18hrs to 24hrs). The errors on the sea surface, the energy and the vorticity prove the incoming wave generates greater errors than the outgoing one. However, even if this is already true for the single-layer model, the incoming wave generates a greater error for the two and four-layer models. Moreover, compared with the linear case, the error generated for the treatment of the open boundaries, with the non-linear models, is smaller. In this test case, the behavior of the two and the four -layer models are almost exactly the same.

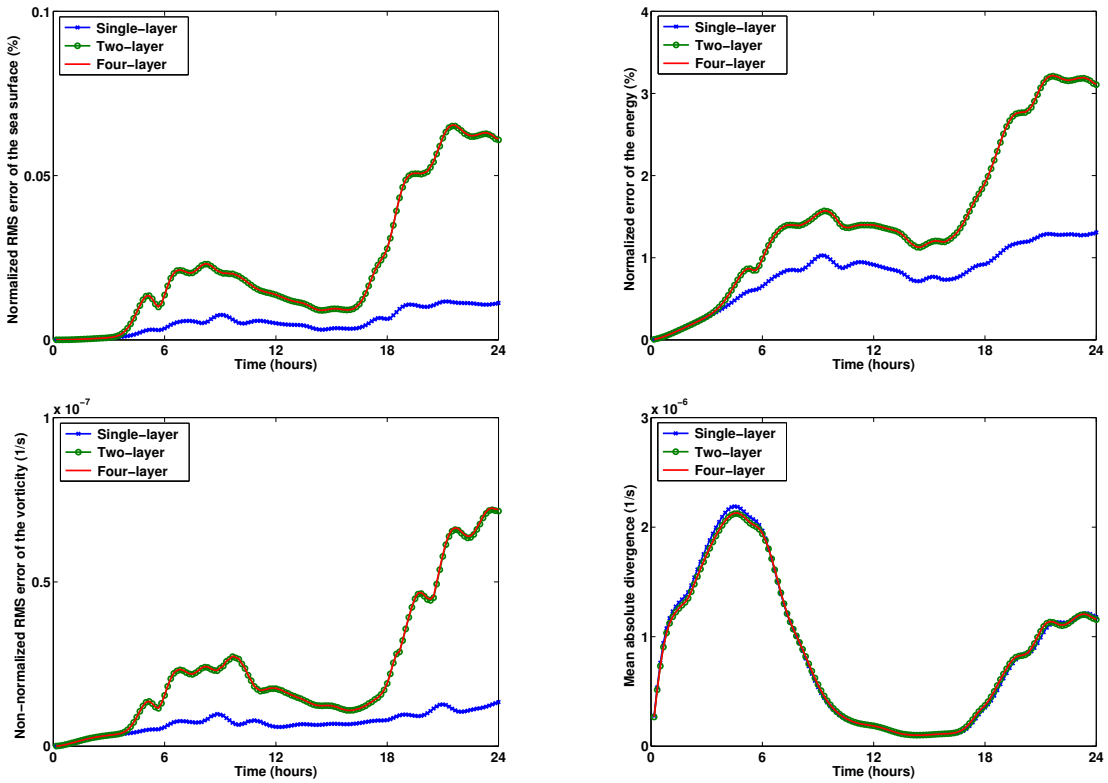

Figure 4.20: Evolution of the diagnostic quantities (non-linear models and test case 1)

4.4.3.2 The barotropic vortex

We consider the propagation of a barotropic vortex in the small domain. The numerical simulations are performed with outgoing conditions on the boundaries of the domain $\mathcal{D}_{ext}$, the following time and space-discretization

$$\begin{cases} \Delta t = 5 \text{ min}, \\ \Delta x = 100 \text{ km}, \end{cases} \tag{4.172}$$

and during 2 days.

In the figures 4.21–4.23, the evolution of the sea surface over the time is represented, for the single-layer model. There is a major difference with the linear case: the vortex has a very small transport velocity. Indeed, in the linear case, we chose this velocity with the constant ${}^{\top}(U_i, V_i)$. In the non-linear one, the vortex moves because of the *Coriolis* force, which generates a small velocity. Note that the barotropic vortex has a long-time existence: it is possible to observe it going out the interior domain $\mathcal{D}$. However, we did not compute a sufficiently long simulation here to observe this phenomenon.

Note that the behavior of the barotropic vortex with the non-linear model is very different compared with the linear model: it is not anymore exactly conserved and

In the figure 4.25, the evolution of the four diagnostic quantities are shown, for the non-linear models and in the second test case. As in the linear case, the two and four-layer models does not get the exact behavior. Moreover, the error generated with the four-layer model is bigger than the two-layer one. However, as the simulation has been performed during two days, the barotropic vortex stayed in the interior domain and the percentage of errors are very small.

To conclude, the general behavior of various diagnostic quantities , in the treatment of the open boundaries, has been clarified in this section, with particular test cases and set of parameters. The errors induced by the multi-layer models are greater than the one of the single-layer model.

4.5 Conclusion and perspectives

The multi-layer model with free-surface describes complex fluid systems. Moreover, to provide a precise underwater forecast, the approximation of this model is not performed on the entire ocean but on a particular part. This induces artificial boundaries.

We clarified the conditions to impose at the open boundaries. These conditions are not exact but asymptotically exact, when the system is weakly stratified in density and velocity. An interesting fact is the error generated with the multi-layer models is always greater than the one with the single-layer model. Consequently, it could be interesting to understand the link between the parameter ε, which controls the density-stratifiaction, and the error generated for the multi-layer model.

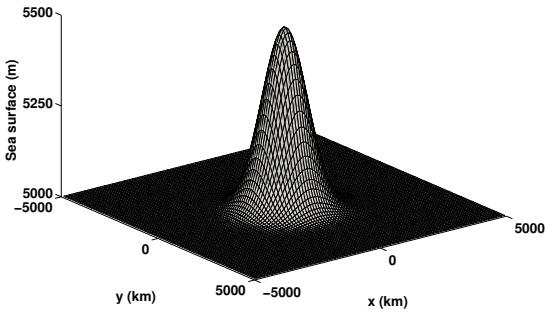

Figure 4.21: Sea surface at $t = 0$h.

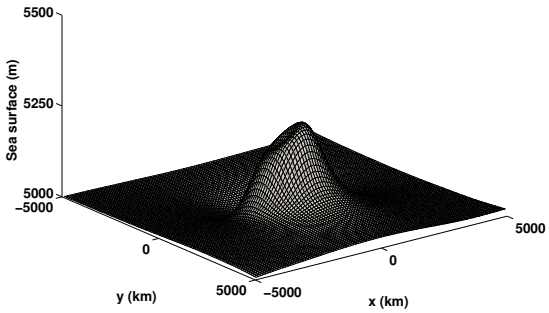

Figure 4.22: Sea surface at $t = 12$h.

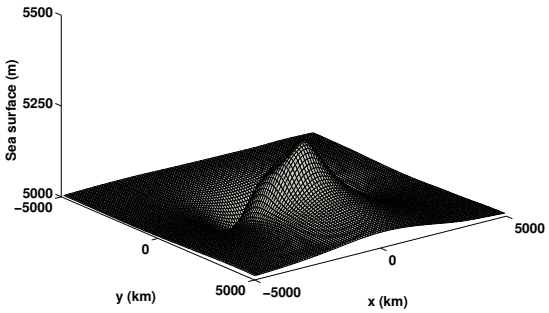

Figure 4.23: Sea surface at $t = 24$h.

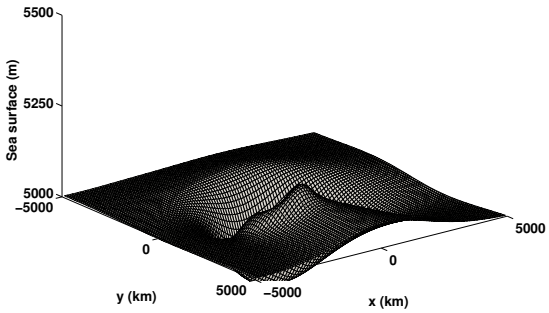

Figure 4.24: Sea surface at $t = 48$h.

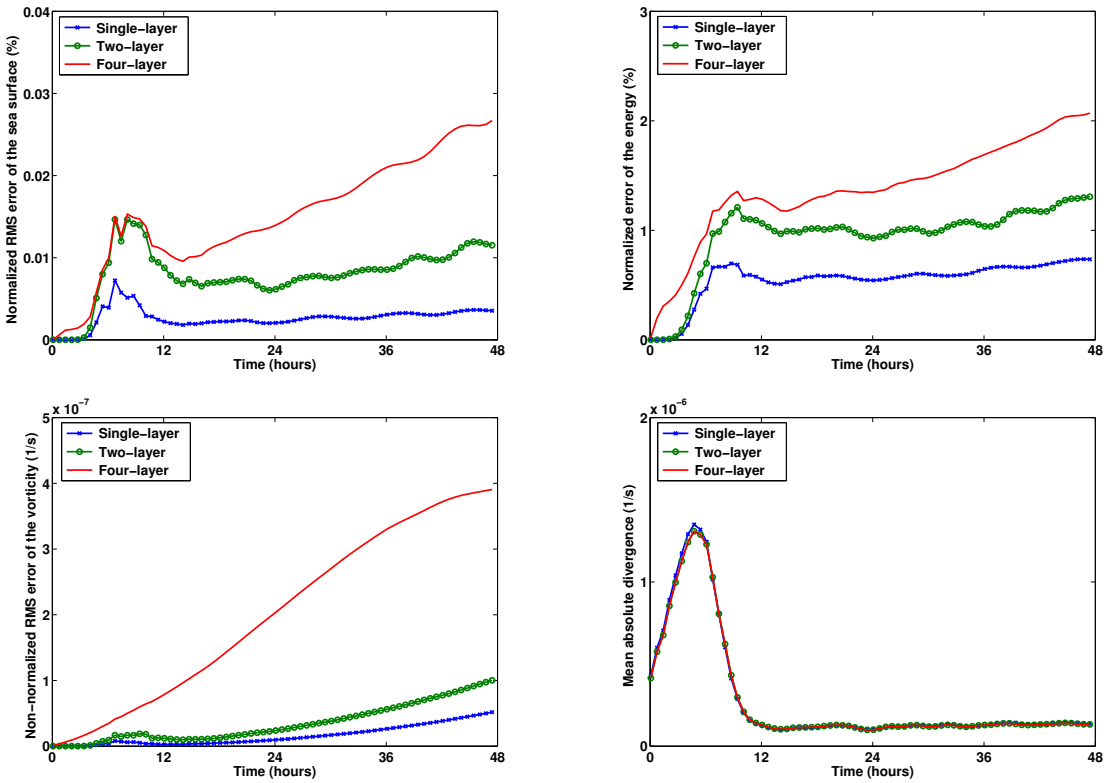

Figure 4.25: Evolution of the diagnostic quantities (non-linear models and test case 2)

Moreover, another point, which would be fascinating to underline, is the validity of the assumptions made in the previous chapter:

- σ is injective,
- the ratio of the thickness, between two consecutive layers, is bounded.

Finally, a comparison of the treatment of the open boundaries, with the asymptotic expansions performed in [50] and the ones proved in the previous chapter, would be really interesting.

Ce qui n'est que difficile ne plaît point à la longue.
Candide ou l'Optimisme, Voltaire, 1759.

Conclusion

Dans ce chapitre, le traitement des frontières ouvertes, pour le modèle de *Saint-Venant* multi-couches, a été détaillé, dans le cas d'un domaine quelconque. Pour les modes barotropes, la condition de *Flather*, introduite dans [49], a été généralisé dans le cas du modèle faiblement stratifiée en densité. Dans cette asymptotique, les conditions limites a prescrire, associées aux modes barotropes, ont aussi été minutieusement décrites.

Après avoir explicité le cas particulier d'un domaine rectangulaire, une comparaison complète, des erreurs générées aux frontières ouvertes, a été effectuée avec :

- deux cas tests : une onde de gravité et un vortex barotrope,
- trois modèles : 1, 2 et 4 couches,
- les modèles linéarisés et non-linéaires.

Bien que les modèles de *Saint-Venant* multi-couches décrivent un système plus complexe et décrivent donc plus précisément le comportement d'un tel système de fluides, l'erreur dans le cas des modèles multi-couches, généré par le traitement des conditions limites ouvertes, reste toujours supérieure à celle du modèle à une couche.
Enfin, la différence d'erreur, entre le modèle à 2 couches et celui à 4 couches, est minime. Dans le cas d'une onde de gravité, elles sont identiques alors que pour le vortex barotrope l'erreur du modèle à 4 couches est légèrement supérieure.

5

Conclusion et perspectives

Contents

5.1 Conclusion

D'innombrables savants, marins, ingénieurs et inventeurs ont tenté de décrypter les océans. Ils les ont explorés, ils ont mesuré ses courants et ses vents, tracé des cartes, construit des navires toujours plus rapides, des submersibles aux prouesses abyssales. Outre les aventures ou mésaventures des différents explorateurs, les océanographes, les physiciens et les mathématiciens ont permis le développement des dispositifs actuels d'aide à la navigation, de télécommunication, de propulsion. De plus, il ont joué un rôle de premier plan pour rendre les prévisions marines efficaces et pertinentes. Par exemple, le développement des technologies modernes ces dernières décennies, notamment l'imagerie satellitale, ont permis une amélioration accrue de la météo marine.

La compréhension des océans est une conquête millénaire. Cependant, les mers sont souvent difficilement accessibles et la connaissance de la mécanique des eaux marines n'est pas encore complète. La dynamique océanique dissimule encore de nombreux secrets que les scientifiques actuels tentent de révéler au grand jour. En effet, les modèles les plus précis, tels que les équations de *Navier-Stokes*, sont trop complexes à mettre en œuvre dans un contexte opérationnel. Dans ce manuscrit, toute l'attention a été portée sur un modèle simplifié : le modèle de *Saint-Venant* multi-couches à surface libre. Dans le cas à une couche, ce modèle a été étudié, de manière exhaustive, depuis presque 150 ans dans [113]. Le cas à deux couches n'est pas encore totalement connu (voir les études récentes dans [43] et [44]) et le cas général à n couches, $n \geq 3$, a été relativement peu étudié (se référer aux

résultats de [125], [126] et [127]).

Le SHOM est chargé des prévisions marines opérationnelles. Le code de calcul HYCOM, développé et utilisé par le SHOM, est principalement basé sur le modèle *Saint-Venant* multi-couches. Les moyens de calcul actuels ne sont pas illimités et que l'attention veut être portée sur certaines zones des océans particulières comme les côtes. Ainsi, il est nécessaire d'introduire des frontières artificielles. Le SHOM a alors besoin de méthodes mathématiques pour traiter ces frontières factices afin qu'elles ne polluent pas les prévisions marines. Cette problématique est donc au cœur des préoccupations du SHOM.

Dans cette thèse doctorale, afin d'améliorer le traitement des frontières ouvertes, de nouveaux résultats ont été prouvés pour le modèle bi-couches rotationnel ainsi que pour le modèle général à n couches.

Dans la première partie de ce manuscrit, l'hyperbolicité et le caractère bien-posé, du modèle bi-couches, ont été prouvés. Les éléments propres de l'opérateur différentiel, associé au modèle, ont pu être caractérisés dans une asymptotique de faible stratification en densité. Une différence majeure, entre le modèle à une dimension d'espace et le modèle à deux dimensions, a été mise en exergue : le domaine d'hyperbolicité n'est borné que dans le second cas. Enfin, un nouveau modèle bi-couches a été introduit, dont le principal atout réside dans la conservativité, sans dégrader les avantages du modèle initial. Il a été démontré que la solution de ce modèle généralise la solution du modèle initial, permettant ainsi de s'affranchir du choix d'un *chemin conservatif* lors de la résolution numérique (voir les détails dans [36], [99] et [2]).

Dans la seconde section, les résultats de la première partie, ainsi que leurs preuves, ont été généralisés au modèle à n couches :

- l'hyperbolicité et le caractère bien-posé du modèle général ont été prouvés à l'aide d'un premier critère explicite, basé sur la symétrisabilité des equations,
- différents cas dégénérés ont été analysés afin de mettre en relief une première condition nécessaire d'hyperbolicité,
- afin de poursuivre les développements, un régime asymptotique particulier a été considéré : toutes les couches ont une hauteurs similaires et les sauts de densité entre les couches sont supposés faibles et représentées par une application injective.

L'analyse de l'opérateur différentiel associé au modèle a permis de mettre en valeur la structure de ses éléments propres. Celle-ci est remarquable car pour chaque interface liquide/liquide, les éléments propres associés sont similaires à ceux de l'interface interne d'un modèle bi-couches. Enfin, le modèle augmenté du rotationnel a été introduit dans le cas général à n couches. Outre le caractère conservatif de ce nouveau modèle, le caractère localement bien-posé et l'hyperbolicité du modèle ont été démontré. De plus, il a été démontré que les solution des deux modèles, non-augmenté et augmenté de la vorticité, sont égales si les conditions initiales sont égales et suffisamment régulières.

Dans la troisième et dernière partie, nous avons effectué la validation numérique du traitement des conditions limites transparentes à l'aide des éléments démontrés dans les deux parties précédentes. En effet, les développements asymptotiques des éléments propres de l'opérateur différentiel associé au modèle permettent d'envisager le traitement des frontières artificielles à l'aide de la méthode des caractéristiques, rappelée dans l'introduction de ce manuscrit. Tout d'abord, le caractère bien-posé du problème initial aux limites, associé au modèle de *Saint-Venant* multi-couches, a été démontré. Les conditions limites à prescrire ont été explicitées dans un cas particulier :

- le domaine considéré est un rectangle
- les modes barotropes et baroclines sont en régime sous-critique sortant pour les frontières Nord et Est, sous-critique entrant pour les frontières Sud et Ouest.

Enfin, le traitement des frontières artificielles a été analysé et validé avec différentes configurations :

- deux cas tests : une onde de gravité et un vortex barotrope,
- trois modèles : 1, 2 et 4 couches.

Cette thèse a donc permis de démontrer plusieurs résultats sur la symétrisabilité et l'hyperbolicité du modèle de *Saint-Venant* multi-couches à surface libre. Ces développements ont induit une méthode de traitement des frontières ouvertes lors de la résolution numérique. Cette méthode a été basée sur la méthode des caractéristiques ainsi que sur les développements asymptotiques prouvés dans les deux premières parties de ce manuscrit. Cependant, l'étude est loin d'être exhaustive et de nombreux autres résultats restent en suspens.

5.2 Perspectives

Cette étude a donc mis en évidence des conditions limites simples, permettant le traitement des frontières transparentes, pour le modèle de *Saint-Venant* multi-couches à surface libre. Non seulement les résultats prouvés dans ce rapport de thèse ont permis de répondre à certaines interrogations,

mais ils ont aussi soulevés de nombreuses questions nouvelles.

Certaines problématiques apparaissent comme conséquence directe du travail effectué durant cette thèse :

- ◇ il serait intéressant d'étudier le développement des éléments propres de l'opérateur différentiel, associé au modèle de *Saint-Venant* multi-couches, dans un régime asymptotique plus général. Par exemple, sans hypothèse sur les hauteurs d'eau de chaque couche,
- ◇ de même, l'analyse du comportement du modèle et des éléments étudiés précédemment, lorsque n tend vers $+\infty$, a un intérêt certain,
- ◇ de plus, il serait pertinent de déterminer l'existence ou non d'invariants de *Riemann*, pour le modèle non-linéaire général à n couches,
- ◇ finalement, l'implémentation et la validation des conditions limites ouvertes dans un code de calcul opérationnel tel que HYCOM.

D'autres problématiques liées au modèle de *Saint-Venant* multi-couches sont apparues au gré de la lecture d'articles sur le sujet :

- ◇ l'étude de la justification rigoureuse du modèle bi-couches rotationnel comme modèle asymptotique issu des équations d'*Euler*, notamment avec l'aide des preuves effectuées pour la justification du modèle à une couche rotationnel [26], ainsi que celle pour le modèle à deux couches irrotationnel [41],
- ◇ le développement et la démonstration de l'existence de solution en temps long pour le modèle de *Saint-Venant* multi-couches, en présence de vorticité, comme développé dans [33] pour le modèle à une couche.

Le modèle de *Saint-Venant* multi-couches à surface libre est un modèle océanique qui dissimule encore de nombreux secrets. Bien que son expression soit simple, les nombreux paramètres qu'il contient rendent encore inaccessibles certains développement théoriques. Cependant, les résultats démontrés pour ce modèle, dans cette thèse, est caractéristique des sciences actuelles et futures. En effet, la collaboration pluridisciplinaire ainsi que le décloisonnement des échanges scientifiques ont permis de repousser les frontières de la connaissance.

Ce qui n'est que difficile ne plaît point à la longue.
Candide ou l'Optimisme, Voltaire, 1759.

Figure 5.1: Kanagawa-oki nami-ura (La grande vague de Kanagawa), Hokusai, 1830-1831

References

[1] ABGRALL, R. & KARNI, S. 2009 Two-layer shallow water system: a relaxation approach. *SIAM Journal on Scientific Computing* **31** (3), 1603–1627. 52, 54, 72, 96, 102, 114

[2] ABGRALL, R. & KARNI, S. 2010 A comment on the computation of non-conservative products. *Journal of Computational Physics* **229** (8), 2759–2763. 40, 184

[3] ALVAREZ-SAMANIEGO, B. & LANNES, D. 2007 A nash-moser theorem for singular evolution equations. application to the serre and green-naghdi equations. *arXiv preprint math/0701681* . 16, 36, 68

[4] AUDUSSE, E. 2005 A multilayer saint-venant model: derivation and numerical validation. *Discrete Contin. Dyn. Syst. Ser. B* **5** (2), 189–214. 59, 68, 71

[5] AUDUSSE, E., BRISTEAU, M.O., PERTHAME, B. & SAINTE-MARIE, J. 2011 A multilayer saint-venant system with mass exchanges for shallow water flows. derivation and numerical validation. *ESAIM: Mathematical Modelling and Numerical Analysis* **45** (01), 169–200. 18, 68

[6] AUDUSSE, E., BRISTEAU, M.-O., PELANTI, M. & SAINTE-MARIE, J. 2011 Approximation of the hydrostatic navier–stokes system for density stratified flows by a multilayer model: kinetic interpretation and numerical solution. *Journal of Computational Physics* **230** (9), 3453–3478. 68

[7] BARNIER, B., MARCHESIELLO, P., DE MIRANDA, A.P., MOLINES, J.M. & COULIBALY, M. 1998 A sigma-coordinate primitive equation model for studying the circulation in the south atlantic. part i: Model configuration with error estimates. *Deep Sea Research Part I: Oceanographic Research Papers* **45** (4), 543–572. 22

[8] BARROS, R. 2006 Conservation laws for one-dimensional shallow water models for one and two-layer flows. *Mathematical Models and Methods in Applied Sciences* **16** (01), 119–137. 55, 115

[9] BARROS, R. & CHOI, W. 2008 On the hyperbolicity of two-layer flows. Proceedings of the 2008 Conference on FACM08 held at New Jersey Institute of Technology. 47, 96, 102

[10] BATCHELOR, G.K. 2000 *An introduction to fluid dynamics*. Cambridge university press. 14

[11] BENKHALDOUN, F., SARI, S. & SEAID, M. 2014 A simple multi-layer finite volume solver for density-driven shallow water flows. *Mathematics and Computers in Simulation* **99**, 170–189. 134

[12] BENZONI-GAVAGE, S. & SERRE, D. 2007 *Multi-dimensional hyperbolic partial differential equations*. Clarendon Press Oxford. 40, 41, 74, 75, 144, 145, 158

[13] BERENGER, J.P. 1994 A perfectly matched layer for the absorption of electromagnetic waves. *Journal of computational physics* **114** (2), 185–200. 24

[14] BLAYO, E. & DEBREU, L. 2005 Revisiting open boundary conditions from the point of view of characteristic variables. *Ocean modelling* **9** (3), 231–252. 22, 53, 57, 125, 158

REFERENCES

[15] BONNET, A. & LUNEAU, J. 1989 Théories de la dynamique des fluides. *Cepadues editions* . 14

[16] BOONKASAME, A. & MILEWSKI, P. 2011 Nonlinear stability of two-layer shallow water flows. *Preprint available at http://www. math. wisc. edu/milewski* . 47

[17] BOUCHUT, F. & MORALES DE LUNA, T. 2008 An entropy satisfying scheme for two-layer shallow water equations with uncoupled treatment. *ESAIM: Mathematical Modelling and Numerical Analysis* **42** (04), 683–698. 72, 134

[18] BOUSQUET, A., PETCU, M., SHIUE, M.-C., TEMAM, R. & TRIBBIA, J. 2013 Boundary conditions for limited area models based on the shallow water equations. *Communications in Computational Physics* **14**, 664–702. 125

[19] BRESCH, D. & RENARDY, M. 2013 Kelvin–helmholtz instability with a free surface. *Zeitschrift für angewandte Mathematik und Physik* **64** (4), 905–915. 47

[20] BROWNING, G.L. & KREISS, H.O. 1986 Scaling and computation of smooth atmospheric motions. *Tellus A* **38** (4), 295–313. 25

[21] BROWNING, G. & KREISS, H.-O. 1982 Initialization of the shallow water equations with open boundaries by the bounded derivative method. *Tellus* **34** (4), 334–351. 25, 69, 158

[22] BRUNEAU, C.H. 2000 Boundary conditions on artificial frontiers for incompressible and compressible navier-stokes equations. *ESAIM: Mathematical Modelling and Numerical Analysis* **34** (02), 303–314. 25

[23] BRUNEAU, C.H. & CREUSÉ, E. 2001 Towards a transparent boundary condition for compressible navier–stokes equations. *International journal for numerical methods in fluids* **36** (7), 807–840. 25

[24] CAMERLENGO, A.L. & O'BRIEN, J.J. 1980 Open boundary conditions in rotating fluids. *Journal of Computational Physics* **35** (1), 12–35. 22

[25] CARPENTER, K.M. 1982 Note on the paper radiation conditions for the lateral boundaries of limited-area numerical models. *Quarterly Journal of the Royal Meteorological Society* **108** (457), 717–719. 22

[26] CASTRO, A. & LANNES, D. 2014 Well-posedness and shallow-water stability for a new hamiltonian formulation of the water waves equations with vorticity. *ArXiv e-prints 1402.0464* . 16, 36, 68, 186

[27] CASTRO, M., FRINGS, J., NOELLE, S., PARÉS, C. & PUPPO, G. 2010 *On the hyperbolicity of two-and three-layer shallow water equations*. Inst. für Geometrie und Praktische Mathematik. 18, 59, 68

[28] CASTRO, M.J., GARCÍA-RODRÍGUEZ, J.A., GONZÁLEZ-VIDA, J.M. & PARÉS, C. 2008 Solving shallow-water systems in 2d domains using finite volume methods and multimedia sse instructions. *Journal of Computational and Applied Mathematics* **221** (1), 16–32. 134

[29] CASTRO DÍAZ, M.J., CHACÓN REBOLLO, T., FERNÁNDEZ-NIETO, E.D. & PARES, C. 2007 On well-balanced finite volume methods for nonconservative nonhomogeneous hyperbolic systems. *SIAM Journal on Scientific Computing* **29** (3), 1093–1126. 134

[30] CASTRO-DÍAZ, M.J., FERNÁNDEZ-NIETO, E.D., GONZÁLEZ-VIDA, J.M. & PARÉS-MADROÑAL, C. 2011 Numerical treatment of the loss of hyperbolicity of the two-layer shallow-water system. *Journal of Scientific Computing* **48** (1-3), 16–40. 46, 71, 96, 102

[31] CHASSIGNET, E.P., HURLBURT, H.E., SMEDSTAD, O.M., HALLIWELL, G.R., HOGAN, P.J., WALLCRAFT, A.J., BARAILLE, R. & BLECK, R. 2007 The hycom (hybrid coordinate ocean model) data assimilative system. *Journal of Marine Systems* **65** (1), 60–83. 18

[32] CHATELIN, R. 2013 Méthodes numériques pour l'écoulement de stokes 3d: fluides à viscosité variable en géométrie complexe mobile; application aux fluides biologiques. PhD thesis, Université Paul Sabatier-Toulouse III. 8

[33] CHENG, B. & TADMOR, E. 2008 Long-time existence of smooth solutions for the rapidly rotating shallow-water and euler equations. *SIAM Journal on Mathematical Analysis* **39** (5), 1668–1685. 186

[34] CHUMAKOVA, L., MENZAQUE, F., MILEWSKI, P., ROSALES, R., TABAK, E. & TURNER, C. 2009 Stability properties and nonlinear mappings of two and three-layer stratified flows. *Studies in Applied Mathematics* **122** (2), 123–137. 72

[35] CORDIER, S., LE, M.H. & MORALES DE LUNA, T. 2011 Bedload transport in shallow water models: Why splitting (may) fail, how hyperbolicity (can) help. *Advances in Water Resources* **34** (8), 980–989. 134

[36] DAL MASO, G., LEFLOCH, P.G. & MURAT, F. 1995 Definition and weak stability of nonconservative products. *Journal de mathématiques pures et appliquées* **74** (6), 483–548. 40, 59, 125, 184

[37] DARBLADE, G., BARAILLE, R., LE ROUX, A.Y., CARTON, X. & PINCHON, D. 1997 Conditions limites non réfléchissantes pour un modele de saint-venant bidimensionnel barotrope linéarisé. *Comptes Rendus de l'Académie des Sciences-Series I-Mathematics* **324** (4), 485–490. 24

[38] DARWIN, C. 1839 *The Zoology of the Voyage of HMS Beagle: Under the Command of Captain Fitzroy, RN, During the Years 1832 to 1836...*. Smith, Elder and Company. 9

[39] DAVIES, H.C. 1976 A lateral boundary formulation for multi-level prediction models. *Quarterly Journal of the Royal Meteorological Society* **102** (432), 405–418. 23

[40] DAVIS, R.A. 1972 Principles of oceanography. In *Principles of oceanography*. Addison-Wesley Publishing. 17

[41] DUCHÊNE, V. 2010 Asymptotic shallow water models for internal waves in a two-fluid system with a free surface. *SIAM Journal on Mathematical Analysis* **42** (5), 2229–2260. 18, 36, 42, 68, 186

[42] DUCHÊNE, V. 2013 A note on the well-posedness of the one-dimensional multilayer shallow water model. *ArXiv e-prints* . 59, 68, 79

[43] DUCHÊNE, V. 2013 On the rigid-lid approximation for two shallow layers of immiscible fluids with small density contrast. *arXiv preprint arXiv:1309.3115* . 71, 183

[44] DUCHÊNE, V., ISRAWI, S. & TALHOUK, R. 2013 Shallow water asymptotic models for the propagation of internal waves. *arXiv preprint arXiv:1306.1000* . 183

[45] DUDZINSKI, M. & LUKÁČOVÁ-MEDVIDOVÁ, M. 2013 Well-balanced bicharacteristic-based scheme for multi-layer shallow water flows including wet/dry fronts. *Journal of Computational Physics* **235**, 82–113. 134

[46] DURRAN, D.R. 2001 Open boundary conditions: fact and fiction. In *IUTAM Symposium on Advances in Mathematical Modelling of Atmosphere and Ocean Dynamics*, pp. 1–18. Springer. 22

[47] ENGQUIST, B. & MAJDA, A. 1977 Absorbing boundary conditions for numerical simulation of waves. *Proceedings of the National Academy of Sciences* **74** (5), 1765–1766. 23, 125

[48] F. BOUCHUT, V. ZEITLIN *et al.* 2010 A robust well-balanced scheme for multi-layer shallow water equations. *Discrete and Continuous Dynamical Systems-Series B* **13** (4), 739–758. 72

[49] FLATHER, R.A. 1976 A tidal model of the northwest european continental shelf. *Mem. Soc. R. Sci. Liege* **10** (6), 141–164. 25, 125, 150, 181

[50] FRINGS, J.T. 2012 *An adaptive multilayer model for density-layered shallow water flows*. Universitätsbibliothek. 18, 72, 179

[51] FULLER, A 1981 Root location criteria for quartic equations. *Automatic Control, IEEE Transactions on* **26** (3), 777–782. 43

[52] GAVRILYUK, SL & KAZAKOVA, M YU 2014 Hydraulic jumps in two-layer flow with a free surface. *Journal of Applied Mechanics and Technical Physics* **55** (2), 209–219. 124

[53] GHADER, S. & NORDSTRÖM, J. 2014 Revisiting well-posed boundary conditions for the shallow water equations. *Dynamics of Atmospheres and Oceans* **66**, 1–9. 158

[54] GILL, A.E. 1982 Atmosphere-ocean dynamics. intenational geophysics series 30. *Donn, Academic, Orlando, Fla* . 16, 36, 68, 163, 164

[55] GUO, D.J. & ZENG, Q.C. 1995 Open boundary conditions for a numerical shelf sea model. *Journal of Computational Physics* **116** (1), 97–102. 25

[56] GUSTAFSSON, B. 2008 *High order difference methods for time dependent PDE*. Springer. 144

[57] GUSTAFSSON, B., KREISS, H.-O. & OLIGER, J. 2013 *Time-dependent problems and difference methods*, , vol. 121. John Wiley & Sons. 144

[58] HEDSTROM, G.W. 1979 Nonreflecting boundary conditions for nonlinear hyperbolic systems. *Journal of Computational Physics* **30** (2), 222–237. 24

[59] HOLTON, J.R. & HAKIM, G.J. 2013 *An introduction to dynamic meteorology*. Academic press. 163

[60] HOU, T.Y. & LEFLOCH, P.G. 1994 Why nonconservative schemes converge to wrong solutions: error analysis. *Mathematics of computation* **62** (206), 497–530. 40

[61] HU, F.Q. 1996 On absorbing boundary conditions for linearized euler equations by a perfectly matched layer. *Journal of Computational Physics* **129** (1), 201–219. 24

[62] HU, F.Q. 2001 A stable, perfectly matched layer for linearized euler equations in unsplit physical variables. *Journal of Computational Physics* **173** (2), 455–480. 24

[63] JAHNKE, T. & LUBICH, C. 2000 Error bounds for exponential operator splittings. *BIT Numerical Mathematics* **40** (4), 735–744. 157

[64] JENSEN, T.G. 1998 Open boundary conditions in stratified ocean models. *Journal of Marine Systems* **16** (3), 297–322. 25

[65] JURY, E & MANSOUR, M 1981 Positivity and nonnegativity conditions of a quartic equation and related problems. *Automatic Control, IEEE Transactions on* **26** (2), 444–451. 43

[66] KARABUT, P.E. & OSTAPENKO, V.V. 2011 Problem of the decay of a small-amplitude discontinuity in two-layer shallow water: First approximation. *Journal of applied mechanics and technical physics* **52** (5), 698–708. 53

[67] KIM, J. & LEVEQUE, R.J. 2008 Two-layer shallow water system and its applications. In *Proceedings of the Twelth International Conference on Hyperbolic Problems, Maryland*. 52, 96, 102

[68] KNAUSS, J.A. 1978 *Introduction to physical oceanography*. Prentice-Hall International, Inc. 17

[69] KNOBEL, R. 2000 *An introduction to the mathematical theory of waves*, , vol. 3. American Mathematical Soc. 19

[70] KREISS, H.O. & LORENZ, J. 1989 *Initial-boundary value problems and the Navier-Stokes equations*, , vol. 136. Academic press. 145

[71] LANNES, D. 2013 A stability criterion for two-fluid interfaces and applications. *Archive for Rational Mechanics and Analysis* **208** (2), 481–567. 38

[72] LANSER, D. & VERWER, J.G. 1999 Analysis of operator splitting for advection–diffusion–reaction problems from air pollution modelling. *Journal of Computational and Applied Mathematics* **111** (1), 201–216. 158

[73] LAX, P. & WENDROFF, B. 1960 Systems of conservation laws. *Communications on Pure and Applied mathematics* **13** (2), 217–237. 155

[74] LAX, P.D. & WENDROFF, B. 1964 Difference schemes for hyperbolic equations with high order of accuracy. *Communications on pure and applied mathematics* **17** (3), 381–398. 155

[75] LEVEQUE, R.J. 1986 Intermediate boundary conditions for time-split methods applied to hyperbolic partial differential equations. *Mathematics of Computation* **47** (175), 37–54. 157

[76] LEVEQUE, R.J. 2002 *Finite volume methods for hyperbolic problems*, , vol. 31. Cambridge university press. 157

[77] LEVEQUE, R.J. & YEE, H.C. 1990 A study of numerical methods for hyperbolic conservation laws with stiff source terms. *Journal of computational physics* **86** (1), 187–210. 158

[78] LEVEQUE, RANDALL JOHN 1982 Time-split methods for partial differential equations. *Tech. Rep.*. DTIC Document. 157

[79] LISKA, R. & WENDROFF, B. 1997 Analysis and computation with stratified fluid models. *Journal of Computational Physics* **137** (1), 212–244. 18, 36, 49, 68

[80] LONG, R.R. 1956 Long waves in a two-fluid system. *Journal of Meteorology* **13** (1), 70–74. 18, 36, 48, 68

[81] MARCHESIELLO, P., MCWILLIAMS, J.C. & SHCHEPETKIN, A. 2001 Open boundary conditions for long-term integration of regional oceanic models. *Ocean modelling* **3** (1), 1–20. 22, 25

[82] MARTINSEN, E.A. & ENGEDAHL, H. 1987 Implementation and testing of a lateral boundary scheme as an open boundary condition in a barotropic ocean model. *Coastal engineering* **11** (5), 603–627. 24

[83] MCDONALD, A. 2002 A step toward transparent boundary conditions for meteorological models. *Monthly weather review* **130** (1), 140–151. 164, 165

[84] MCDONALD, A. 2003 Transparent boundary conditions for the shallow-water equations: testing in a nested environment. *Monthly weather review* **131** (4), 698–705. 166

[85] MCLACHLAN, R.I. & QUISPEL, G.R.W. 2002 Splitting methods. *Acta Numerica* **11**, 341–434. 158

[86] MCWILLIAMS, J.C. & FLIERL, G.R. 1979 On the evolution of isolated, nonlinear vortices. *Journal of Physical Oceanography* **9** (6), 1155–1182. 166

[87] MILLER, M.J. & THORPE, A.J. 1981 Radiation conditions for the lateral boundaries of limited-area numerical models. *Quarterly Journal of the Royal Meteorological Society* **107** (453), 615–628. 22

[88] MONJARRET, R. 2014 Local well-posedness of the two-layer shallow water model with free surface. *arXiv preprint arXiv:1402.3194* . 68, 71, 82, 96, 102, 104

[89] MOORE, G.E. *et al.* 1965 Cramming more components onto integrated circuits. 13

[90] MOORE, G.E. *et al.* 1975 Progress in digital integrated electronics. *IEDM Tech. Digest* **11**. 14

[91] MUÑOZ-RUIZ, M.L. & PARÉS, C. 2011 On the convergence and well-balanced property of path-conservative numerical schemes for systems of balance laws. *Journal of Scientific Computing* **48** (1-3), 274–295. 40

[92] NAVON, I.M., NETA, B. & HUSSAINI, M.Y. 2004 A perfectly matched layer approach to the linearized shallow water equations models. *Monthly Weather Review* **132** (6), 1369–1378. 24, 162, 164, 165, 166, 167

[93] NDANOU, S., FAVRIE, N. & GAVRILYUK, S. 2014 Criterion of hyperbolicity in hyperelasticity in the case of the stored energy in separable form. *Journal of Elasticity* **115** (1), 1–25. 38

[94] NYCANDER, J. & DÖÖS, K. 2003 Open boundary conditions for barotropic waves. *Journal of Geophysical Research: Oceans (1978–2012)* **108** (C5). 22, 23, 24, 25

[95] ORGANIZATION, INTERNATIONAL MARITIME 1999 *Convention SOLAS: Convention internationale de 1974 pour la sauvegarde de la vie humaine en mer: amendements de 1996 en vigueur à compter de juillet 1998*. IMO Publishing. 7

[96] ORLANSKI, I. 1976 A simple boundary condition for unbounded hyperbolic flows. *Journal of computational physics* **21** (3), 251–269. 22, 125

[97] OVSYANNIKOV, L.V. 1979 Two-layer shallow water model. *Journal of Applied Mechanics and Technical Physics* **20** (2), 127–135. 18, 36, 52, 68, 96, 102

[98] PALMA, E.D. & MATANO, R.P. 1998 On the implementation of passive open boundary conditions for a general circulation model: the barotropic mode. *Journal of Geophysical Research: Oceans (1978–2012)* **103** (C1), 1319–1341. 22, 24, 25

[99] PARÉS, C. 2006 Numerical methods for nonconservative hyperbolic systems: a theoretical framework. *SIAM Journal on Numerical Analysis* **44** (1), 300–321. 40, 184

[100] PEDLOSKY, J. 1982 Geophysical fluid dynamics. *New York and Berlin, Springer-Verlag, 1982. p. 636* **1**. 16, 36, 68, 163

[101] PELANTI, M., BOUCHUT, F. & MANGENEY, A. 2008 A roe-type scheme for two-phase shallow granular flows over variable topography. *ESAIM: Mathematical Modelling and Numerical Analysis* **42** (05), 851–885. 134

[102] PENVEN, P., DEBREU, L., MARCHESIELLO, P. & MCWILLIAMS, J.C. 2006 Evaluation and application of the roms 1-way embedding procedure to the central california upwelling system. *Ocean Modelling* **12** (1), 157–187. 166

[103] PERKINS, A.L., SMEDSTAD, L.F., BLAKE, D.W., HEBURN, G.W. & WALLCRAFT, A.J. 1997 A new nested boundary condition for a primitive equation ocean model. *Journal of Geophysical Research: Oceans (1978–2012)* **102** (C2), 3483–3500. 22

[104] PETCU, M. & TEMAM, R. 2013 An interface problem: the two-layer shallow water equations. *DCDS-A* **6** (2), 401–422. 125

[105] PIDWIRNY, M. 2006 Surface and subsurface ocean currents: Ocean current map. *Univ. of British Columbia, Okanagan, BC, Canada.(Available at http://www. physicalgeography. net/fundamentals/8q_1. html)* . 9

[106] POINSOT, T.J. & LELEF, S.K. 1992 Boundary conditions for direct simulations of compressible viscous flows. *Journal of computational physics* **101** (1), 104–129. 25

[107] RAYMOND, W.H. & KUO, H.L. 1984 A radiation boundary condition for multi-dimensional flows. *Quarterly Journal of the Royal Meteorological Society* **110** (464), 535–551. 22

[108] RENARDY, M. & ROGERS, R.C. 2004 *An introduction to partial differential equations*, , vol. 4. Springer. 144

[109] RENNELL, J. & PURDY, J. 1832 *An investigation of the currents of the Atlantic Ocean: and of those which prevail between the Indian Ocean and the Atlantic*. Published for Lady Rodd by JG & F. Rivington. 9

[110] RICHTMYER, R.D. 1962 *A survey of difference methods for nonsteady fluid dynamics*. NCAR. 155

[111] RØED, L.P. & COOPER, C.K. 1987 A study of various open boundary conditions for wind-forced barotropic numerical ocean models. *Elsevier oceanography series* **45**, 305–335. 22, 24, 25, 125

[112] ROSS, J.C. 1847 *A Voyage of Discovery and Research in the Southern and Antarctic Regions, during the Years 1839-43*. Murray. 9

[113] DE SAINT-VENANT, A.B. 1871 Théorie du mouvement non permanent des eaux, avec application aux crues des rivières et a l'introduction de marées dans leurs lits. *Comptes rendus des séances de l'Académie des Sciences* **36**, 174–154. 16, 36, 68, 183

[114] SCHIJF, J.B. & SCHONFLED, J.C. 1953 Theoretical considerations on the motion of salt and fresh water. IAHR. 18, 36, 52, 68, 96, 102

[115] SCHOT, S.H. 1992 Eighty years of sommerfeld's radiation condition. *Historia Mathematica* **19** (4), 385–401. 22

[116] SEGAR, D.A. & SEGAR, E.S. 1998 *Introduction to ocean sciences*. Wadsworth Pub. 15

[117] SERRE, D. 1996 *Systèmes de lois de conservation*. Diderot Paris. 39, 40, 41, 73, 74, 75

[118] SMOLLER, J. 1983 Shock waves and reaction-diffusion equations, vol. 258 of fundamental principles of mathematical science. 41, 76

[119] SOMMERFELD, A. 1896 Mathematische theorie der diffraction. *Mathematische Annalen* **47** (2), 317–374. 22

[120] SOMMERFELD, A. 1909 Über die ausbreitung der wellen in der drahtlosen telegraphie. *Annalen der Physik* **333** (4), 665–736. 22

[121] SOMMERFELD, A. 1910 Die greensche funktion der schwingungsgleichung für ein beliebiges gebiet. *Physikal. Zeitschr* **11**, 1057–1066. 22

[122] SOMMERFELD, A. 1949 Partial differential equation in physics. *Lectures on Theoretical Physics-Pure and Applied Mathematics, New York: Academic Press, 1949* **1**. 22, 125

[123] SPALL, M.A. & HOLLAND, W.R. 1991 A nested primitive equation model for oceanic applications. *Journal of Physical Oceanography* **21** (2), 205–220. 166

[124] SPORTISSE, B. 2000 An analysis of operator splitting techniques in the stiff case. *Journal of Computational Physics* **161** (1), 140–168. 158

[125] STEWART, A.L. & DELLAR, P.J. 2010 Multilayer shallow water equations with complete coriolis force. part 1. derivation on a non-traditional beta-plane. *Journal of Fluid Mechanics* **651**, 387–413. 17, 184

[126] STEWART, A.L. & DELLAR, P.J. 2012 Multilayer shallow water equations with complete coriolis force. part 2. linear plane waves. *Journal of Fluid Mechanics* **690**, 16–50. 17, 184

[127] STEWART, A.L. & DELLAR, P.J. 2013 Multilayer shallow water equations with complete coriolis force. part 3. hyperbolicity and stability under shear. *Journal of Fluid Mechanics* **723**, 289–317. 18, 47, 49, 52, 59, 68, 71, 96, 102, 104, 184

[128] STRANG, G. 1964 Accurate partial difference methods. *Numerische Mathematik* **6** (1), 37–46. 145

[129] STRANG, G. 1968 On the construction and comparison of difference schemes. *SIAM Journal on Numerical Analysis* **5** (3), 506–517. 157

[130] TAYLOR, M.E. 1996 *Partial differential equations III: Nonlinear equations*. Springer. 41, 76

[131] THOMPSON, P.A. & BEAVERS, G.S. 1972 Compressible-fluid dynamics. *Journal of Applied Mechanics* **39**, 366. 14

[132] TORO, E.F. 1999 *Riemann solvers and numerical methods for fluid dynamics*, , vol. 16. Springer. 38

[133] TORO, E.F. 2009 *Riemann solvers and numerical methods for fluid dynamics: a practical introduction*. Springer. 76

[134] TRÉGUIER, A.M., BARNIER, B., MIRANDA, A.P. DE, MOLINES, J.M., GRIMA, N., IMBARD, M., MADEC, G., MESSAGER, C., REYNAUD, T. & MICHEL, S. 2001 An eddy-permitting model of the atlantic circulation: Evaluating open boundary conditions. *Journal of Geophysical Research: Oceans (1978–2012)* **106** (C10), 22115–22129. 22

[135] TREVES, T. 2008 United nations convention on the law of the sea. *United Nations Audiovisual Library of International Law* . 7

[136] VREUGDENHIL, C.B. 1979 Two-layer shallow-water flow in two dimensions, a numerical study. *Journal of Computational Physics* **33** (2), 169–184. 71, 134

Abstract

This PhD dissertation, conducted as a collaboration between the SHOM and the University of Toulouse, deals with improving the treatment of open boundary conditions, for the multi-layer shallow water model with free surface. One of the main difficulties with such an objective is the determination of the modes associated to the internal surfaces liquid/liquid: the baroclinic modes.

The work of this thesis focusses on two axes:

- ◇ The first one concerns the eigenstructure of the differential operator, associated to the general model. This allows to insure conditions of hyperbolicity and local well-posedness of the system of equations. This axis is divided in two chapters. The analysis of the two-layer model is performed in the first chapter: the calculus are exact and it is proved the gap is important compared with the single-layer model. The model with n layers, $n \geq 3$, is studied in the second chapter: the main difficulty of these equations is the number of parameters, which obliges to concede assumptions. A new conservative multi-layer model is introduced and analyzed.
- ◇ The second axis deals with practical treatment of the open boundary conditions. The conditional local well-posedness of the initial-boundary value problem is proved. Afterwards, the boundary conditions are clarified for a general domain and a particular one: a rectangle. Comparison of the errors is performed between the single-layer model and the two and four-layer models, with two test case: the propagation of a gravity wave and a barotropic vortex.

Keywords: shallow water, multi-layer, free surface, hyperbolicity, local well-posedness, vorticity, open boundaries.

Résumé

Ce travail de thèse, mené en collaboration entre le SHOM et l'Université de Toulouse, s'inscrit dans un contexte d'amélioration du traitement des conditions limites ouvertes, pour le modèle de *Saint-Venant* multi-couches à surface libre. L'une des principales difficultés rencontrée dans cette démarche concerne la détermination des modes associés aux surfaces interne liquide/liquide: les modes baroclines.

Les travaux de cette thèse s'articulent autour de deux axes principaux :

- ◇ Le premier traite l'analyse des éléments propres de l'opérateur différentiel, associé au modèle général. Cela permet d'assurer des conditions d'hyperbolicté et de caractère bien-posé du système d'équations. Cet axe est divisé en deux chapitres. L'analyse du modèle bi-couche est menée dans le premier chapitre : les calculs sont exacts et il y est prouvé que la différence avec le modèle à une couche est importante. Le modèle à n couches, avec $n \geq 3$, est étudié dans le second chapitre : la difficulté principale pour l'analyse de ces équations est le nombre de paramètres, ce qui nécessite de supposer des hypothèses. Un nouveau modèle multi-couches conservatif est introduit et analysé.
- ◇ Le second axe traite le traitement opérationnel des conditions limites ouvertes. Le caractère bien-posé du problème initial aux limites est démontré, sous certaines conditions. Ensuite, les conditions limites à prescrire sont clairement explicitées pour un domain général et un domain particulier : un rectangle. La comparaison des erreurs, des modèles à une, deux et quatre couches, est menée avec deux cas tests : la propagation d'une onde de gravité et d'un vortex barotrope.

Mots clés : *Saint-Venant*, multi-couches, surface libre, hyperbolicité, localement bien-posé, vorticité, conditions limites ouvertes

La mer est un espace de rigueur et de liberté.

V. Hugo.